SEDIMENTOLOGY AND TECTONICS OF THE WESTERN CAMEROS BASIN PROVINCE OF BURGOS NORTHERN SPAIN.

D. Phil. Thesis

Department of Earth Sciences

University of Oxford.

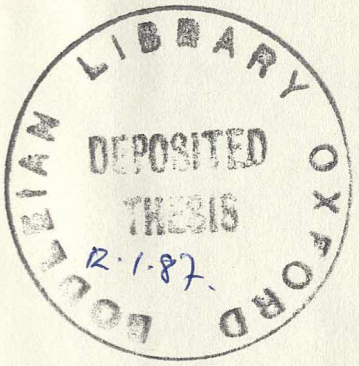

Trinity 1986.

Volume 2: Figures.

NIGEL HOWARD PLATT

Worcester College

Oxford.

Fig 1.1. Iberia: location map, showing provinces.

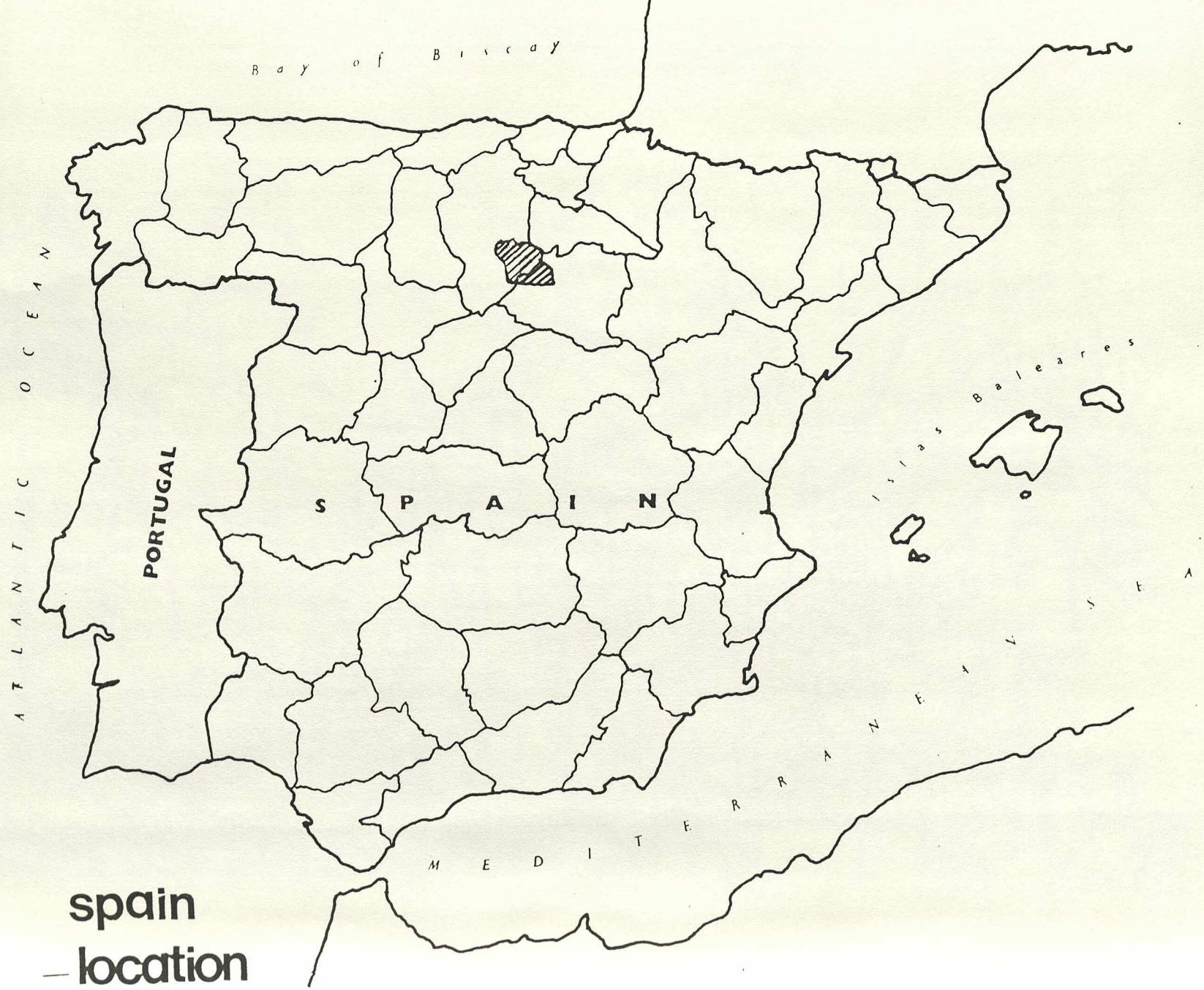

spain
– location

Fig 1.2. Study area: location map, showing major roads.

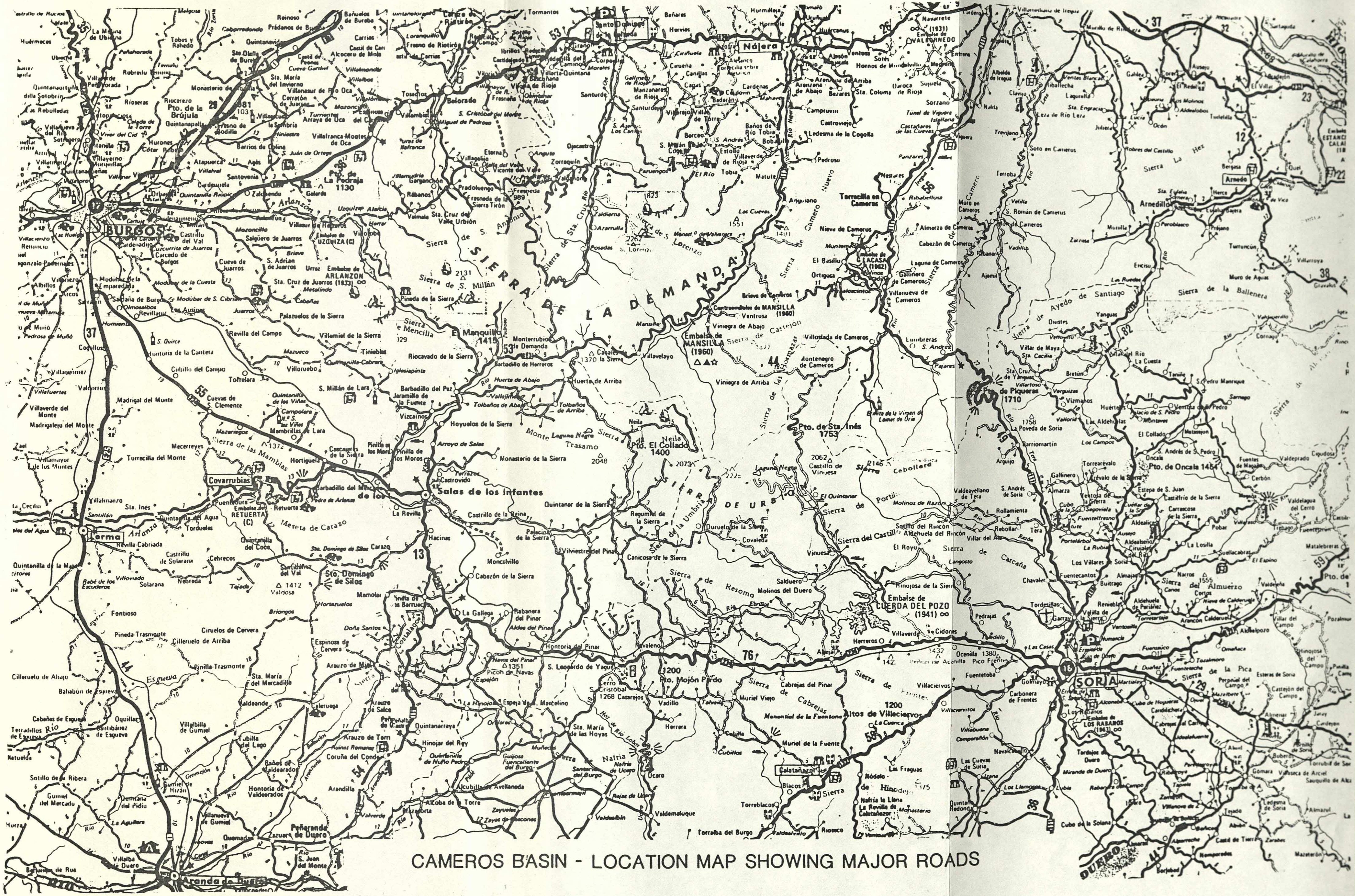

CAMEROS BASIN - LOCATION MAP SHOWING MAJOR ROADS

Fig 1.3. Iberia: simplified geology, showing Mesozoic Basins.

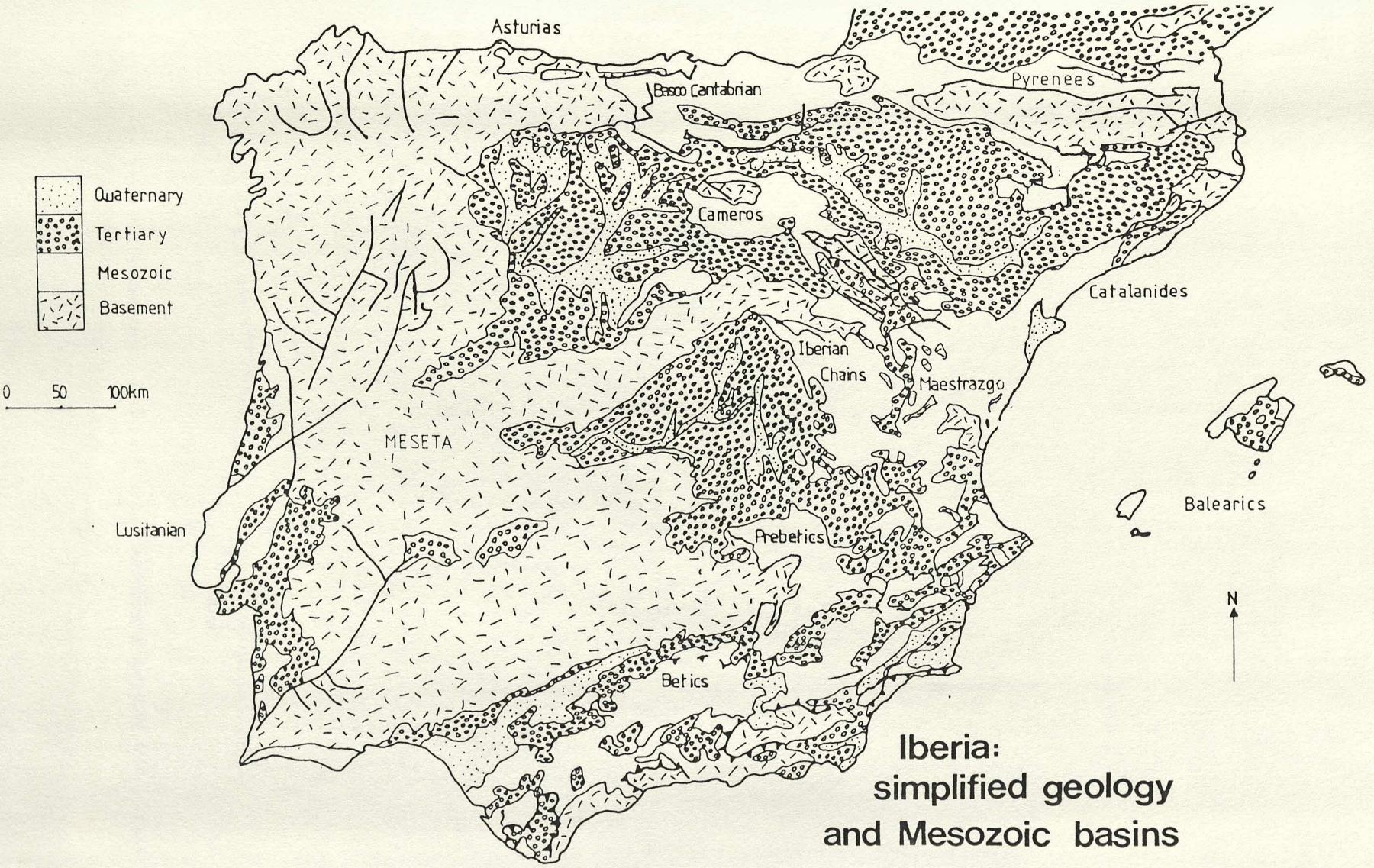

Iberia:
simplified geology
and Mesozoic basins

Fig 1.4. Iberia: physical, showing major mountain ranges and rivers.

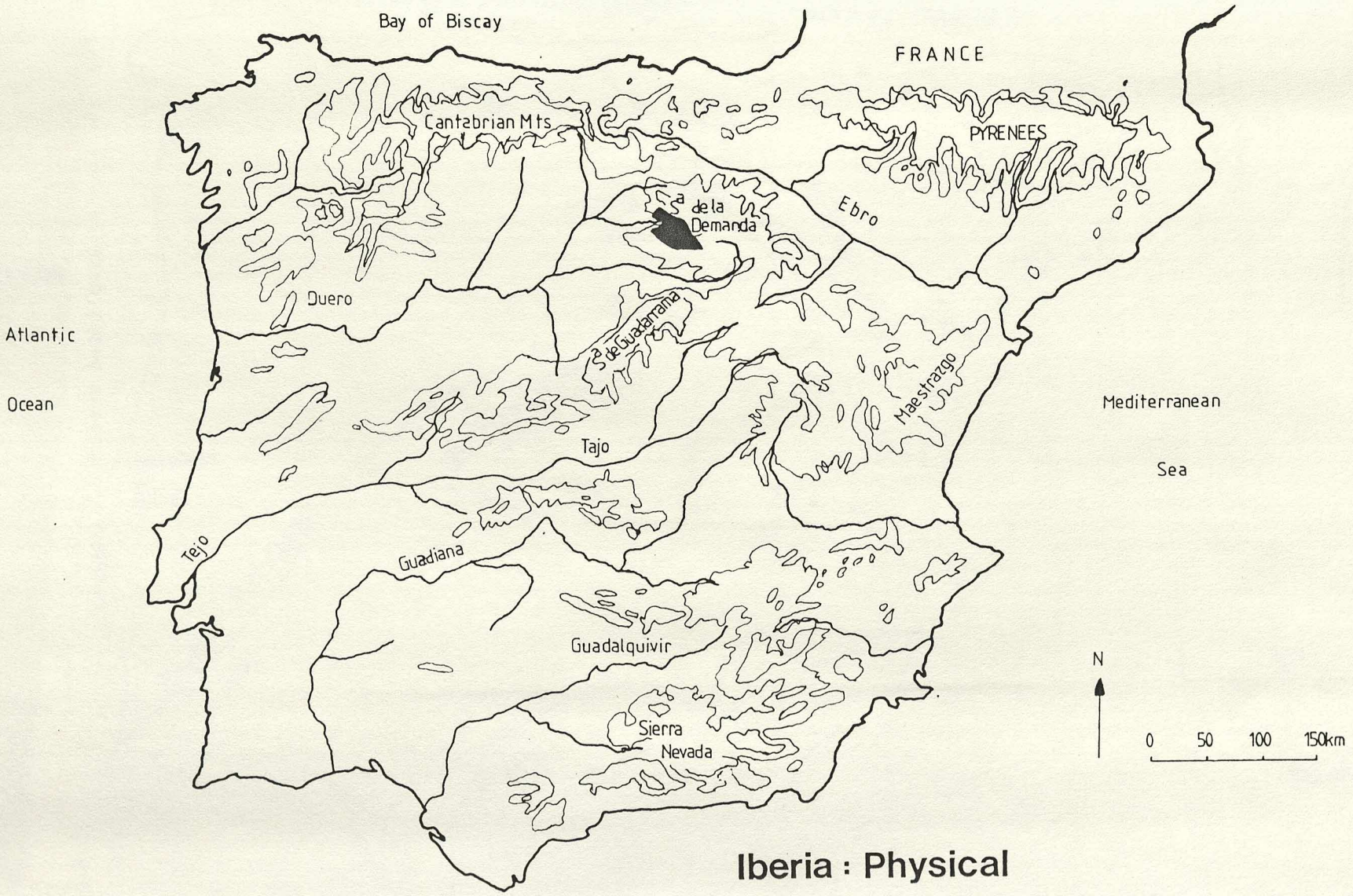

Iberia : Physical

Fig 1.5. Iberia: simplified structural map.

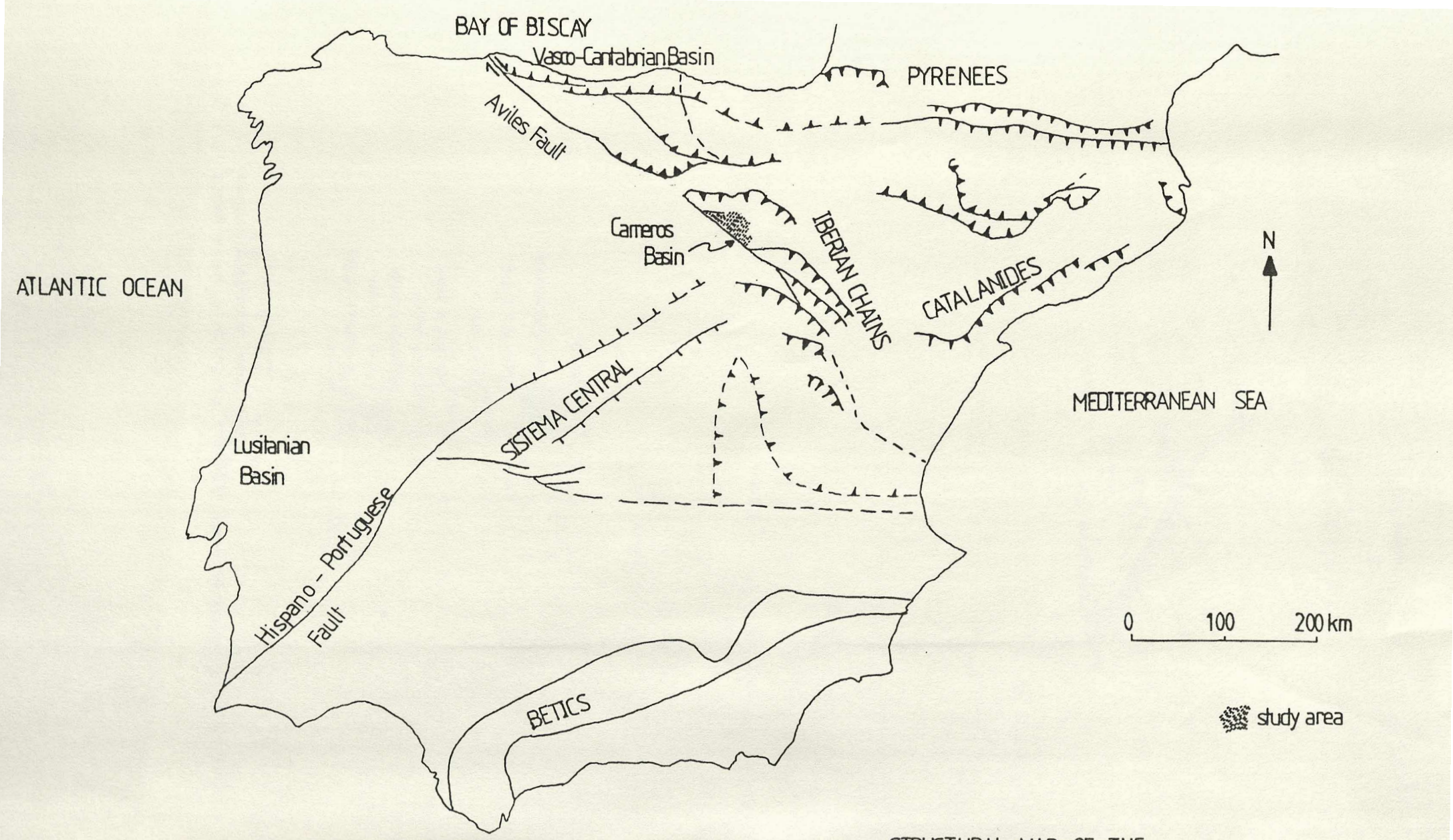

STRUCTURAL MAP OF THE IBERIAN PENINSULA

Fig 1.6. Study area: simplified geology, showing location of logged sedimentological sections.

Roads
Sections
Scale: 0 2 4 6 8 10 km

Key:

- Quaternary
- Plio-Quaternary (Rañas)
- Oligocene & Miocene
- Palaeocene & Eocene
- Upper Cretaceous
- Salas Group & Utrillas
- Pedroso Group
- Tierra de Lara Group
- Triassic & Marine Jurassic
- Palaeozoic

N

Sierra de la Demanda

To Burgos
To Burgos
Torrelara
Cuevas de San Clemente
Rupelo
To Nájera, Logroño
Quintanilla de las Viñas
Jaramillo Quemado
Vizcainos
Barbadillo del Pez
Marmolillas de Lara
Hortigüela
Valparaso
Piedrahita del Muñó
Castrovido
Terrazas
To Lerma
Covarrubias
Salas de los Infantes
To Laguna Negra
To Neila
Quintanar de la Sierra
To Soria
Palacios de la Sierra
Moncalvillo
To Lerma
SILOS BASIN
S. Domingo de Silos
Tejada
Pinilla de los Barruecos
Hortezuelos
Mamolar (Ladera)
Tenadillas
La Gallega
Atlea del Pinar
To Madrid
Las Pinarejas (Doña Santos)
Hontoria del Pinar
To Madrid
Sierra de Brezales
San Leonardo de Yagüe
Puerto Mojon Pardo
To Soria
Espejon
Yadillo
To Madrid
Huerta del Rey
Talveila
Espeja
La Hinojosa
Cubillo
To Burgo de Osma

Duero Basin

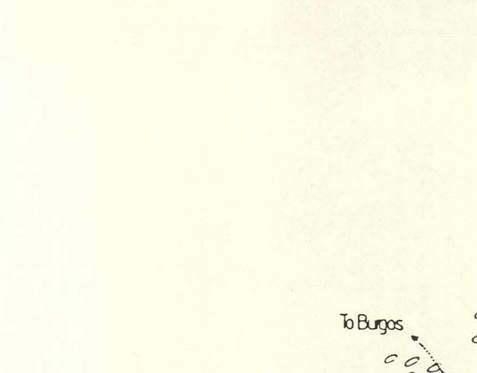

SIMPLIFIED GEOLOGICAL MAP OF THE W CAMEROS BASIN (modified after Salomon 1982).

Fig 1.7. Sketch map of study area, showing areas selected for detailed mapping.

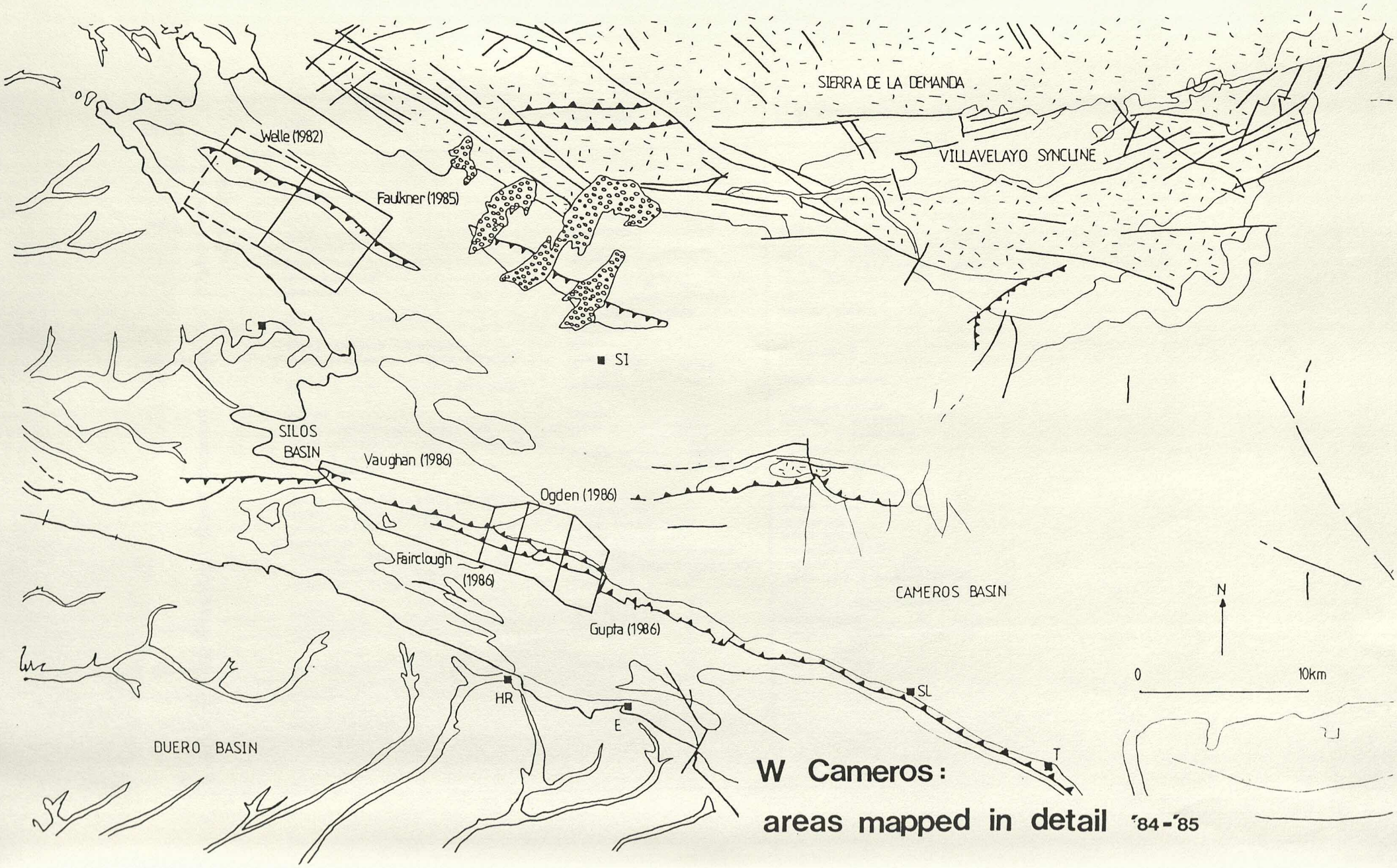
SIERRA DE LA DEMANDA
VILLAVELAYO SYNCLINE
Welle (1982)
Faulkner (1985)
SI
SILOS
BASIN
Vaughan (1986)
Ogden (1986)
Fairclough
(1986)
Gupta (1986)
CAMEROS BASIN
DUERO BASIN
HR
E
SL
T
N
0
10km
W Cameros:
areas mapped in detail '84-'85

Fig 2.1. Stratigraphy of the W Cameros Basin and correlation with S England.

STRATIGRAPHY OF THE W CAMEROS BASIN

PERIOD	STAGE	LOCAL NAME	U. K. EQUIVALENT (IF ANY)
QUATERNARY			
	PLIO-PLEISTOCENE	RANAS	
TERTIARY	MIOCENE	LA HINOJOSA	
	OLIGOCENE	COVARRUBIAS	BEMBRIDGE / BOVEY
	PALAEOCENE	GARUMNIAN /	READING / BARTON
	MAASTRICHTIAN	SANTIBANEZ DEL VAL	MAASTRICHTIAN / DANIAN CHALKS
	CAMPANIAN	S^{O} DOMINGO DE SILOS	UPPER CHALK
		BURGO DE OSMA	
	CONIACIAN - CAMPANIAN	HONTORIA DEL PINAR	MIDDLE CHALK
		HORTEZUELOS	
	UPPER TURONIAN - CONIACIAN	MUNECAS	
CRETACEOUS	UPPER CENOMANIAN - LOWER TURONIAN	PICOFRENTES	LOWER CHALK
		S^{a} MARIA DE LAS HOYAS	
	UPPER ALBIAN - LOWER CENOMANIAN	UTRILLAS	UPPER GREENSAND
	APTIAN	SALAS	LOWER GREENSAND
	UPPER VALANGINIAN - BARREMIAN	PEDROSO / PIEDRAHITA	WEALDEN / HASTINGS
	UPPER BERRIASIAN - LOWER VALANGINIAN	/ HORTIGUELA	/ FAIRLIGHT
	? LOWER BERRIASIAN	TIERRA DE LARA / RUPELO	PURBECK
	? PORTLANDIAN	/ SENORA DE BREZALES	PORTLAND SANDS
	UPPER OXFORDIAN - LOWER KIMMERIDGIAN	TALVEILA	CORALLIAN & KELLOWAYS
	MIDDLE - UPPER CALLOVIAN	VILLAVELAYO	LOWER OXFORD CLAY
JURASSIC	LOWER CALLOVIAN	UPPER ORANGE BEDS	CORNBRASH
	BATHONIAN	LOWER ORANGE BEDS	GREAT OOLITE
	AALENIAN - BAJOCIAN	LIMESTONES WITH SPONGES	INFERIOR OOLITE
	PLIENSBACHIAN - TOARCIAN	LIMESTONE LIAS & MARLY LIAS	MIDDLE & UPPER LIAS
	RHAETIAN - SINEMURIAN	CARNIOLAS	LOWER LIAS & PENARTH GROUP
	KEUPER	KEUPER	KEUPER / MERCIA MUDSTONE
TRIASSIC	MUSCHELKALK	MUSCHELKALK	WATERSTONES
	BUNTER	BUNTER	BUNTER / SHERWOOD SANDSTONE
CARBONIFEROUS	WESTPHALIAN B - C	WESTPHALIAN B - C	COAL MEASURES
ORDOVICIAN	TREMADOC	BARRIOS	
CAMBRIAN	LOWER - MIDDLE	BARBADILLO DEL PEZ	

PLATT N (1986)

Fig 2.2. Palaeozoic stratigraphy of the Sierra de la Demanda, from Colchen (1970).

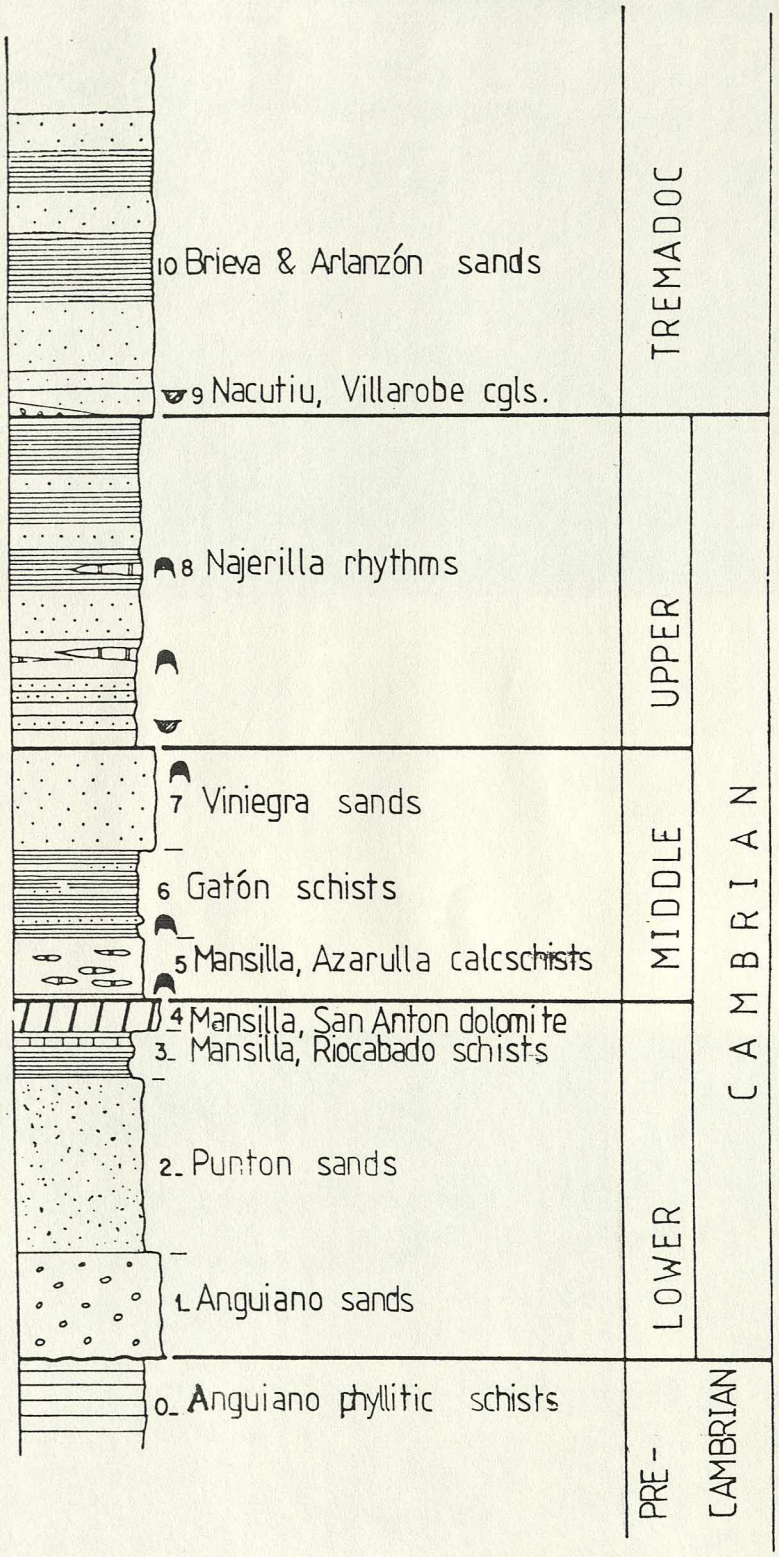

M. Colchen, 1969

LOWER PALAEOZOIC STRATIGRAPHY.

Fig 2.3. Well-cleaved phyllites at the junction of the C-113 with the local road to Pineda del Sierra and Riocavado de la Sierra, approximately 5km N of Barbadillo del Pez.

Fig 2.4. Phyllites at the same locality as fig 2.3, showing bedding. Agnostid trilobite found at this locality by D C Edwards. The presence of thin and graded clastic laminae in a fine-grained background indicates quiet, possibly deep water, sedimentation.

Fig 2.5. Triassic stratigraphy of N Spain (Virgili et al, 1977).

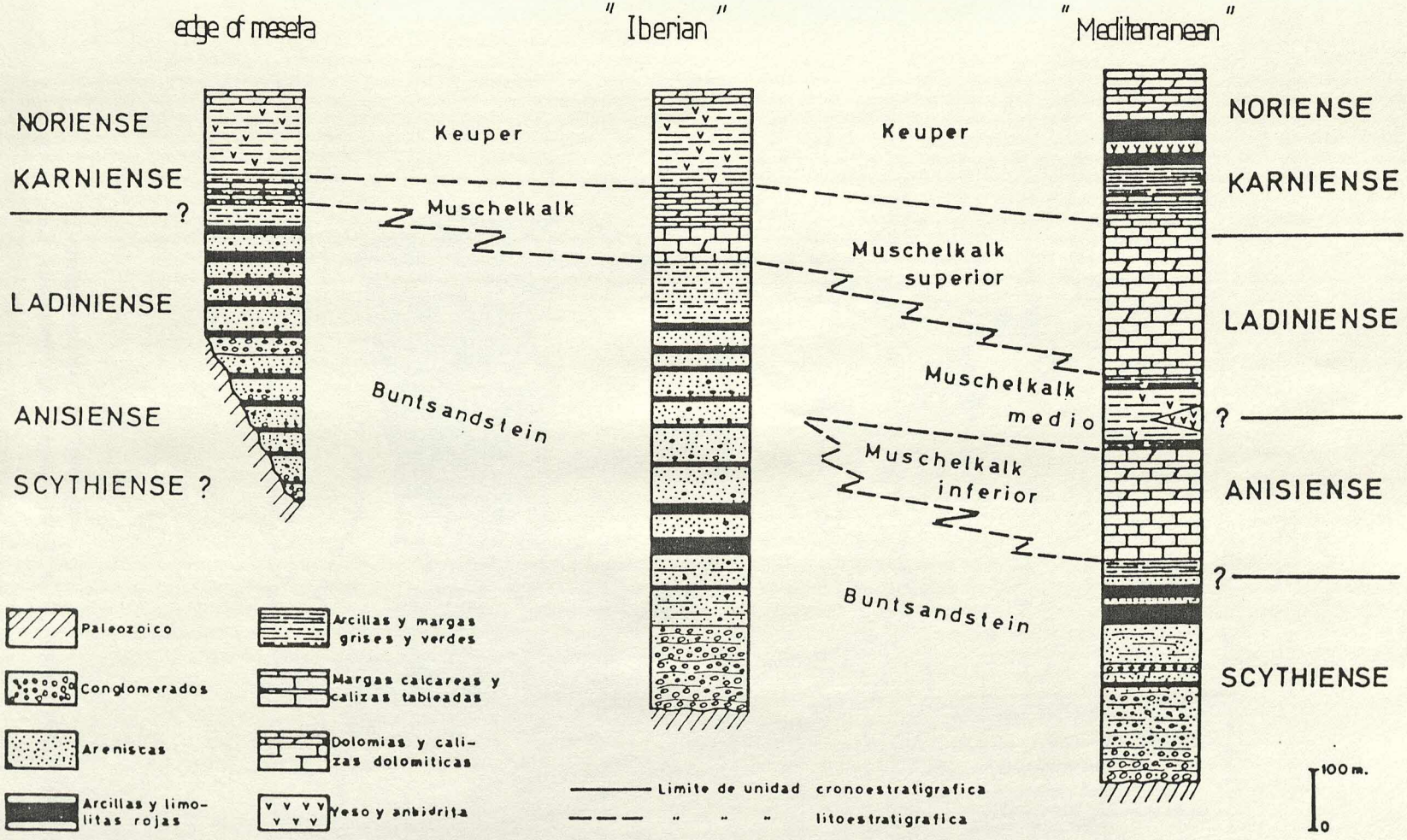

TRIASSIC—LITHOSTRATIGRAPHIC UNITS

Fig 2.6. Map showing the areal limits of the Middle Triassic transgression in Iberia.

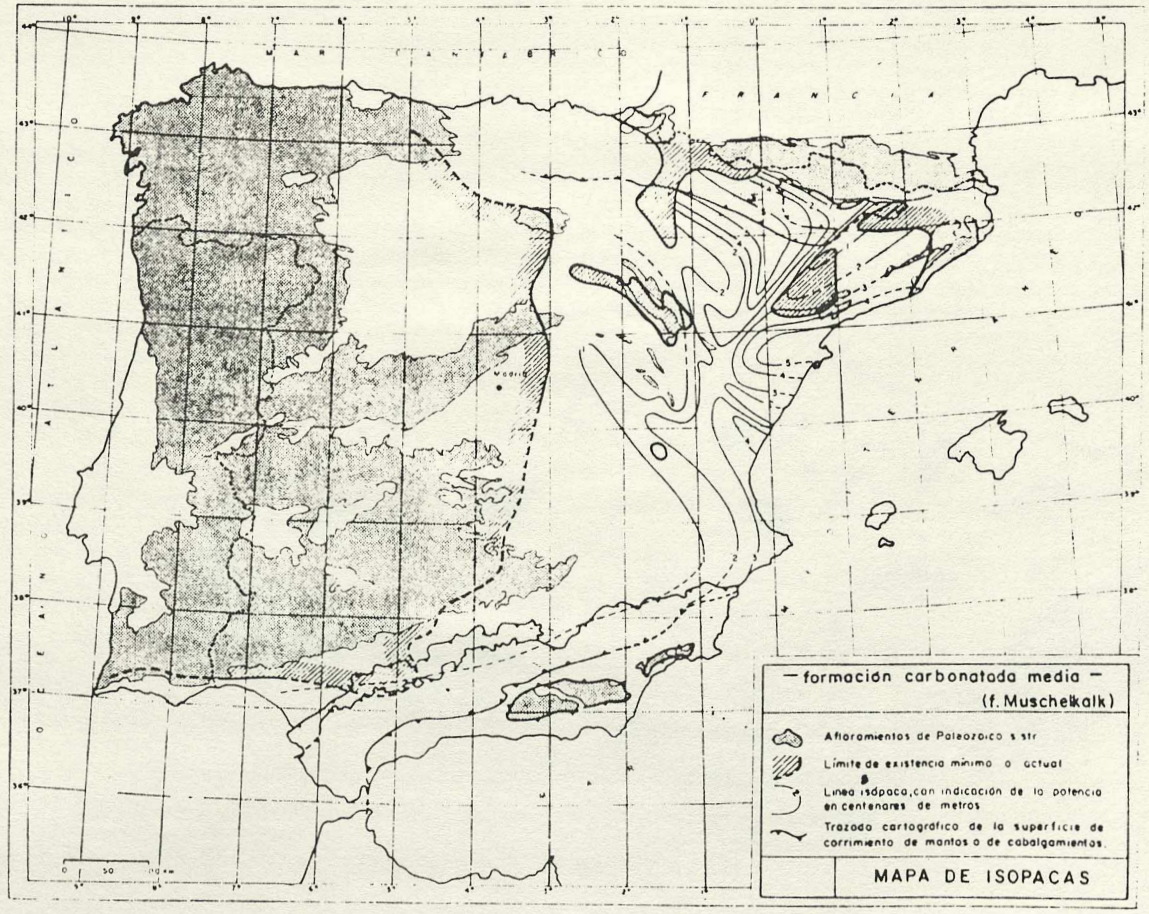
— formación carbonatada media —
(f. Muschelkalk)
Afloramientos de Paleozoico s str
Límite de existencia mínimo o actual
Línea isópaca, con indicación de la potencia en centenares de metros
Trazado cartográfico de la superficie de corrimiento de mantos o de cabalgamientos
MAPA DE ISOPACAS

Fig 2.7. Hand-specimen of vuggy dolomite showing many angular voids (?evaporite pseudomorphs). Carniolas. San Leonardo Fault Zone, Near Tenadillas, 1km SSE of Pinilla de los Barruecos.

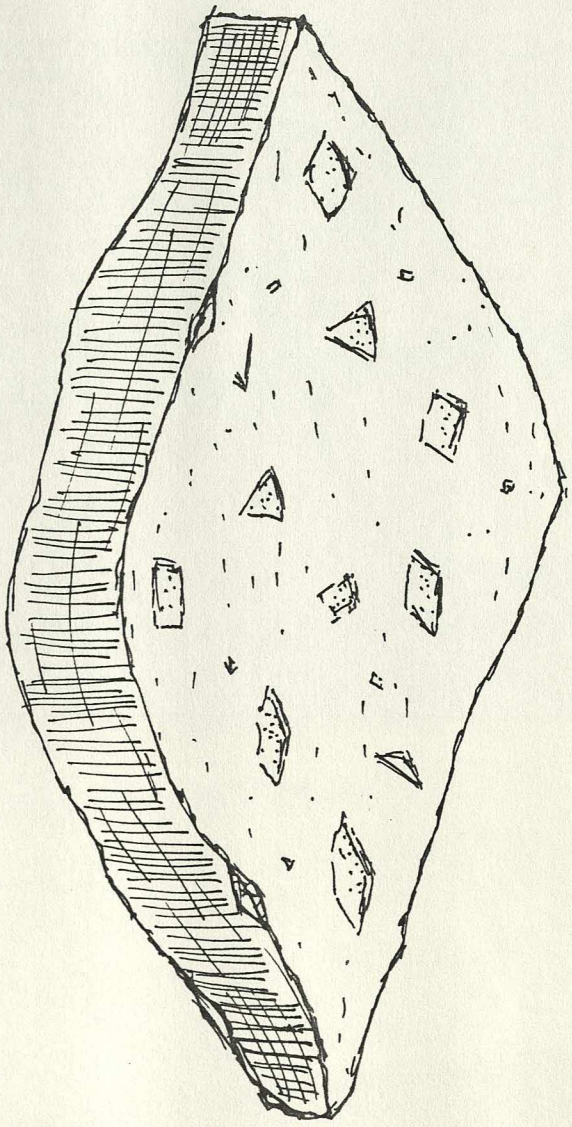

Fig 2.8. Outcrop photograph of laminated carbonate, showing vuggy texture (top of outcrop) and teepee structures. Carniolas. 1km N of Vadillo, near San Leonardo.

Fig 2.9. Palaeogeography for the W Cameros Basin during Liassic times, from Valladares (1980).

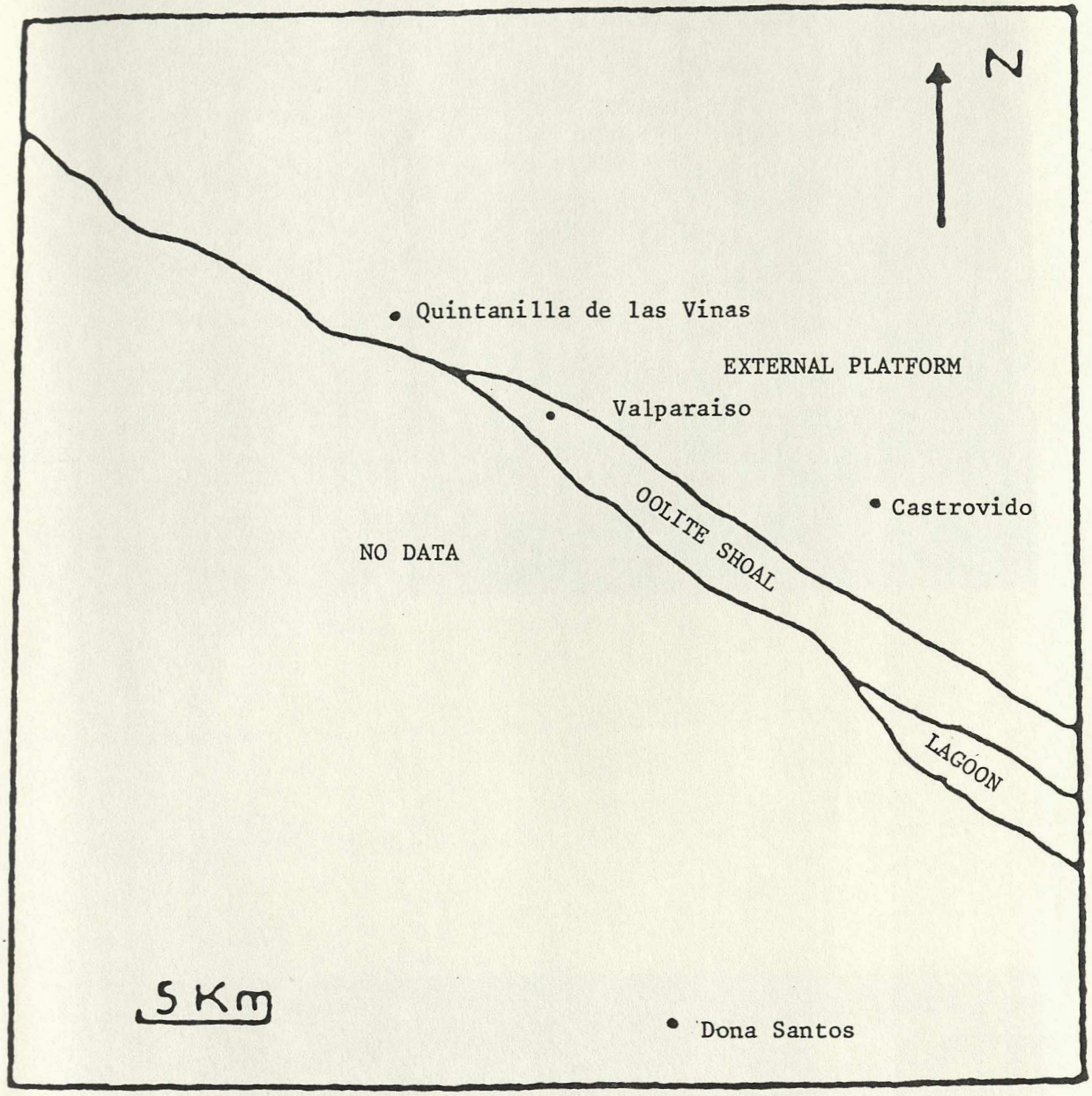

Valladares (1980). Palaeogeography: Upper Sinemurian.

Fig 2.10. Well-bedded limestone-marl rhythms "Limestone Lias". Hammer rests on minor fault. Note also fault, lower centre, dying out / accommodated up-section? Looking NW, Piedrahita de Muno.

Fig 2.11. Marls with only thin intercalated limestones. "Marly Lias". Abundant ammonites at this locality. Looking E. 1km SSE of Pinilla de los Barruecos.

Fig 2.12. Bedded limestones with intercalated marls. ?Aalenian. Near Cubillo del César.

Fig 2.13. Marine Jurassic sequence. Liassic marls (poor outcrop, scree left) overlain by bedded Aalenian (upper left) and left of house (right). Well-bedded limestones of Middle Bajocian - Bathonian passing up into orange limestones of Lower Callovian. Senora de Brezales Formation above (right, on ridge crest below pointed hill). Snow on horizon (left) on Palaeozoic of Sierra de la Demanda. Snow on horizon (right) lying on Pedroso Group dip slope, near Laguna Negra. Castrovido. Left: looking NE; right: looking E.

Fig 2.14. Discontinuity in marine Jurassic sequence, exhibiting considerable relief. Well-bedded limestones of Middle Bajocian - Bathonian rest on massive Upper Aalenian - Lower Bajocian limestones with sponges. Relief classically interpreted as product of sponge bioherm topography, but this view suggests folding at this horizon. Quintanilla de las Vinas. Looking W.

Fig 2.15. Bathonian - Callovian. Well-bedded grey limestones of Bathonian overlain by yellow-orange weathering "orange beds" (?Lower Callovian). Mambrillas de Lara.

Fig 2.16. Lower Callovian limestones showing micritic carbonate nodules (pale grey) set in matrix of yellow-orange weathering carbonate rich in 1mm quartz grains. Mambrillas de Lara.

Fig 2.17. Well-bedded yellow-orange weathering limestones ("orange beds") of Lower Callovian overlain by:
a) grey limestone, Senora de Brezales Fm equivalent, eg centre right, under stubby spreading tree;
b) red marls, Las Vinas Member, (not outcropping, scrub-covered bank);
c) massive limestones of Ladera Member. Looking SE. Mambrillas de Lara.

Fig 2.18. Yellow limestones ("orange beds") with ammonite. 1km N of Torrelara. Macrocephalus zone. Lower Callovian.

Fig 2.19. Block of yellow limestone ("orange beds") with ammonite. 1km N of Torrelara. Macrocephalus zone. Lower Callovian.

Fig 2.20. Map showing age of youngest preserved marine Jurassic strata, NW Iberian Chains. From Mensink & Schüdack (1982).

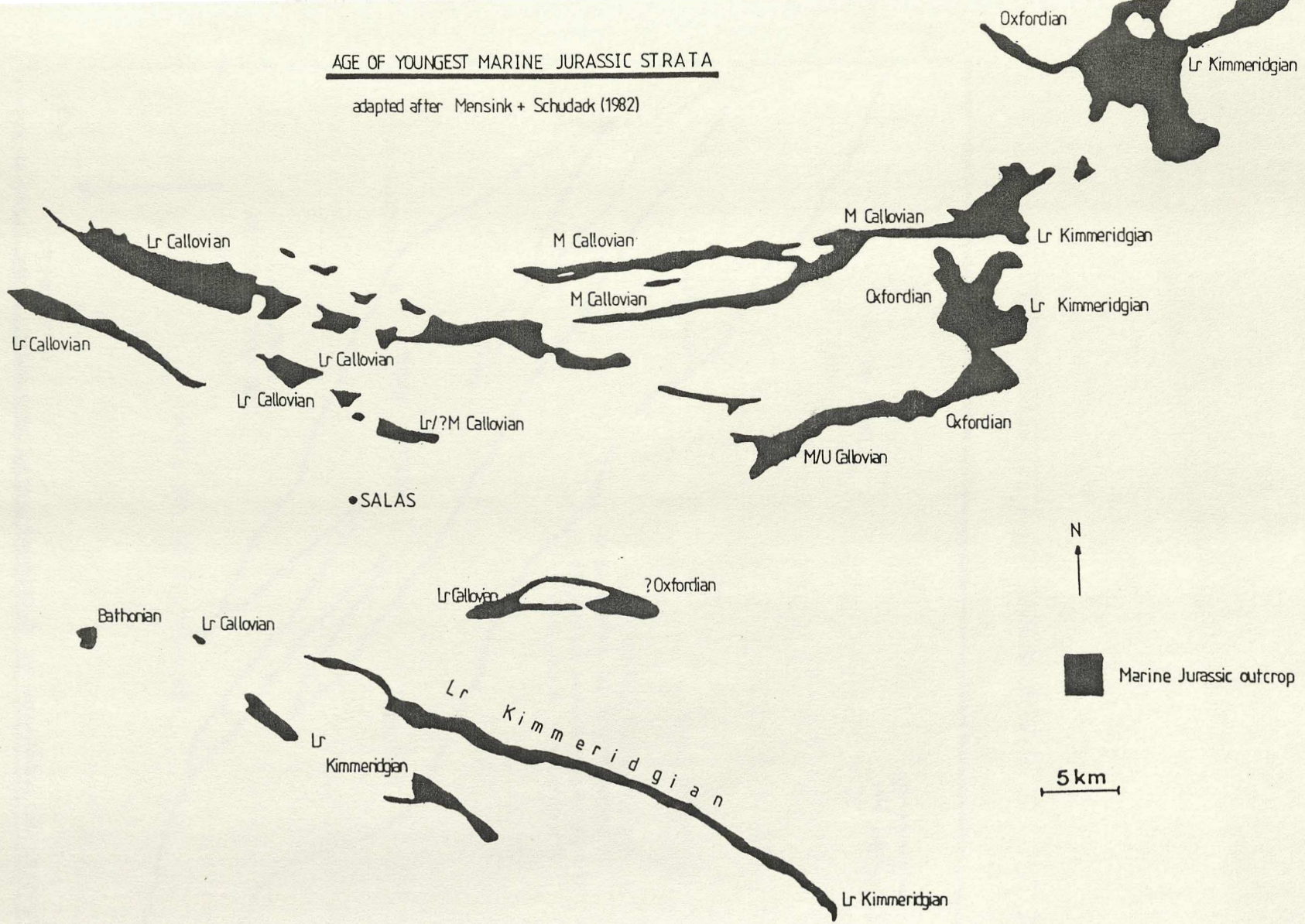
AGE OF YOUNGEST MARINE JURASSIC STRATA
adapted after Mensink + Schudack (1982)
Oxfordian
Lr Kimmeridgian
M Callovian
Lr Kimmeridgian
Lr Callovian
M Callovian
Oxfordian
Lr Kimmeridgian
Lr Callovian
Lr Callovian
Lr Callovian
Lr/?M Callovian
Oxfordian
M/U Callovian
SALAS
N
Lr Callovian
?Oxfordian
Bathonian
Lr Callovian
Marine Jurassic outcrop
Lr Kimmeridgian
Lr
Kimmeridgian
5 km
Lr Kimmeridgian

Fig 2.21. Lower Callovian palaeogeography as envisaged by Valladares (1976).

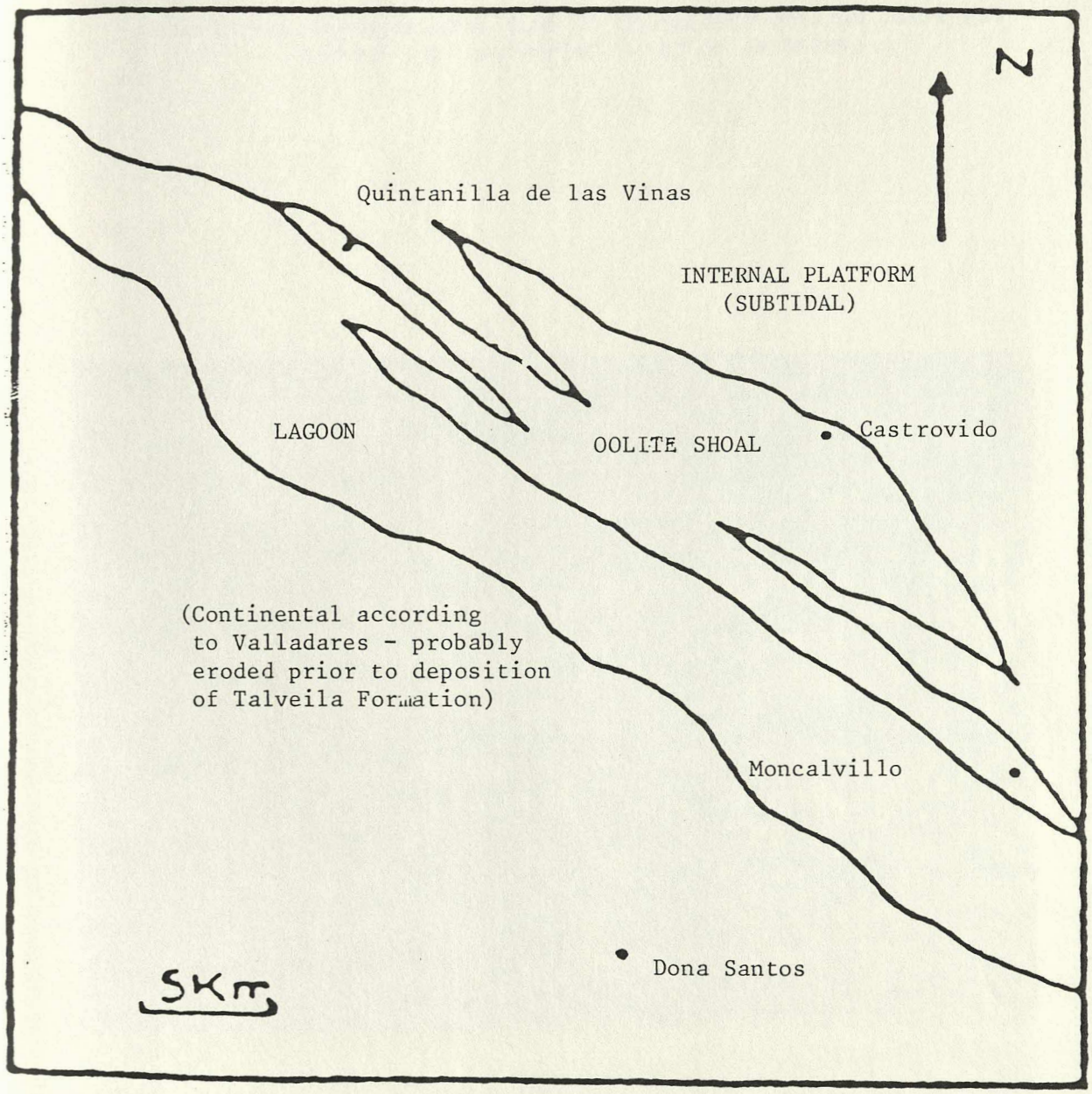

Lower Callovian Palaeogeography (after Valladares, 1980).

Fig 2.22. Outcrop photograph of dark grey to black limestones. (?Middle) to Upper Callovian. Villavelayo.

Fig 2.23. Middle Oxfordian palaeogeography of the Iberian Chains. Errenst (1984).

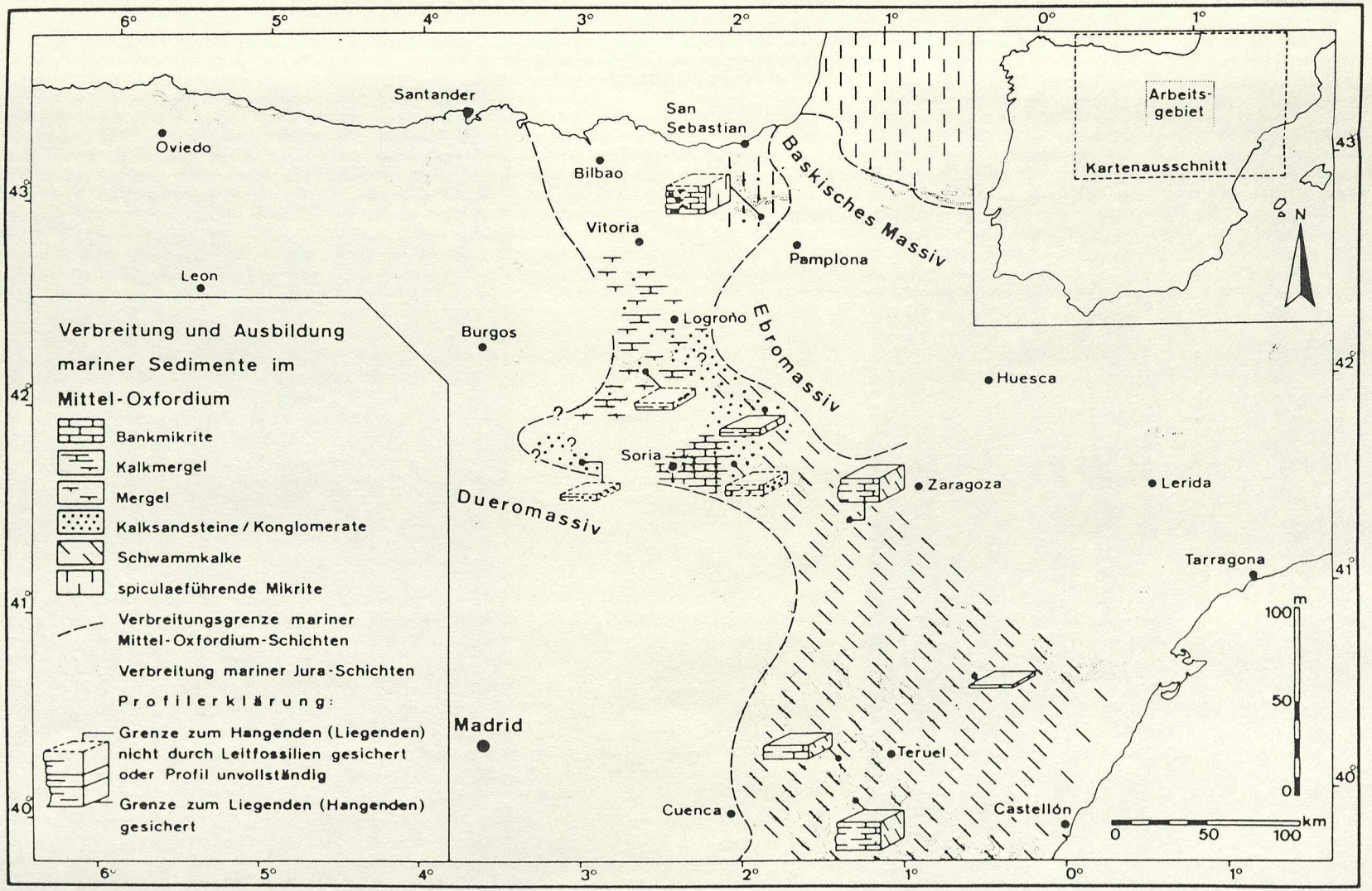

Middle Oxfordian Palaeogeography. Errenst (1984).

Fig 2.24. Micrograph of sandy calclithite showing abundant bioclasts including bivalves. Numerous irregular quartz grains and opaque grains. Note preferred grain orientation of larger allochems. Stained section. Field of view: 9mm. Lower Talveila Formation. Hortezuelos.

Fig 2.25. Coarse cross-bedded calclithites. Planar and trough cross-sets. Mapping board in bottom right of picture is 23cm across. Lower Talveila Formation. Hortezuelos.

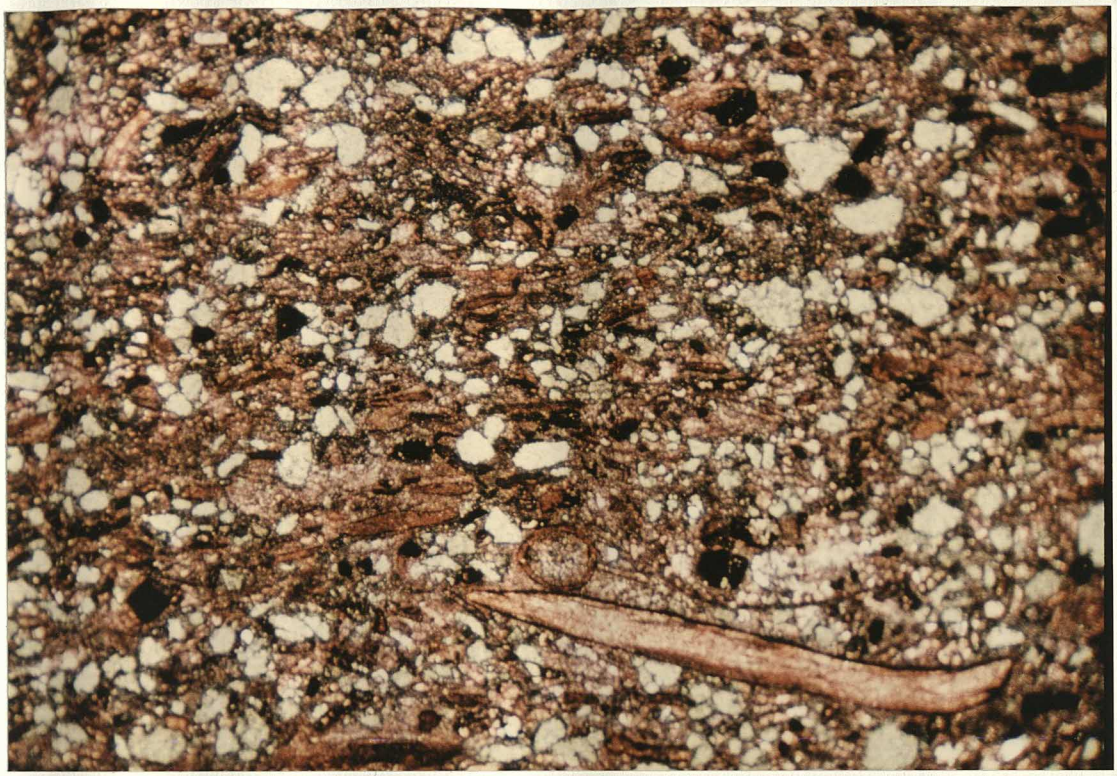

Fig 2.26. Coarse cross-bedded arenites. Note continuous thickness of sands - 10m. Lower Talveila Formation, (about 10m above base). Hortezuelos.

Fig 2.27. Interbedded arenites and quartz-pebbly conglomerates. Planar cross-bedding of arenites. Consistent set accretion direction in this example (towards S). Numerous reactivation surfaces. Some upward-fining discernible. Channelled base of conglomerate unit above hammer. Red-weathering horizons near base. Lower Talveila Formation. Hortezuelos. Looking E.

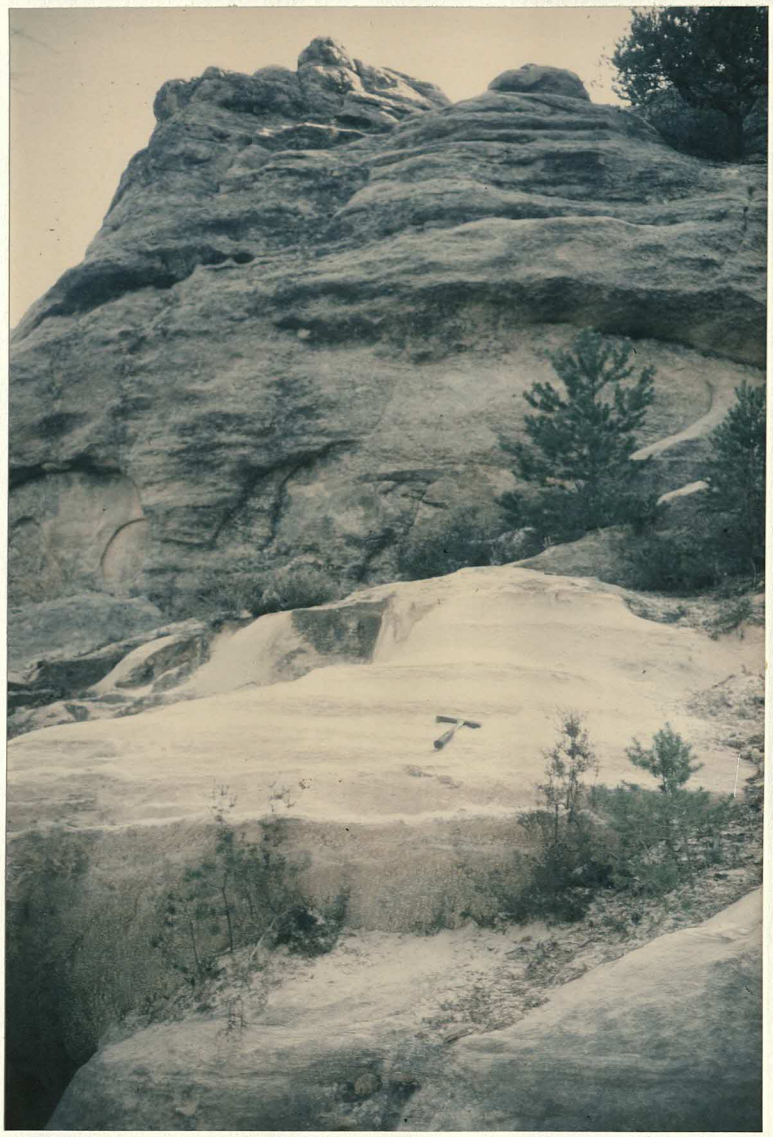

Fig 2.28. Yellow biomicrites forming 5-20cm beds. This is the entire thickness of carbonate preserved in the Talveila Formation at this locality, (and even here is only preserved on the E side of the anticline). Top of Talveila Formation. Hortezuelos.

Fig 2.29. View of Talveila Formation section at Hortezuelos showing thick cross-bedded arenites (lower part of sequence) overlain by yellow limestones (forming prominent horizon marking upper part of sequence; as in fig 2.28).

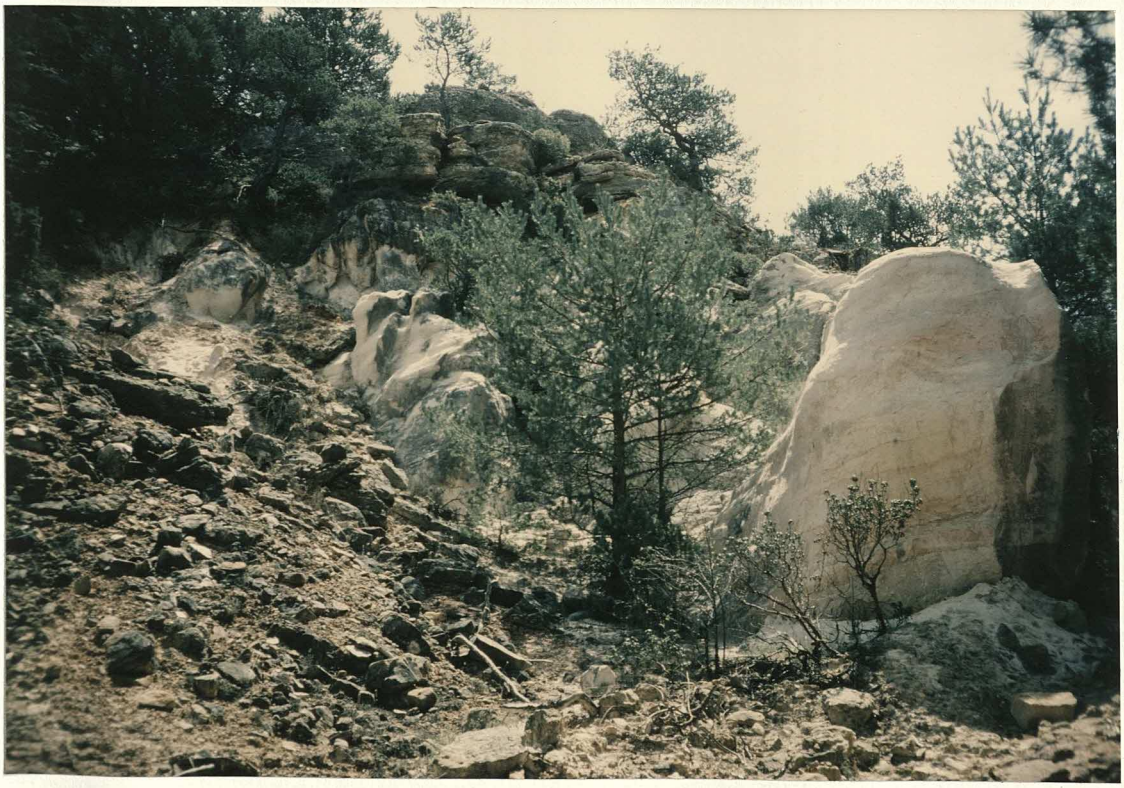

Fig 2.30. Breccia developed on karst surface of upper Talveila Formation limestones. Near vertical beds - younging to left. Red sand containing numerous irregular clasts of yellow limestone (left of hammer) derived locally from brecciated yellow limestone (right of hammer). Breccia apparently present below upper surface of limestone (horizon marked by position of notebook). Red sands above (extreme left contains fewer clasts of yellow limestone. Basal contact of Senora de Brezales Formation. Looking ESE. 1km SE of Pinilla de los Barruecos.

Fig 2.31. Breccia developed on karst surface of upper Talveila Formation limestone. Near vertical beds - younging to left. Brecciated top of yellow limestone (upper centre) overlain by red sand with abundant angular and locally-derived clasts of yellow limestone. Gritty lag (left of lens cap). Basal contact of Senora de Brezales Formation. Looking ESE. 1km SE of Pinilla de los Barruecos.

Fig 2.32. Ferruginous crust marking contact between yellow arenites of lower Talveila Formation and red sands of basal Senora de Brezales Formation. Coarse conglomerates 3m above at this locality (out of picture). 2km SE of Aldea del Pinar, near Hontoria del Pinar.

Fig 2.33. Stratigraphy of continental sequence, Sanchez Lozano (1894).

Fig 2.34. Stratigraphy of continental sequence, Saenz Garcia (1932).

<table>
<tr><th>R. SANCHEZ-LOZANO (1894)</th><th>C. SAENZ-GARCIA (1932)</th><th colspan="2">BEUTHER-TISCHER (1966)</th></tr>
<tr><td colspan="4">CENOMANIENSE MARINO</td></tr>
<tr><td>Arcosas lignitíferas</td><td>V</td><td colspan="2">Utrillas</td></tr>
<tr><td>Grupo detrítico denominado : "Urgo - Aptiense"</td><td>IV</td><td rowspan="3">Grupos Tera... Olivan</td><td rowspan="3">"wealdiense"</td></tr>
<tr><td>Grupos E D C "weald"</td><td>III II</td></tr>
<tr><td>Grupos B A "Purbeck"</td><td>I</td></tr>
<tr><td colspan="4">JURASICO MARINO</td></tr>
</table>

modified after Salomon (1982)

Fig 2.35. Stratigraphy of continental sequence, Beuther (1966) and Tischer (1966). This scheme formed the basis for the subdivisions used on the 1:50 000 and 1:200 000 IGME geological maps.

Fig 2.36. Stratigraphy of the continental sequence. Salomon (1982).

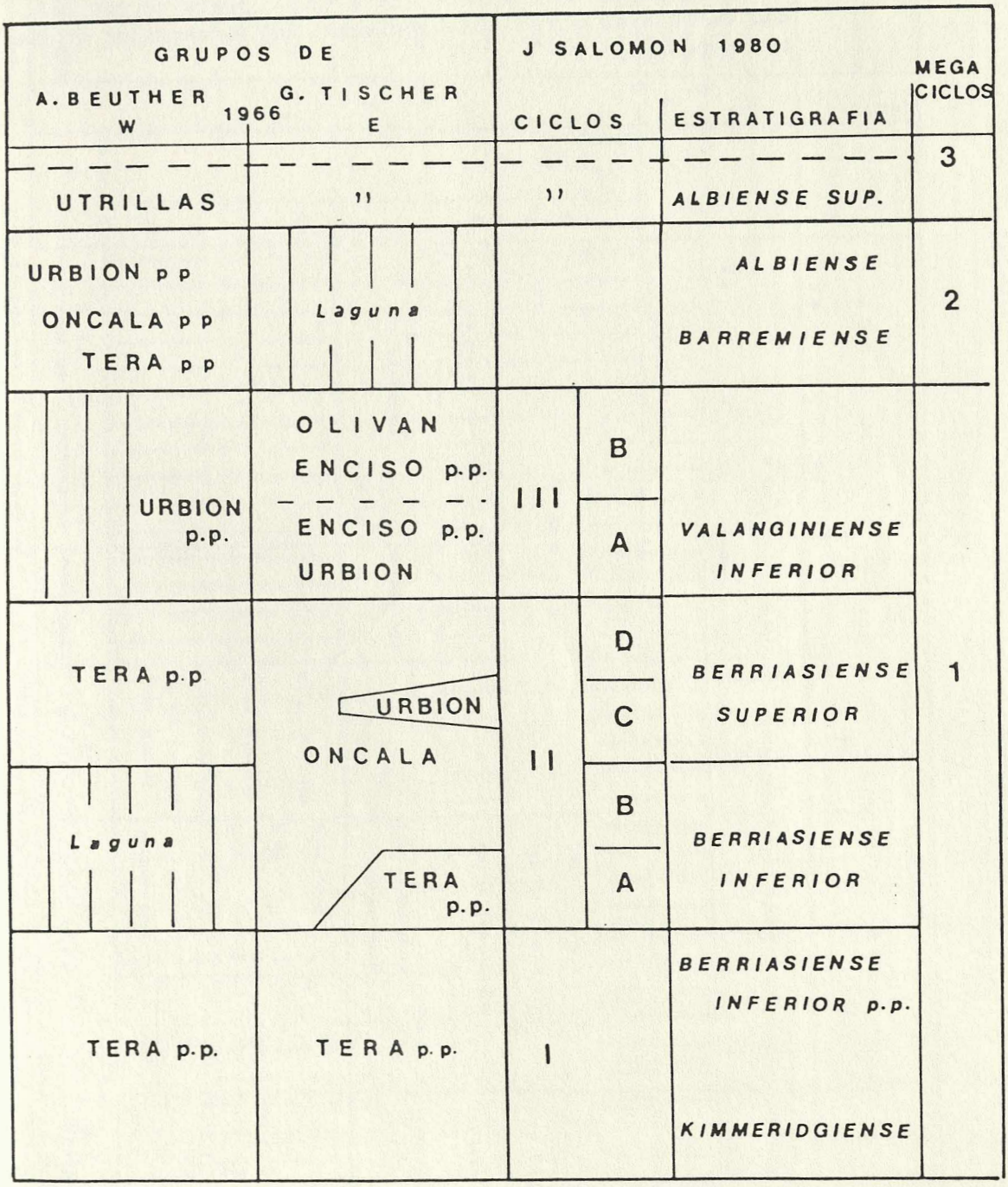

Salomon (1982)

Fig 2.37. Stratigraphy of the continental sequence (Salomon, 1982), showing Groups defined for the E and W parts of the Basin and indicating correlation between the successions of the two zones.

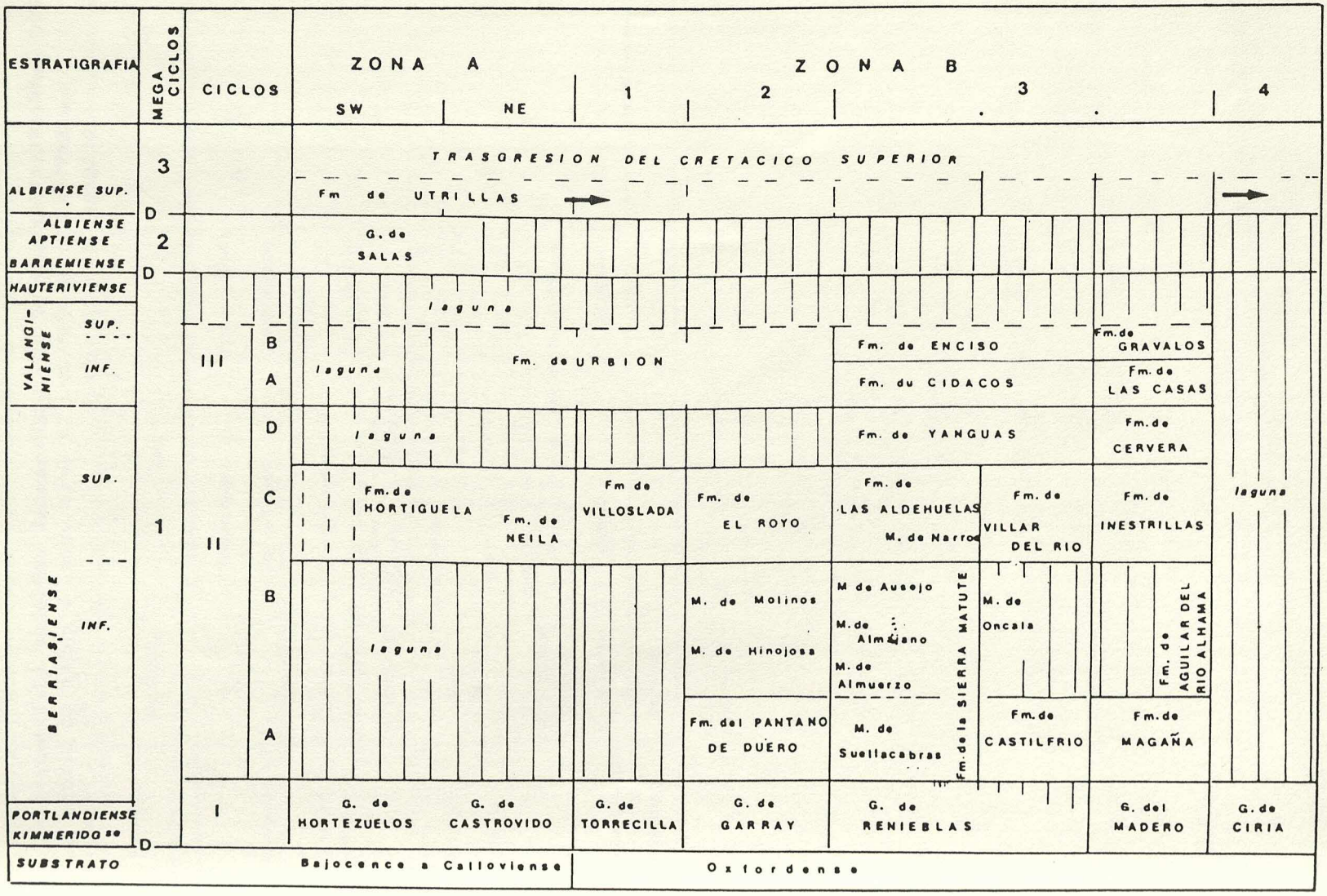

Salomon (1982)

Fig 2.38. Stratigraphy of the continental sequence (Salomon, 1983). Revised nomenclature. In this work, I refer to Salomon's original (1982) scheme.

Groupe 1 : Kimméridgien - Valanginien ;
Groupe 2 : Barrémien - Albien ;
Groupe 3 : Albien supérieur..

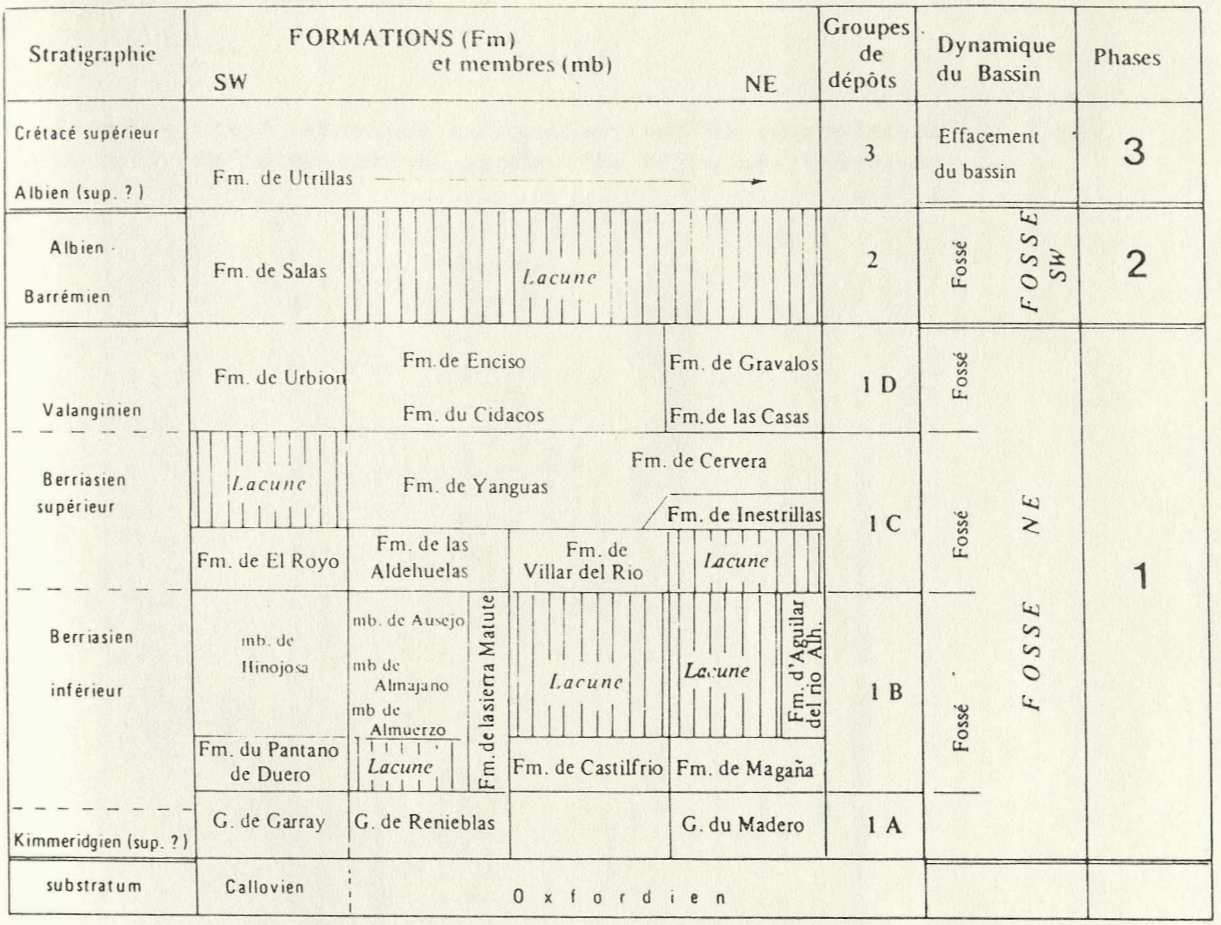

Fig 2.39. Stratigraphy of the continental sequence. Correlation of newly-defined units with those of Salomon (1982; figs 2.36 & 2.37).

UPPER JURASSIC - LOWER CRETACEOUS: CORRELATION WITH PREVIOUSLY DEFINED STRATIGRAPHIC UNITS

AGE	SALOMON (1982)	SALOMON (1982) ALONSO et al (1982)	PLATT (1986)
Lower Cenomanian Upper Albian	Group V	Utrillas Fm (Tejada Mb)	Utrillas Fm (Tejada Mb)
?Aptian Barremian	Group IV	Salas Group	Salas Group
Lower Valanginian Upper Berriasian	Group IIC	Neila Fm Hortigüela Fm	Pedroso Gp) Piedrahita de Muno Fm) Hortigüela Fm
Lower Berriasian Kimmeridgian	Group I	Castrovido Gp = Hortezuelos Gp	Tierra de Lara Gp) Rupelo Fm) Senora de Brezales Fm
Lower Kimmeridgian Upper Oxfordian	"Jurassique détritique"		Talveila Fm

PLATT N (1986)

Fig 2.40. Revised detailed lithostratigraphy of the Late Jurassic - Early Cretaceous continental sequence in the W Cameros Basin, showing likely correlation with the sequence in SW Cantabria (Aguilar del Campoo area).

STRATIGRAPHY OF THE "PURBECK" / "WEALDEN" SEQUENCE OF THE W CAMEROS & SW CANTABRIA.

W CAMEROS							SW CANTABRIA		
PEDROSO GROUP	~ 40m HORTIGUELA FM	ZURRAMUJERES MB	oncoidal limestones	clastics	TERRAZAS MB up to 2000m+	PIEDRAHITA DE MUNO FM	sandstones & oncoidal lsts	UPPER	CORVIO & EMBALSE DE PISUERGA MBS
			----------black limestones---------						
	~ 20m	SAN MARTIN MB	marls	clastics	VIZCAINOS MB ~200m ?				
----------desiccation-cracked surface----------							----------		
	0-20m	RIO CABRERA MEMBER	red ostracod lst chert yellow/vuggy lsts				chert	UPPER-MIDDLE	LOMILLA
			----------				----------		
	0-90m	MAMBRILLAS DE LARA MB	Dinosaur Bed dark biomicrites & charophyte marls				fossiliferous	MIDDLE	AGUILAR SUP.
TIERRA DE LARA GROUP	RUPELO FM	----------Torrelara Bed----------							
		--------brecciated surface----------					----------		
	0.5-70m	LADERA MB	white lsts (brecc/pelleted) mottled lsts	red marls	LAS VINAS MB 0-40m		microkarst mottled	LOWER	AGUILAR INF.
----------laminated limestone----------							----------		
	SENORA DE BREZALES FM 2-70m		crusts polygenetic cgl red sands				crusts polygenetic cgl	BASAL	VILLAESPINOSO
----------karstic surface / Fe crust----------							----------		
	TALVEILA FM 0-75m		lsts with corals ssts/yellow calclithites						MISSING
----------karst / erosive surface----------									
			MARINE JURASSIC					MARINE JURASSIC	

Fig 2.41. Brecciated surface marking the top of the Ladera Member. Large black chert pebble to left of hammer. Angular limestone clasts in surface. The blocks have clearly not been significantly transported - brecciation more or less in situ, probably as a result of emergence. At Ladera, the clasts forming this surface are "calcretised" - they show strong pedogenic overprint. Example shown here from 1km N of Torrelara.

Fig 2.42. Cracked surface at top of Rupelo Formation. Note polygonal pattern of dominantly straight cracks, angular termination - permits interpretation as subaerial desiccation features and distinction from subaqueous synaeresis cracks. Host carbonate is very white, slightly marly micrite, rarely fossiliferous. Occurs 2m above "Dinosaur Bed" of Mambrillas de Lara Member. Top of Rio Cabrera Member (yellow limestones and cherts not found at this locality). Mambrillas de Lara.

Fig 2.43. Cracked surface at top of Rupelo Formation. Straight cracks with angular terminations developed in white, marly micrite. Top of Rio Cabrera Member. 1km S of Rupelo.

Fig 2.44. Stratigraphy of the continental sequence according to Gil Serrano & Zubieta (1978). Note highly diachronous nature of the units. See critical discussion in text.

ESQUEMA DE CORRELACCION DE LAS FACIES CONTINENTALES

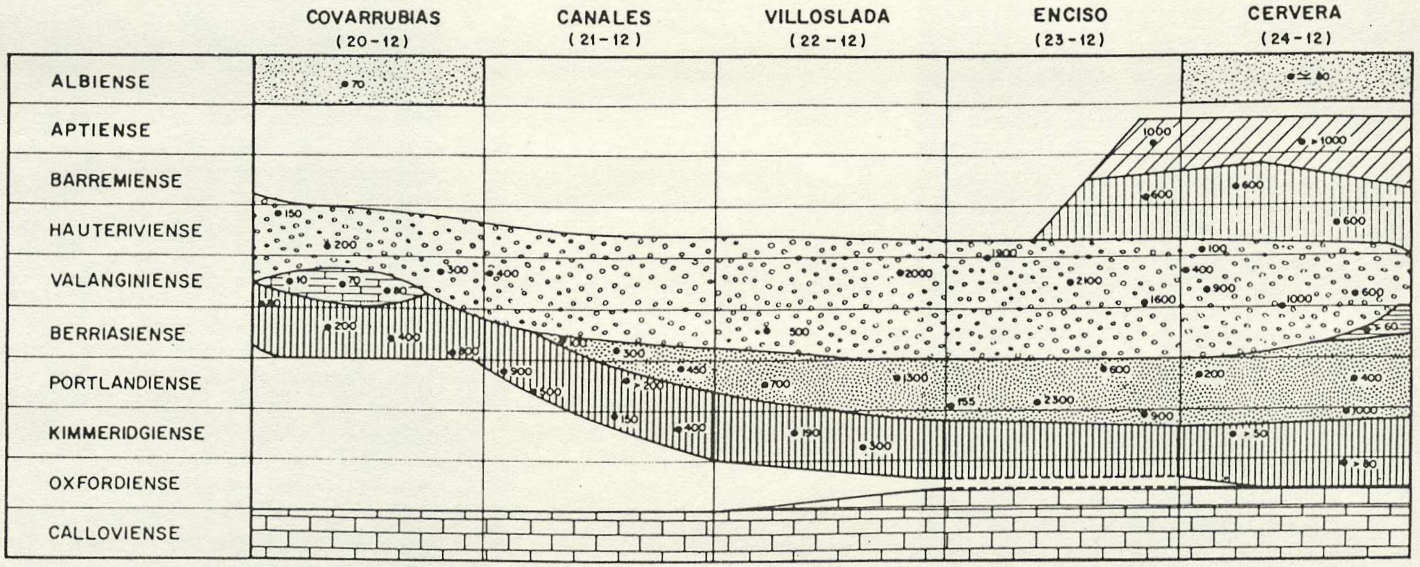

UTRILLAS
OLIVAN
ENCISO
URBION
CABRETON

ONCALA
CALIZAS PISOLITICAS
TERA
JURASICO MARINO

CONTACTO ENTRE FORMACIONES O GRUPOS
CONTACTO ENTRE FORMACIONES O GRUPOS NO AFLORANTES
POTENCIA EN METROS

Fig 2.45. Upper Cretaceous sequence. Road lies on Lower Cretaceous clastics, probably Salas Group. Utrillas sands, base of slope (exposing, centre). Santa Maria de las Hoyas Formation marls (Upper Cenomanian) above, not exposing. Marls of Picofrentes Formation (Lower Turonian), also not exposing. Prominent bed at base of limestone marl alternations is probably glauconitic sandstone reported at top of marl sequence by Faulkner (1985) - ?equivalent to Santa Cruz del Tozo Formation of SW Cantabria. Thinly-bedded limestone-marl alternations are assigned to the Munecas Formation (bioclastic limestones; Upper Turonian - Lower Coniacian). Just beneath scarp crest, poorly exposing interval represents massive limestone mudstones of Hortezuelos Formation (Coniacian). Massive carbonates forming scarp are rudistid and foraminiferal limestones of Hontoria del Pinar Formation (Lower Santonian). Upper parts of sequence not visible - (?Santo Domingo de Silos Formation and) Santibanez del Val Formation probably absent here - apparently significant truncation below OligoMiocene at this locality. Barbadillo del Mercado. Looking W.

Fig 2.46. Upper Cretaceous sequence. Upper Cenomanian and Lower Cenomanian marl is covered by scree of Upper Turonian limestone. Basal sandstone and limestone of Upper Turonian forms prominent bands. Well-bedded Munecas Formation (Upper Turonian). Limestone mudstones of Hortezuelos Formation above thick conifers (upper left). Crest of hill formed by resistant rudistid and foraminiferal limestones of Hontoria del Pinar Formation (Lower Santonian). El Molar, near Mambrillas de Lara.

Fig 2.47. Upper Cretaceous stratigraphy. From Alonso et al (1982).

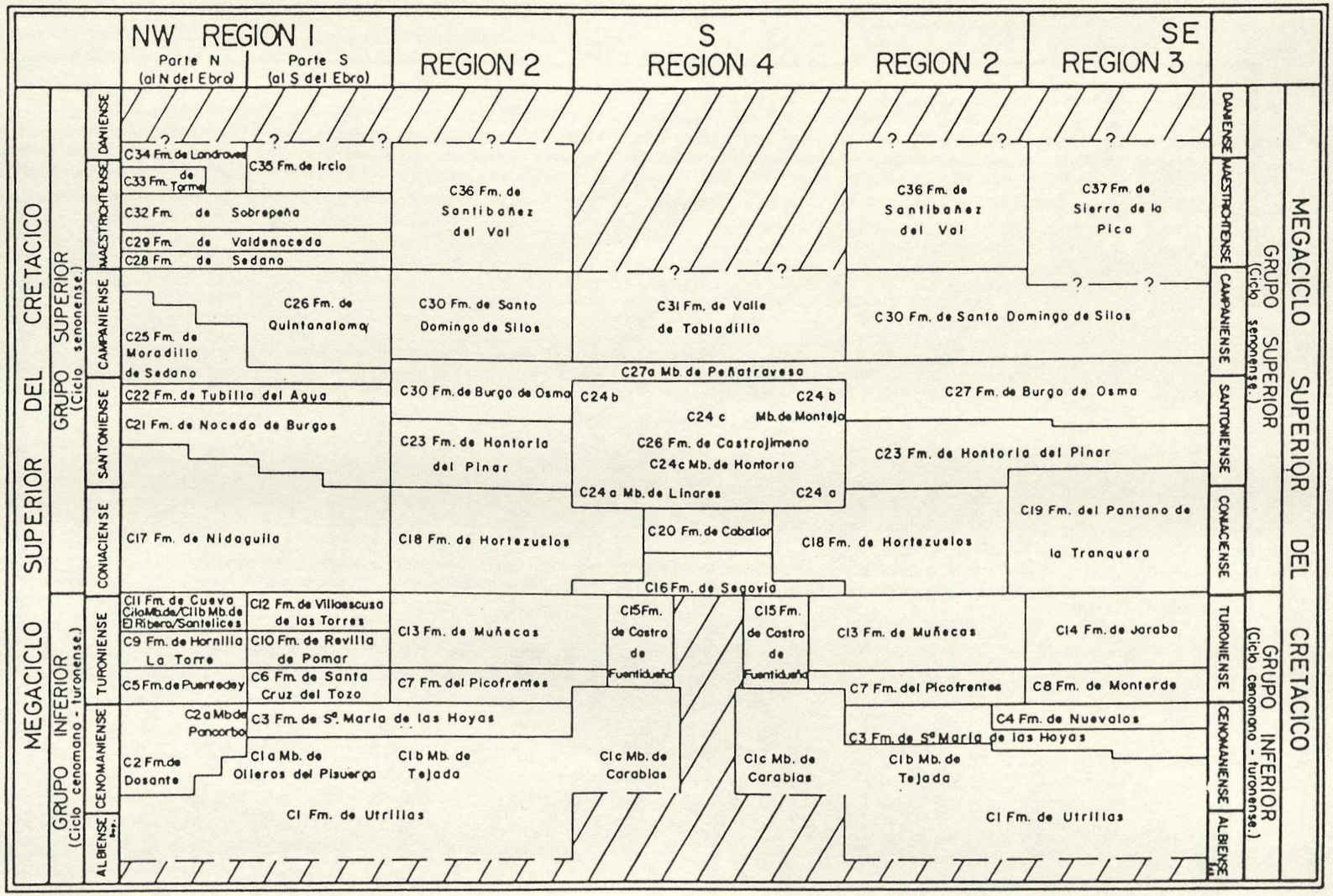

Alonso et al (1982)

Fig 2.48. Map showing location of areas defined for fig 2.47.

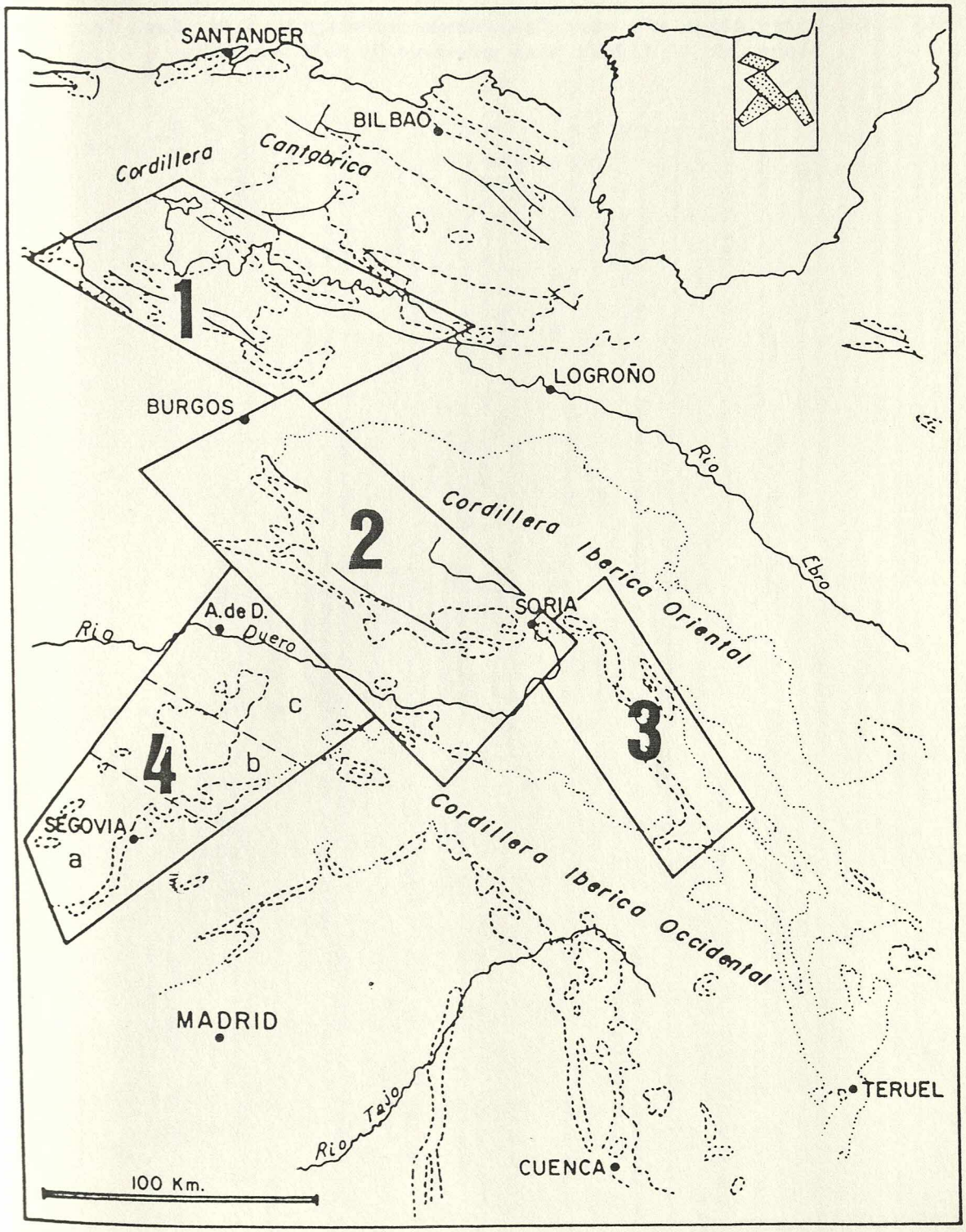

Alonso et al (1982)

Fig 2.49. Correlation of Upper Cretaceous stratigraphy as given in Alonso et al (1982) with previously defined units.

UPPER CRETACEOUS STRATIGRAPHY - CORRELATION CHART OF PREVIOUS WORKS.

VALLADARES(1976)	VALLADARES (1976)		FLOQUET (1979)	AGE	FLOQUET et al (1982)
f. de oncolitos y algas f. de intraclastos y fosiles	IV areniscas, arcillas y calizas			Palaeocene Maastrichtian	Santibanez del Val
f. de mudstones f. de dolomias f. de calizas cristalinas	III carniolas y calizas dolomiticas			Campanian	Santo Domingo de Silos
f. de rudistas		c) calizas bioclasticas construidos por rudistas			Burgo de Osma
f. de wackestones de foram. f. de calizas de equinidos f. de wackestones de moluscos f. de oolitos f. de calizas bioclasticas, stromatoliticas f. de ostracodos y serpulitos	II calizas bioclasticas y calizas masivas	b) calizas biogenicas construidos por ostreidos a) calizas bioclasticas oolitos stromatolitos	D) calcaires fins mal stratifiés C) calcaires variés	Campanian - Coniacian Coniacian - Turonian	Hontoria del Pinar Hortezuelos Munecas
f. de calizas mudstones f. de calizas glauconiticas y fosilifaras	I alternancia de margas y calizas	alternancia de margas con calizas arenosas o glauconiticas.	B) ensemble marneux fosilifère	Lower Turonian -	Picofrentes
					Sa Cruz del Tozo
f. de margas		arcillas grisas muy oscuro	A) argillo-calcaire 1) marnocalcaire 2) argilleuse	Upper Cenomanian	Sa Maria de las Hoyas
Utrillas	Utrillas		Utrillas	Lower Cenomanian Upper Albian -	Tejada

PLATT N (1986)

Fig 2.50. Correlation of Upper Cretaceous sequence of W Cameros (data from Alonso et al, 1982) with the Upper Cretaceous sequence of S England (as given by Anderton et al, 1979).

UPPER CRETACEOUS STRATIGRAPHY - CORRELATION CHART OF PREVIOUS WORKS.

FLOQUET et al (1982) ALONSO et al (in press)	FAULKNER (1985)	VAUGHAN (1986)	S ENGLAND EQUIVALENT (ANDERTON et al, 1979)	AGE
Santibanez del Val		Santibanez del Val Fm	Maastrichtian - ~~ Danian Chalks ~~	Palaeocene Maastrichtian
Santo Domingo de Silos		Santo Domingo de Silos Fm		Campanian
Burgo de Osma			Upper Chalk	
Hontoria del Pinar Hortezuelos	massive mudst lst bedded mudst lsts	Yecla Group		Campanian - Coniacian
Munecas	oolitic lsts bioclastic lsts lst	Munecas Fm	Chalk Rock	Coniacian - Turonian
Picofrentes		Picofrentes Fm	Middle Chalk	Lower Turonian
Sa Cruz del Tozo	glauconitic sst		Melbourn Rock	
Sa Maria de las Hoyas	marls	Santa Maria de las Hoyas Fm	Lower Chalk - Plenus Marls - Grey Chalk & - Chalk Marl	Upper Cenomanian
Tejada	sands	Tejada Fm	Glauconitic Marl	Lower Cenomanian
			U Greensand	Upper Albian

hardground ------- non sequence / unconformity.

PLATT N (1986)

Fig 2.51. Upper Cretaceous sequence. Cornfield, foreground, is developed on Utrillas sands (Upper Albian - Lower Cenomanian). Break of slope (darker brown field, right) occurs at Santa Maria de las Hoyas Formation "oyster bed". Line of dark green scrub at top of darker brown field marks outcrop of fossiliferous marls rich in echinoids and ammonites (Picofrentes Formation, Lower Turonian). Upper Turonian - Lower Santonian sequence above, as figs 2.45 & 2.46. Mountain on right is La Muela, to left is El Molar ("the tooth"). Mazariegos, 3km SE of Cuevas de San Clemente.

Fig 2.52. "Oyster Bed". Abundant encrusting oysters (Ostrea). Brown (?ferruginous) matrix - possibly indicating slow sedimentation. Scale bar is 15cm long. Base of Santa Maria de las Hoyas Formation. Upper Cenomanian. Penacoba.

Fig 2.53. Upper Cretaceous sequence. Upper Cenomanian and Lower Turonian marls covered by scree. Sandstone forms prominent band below well-bedded bioclastic limestones and intercalated marls of Upper Turonian Munecas Formation. Conifers growing on scree slope developed on mudstone limestones of Hortezuelos Formation. Hill top consists of massive rudistid and foraminiferal limestones of Hontoria del Pinar Formation (Lower Santonian). La Muela (Mambla), near Mambrillas de Lara. Looking W. (Mountain takes its name from evocative morphology).

Fig 2.54. Micrograph sketch of glauconitic sandstone. From Faulkner (1985). Field of view: 9mm. Base of Upper Turonian (Munecas Formation, facies cf Santa Cruz del Tozo Formation?). Penalara, near Quintanilla de las Vinas.

Fig 2.55. Micrograph sketch of bioclastic limestone. From Faulkner (1985). Field of view: 9mm. Munecas Formation (Upper Turonian). Penalara, near Quintanilla de las Vinas.

Fig 2.56. Micrograph sketch of oolitic limestone. From Faulkner (1985). Near top of Munecas Formation (Upper Turonian). Penalara, near Quintanilla de las Vinas.

Glauconitic sandstone.

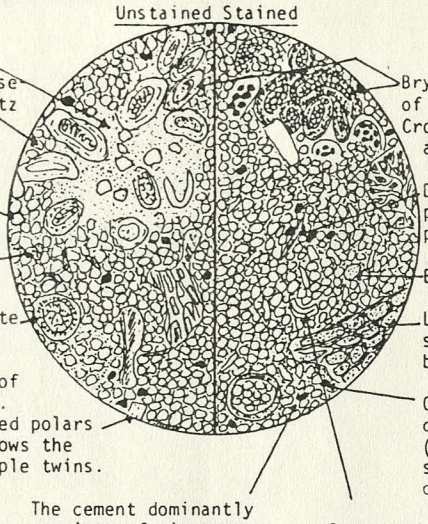

The cement dominantly consists of microspar in between the quartz grains. However the larger voids, such as within the bryzoan calcite case are filled with a blue ferroan calcite.

Scattered throughout the section are small rounded bio-clasts of brachiopods and possibly some molluscs as well.

Bioclastic Limestone.

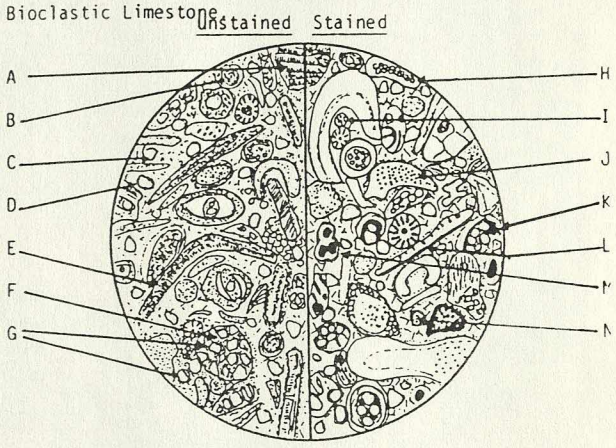

A) Broken piece of coral.

B) Structureless grain of micrite.

C) Angular quartz grains

D) Small moderate relief mineral with yellow pleochroism possibly a detrital grain of tourmaline.

E) Rounded grains of mollusc shells- these shells generally have several layers of internal structure.

F) Bryzoan fragments- internally layered honey comb structure. Occasionally the pores of the bryzoan are filled with glauconite.

G) Glauconite- small rounded grains.

H) Sparite clasts- coarse blocky sparite surrounded with micrite envelope.

I) Echinoderm spines.

J) Echinoderm fragments; some of these fragments show syntaxial growth. There is one unusual clast which displays twinning within one fragment of an echinoderm.

K) Rock fragments- clasts of quartz, glauconite, coarse micrite bounded by an opaque. These clasts were possibly derived from the rock below.

L) Rounded grains of brachiopod shells- some of these shells are pseudopunctate.

M) Foraminifera- multiocular foraminifera.

N) Occasional pieces of chert are present.

Oolitic Limestone.

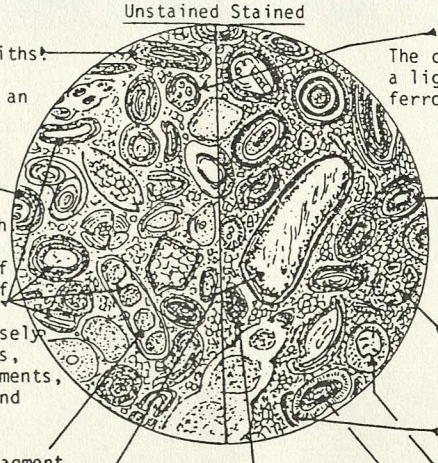

Fig 2.57. Domal stromatolite from the Munecas Formation (Upper Turonian). Scale bar is 15cm long. Penacoba.

Fig 2.58. Exposure of sandstones and silty clays of the fluvial units of the Santibanez del Val Formation. Beds overturned - younging to right. Prominent beds are tabular sandstones (?local very weak channelling), interbedded mottled silty clays and nodular white carbonates with prismatic texture. Interpretation: Fluvial sandbodies are probably crevasse-splays encroaching over fine grained overbank deposits. Interchannel areas intermittently submerged shallow, temporary carbonate-producing lakes. Strong pedogenesis: overbank silts mottling, development of carbonate nodules; carbonates prismatic texture. Base of SVF^{C}. La Yecla, near Santo Domingo de Silos. Looking W.

Fig 2.59. Facies sequences of the Santibanez del Val Formation. After Vaughan (1986).

STRATIGRAPHY AND FACIES OF THE SANTIBANEZ DEL VAL FORMATION.

NAME OF SUBDIVISION	LITHOLOGIES	INTERPRETATION
SVF^e	Sandstones and silty clays - unexposed	Fluvial channel and overbank deposits
SVF^d	Mudstone-limestones with desiccation brecciation and gastropods	Palustrine deposits
SVF^c	Sandstones and silty clays - mainly unexposed except at the base	Fluvial channel and overbank deposits
SVF^b	Mudstone-limestones with desiccation brecciation, root-traces, and red micrite intraclasts	Palustrine deposits
SVF^a	Sandstones and silty clays - mainly unexposed. ? gradational contact with underlying Santo Domingo de Silos Fm	Fluvial channel and overbank deposits

Data from Vaughan (1986) after Floquet et al, (1985).

Fig 2.60. Thick conglomerate sequence showing dip (possibly partly depositional - large scale accretion surfaces of alluvial fans) to left. Note extremely coarse clasts of Upper Cretaceous limestone (left) - up to 1m. OligoMiocene. 2km E of Covarrubias. (Cave upper left - Covarrubias derives its name from the many, often formerly inhabited, caves in OligoMiocene clastics: "cueva" = cave, rubias" = red).

Fig 2.61. Coarse, immature, polymict conglomerate with numerous poorly-sorted and irregular angular clasts of Upper Cretaceous limestone. Rare quartz pebbles. Some clasts of yellow limestone - probably derived from Marine Jurassic sequence.
Interpretation: Erosion of entire Mesozoic sequence.
OligoMiocene, La Hinojosa.

Fig 2.62. Sands with few, scattered, clasts of Upper Cretaceous limestone.
Interpretation: Sediment sourced dominantly from recycling of subjacent molasse - limited erosion of Upper Cretaceous only.
Miocene. La Hinojosa.

Fig 2.63. Red, weakly laminated sands.
Interpretation: Maturity and absence of coarse clasts may indicate less active erosion.
Miocene. La Hinojosa.

Fig 2.64. Regional distribution of Miocene facies. From IGME (1970).

Esquema de distribución de facies del Mioceno, Hoja n.º 20 a escala 1:200.000 con la división en Hojas escala 1:50.000 (según informe de AEROSERVICE).

Fig 2.65. Lithostratigraphic units of the Tertiary sequence, W Burgos. Pol (1985).

TERTIARY LITHOSTRATIGRAPHIC UNITS (POL, 1985): Palaeogeographies

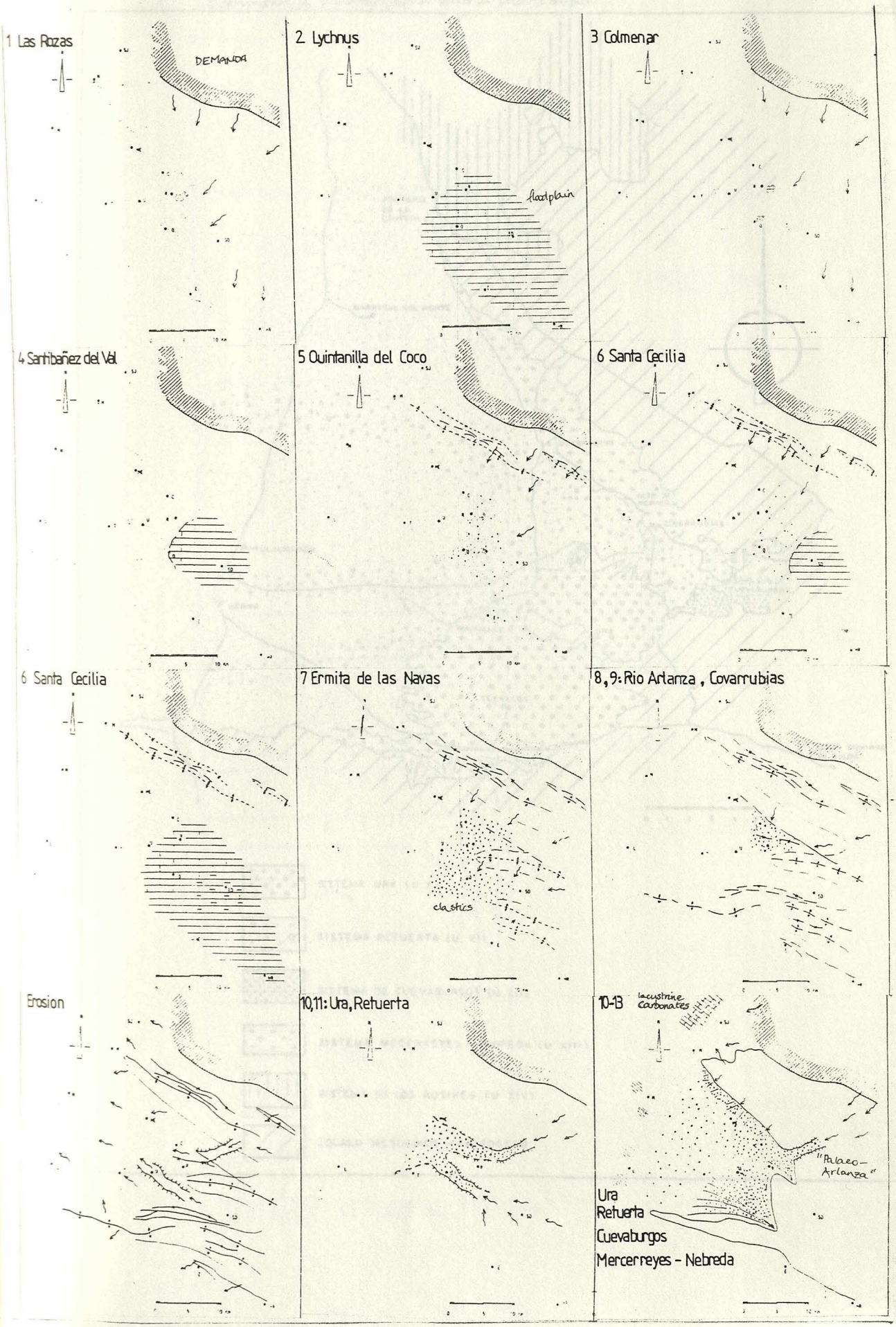

Distribution of lithostratigraphic units on present surface

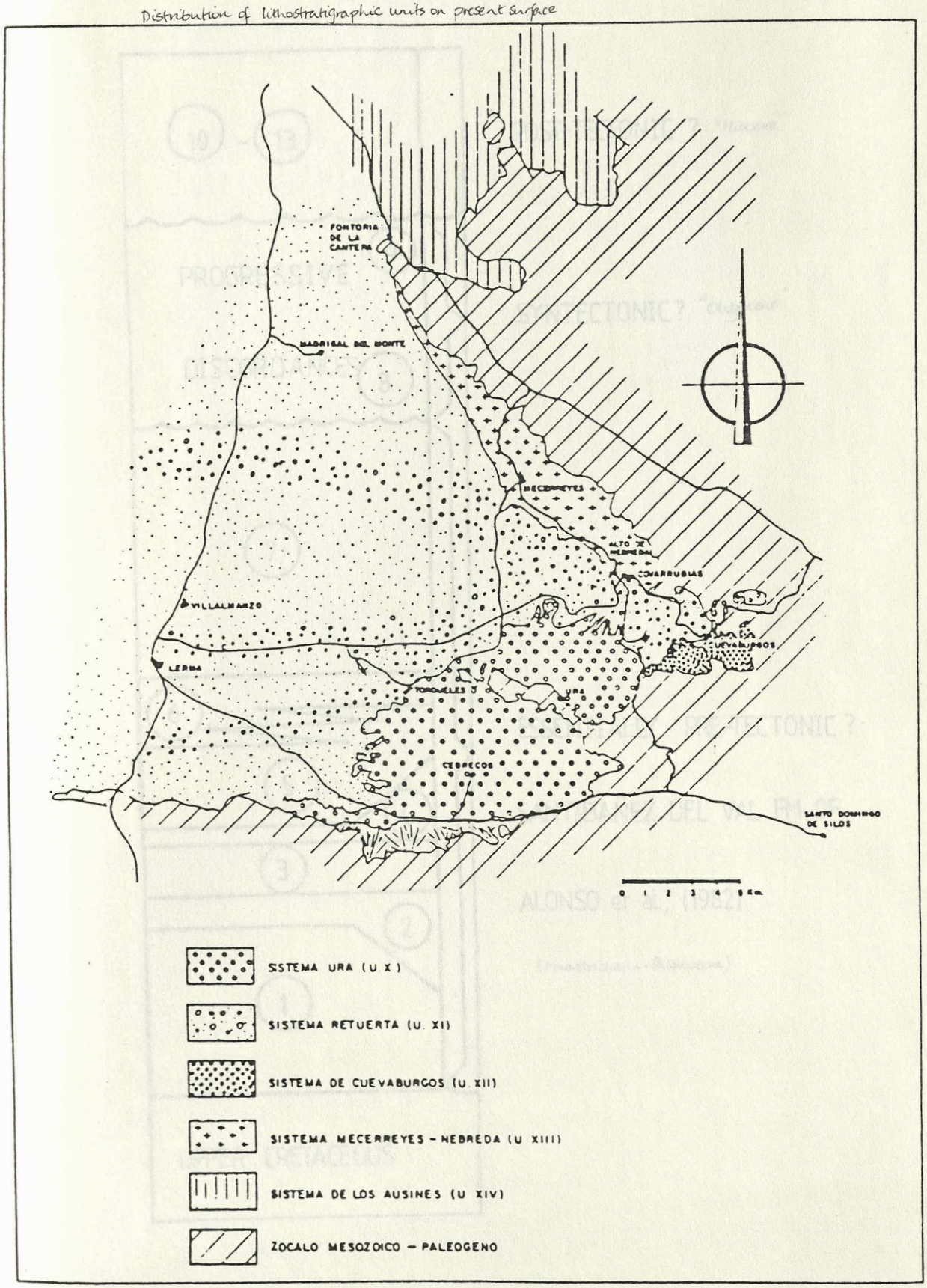

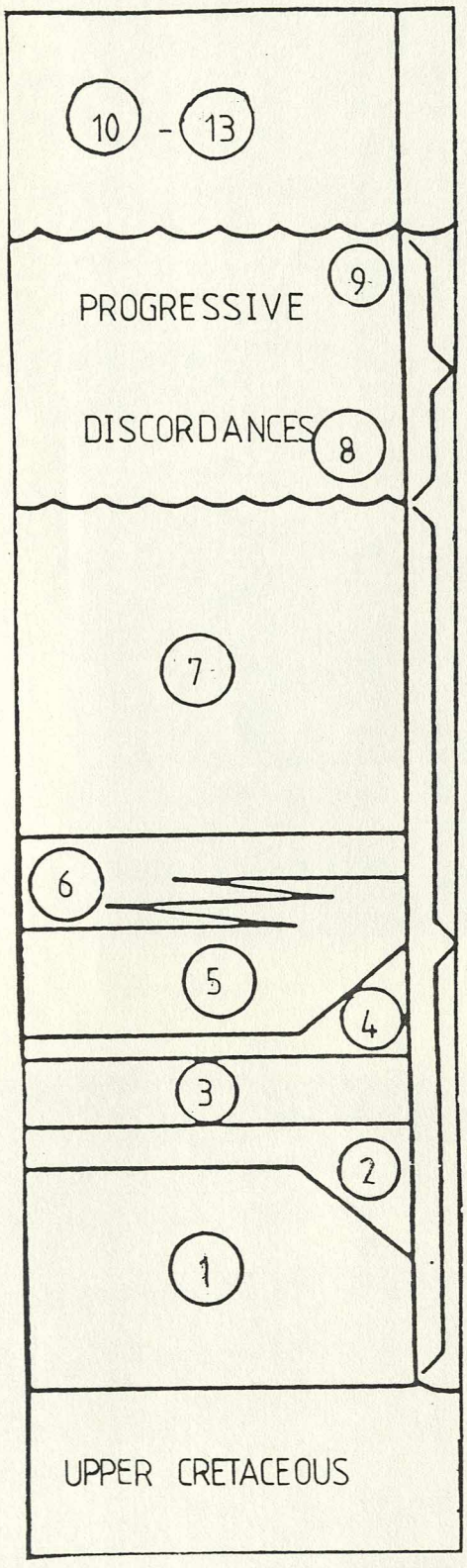

TERTIARY LITHOSTRATIGRAPHY

after Pol (1985)

Fig 3.1. Typically homogeneous red sands, Senora de Brezales Formation. Senora de Brezales, 3km N of Espejon.

Fig 3.2. Senora de Brezales Formation red sands exhibiting trough cross-bedding. Looking E. El Cangrejo, 3km N of Huerta del Rey.

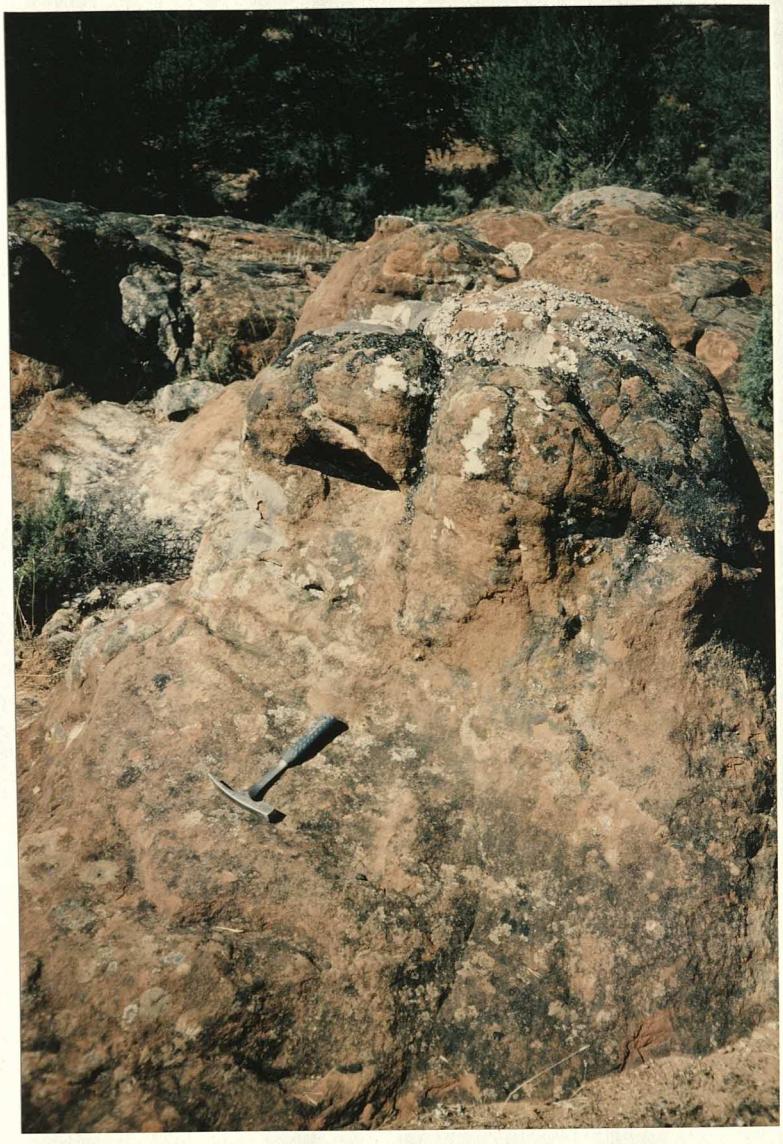

Fig 3.3. Close-up view of the right-hand side of outcrop shown in fig 3.2. Looking E.

Fig 3.4. Red sands, Senora de Brezales Fm, exhibiting erosive bases, thin pebbly lags, trough cross-bedding and progressive homogenisation. Looking NW at El Cangrejo.

Fig 3.5. Plane-laminated Senora de Brezales Fm red sands. Ladera, near Mamolar.

Fig 3.6. Red sands, Senora de Brezales Fm, exhibiting small burrows. El Cangrejo.

Fig 3.7. Red sands, Senora de Brezales Fm, exhibiting well-defined white mottling, possibly the product of bioturbation (roots and/or sand-dwelling burrowers). Ladera, near Mamolar.

Fig 3.8. Mottled profile of red sands truncated by erosive-based coarser grit unit, Senora de Brezales Fm. Ladera, near Mamolar.

Fig 3.9. Red sands in truncated profile exhibiting tubular (root?) mottles and fine angular (desiccation or root hair?) cracks, Senora de Brezales Fm. Senora de Brezales.

Fig 3.10. Red sands, showing rounded mounds and depressions (bush/tree stumps?), Senora de Brezales Fm. El Cangrejo.

Fig 3.11. Homogeneous red sands and tubular carbonate structure (left of lens cap) - probably a petrified root. Senora de Brezales Fm. Castrovido.

Fig 3.12. Red sands exhibiting abundant angular cracks, Senora de Brezales Fm. 2km NW of La Gallega.

Fig 3.13. Red sands, showing well-developed horizontal and vertical angular (?desiccation) cracks. Profile truncated by erosive base of conglomerate unit. Conglomerate contains clasts of grey micritic limestone and of laminated limestone "crusts". See discussion of conglomerate clast derivation (Chapter 8). Senora de Brezales Fm. Hortezuelos.

Fig 3.14. Heavily mottled impure carbonate. Fabric shows weakly developed horizontal and vertical elements. Truncation by erosive, channelled base of sandstone unit which faintly show trough cross-bedding towards top. Senora de Brezales Fm. Senora de Brezales.

Fig 3.15. Structureless red sandstones overlain by weakly nodular impure limestone with abundant fine carbonate strings (root hairs or desiccation features). Limestone is heavily brecciated above hammer. Senora de Brezales Fm. Ladera, near Mamolar.

Fig 3.16. Close-up view of limestone shown in fig 3.15; fabric showing well-developed horizontal elements - thicker root "crusts". Senora de Brezales Fm. Ladera, near Mamolar.

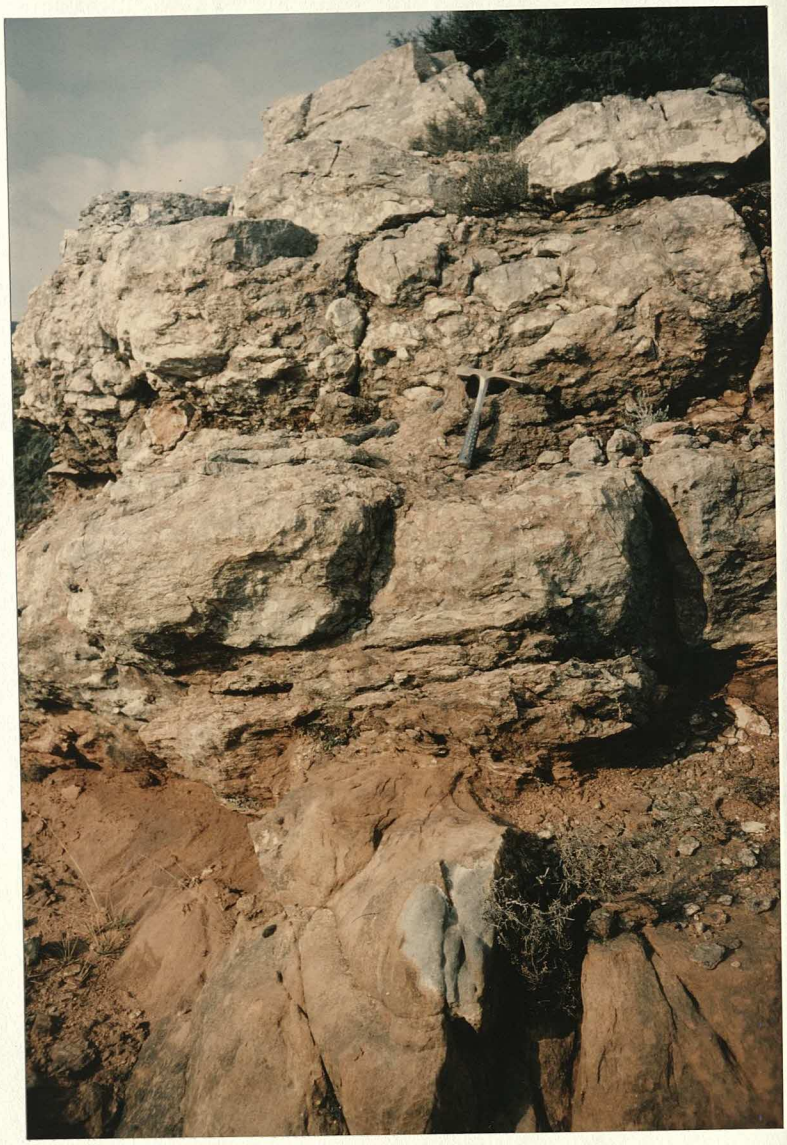

Fig 3.17. Profile from bedded, ?rippled, red sandstone with upward-increasing carbonate content (desiccating hardpan) into grey carbonate (?temporary lake) into heavily mottled and eventually brecciated rubbly limestone (palaeosoil). Senora de Brezales Fm. Ladera, near Mamolar.

Fig 3.18. Fine red sandstone with angular (desiccation) cracks and cm-scale carbonate nodules ("cornstones"). Old Red Sandstone, Freshwater East, U.K..

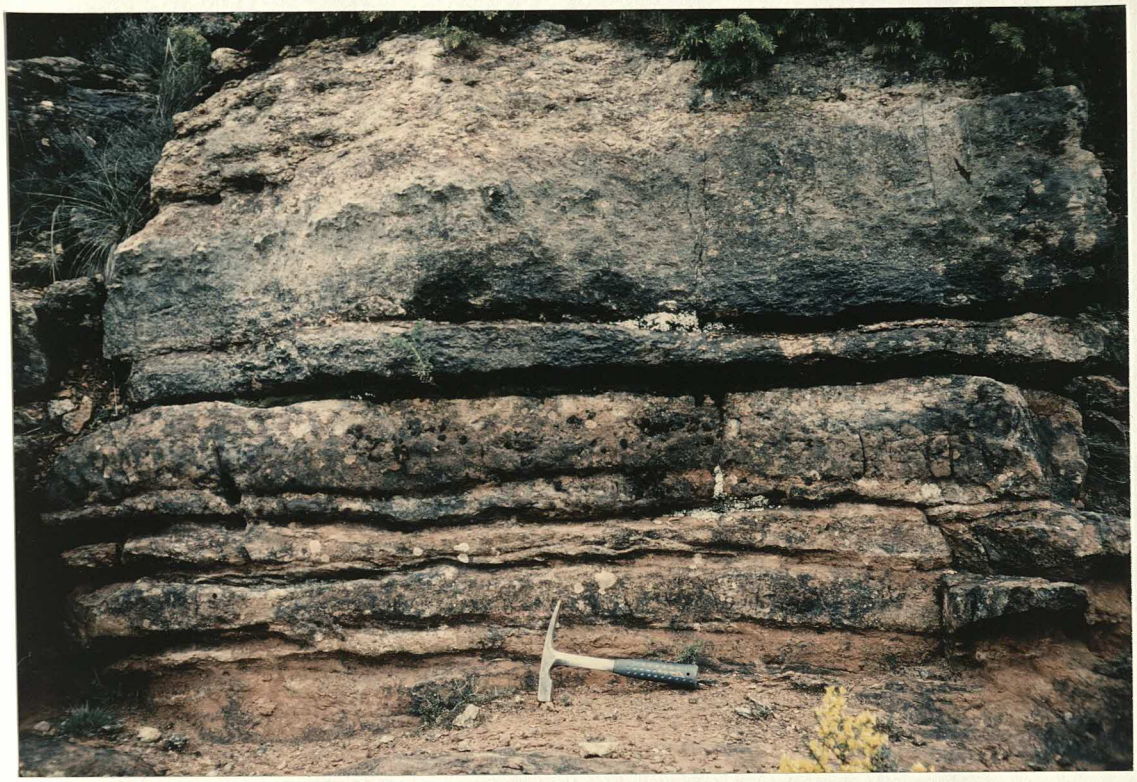

Fig 3.19. Fine red sands with abundant carbonate nodules, truncated by laminated sands. Old Red Sandstone. Freshwater East, U.K..

Fig 3.20. Conglomerate channels (just above track, lower centre). Senora de Brezales Fm. Espejon, looking E. Limestones in foreground belong to marine Jurassic. Rupelo Formation limestone forming ridge above channels, bedding near vertical. Village and cornfields lie on Utrillas (Upper Albian - Lower Cenomanian) sands. Mountain behind village consists of Upper Cretaceous limestones.

Fig 3.21. Closer view of channels shown in fig 3.20. Utrillas (cornfields) and Upper Cretaceous limestones (mountain) behind. Looking S.

Fig 3.22. Close-up view of channel shown in figs 3.20 & 3.21. Channel displays erosive base to left and fining upwards. Point bar deposits of trough cross-bedded sandstone in foreground. Channel cut into poorly-exposing palaeosoil (see fig 3.39). Looking SE.

Fig 3.23. Interpretative sketches of Senora de Brezales Fm palaeochannels shown in figs 3.20 - 3.22, Espejon.

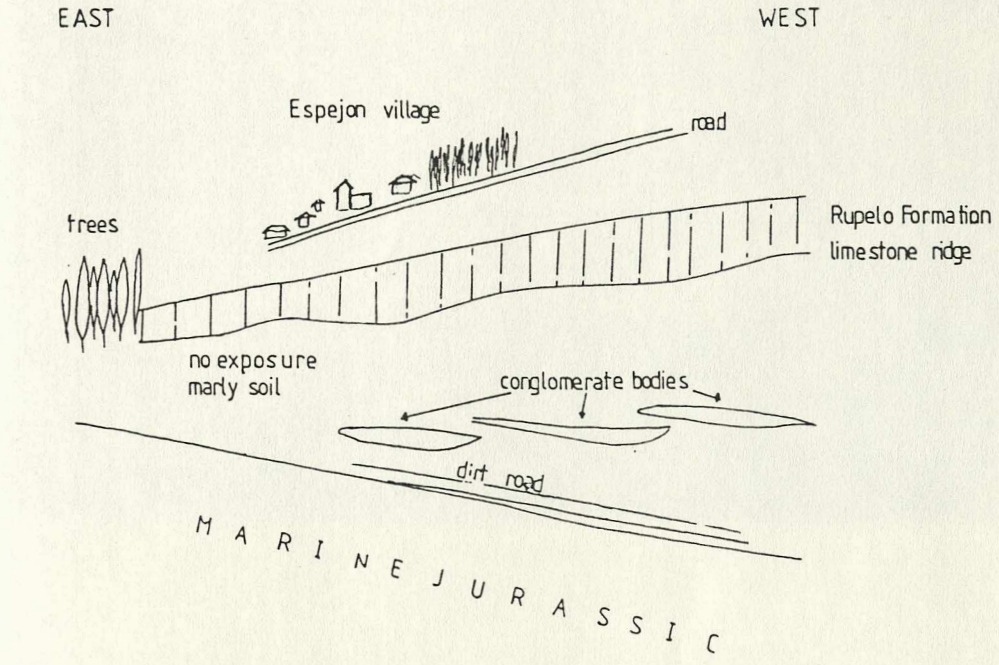
EAST
WEST
Espejon village
road
trees
Rupelo Formation
limestone ridge
no exposure
marly soil
conglomerate bodies
dirt road
M A R I N E J U R A S S I C

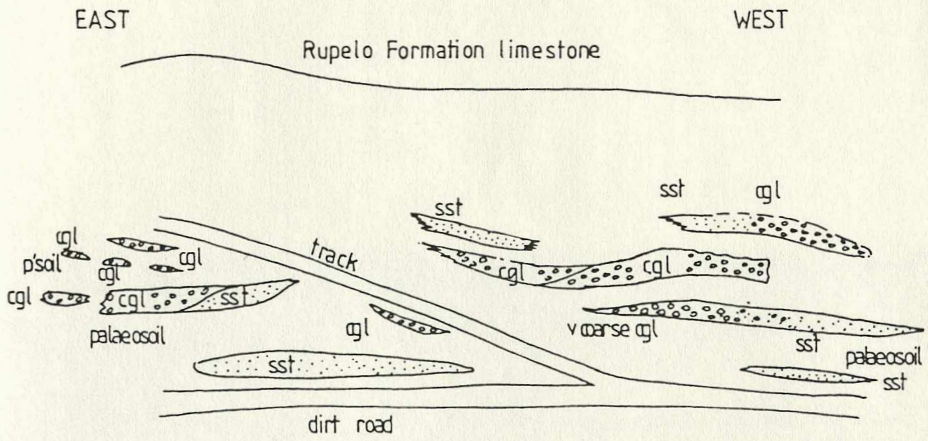
EAST
WEST
Rupelo Formation limestone
sst
cgl
track
p'soil
cgl
cgl
cgl
cgl
sst
palaeosoil
cgl
sst
cgl
cgl
sst
v coarse cgl
sst
palaeosoil
sst
dirt road

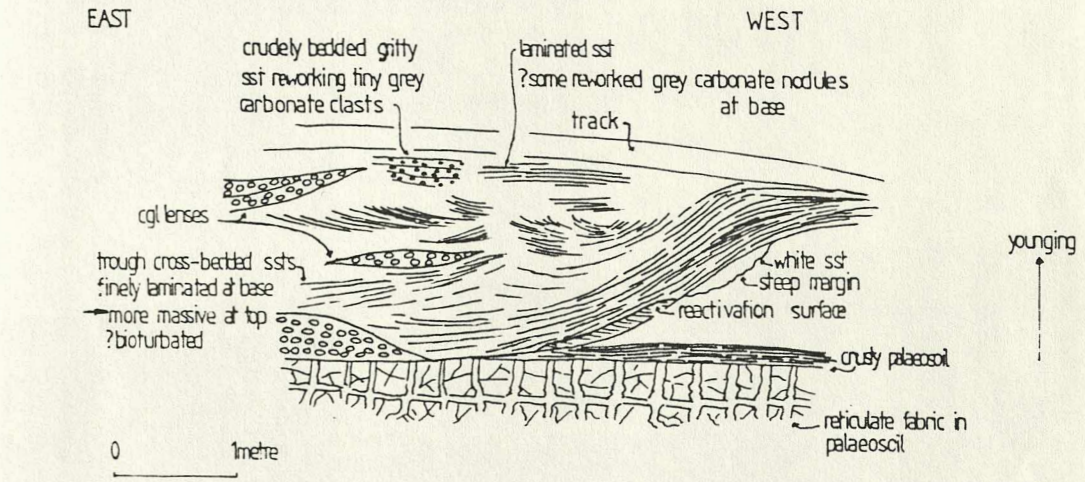
EAST
WEST
crudely bedded gritty
sst reworking tiny grey
carbonate clasts
laminated sst
?some reworked grey carbonate nodules
at base
track
younging
cgl lenses
trough cross-bedded ssts
finely laminated at base
more massive at top
?bioturbated
white sst
steep margin
reactivation surface
crusty palaeosoil
reticulate fabric in
palaeosoil
0
1metre

Fig 3.24. Coarse monomict conglomerates, with intercalated lens of red sandstone. Senora de Brezales Fm, Hortezuelos.

Fig 3.25. Thick channelled monomict conglomerate truncating pedogenically-modified red sandstone. Suggestion of large-scale cross-stratification in conglomerate (?sets dipping to right/E). Senora de Brezales Fm, Hortezuelos. Looking N.

Fig 3.26. Interbedded sandstone and fine conglomerate lenses, cross-stratified. Coarse, polymict, matrix-supported conglomerates visible above and to left. Senora de Brezales Fm, Castrovido.

Fig 3.27. Coarse polymict conglomerates above cross-bedded coarse pebbly sandstone/fine grit. Conglomerate includes irregular 2-8cm yellow, grey and pink mottled limestone clasts (see text for discussion of derivation) and 2-5mm rounded quartz pebbles. Senora de Brezales Fm, 2km SSE of La Gallega, just W of forest track to Espejon.

Fig 3.28. Coarse channel fill conglomerate. Coarse, pebbly, friable red quartz sand matrix, clasts of grey, yellow and pink-mottled limestone. Senora de Brezales Fm. Mambrillas Fault Zone (see also Chapter 8).

Fig 3.29. Close-up view of polymict conglomerate, Senora de Brezales Fm. Quintanilla de las Vinas.

Fig 3.30. Matrix- and clast-supported conglomerates. Note irregular clasts, poor sorting, erosive-based unit of fine conglomerate; Senora de Brezales Fm. Senora de Brezales.

Fig 3.31. Particularly coarse polymict conglomerates with abundant clasts of yellow fossiliferous limestone (Lower Callovian). Locality is close to Jaramillo-Covarrubias Fault - a major transfer structure. Senora de Brezales Formation. Approximately 1km NW of Jaramillo Quemado.

Fig 3.32. Grey carbonate structure (root) cross-cutting red sandstone. Note bifurcation. Senora de Brezales Fm. Ladera, near Mamolar.

Fig 3.33. Close-up view of structure similar to that in fig 3.32. Senora de Brezles Fm. Jaramillo Quemado.

Fig 3.34. Undulating carbonate string/crust in polymict conglomerate. Several other thin strands of grey carbonate; thicker crust above lens cap, laminar fabric just discernible. Senora de Brezales Fm, Ladera, near Mamolar.

Fig 3.35. Rubbly, mottled limestone resting on yellow marine limestones (probably Lower Callovian). Elsewhere, a lithologically-similar limestone occurs above the Senora de Brezales Fm conglomerates. Cornfield behind with no exposure lies on Las Vinas Member Marls. 500m NW of Mambrillas Fault Zone.

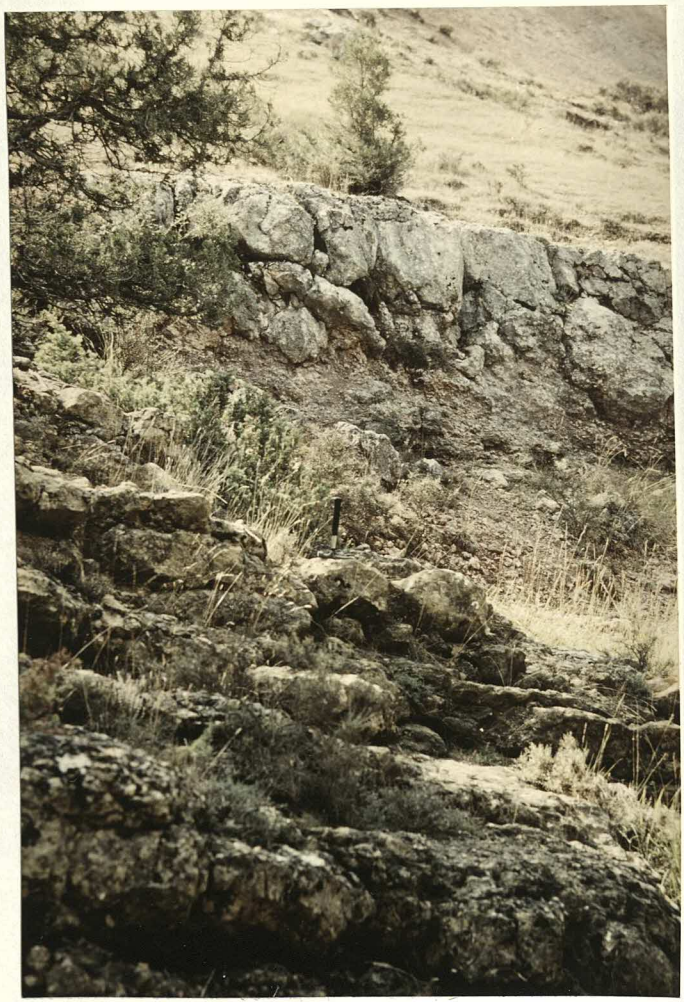

Fig 3.36. Undulating laminar crust developed on marine Jurassic pediment. Note less obvious crust further to right, conglomerate to left. Castrovido.

Fig 3.37. Laminar crusts interbedded with red sandstones. Note also fine horizontal carbonate strings. Individual laminae visible (right of hammer handle end and bottom right of outcrop). Senora de Brezales Fm. Castrovido.

Fig 3.38. Undulating laminar crusts, weathering out as white bands, developed on top of (and within uppermost layers of) marine Jurassic (Lower Callovian) pediment. Senora de Brezales Fm equivalent. Mambrillas de Lara.

Fig 3.39. Palaeosoil displaying horizontal (root crusts) and vertical (root columns) elements making up reticulate "latticework" fabric. Conglomerate channels are incised into this (see figs 3.21 - 3.24).
Reticulate fabric formed by growth of lateral roots and pneumatophores. Senora de Brezales Fm. Espejon.

Fig 3.40. Thick polymict conglomerate truncating heavily-mottled "laminite" palaeosoil. Fabric dominated by horizontal elements, but some vertical structure. Senora de Brezales Fm. Senora de Brezales.

Fig 3.41. Heavily orange-purple mottled "laminite" palaeosoil. Senora de Brezales Fm, Senora de Brezales.

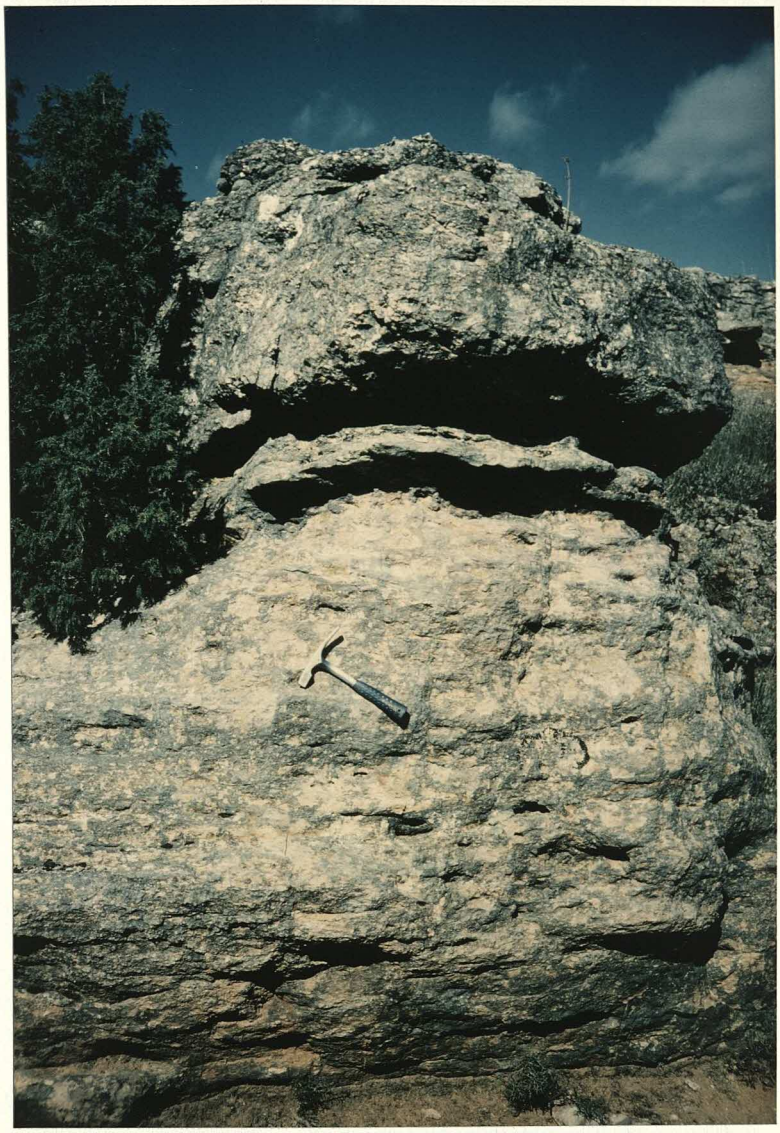

Fig 3.42. Brecciated, mottled limestone with included pockets/fissures filled by laminated red sand. Limestone itself has been brecciated to give weak horizontal fabric. Senora de Brezales Fm. Ladera, near Mamolar.

Fig 3.43. Limestone breccia passing up into more massive limestone with strongly-developed horizontal "laminite" fabric. Senora de Brezales Fm. La Gallega.

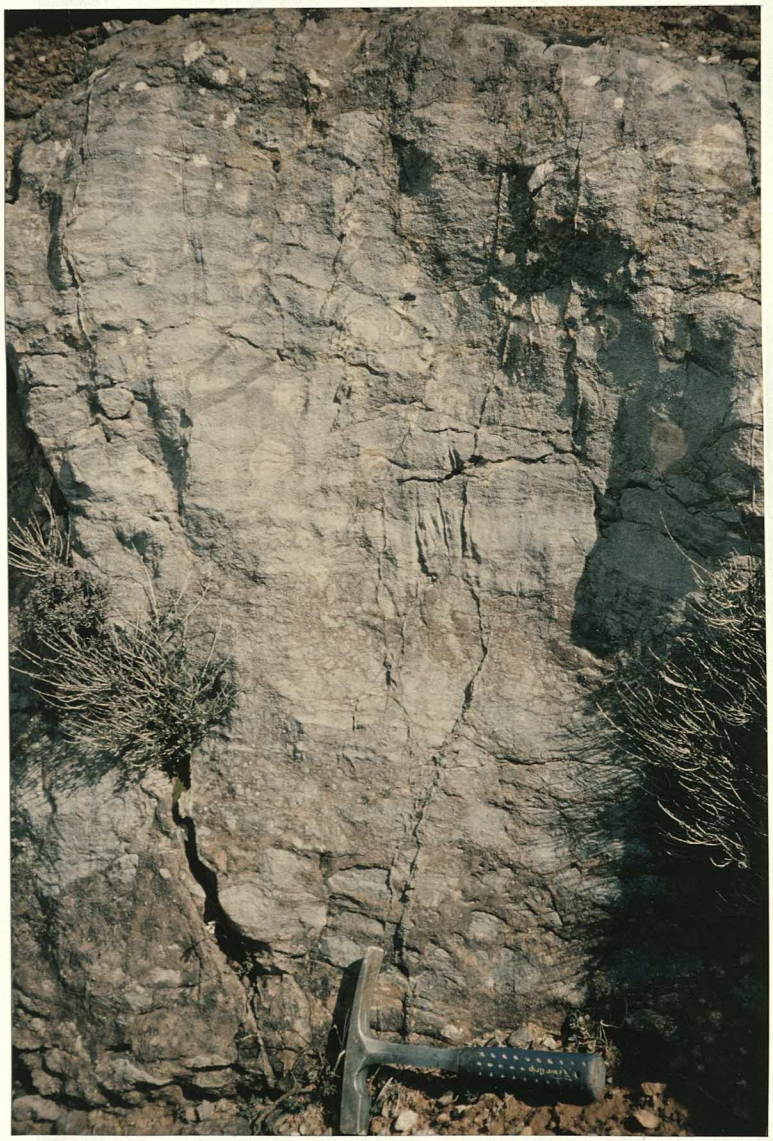

Fig 3.44. Undulating, bedded laminar crusts alternating with marls. Also spaced vertical elements (root columns). Result is poorly-developed reticulate "latticework" fabric. Thicker root crust above small bush, upper left. Senora de Brezales Fm. Talveila.

Fig 3.45. Thin root crusts alternating with red marly limestones. Slight (?desiccation or root) brecciation. Senora de Brezales Fm / Ladera Mb of Rupelo Fm. Talveila.

Fig 3.46. Bedded root crusts in problematic domal mass (?root bioherm). Senora de Brezales Fm. Senora de Brezales.

Fig 3.47. Closer view of second domal mass of bedded (here more undulating) root crusts. Senora de Brezales Fm. Senora de Brezales.

Fig 3.48. Red marls of Las Vinas Member (outcropping behind tree). Rubbly limestone surface (foreground) overlying patchy conglomerates on top of marine Jurassic (Lower Callovian) pediment. Limestones of Ladera Member above marls. Sandstones and conglomerates of Pedroso and Salas Groups in fields with brown soil in left middle distance (thin limestones lenses on intermittent bushy ridges), Utrillas sands in fields with pinkish-yellow soil in right, far distance. Limestones forming scarp on horizon belong to Upper Cretaceous. View looking WSW, 2km W of Torrelara.

Fig 3.49. Micrograph of green marl with intraclast (pink, cracked), charophyte oogonia, ostracod shell fragments (thin shell material). Possible bivalve fragment (thicker shell material). Abundant fine terrigenous material (small white clasts). Stained section. Intensity of stain reflects fine grain size, and presence of Fe and clay impurities. Field of view: 9mm. Las Vinas Member. Quintanilla de las Vinas.

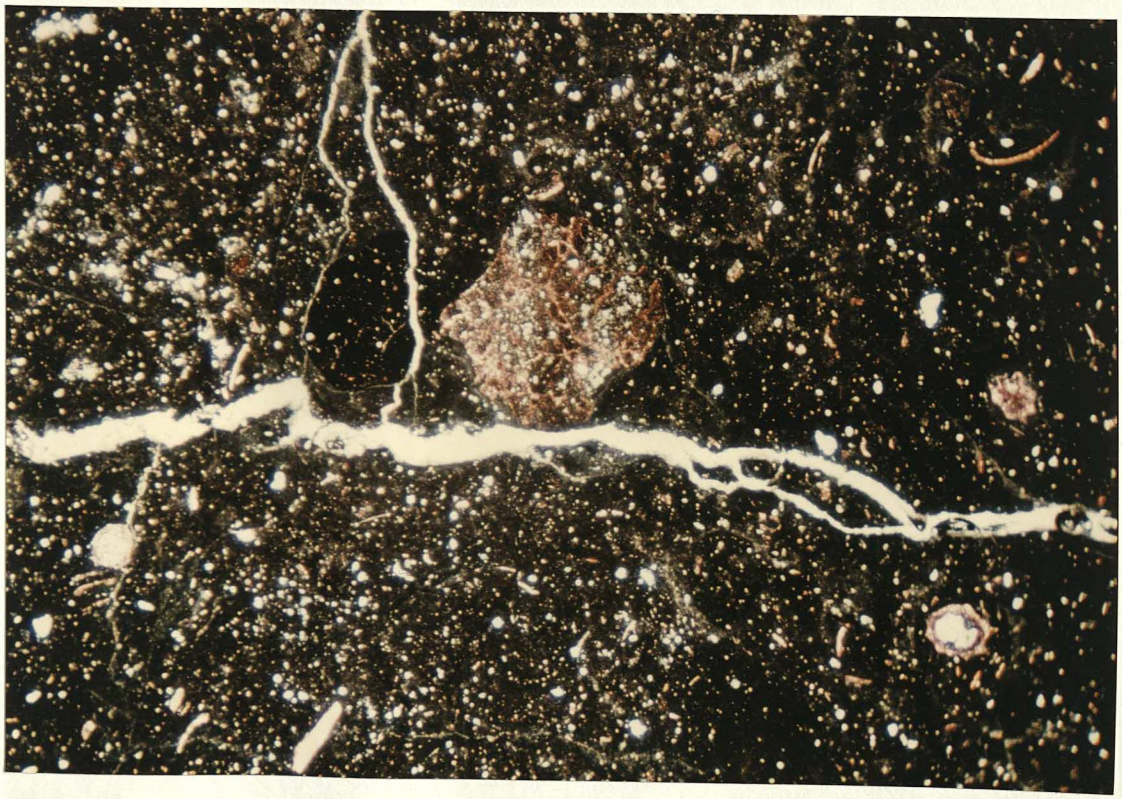

Fig 3.50. Mottled limestone including abundant fine red clasts, yellow clasts, black clasts. Ladera Member. Ladera, near Mamolar.

Fig 3.51. Mottled limestone with weakly developed laminar fabric. Rock is rich in angular-branching and circumgranular cracks. Progressive microbrecciation of rock grainstone texture. Ladera Member. Mambrillas de Lara.

Fig 3.52. Exceptionally marly limestones, grading up from green marls. Ladera Member. Torrelara.

Fig 3.53. Carbonate showing strong mottling reflecting redistribution of Fe on subaerial exposure. Irregular thin spar-filled string-like voids are root tubules. Larger, spar-filled planar or curved cracks are desiccation features; smaller examples are often associated with circumgranular cracks induced by shrinkage of incipient glaebules (eg arrowed centre right). Black pebbles indicate source of reworked stabilised organic carbon (see section 3.3.10) and hence possibly proximity to emergent vegetated areas. Interpretation: Development of pedogenic features on original lacustrine carbonate host.
Ladera Member. Mambrillas de Lara.

Fig 3.54. Carbonate showing local mottling and abundant fine spar associated with root tubules and larger, possibly solutional cavities filled with coarse blocky spar (centre). Needle-fibre calcite crystals (see text) in cavity, which is filled by palisade (speleothem) carbonate crystals showing zoning under cathodoluminescence (figs 3.187 & 3.188). Ladera Member. Mambrillas de Lara.

Fig 3.55. Glaebule / "peloid" / "caliche pisoid" with dark stain (fine grain size, clay impurities) and included detrital material. Circumgranular crack developing as extension of larger spar-filled curving desiccation crack. Smaller branching cracks at initial stages. Smaller glaebule (top left) showing incipient differentiation from matrix. Stained section. Field of view: 9mm. Ladera Member. Mambrillas de Lara.

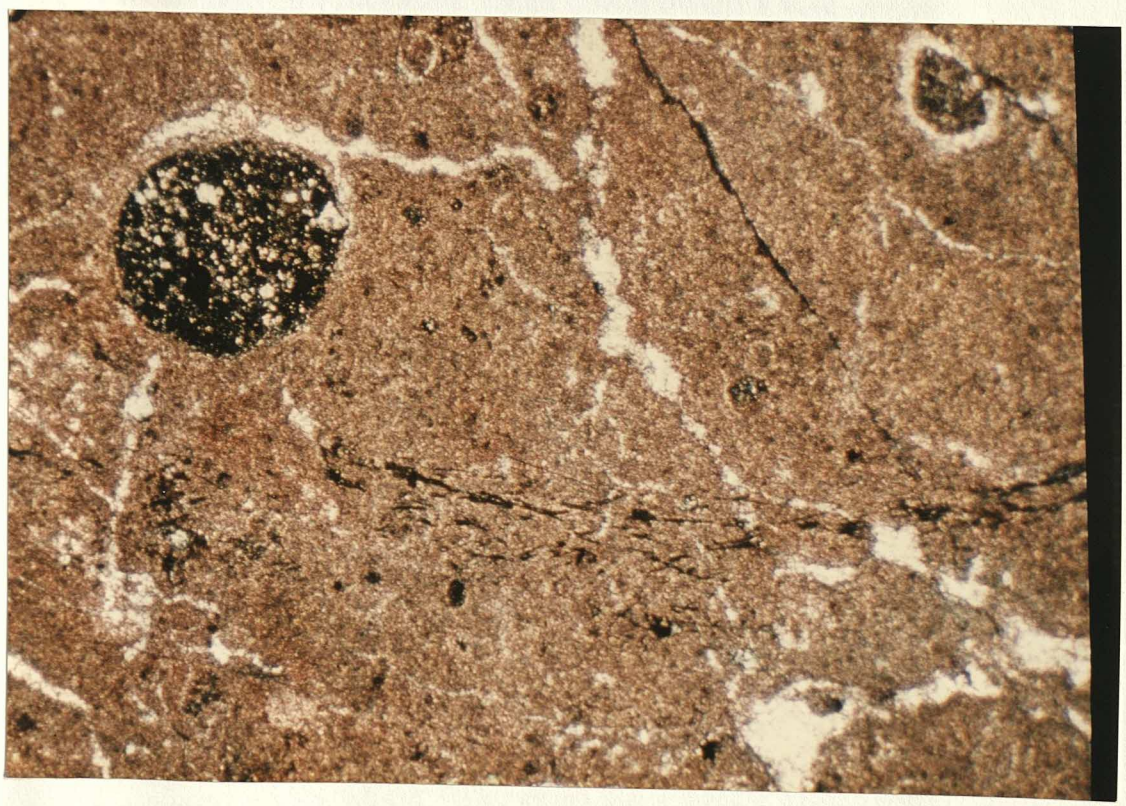

Fig 3.56. Large dark-stained glaebules with some included detrital material, surrounded by circumgranular spar-filled crack, smaller incipient glaebules in first stages of differentiation from micrite matrix. Cracks develop as a result of grain shrinkage and rotation during desiccation. Stained section. Field of view: 4mm. Ladera Member. Mambrillas de Lara.

Fig 3.57. Tubular spar-filled irregular voids in dark, clotted peloidal micrite. Some evidence of minor geopetal filling with crystal silt.
Interpretation: root tubules, subsequent minor fill from cavity walls.
Stained section. Field of view: 9mm. Ladera Member. Mambrillas de Lara.

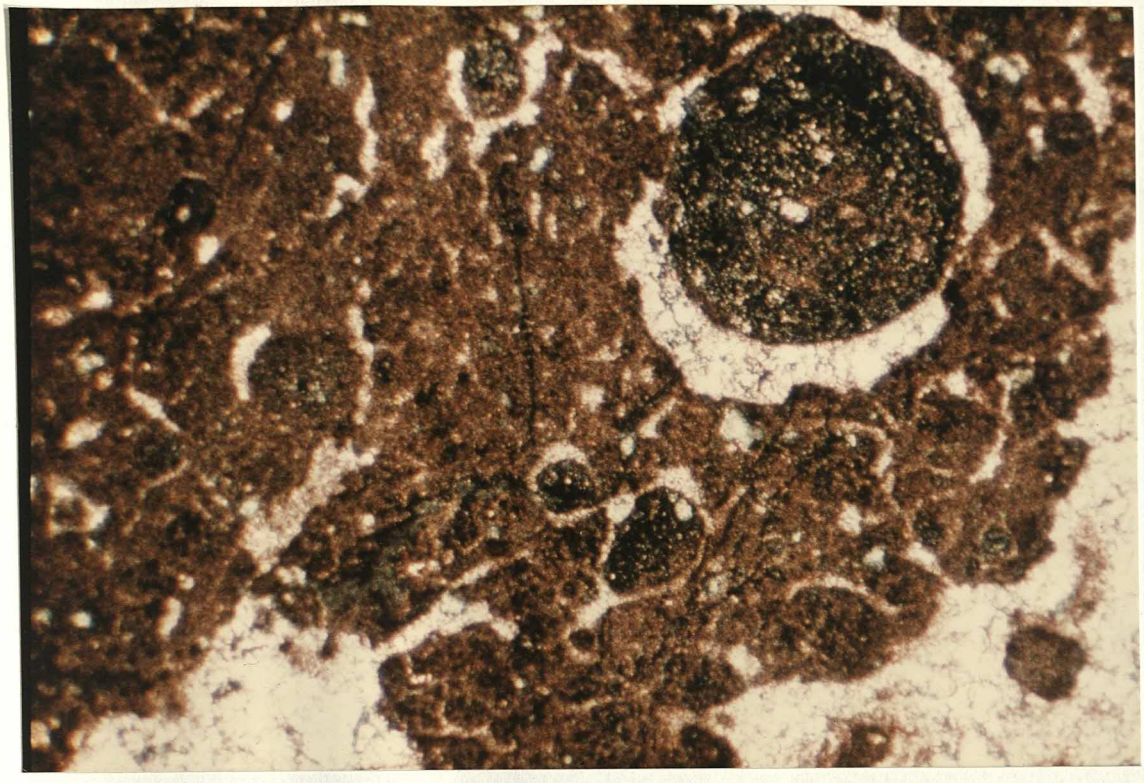

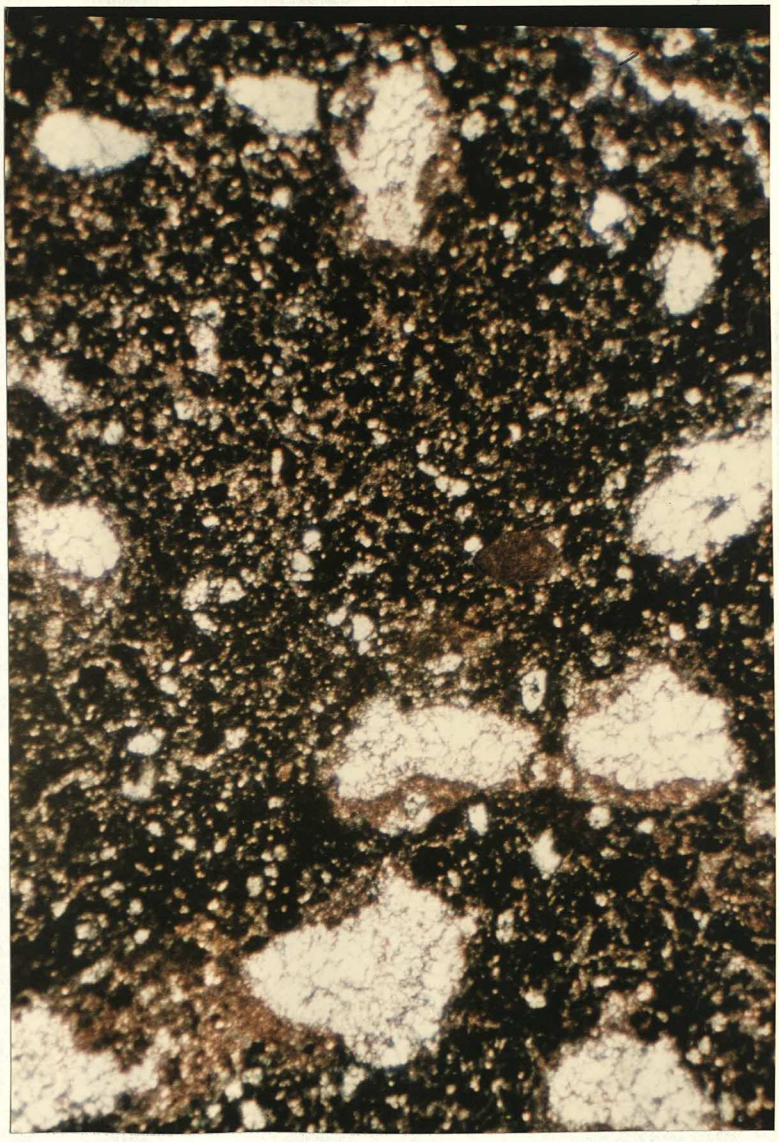

Fig 3.58. Irregular spar-filled voids, some dark glaebules. Abundant needle-fibre calcite crystals. Peloidal micrite matrix. See hand specimen (fig 3.54) and micrographs under cathodoluminescence (figs 3.187 & 3.188). Ladera Member. Mambrillas de Lara.
Interpretation of needle fibre crystals: leaves or straight root hairs?
Stained section. Field of view 9mm.

Fig 3.59. Close-up view of same sample. Field of view: 4mm. Ladera Member. Mambrillas de Lara.

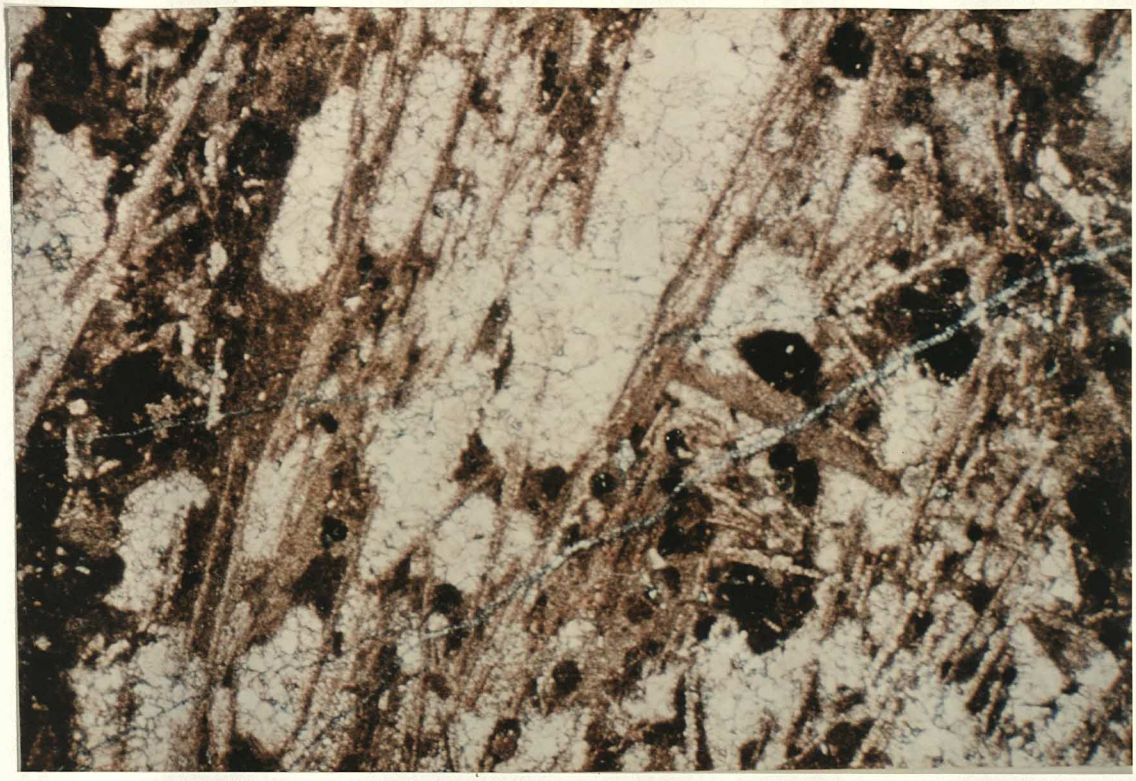

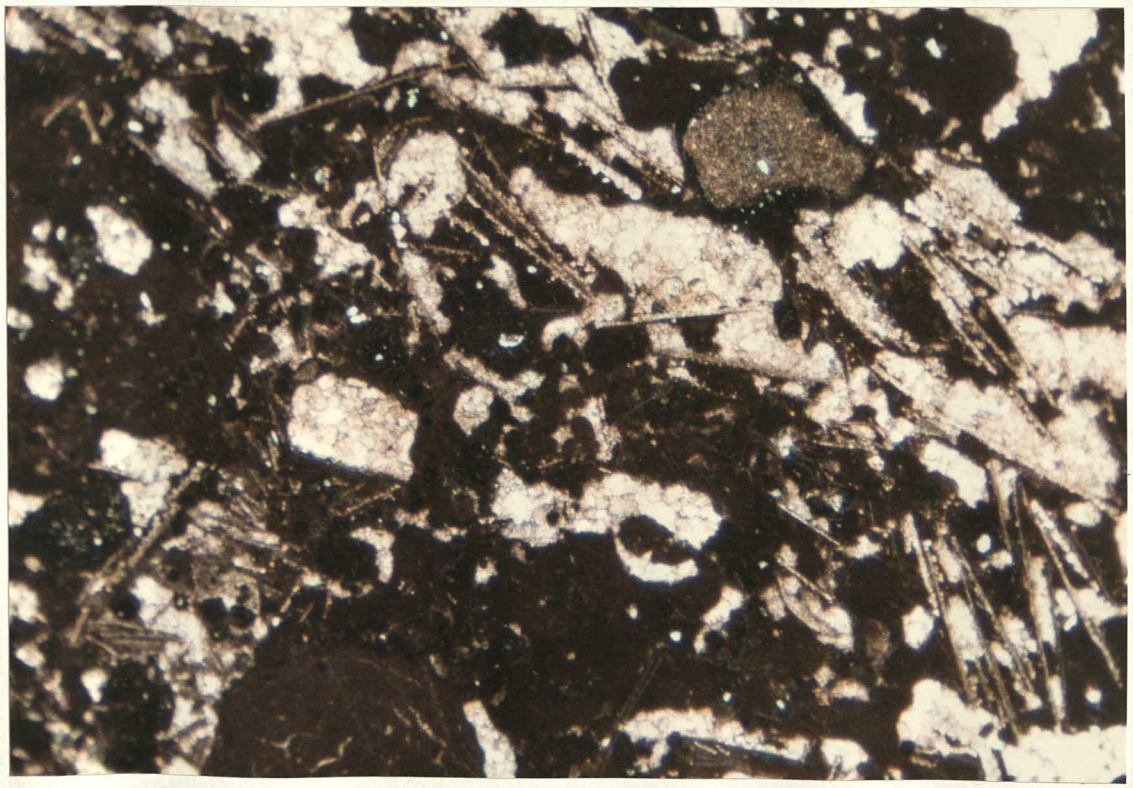

Fig 3.60. Palisade calcite crystals infilling cavity in same sample as figs 3.187 & 3.188. Some are arranged in radial fan-like arrays. Stained section. Field of view: 9mm. Ladera Member. Mambrillas de Lara.

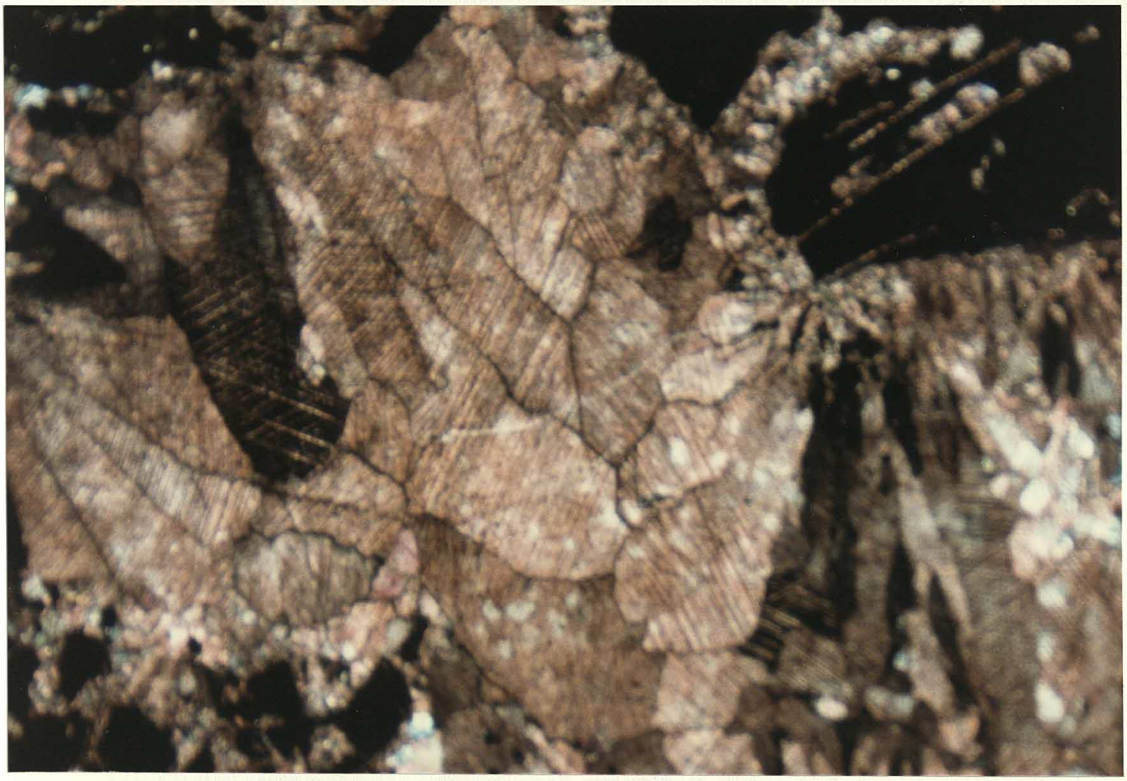

Fig 3.61. Morphology of desiccation cracks in carbonates. Freytet & Plaziat (1982)

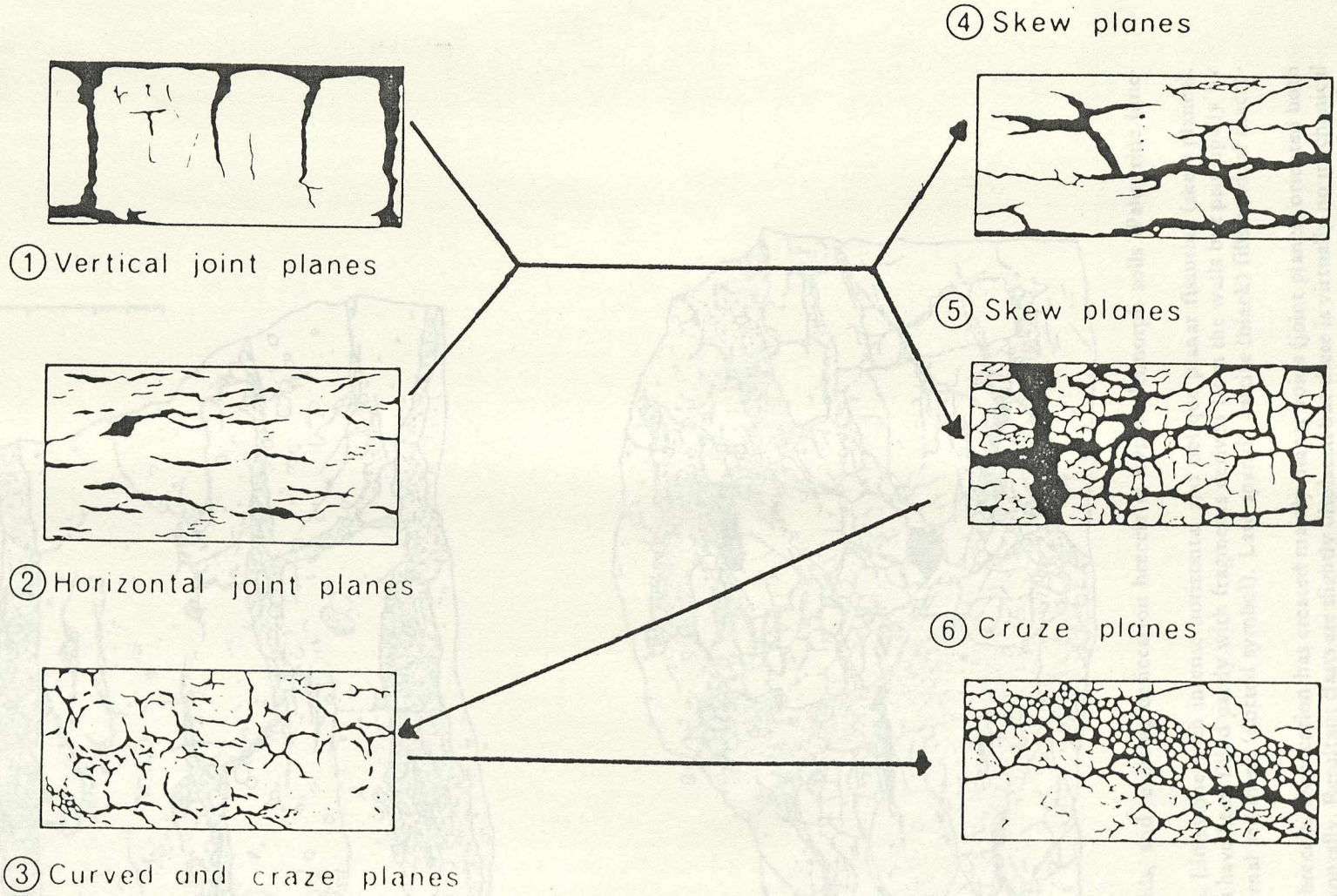

Elements of soil micromorphology: desiccation planes (from palustrine limestones in Languedoc, Limagne, Paris Basin).

modified after Freytet & Plaziat (1982)

A

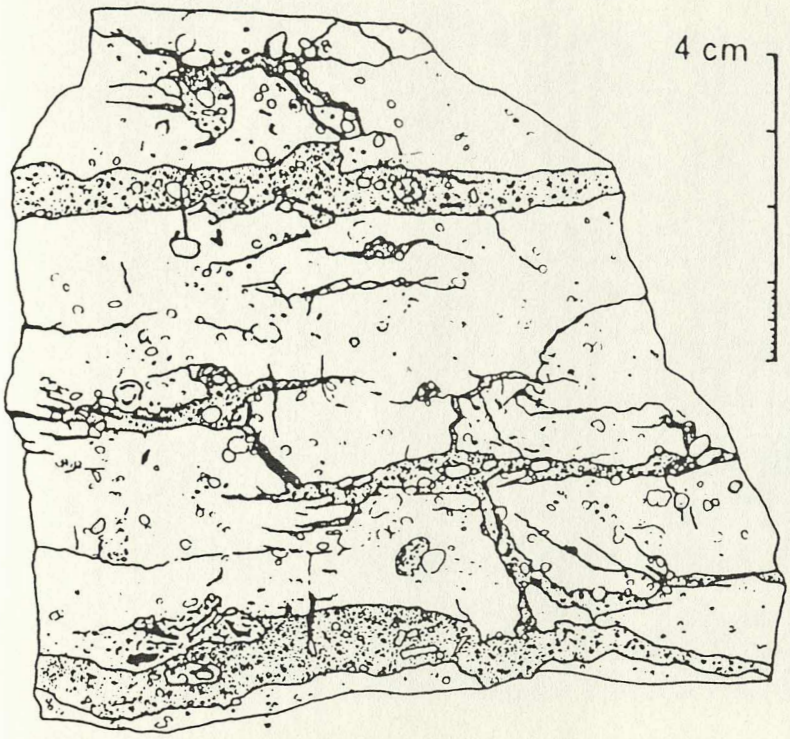

B

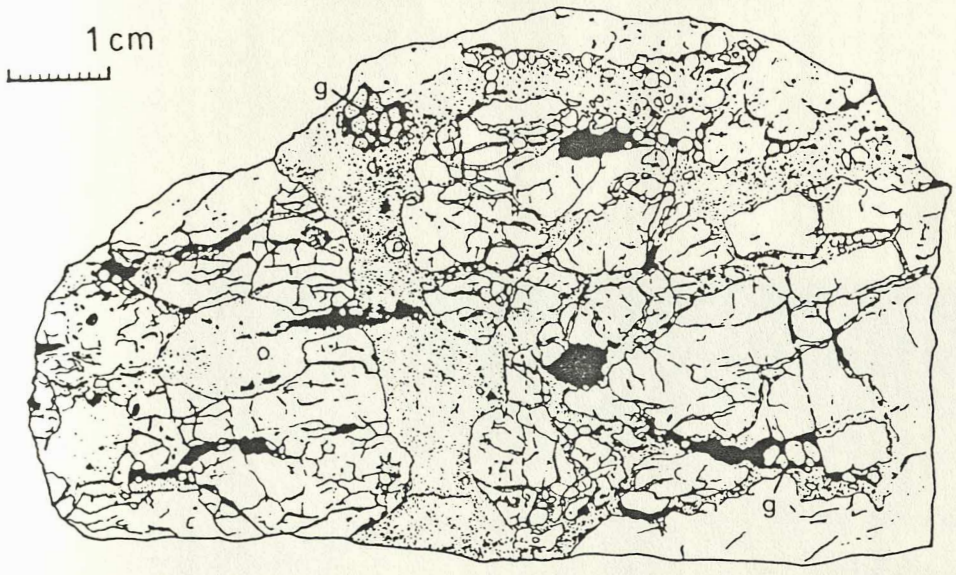

Planar voids, and resulting desiccation breccia in hypercalcimorph soils (Palustrine limestone).

A. Skew planes. Limestone with intense horizontal and oblique planar fissuring (skew planes). The resulting voids have been filled partly with fragments derived from the walls but principally by infiltration of external sediment (dotted symbol). Late sparitic calcite (black) fills residual macroporosity.

B. Desiccation breccia. Desiccation has created mainly planar voids (joint planes) oriented both vertically and horizontally. Resultant clasts are slightly displaced but there is virtually no mechanical reworking. Fissure and cavity filling is fine carbonate material (stippled) probably introduced during flooding. A second series of desiccation fissures (in black) cut, or enlarge, certain first-phase fissures has locally winnowed the first-phase internal sediment producing patches of grainstone texture (g). plus their filling. Water circulating through this secon series of fissures has locally winnowed the first-phase internal sediment, producing patches of grainstone texture (g). Residual voids are filled with sparite (black).

A and B, Cuiso-Lutetian, Ventenac Limestone, Minerve; tracing from polished surface.

Freytet & Plaziat (1982)

Fig 3.62. Polished slab of hand specimen showing strong and irregular mottling (redistribution of Fe) and tiny irregular spar-filled root tubules (just above centre of scale bar). Senora de Brezales Fm equivalent. 1km NW of Mambrillas Fault Zone (same horizon as fig 3.35).

Fig 3.63. Hand specimen of heavily mottled impure carbonate, showing typical purple - yellow colours in cm-scale mottle patterns. Ladera Member. Las Pinarejas.

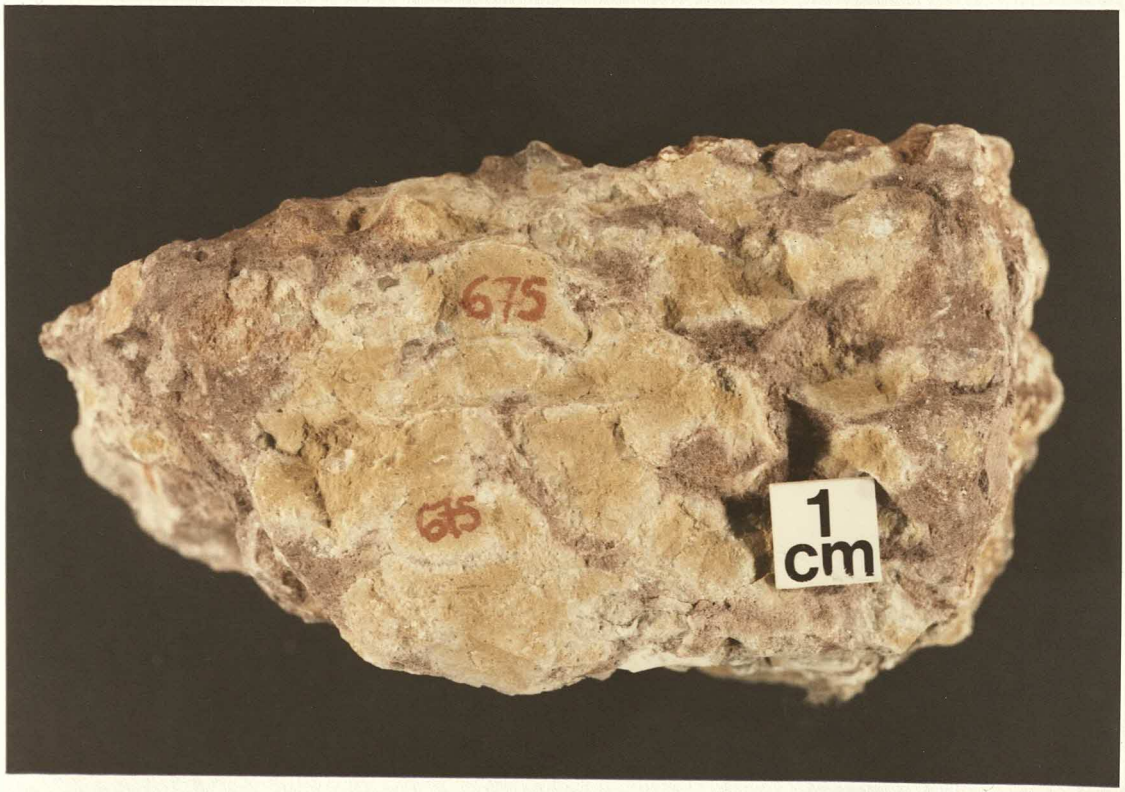
675
675
1
cm

Fig 3.64. Nodular carbonate developed in red marl host. Weakly-developed vertical fabric, suggesting formation *in situ* (eg by roots). However, greater carbonate content and extreme brecciation at base suggests some reworking from thick carbonate unit below (ie to left in photograph - younging to right of photograph, near vertical bedding). Rio Cabrera Member. 800m S of Rupelo.

Fig 3.65. Highly mottled, heavily brecciated, slightly impure, limestone. Weak vertical ("prismatic") fabric discernible in upper right of photograph. Ladera Member. Hortezuelos.

Fig 3.66. Thick limestone bed, overlying red-purple mottled marls (poor exposure under scree, bottom of photograph). Limestone is massive at the top, mottled and brecciated at the base with vertical 5-10cm tubular structures defining prismatic fabric.
Interpretation: large roots. Sequence: marl → brecciated limestone → massive limestone indicates succession of environments: distal alluvial → littoral → permanent lacustrine / paludal. Ladera Member. El Cangrejo, 3km N of Huerta del Rey.

Fig 3.67. Vertical cylindrical structures similar to those shown in fig. 3.66, here developed in marl at base of limestone. One column showed a red central cortex with a weakly-discernible radial mottling pattern.
Interpretation: large roots.
Ladera Member. 2km N of Huerta del Rey.

Fig 3.68. Abundant vertical cylindrical carbonate structures set in red mottled marly limestone, and penetrating up to 50-100cm, defining prismatic fabric.
Interpretation: large roots.
Ladera Member. Rupelo.

Fig 3.69. Closer view of cylindrical carbonate structure as in fig 3.68. Note nodular character of limestone (possibly reflecting irregular surface of tubercled root or concretionary growth around it) and, in this case, paler cortex. Ladera Member. Rupelo.

Fig 3.70. Well-developed prismatic fabric with abundant dark, vertical, elements in highly mottled fresh-water limestone showing evidence of strong pedogenic modification. Presence of some uncemented fissure fillings suggests fabric may locally have been accentuated by Recent pedogenesis before excavation of the road cut. Limestone occurs interbedded between channellised OligoMiocene conglomerates. Tejada.

Fig 3.71. Excellent example of prismatic fabric from pedogenically modified fresh-water limestone. Interbedded with coarse conglomerates. The vertical "joints" are pedogenetic, not neotectonic, features. OligoMiocene. Jaca Basin. Photograph courtesy of E J Jolley and D C Edwards.

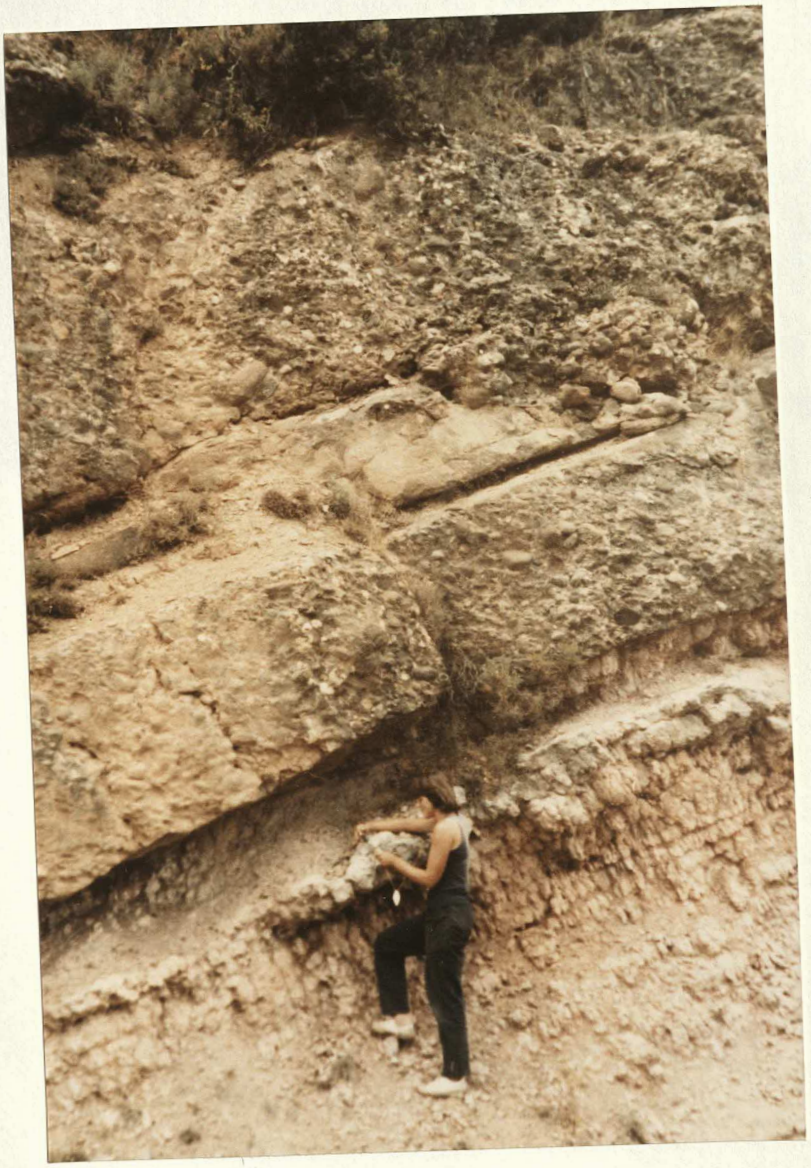

Fig 3.72. Prismatic fabric displayed in seatearth (pedogenically altered sandstone beneath coal horizon). Vertical cracks mark root-traces. Carboniferous. Amroth, near Tenby, U.K.

Fig 3.73. Morphology of Recent root structures reported from the Bahamas by Hoffmeister & Multer (1965).

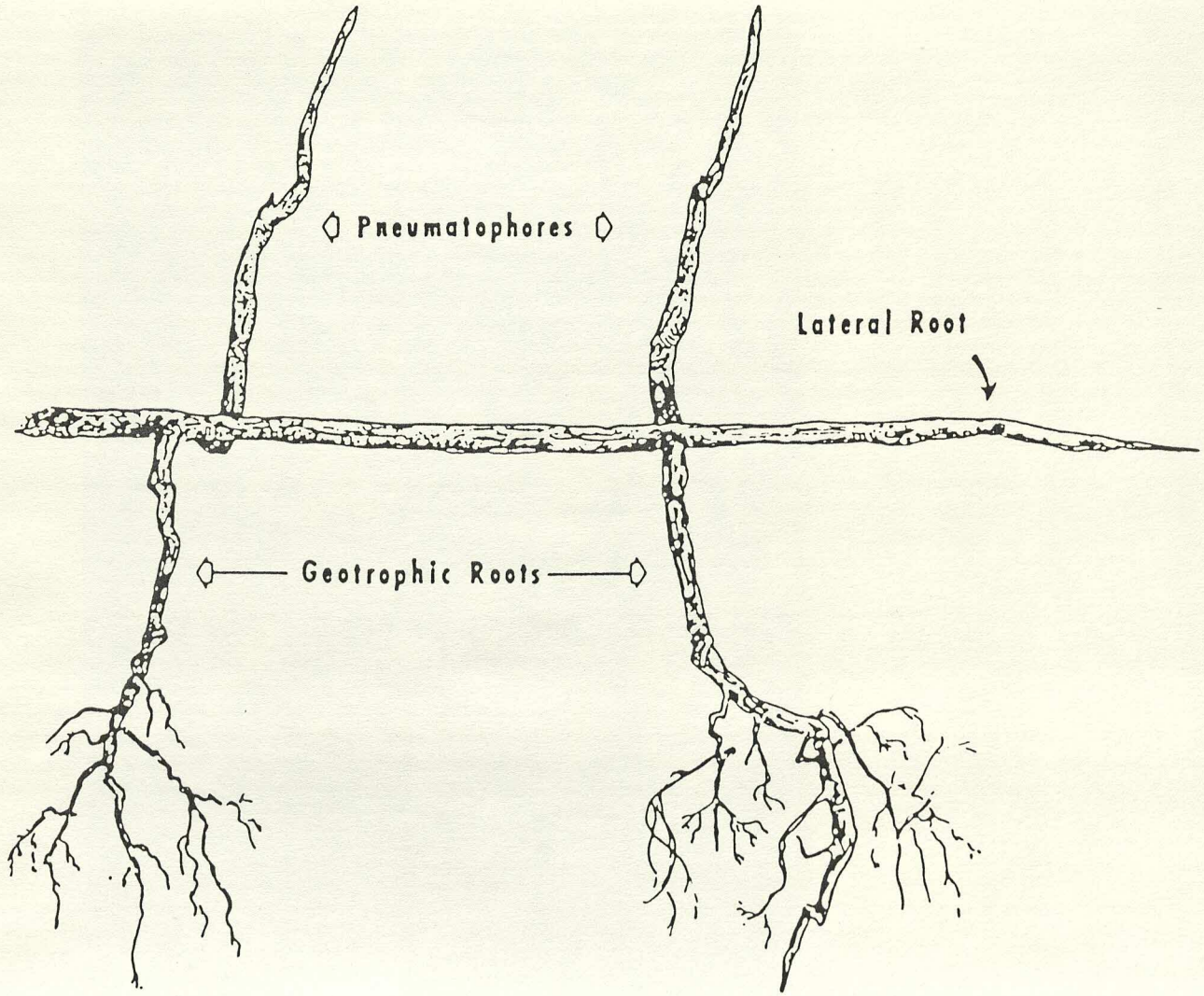

Basic root structure of *Avicennia nitida*

Fig 3.74. Red horizons ("terra rossa") up to 1m in thickness interbedded with massive and peloidal limestones. Red horizons locally appear to pipe down joints (eg above roughly cuboid loose block, in heavy shade, centre right of photograph) - possible evidence for karstic processes. Ladera Member. Mambrillas de Lara.

Fig 3.75. Close-up view of part of red horizon. Matrix-supported, (matrix of impure mottled grey-pink carbonate), abundant ½-5cm irregular clasts of red marl of apparently local derivation. Ladera Member. Mambrillas de Lara.

Fig 3.76. Looking down on bedding plane, showing angular 1-5mm wide cracks filled with grey carbonate. Red mottled limestone matrix. Cracks probably developed as a result of both root- and desiccation brecciation. Ladera Member. Mambrillas de Lara.

Fig 3.77. Mechanism for the formation of subjacent karst.

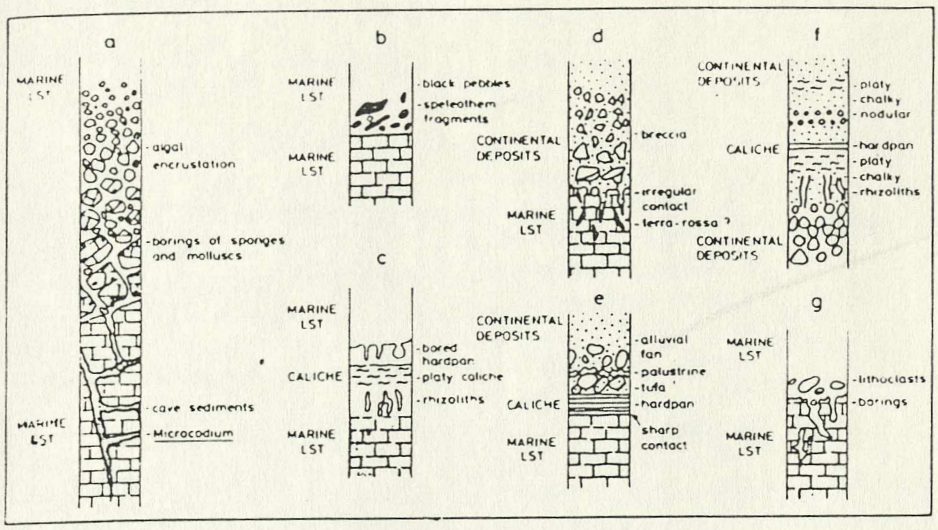

Generalized sequences containing exposure surfaces based on known examples. (a) Karstified Mesozoic limestone reworked in Miocene coastal environment. Most of the karst profile is preserved, with clear evidence of proximity of soil cover, Barcelona, Spain. (b) Same exposure surface as in (a) but karst profile is not preserved; sequence is diagnostic of close proximity of karst and soil. (c) Caliche profile in Tertiary marine limestone reworked in Plio Pleistocene coastal environments, Yucatan, Mexico. (d) Sequence probably contains subaerial exposure but no diagnostic evidence is found, except for relics of possible terra-rossa in deep joints. Same exposure surface as (a) and (b). (e) Mesozoic limestone, intensively calichified, followed by Paleocene palustrine sediments and alluvial fans, Barcelona, Spain. (f) Calichified overbank deposits of Triassic alluvial fan complex, Barcelona, Spain. (g) Same exposure surface as (a), (b) and (d), but without traces of subaerial exposure facies. Only coastal exposure facies are recorded.

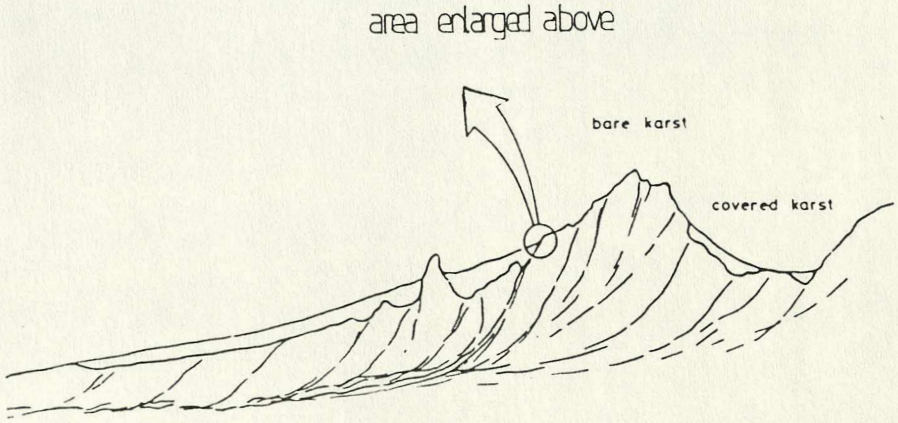

Fig 3.78. Polished slab of pale grey limestone host; some root tubules and fine desiccation cavities, with patchy, but well-developed, laminar fabric defined by abundant, 1mm diameter, spar-filled cavities concentrically lined by pale micrite. Green marl above and below, also some included along laminae.
Interpretation: discontinuous mats of root tubules ("root crusts"). Root colonisation in marginal lacustrine environment. Horizontal roots may reflect necessity for wide catchment in semi-arid climate or early lithification of subjacent sediment. Green marls might record terrigenous input and reduction in soil (or subaqueously?).
Ladera Member (upper part). Mambrillas de Lara.

Fig 3.79. Slab of part of thick (1m) bedded unit with laminar fabric and abundant 1mm spar-filled root tubules.
Interpretation: Thick root mat / crust. This example from top of Rio Cabrera Member, Rupelo, but many other excellent examples in Ladera Member, eg at Ladera, near Mamolar.


1
cm

Fig 3.80. Micrograph of root mat / crust shown in previous figure. Note: some small, rounded peloids; local presence of lacy fabric of interlocking fine walls and cavities - this is "alveolar texture". Unstained section: field of view: 9mm. Top of Rio Cabrera Member, Rupelo. (See figs 3.84 & 3.85).

Fig 3.81. Micrograph of root mat / crust. Intricate fabric made up of abundant spar-filled root cavities and interlocking micritic cavity walls/linings. Stained section. Field of view: 9mm. Ladera Member. Senora de Brezales.

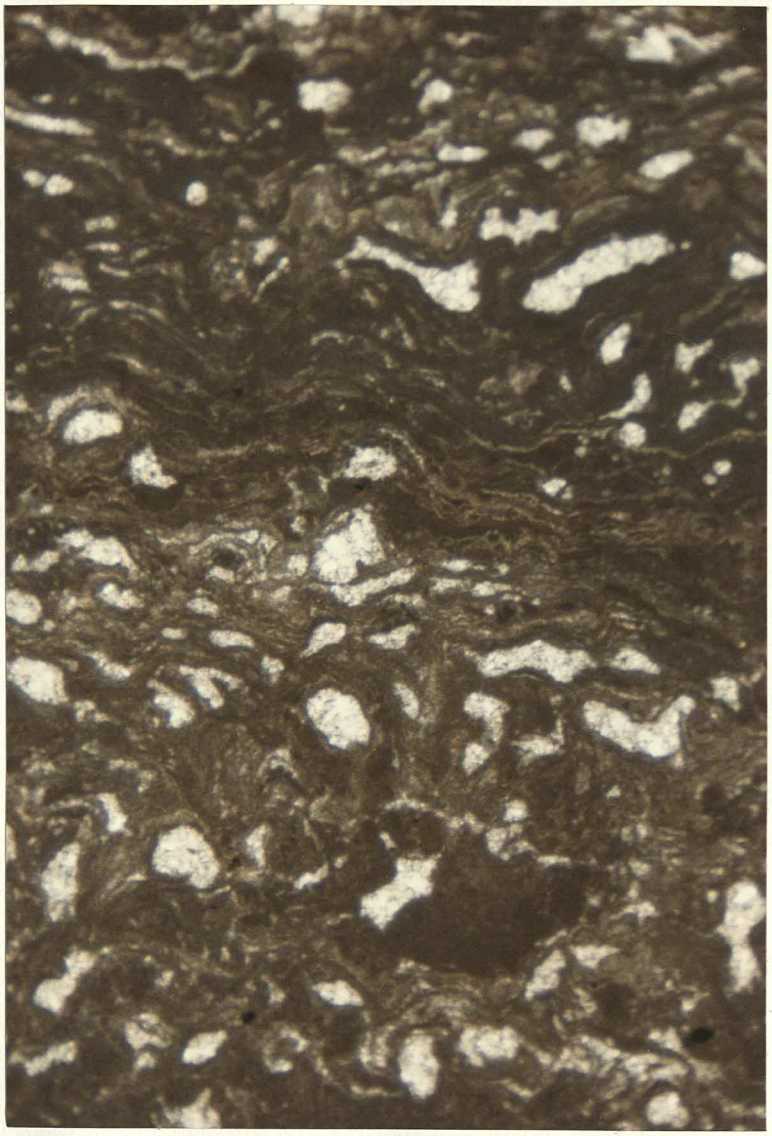

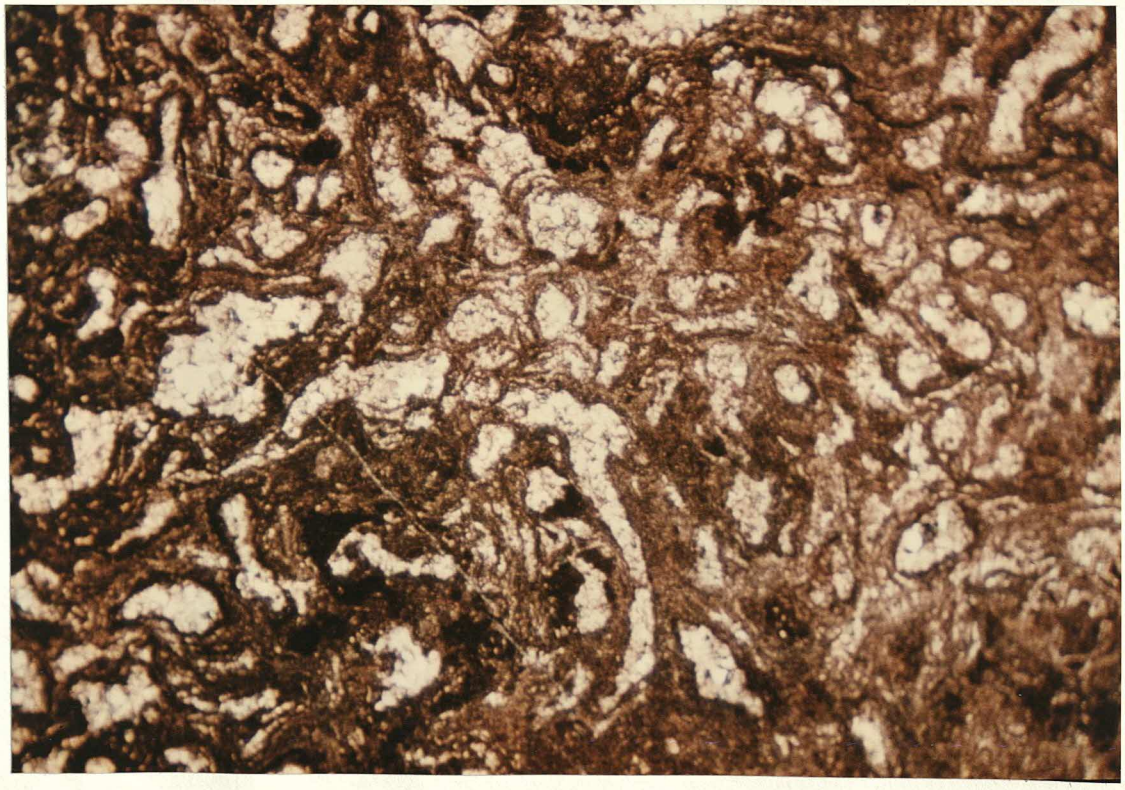

Fig 3.82. Micrograph of root mat / crust. The sparry areas are filled voids marking the vascular system, while the micrite displaying concentric structure represents the cavity walls / linings. Dark grains are individual soil grains (glaebules). Late fill of root porosity with ferroan calcite. Stained section. Field of view: 4mm. Ladera Member. Mambrillas de Lara.

Fig 3.83. Micrograph showing similar structures to those in fig 3.81, but also showing irregularly shaped (interstitial?) glaebules (dark areas) and weakly-discernible alveolar texture within the root cavities - complex lacy network reflecting smaller-scale aspects of root structure. Ladera Member. Mambrillas de Lara.

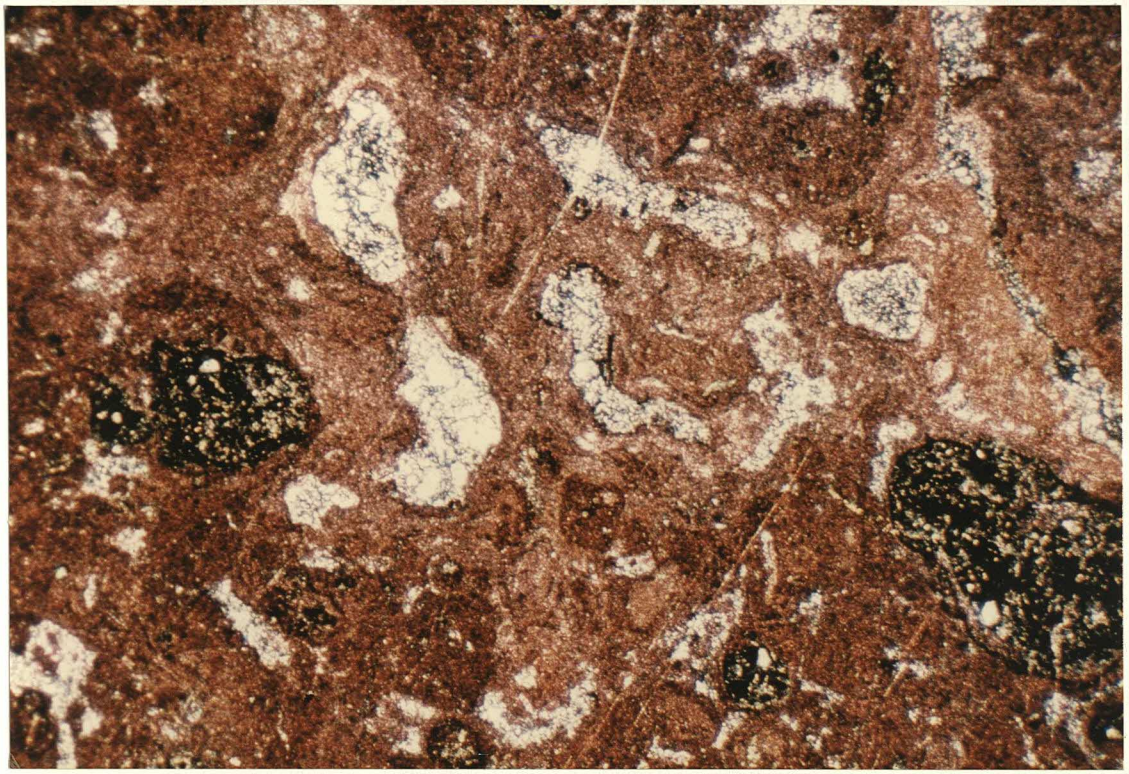

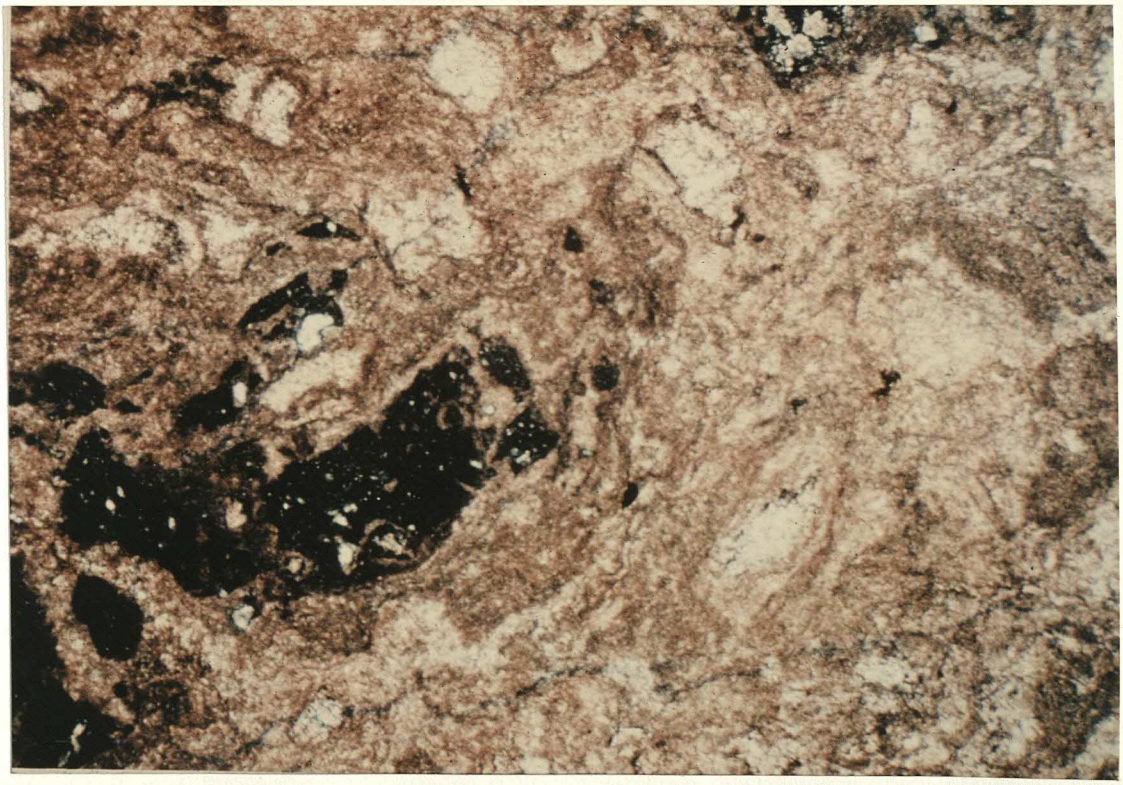

Fig 3.84. Classification of rhizoliths (Klappa, 1980).

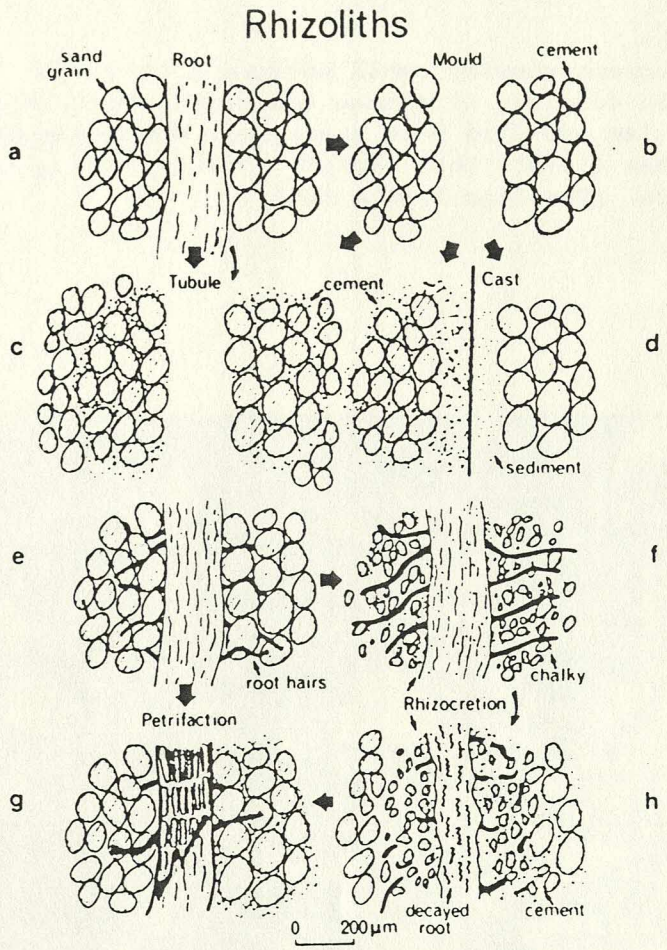

Fig. 1. Schematic representation of types of rhizoliths and their relationships. (a) Hairless part of root in lime sand. (b) Root mould in lime sand. Vadose fringe cement (low magnesian calcite) prevents mould from collapse. (c) Root tubule. Intergranular pore space in proximity of root mould has been filled with low magnesian calcite cement. Remainder of lime sand is uncemented or weakly cemented. Cementation took place either during lifespan of root which has since decayed ($a \rightarrow c$) or from wall of a root mould because of greater porosity and permeability and hence greater availability of percolating $CaCO_3$-bearing solutions through the mould ($b \rightarrow c$). (d) Root cast formed by filling root mould or tubule with sediment and/or calcite cement. (e) Root with root hairs in lime sand. (f) Rhizocretion. Etching by root hairs of lime sand and localized reprecipitation of dissolved calcite as isolated micritic grains produces a chalky rhizocretion (compare with *e*). (g) Root petrifaction. Partly decayed root and root hairs impregnated with calcite (see text and Figs 7 and 8 for details). (h) Rhizocretion. Partly decayed root and sloughed off root hairs encased in partly etched lime sand. Root materials are not calcified (contrast with *g*).

Fig 3.85. Micrograph showing small patches of alveolar texture. This fabric consists of a more delicately lacy network of cavities and fine root structure. Fabric first described by Esteban (1974). This example from top of Rio Cabrera Member, Rupelo. (See figs 3.80 & 3.81).

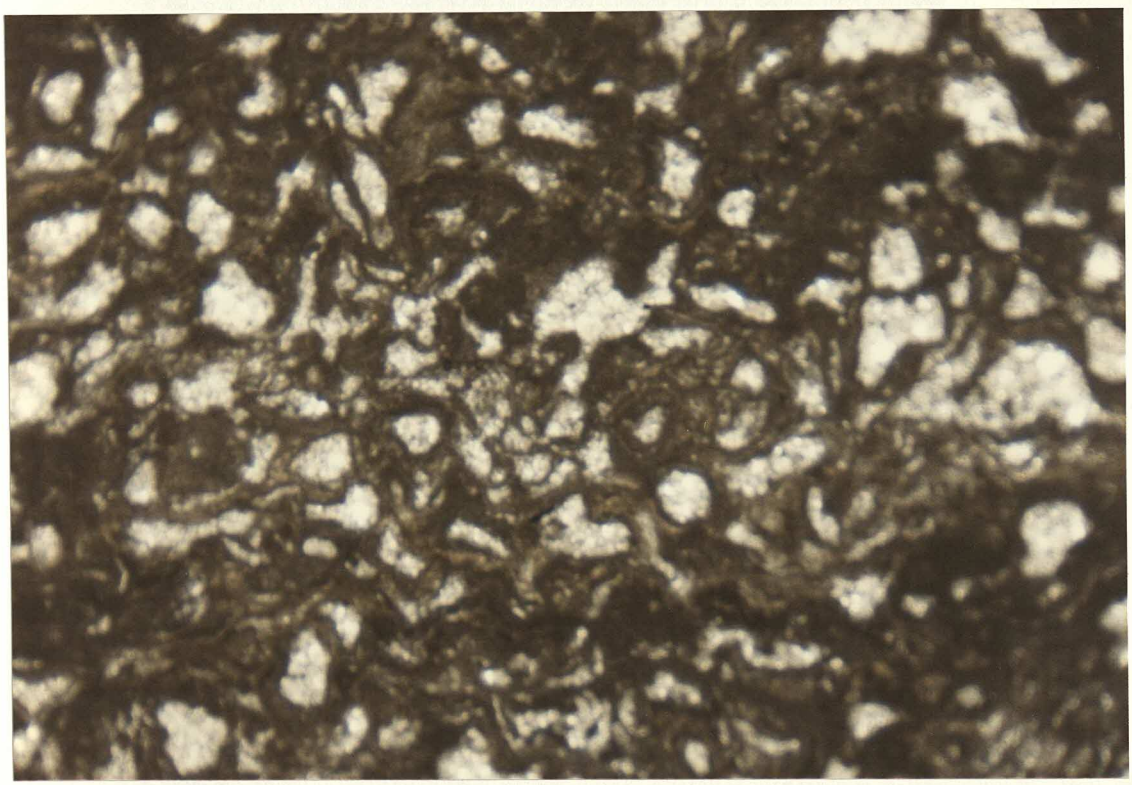

Fig 3.86. Laminated crust developed above limestone with glaebules and included quartz grains which show evidence of calcite replacement. Crust shows dense, weakly undulating, laminar fabric which contrasts strongly with porous crusts. The fabric is more similar to those described by Multer & Hoffmeister (1968) and to "croute zonaire" of French workers. Problematic - it is not clear if this is an ancient crust formed by the action of roots or epilithic lichens (Klappa, 1981), or if it is a recent crust formed by lichens or related to tufa deposition. Hand specimen in upper photograph is 15cm in length. ?Ladera Member. Quintanilla de las Vinas.

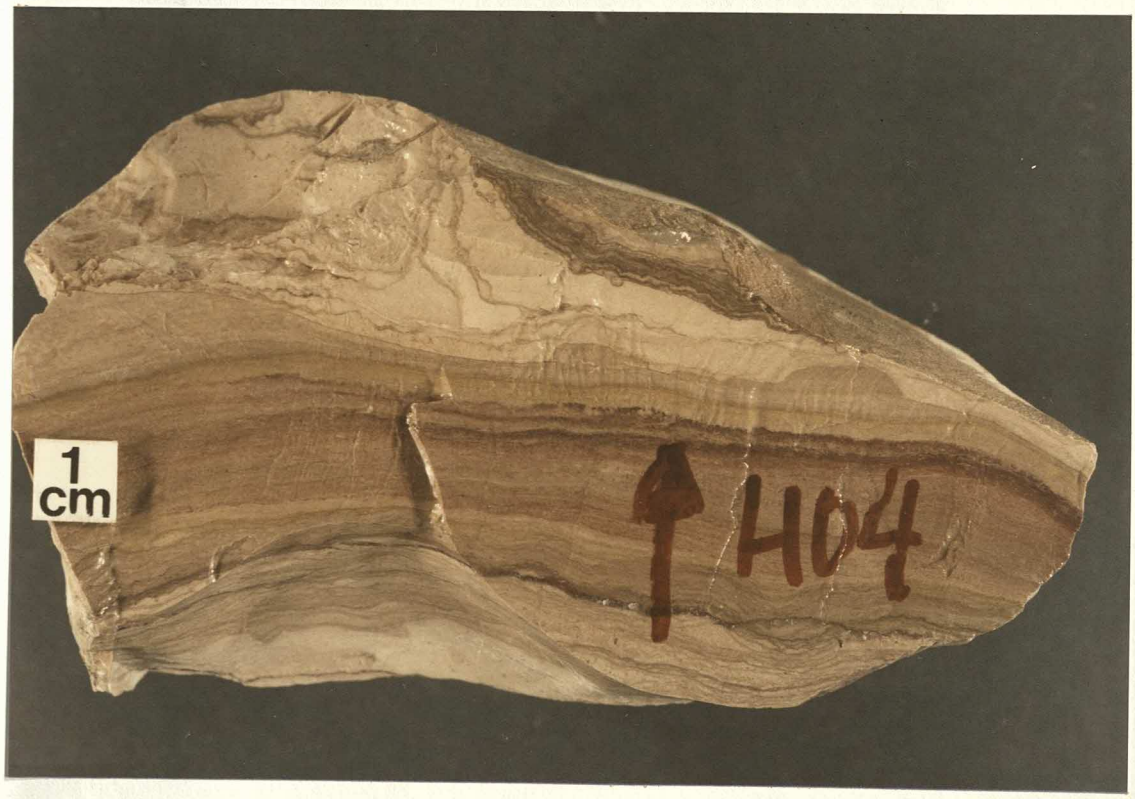
1
cm
H04

Fig 3.87. (Above) Mottled limestone. Abundant geopetally-filled cavities evident in hand specimen. Pure white nature of the geopetal carbonate allows easy identification as vadose silt. Some 5mm black pebbles. Ladera Member. Las Pinarejas. (Below) Mottled, very brecciated limestone from a little higher in the same section. Red angular intraclasts, pale carbonate matrix, probably of vadose silt.
Interpretation: Microkarst processes associated with brecciation at higher levels within a soil profile. At greater depth there is less brecciation, and original cavities can be recognised. The association with mottling may indicate more prolonged exposure or it may signify the superposition of microkarst processes on an already modified sediment.

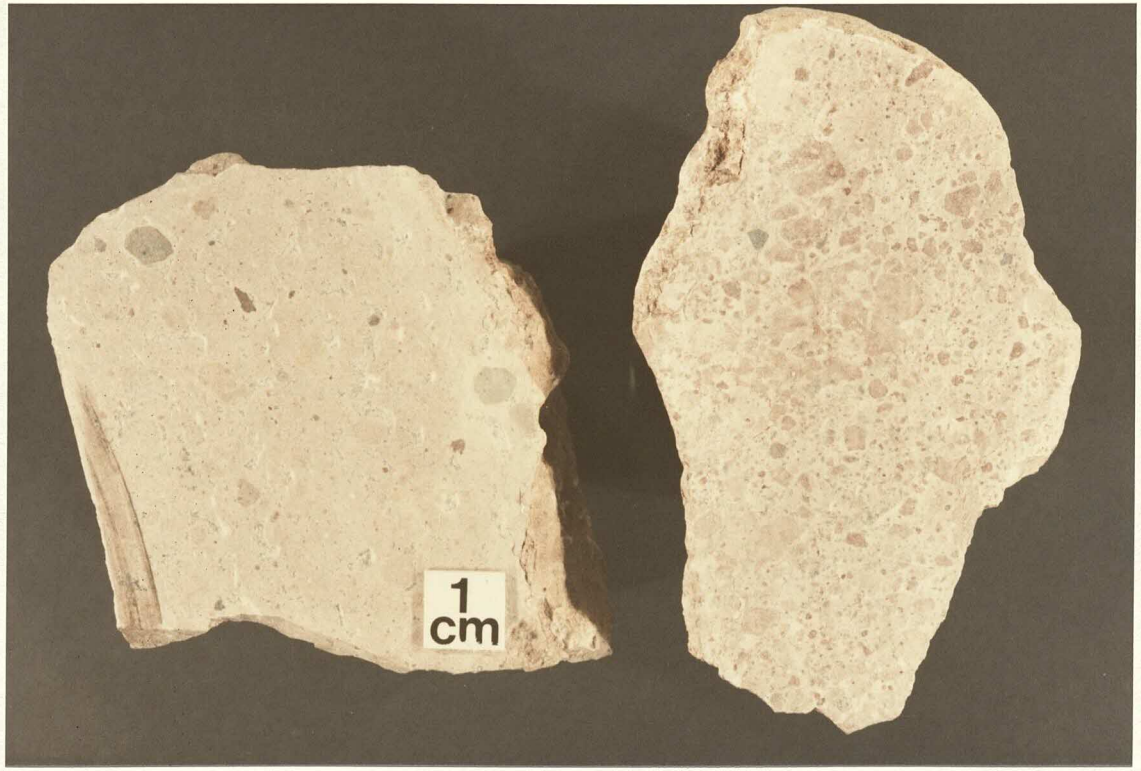
1
cm

Fig 3.88. Large and often elongate solutional cavities showing sequential filling by:
1) dark micrite
2) vadose silt (sometimes several generations)
3) blocky fresh-water phreatic cement.
Abundant circumgranular cracks in host sediment and some glaebules / "pisoids" in cavities.
Interpretation: Spectacular example of the action of microkarst processes. In extreme cases, vadose silt may replace much of the rock (see figs 3.89 & 3.92). Recognition of totally-filled cavities is difficult using optical microscopy, but may be facilitated by the use of cathodoluminescence, as the vadose silts are non-luminescent (see figs 3.180 & 3.181). Stained section. Field of view: 9mm. Top of Mambrillas de Lara Member, Senora de Brezales.

Fig 3.89. Vadose silt from microkarst cavities making up much of the rock - in this instance vadose silt is difficult to distinguish from micrite matrix, which itself may have been subject to partial recrystallisation (see Chapter 7). Rounded intraclasts of more organic-rich biomicrite. Unstained section. Field of view: 9mm.

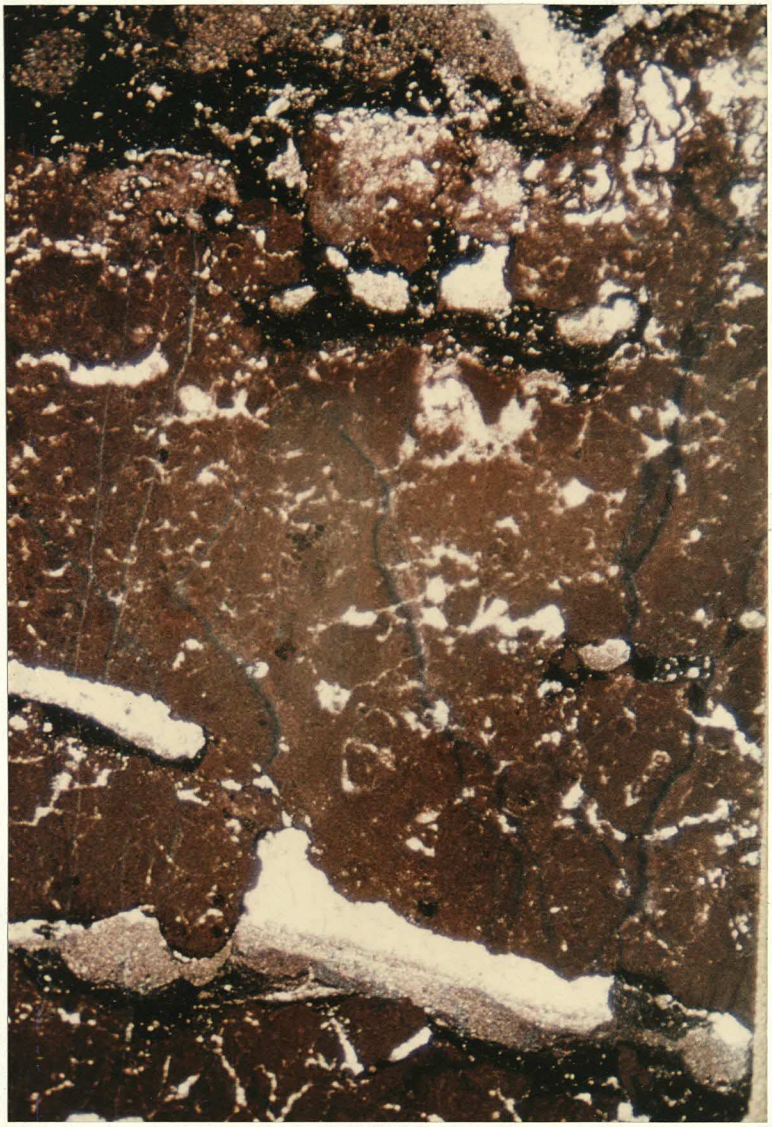

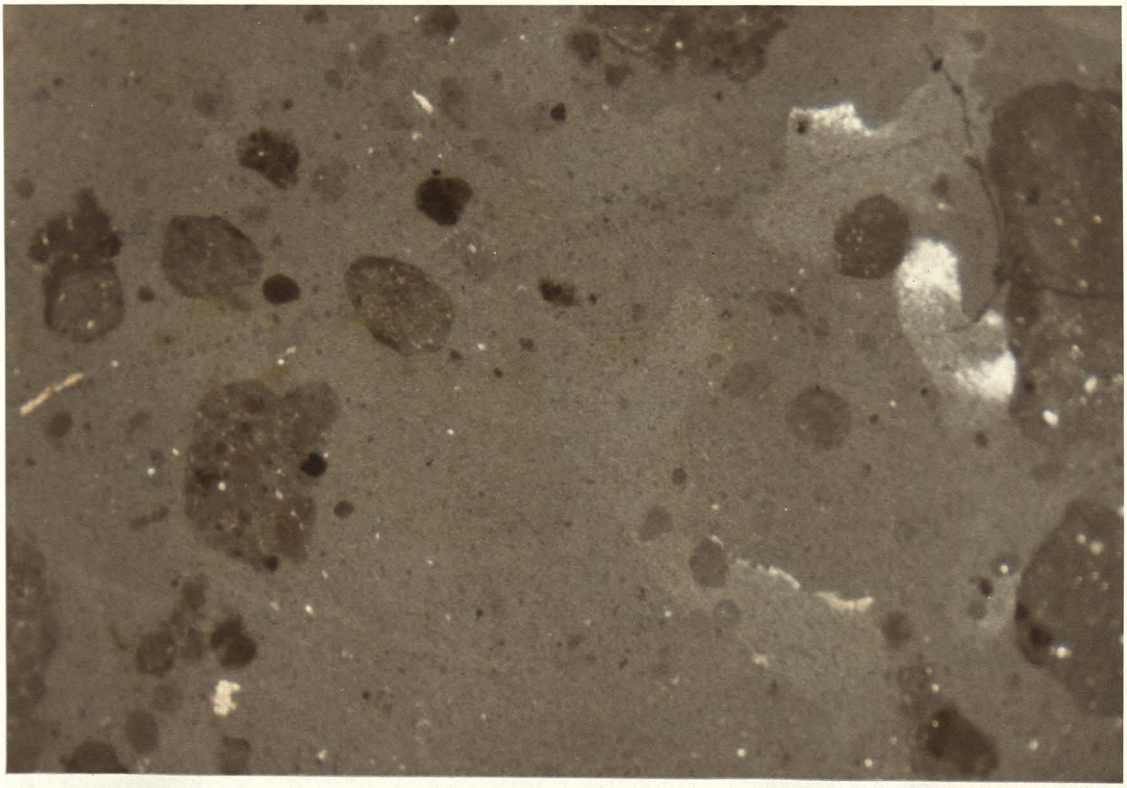

Fig 3.90. Field view of microkarst cavities (upper left, above hammer end, and centre, to right of pick end. Younging in direction of pick end. Cavities penetrate vertically up to 10cm from irregular subhorizontal surface. Abundant included intraclasts. Black pebbles also visible (upper centre). Rio Cabrera Member. 800m S of Rupelo.

Fig 3.91. Micrograph of subvertical microkarst cavity / fissure. Abundant perched fills of microspar - "vadose silt" - between intraclasts of dark-staining micrite including charophyte stem. Later void-filling blocky fresh-water phreatic cement.
Interpretation: Microkarst processes causing brecciation of open lacustrine biomicrite.
Stained section. Field of view: 9mm.
Mambrillas de Lara Member. Torrelara.

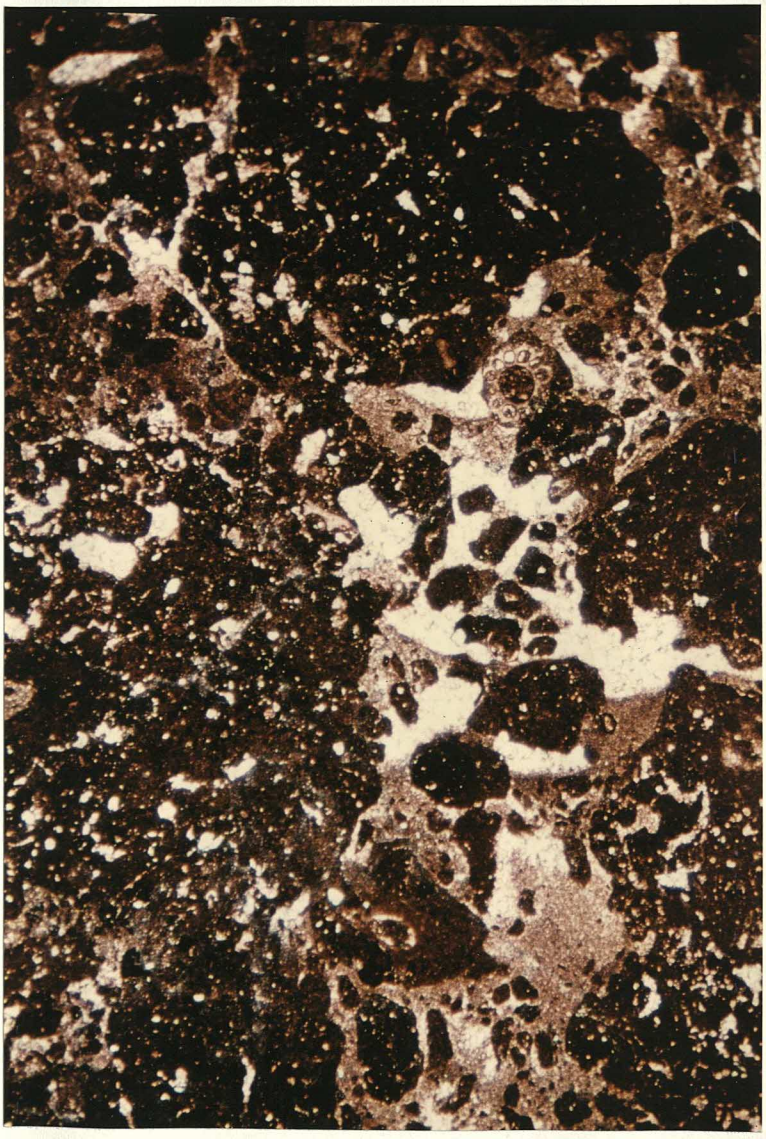

Fig 3.92. Large cavities showing perched fills of microspar making up much of the rock. Host sediment shows abundant circumgranular cracks and development of glaebules which are then released into the cavities, or reworked and subsequently washed in as inverse-graded "grainstone" cavity fills. Later isopachous, and final slightly ferroan phreatic void-filling cements.
Interpretation: Combined action of desiccation brecciation and microkarst processes can ultimately lead to development of isolated patches of grainstone texture.
Stained section. Field of view: 9mm. Ladera Member. Mambrillas de Lara.

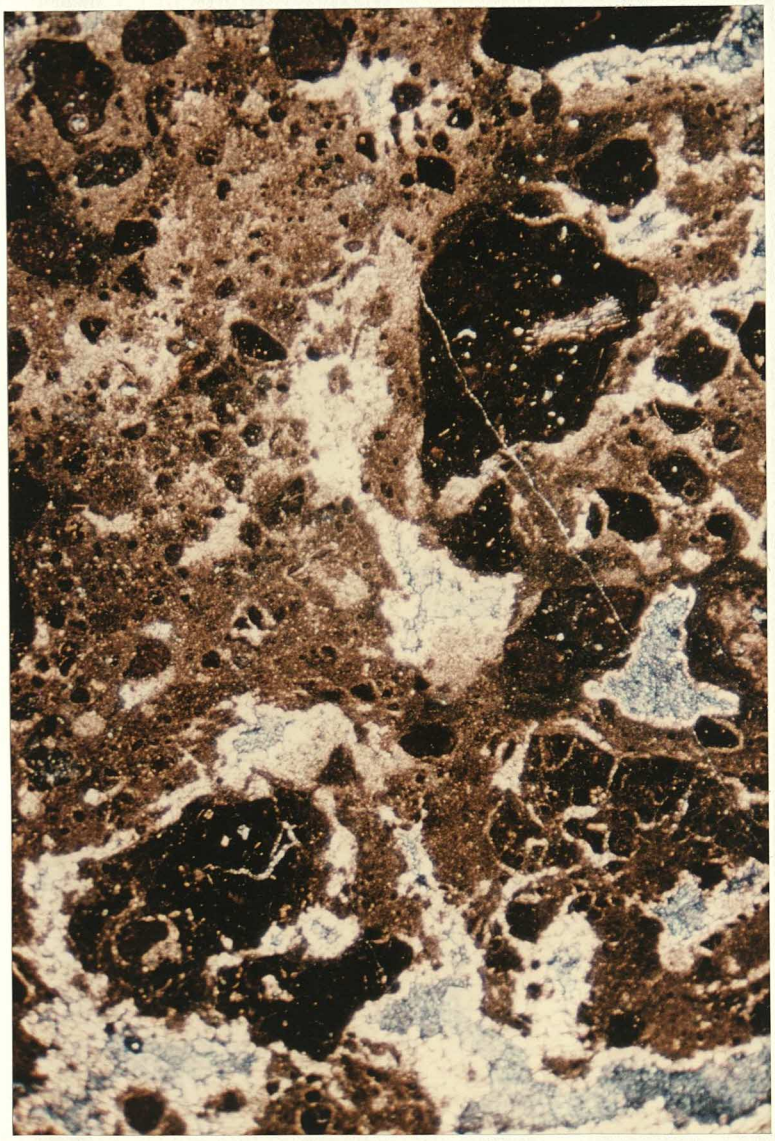

Fig 3.93. Mechanism for the formation of microkarst cavities. From Freytet & Plaziat (1982).

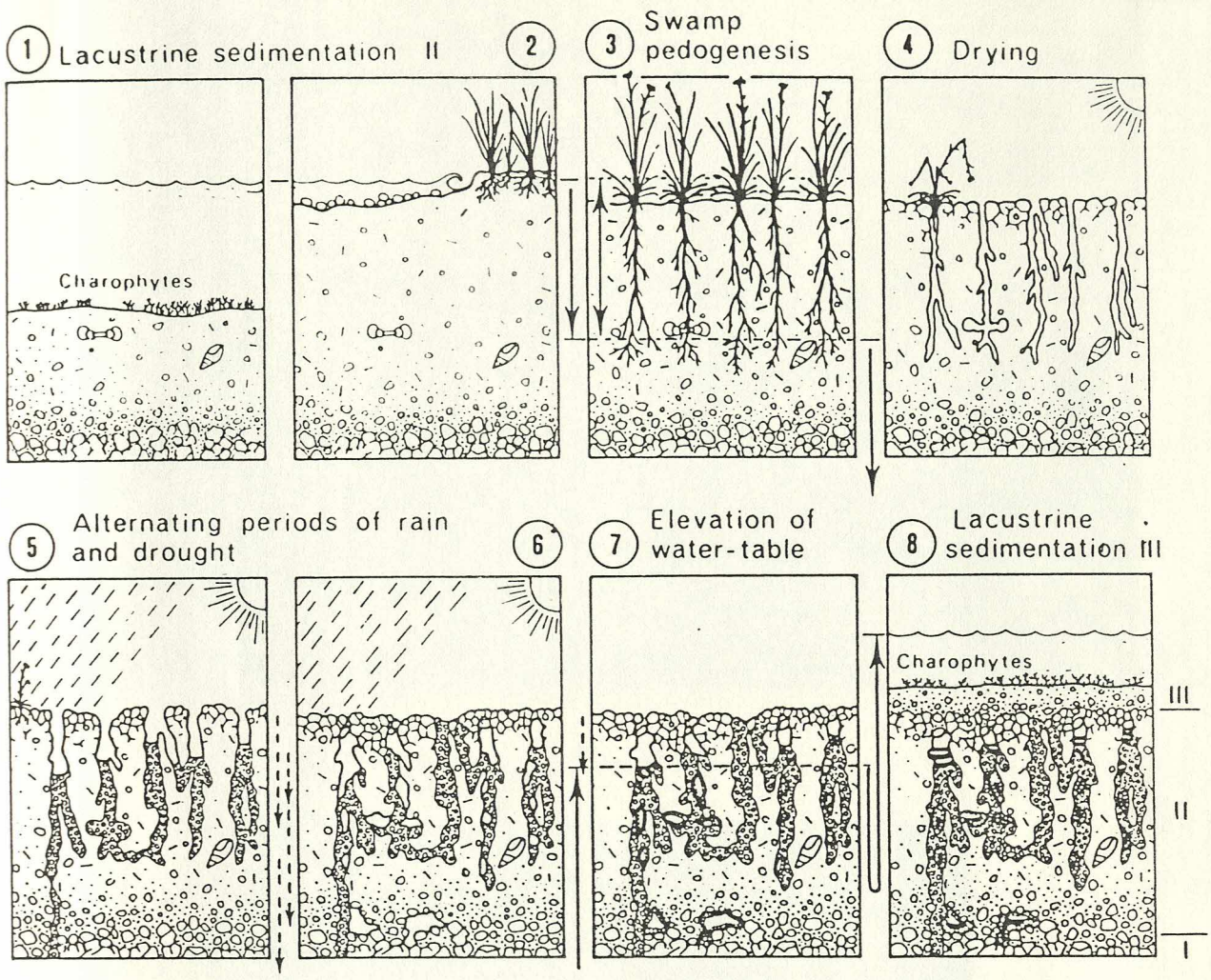

Schematic evolution of pedogenetic pseudo-microkarst (after Plaziat & Freytet 1978). A phase of lacustrine sedimentation (with charophytes, *Planorbis, Lymnaea*, etc.) (1) was terminated by a layer of muddy gravel sediment, furnished by littoral erosion (2). A lowering of water-level permitted colonization by a deep-rooted vegetation (3), the depth of root-traces indicates that the water-table was periodically deeper than 1 m. During fluctuation of the water-table dissolution of molluscs shells was locally active.

A permanent drying (4), following the lowering of the water-table below the limit of root penetration caused the disappearence of this vegetation and the formation of desiccation fissures (joint, skew, craze and curved planes). Sudden rainfall periodically interrupted the drying and determined concurrently widening and filling of the voids by eroding pulverulent gravelly material from the desiccated walls (5). The initial heterometric filling was partly eroded by subsequent rains (6), and the filling of the new cavities was achieved in successive stages, minor discontinuities separating individual lenses of laminated deposits. Rise of the water-table (7) cut off internal filling. The cavities, thus situated in a phreatic environment, are lined by isopachous sparitic calcite. When the water-table was slightly lower (7–8) a second phase of finer internal sediment was introduced both into lower voids, where it overlies the sparitic lining, and into the upper. The return to transgressive lacustrine conditions (8) interrupted the development of this pseudo-karst. However, it is possible that a subsequent emersion permitted a new generation of roots to reach the buried sequence causing superimposed networks which could re-open ancient cavities (with superimposed fillings, see Fig. 42). Although this type of evolution requires a slow rate of lithification (loose matrix when water-filled), the permanence of vertical cylindrical voids (Fig. 43) shows that consolidation occurs before any cementation, due to lime cohesion during periods of dryness.

Freytet & Plaziat (1982)

Fig 3.94. Vertical microkarst cavities in Aguilar Fm, SW Cantabria. Locality first described by Comas (1981). Cavities (slightly darker grey carbonate) penetrate up to 30cm through grey limestone with abundant angular-branching (desiccation) cracks. Numerous included peloids / intraclasts. Horizontally elongate areas of spar visible, left centre. Aguilar Inferior Member. Quarry 1km N of Aguilar del Campoo.

Fig 3.95. Close-up view of cavities shown in fig 3.88. Heavily-cracked carbonate host showing strong incipient brecciation. Intraclasts / peloids in cavities strongly rounded. Aguilar Inferior Member. Quarry 1km N of Aguilar del Campoo.

Fig 3.96. Green marls associated with pedogenically modified horizon. "Dirt Bed". Basal Purbeck. Portland, U.K..

Fig 3.97. Torrelara Bed. 1m bed of limestone conglomerate, clasts irregular, 2-40mm, set in matrix of limestone granules. Passes up into 50cm thick cross-bedded arenites. Marking base of Mambrillas de Lara Member. 1km N of Torrelara.

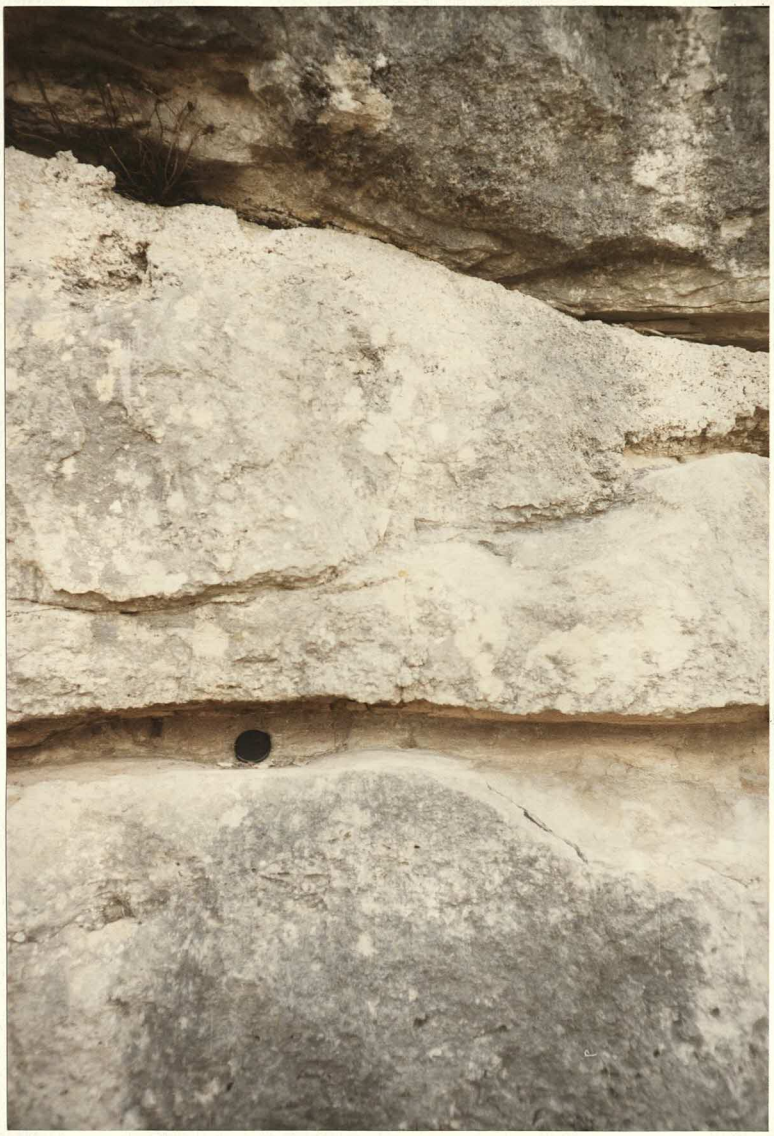

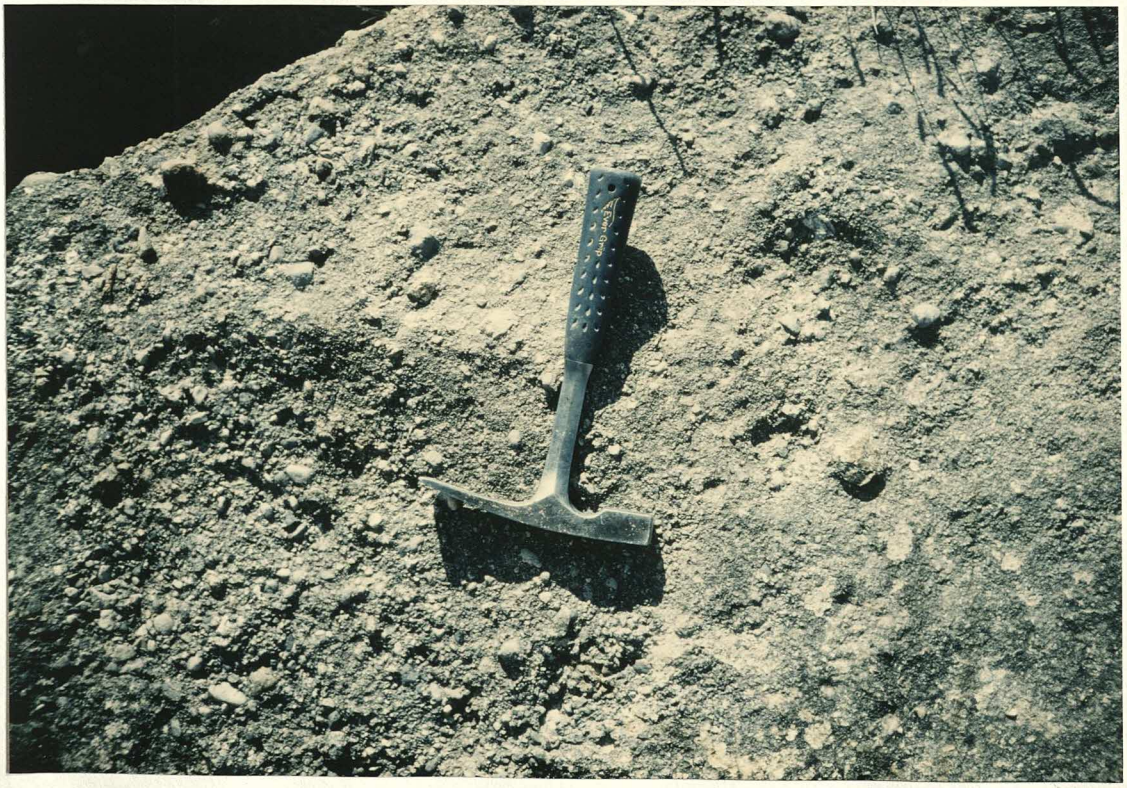
Vaughan
Power Grip

Fig 3.98. Field view of Rupelo Formation succession, NW sector of study area. Marine Jurassic (Lower Callovian) under bushy area, extreme left. Marls (Las Vinas Member) not outcropping under cornfield (centre left). Scarp (centre) Ladera Member massively bedded marly limestones. Torrelara Bed (limestone conglomerate and arenites) outcrops behind bushes extreme right. Cornfield (centre right) over non-exposing marly limestones and marls (base of Mambrillas de Lara Member). Small scarp behind bushes, extreme right, consists of thinly-bedded fossiliferous biomicrites of Mambrillas de Lara Member. Cornfields behind and to right - clastics of Pedroso and Salas Groups and Utrillas Formation. Mountain in distance of Upper Cretaceous limestones. Looking SE, 1km N of Torrelara.

Fig 3.99. Metre-scale interbeds of open lacustrine biomicrites and marls. Erosion surface shown in fig 3.129 occurs by tiny yellow gorse blooms above road side, centre. Mambrillas de Lara Member. Mambrillas de Lara, looking W.

Fig 3.100. Thick sequence of metre-scale dark fossiliferous biomicrites and thin dark marl interbeds.
Interpretation: open lacustrine.
This is an unusually thick sequence of open lacustrine deposits - 20m - elsewhere the Mambrillas de Lara Member is often only 1-3m thick.
Field vehicle is 3.06m in length. Mambrillas de Lara Member. Tenadillas, 3km S of Pinilla de los Barruecos, looking S.

Fig 3.101. Thick sequence of dark fossiliferous biomicrites (charophytes, ostracods), thin partings of marl (proportional thickness reduced by strong differential compaction). Limestone beds above and to left of hammer show weak lensoid geometry - possible evidence for current action? Mambrillas de Lara Member. Tenadillas, 3km S of Pinilla de los Baruecos.


GB ODU 857W

Fig 3.102. Wackstone, showing pale and dark micrite intraclasts (clasts reworked from marginal lacustrine areas and "black pebbles"). Also thin- and thick-shelled fossil débris - ostracods and gastropods / bivalves respectively. Mambrillas de Lara Member, Mambrillas de Lara.

Fig 3.103. Charophytes from the Rupelo Formation.

CHAROPHYTES FROM THE TIERRA DE LARA GROUP.

SAMPLE	LOCATION	LITHOLOGY	CHAROPHYTES	SOURCE OF IDENTIFICATION
SP 22	Mambrillas de Lara (upper part of Mambrillas de Lara Mb)	green - grey marl	Nodosoclavator bradleyi	P. O. Mojon (Neuchâtel)
			Porochara c.f. Kimmeridgiensis?	
SP 17	Mambrillas de Lara (base of Mambrillas de Lara Mb)	dark grey marl	Globator incrassatus	
			Globator maillardi	
			Nodosoclavator bradleyi	
			Flabellochara gravesi	
	Quintanilla de las Vinas (? top of Mambrillas de Lara Mb)	? grey biomicrites	T. forbesii	Salomon (1982)
			Perimneste horrida	
			Nodosoclavator aff. bradleyi	
229 C	Hortezuelos (? Rio Cabrera Mb / Hortigüela Fm)	dark grey marls (dedolomitised)	Perimneste horrida	P. O. Mojon (Neuchâtel)
			Clavator reidi	
			Nodosoclavator bradleyi	
			Porocharaceans sp.	

Fig 3.104. Charophytes from the Aguilar Formation (Sbeta, 1976).

CHAROPHYTES FROM THE AGUILAR FORMATION.

SAMPLE	LOCATION	UNIT	CHAROPHYTES	AGE
3-5AL	Camesa	2	Flabellochara gravesi (Harris) Grambast Perimneste horrida Harris Porochara c.f. maxima Donze Porochara sp.	Berriasian
3-5DL	Camesa	2	Nodosoclavator bradleyi (Harris) Grambast Flabellochara gravesi (Harris)	Berriasian
3-5L	Camesa	2	Porochara c.f. maxima Porochara sp.	Berriasian
V73-3	Villela	1	Porochar?	Jurassic?

Data from Sbeta (1976).

Fig 3.105. Biomicrite containing a variety of faunal elements: charophyte stem ("telephone dial", lower left), ostracod fragments (thin shell material above charophyte stem, gastropod débris (large curving thin shell fragment, extreme right) and bivalve fragments (thicker shell material). Intraclast (upper centre, uniform purple stain).
Interpretation: No evidence of emergence. Absence of lamination indicates oxygenation / bioturbation. Open lacustrine, moderate energy (fragmentation of fossil material and input of (?marginal lacustrine) intraclast.
Stained section. Field of view: 9mm. Mambrillas de Lara Member. Mambrillas de Lara.

Fig 3.106. Charophyte oogonia, longitudinal section, present in clast surrounded by incipient circumgranular crack.
Interpretation: Pedogenic modification of open lacustrine carbonate. Unstained section. Field of view: 4mm. Ladera Member. Ladera.

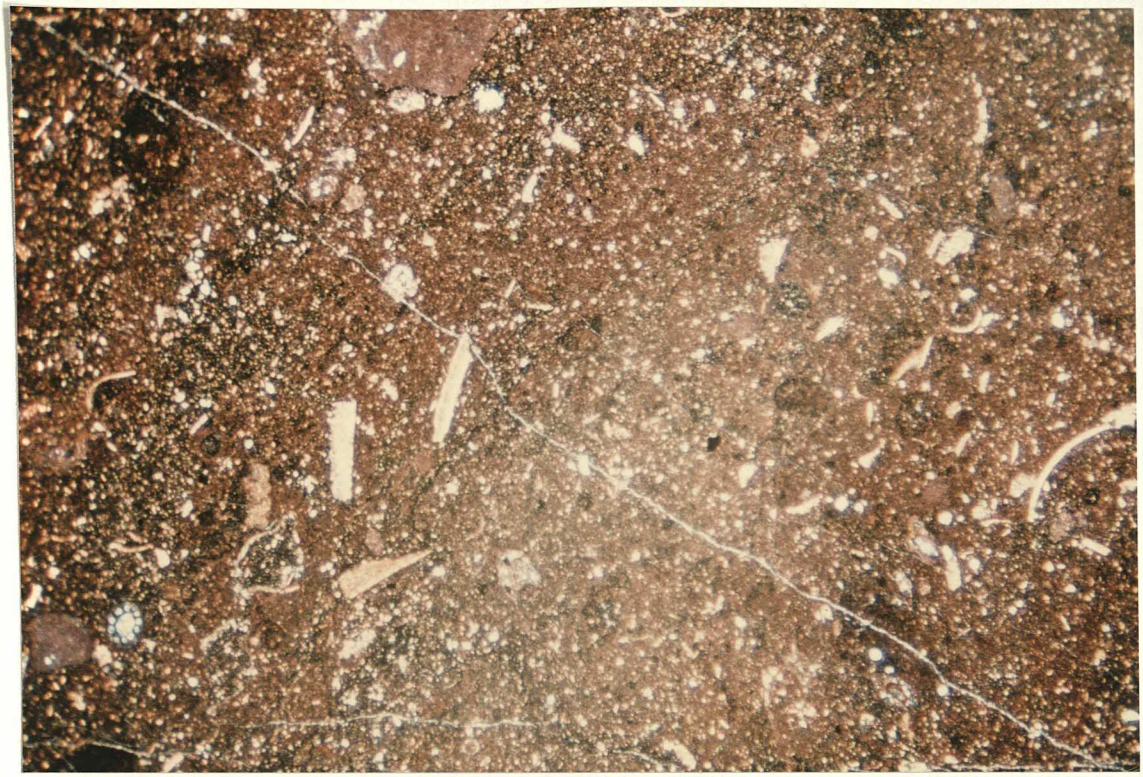

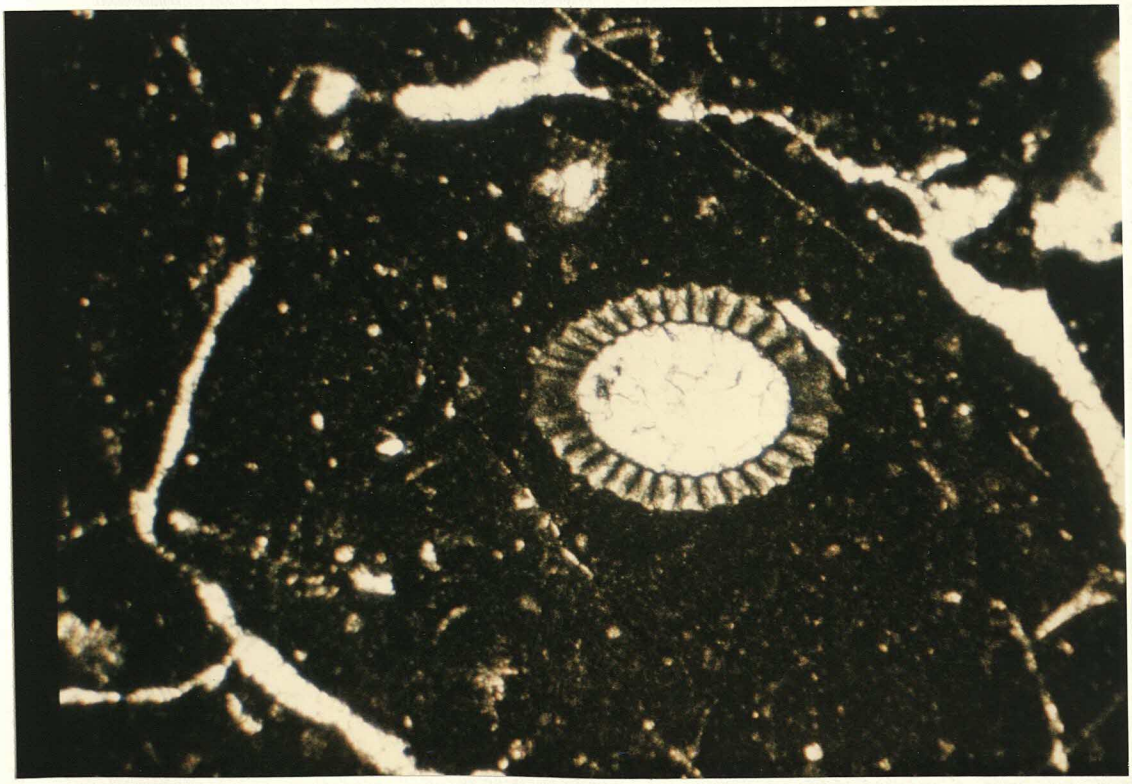

Fig 3.107. Charophyte dedolomite (see facies 14, figs 3.176 - 3.178) showing charophyte stem sections in a variety of orientations. Rhombic crystals of spar nucleated on stems showing slight staining (dedolomitised). ?Rio Cabrera Member / Hortigüela Formation. Rio Helechal, Hortezuelos.

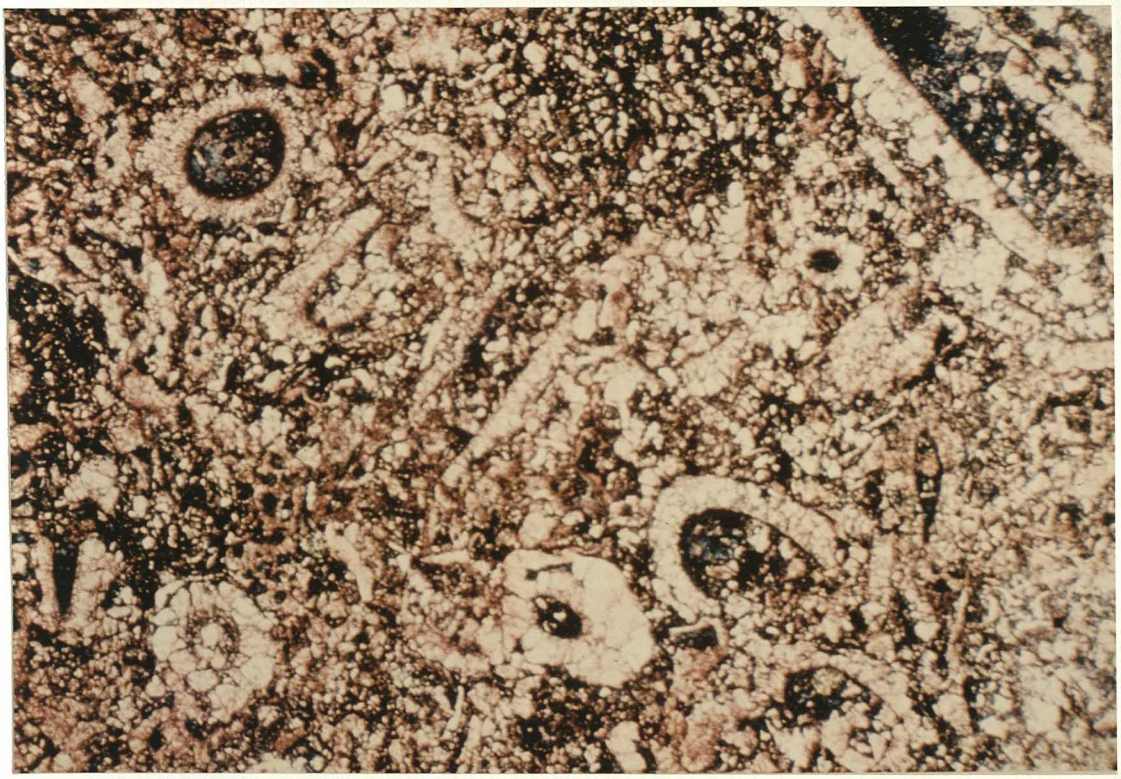

Fig 3.108. Biomicrite with abundant charophyte stems in transverse section, often disarticulated (cortical cells removed). Also some oblique sections. Gastropod section lower right. Interpretation: shallow water, open lacustrine. Stained section. Field of view: 9mm. Mambrillas de Lara Member. Espejon.

Fig 3.109. Biomicrite with transverse section of charophyte stem ("telephone dial"), also thin shell débris (ostracods and gastropods). Red / blue staining object may be fragment of charophyte node (oblique section) with late ferroan cement filling central cavity. Dark stain reflects small grain size and presence of organics and clay impurities. Interpretation: No evidence of emergence, fresh-water fauna/flora open lacustrine. Stained section. Mambrillas de Lara Member. Mambrillas de Lara.

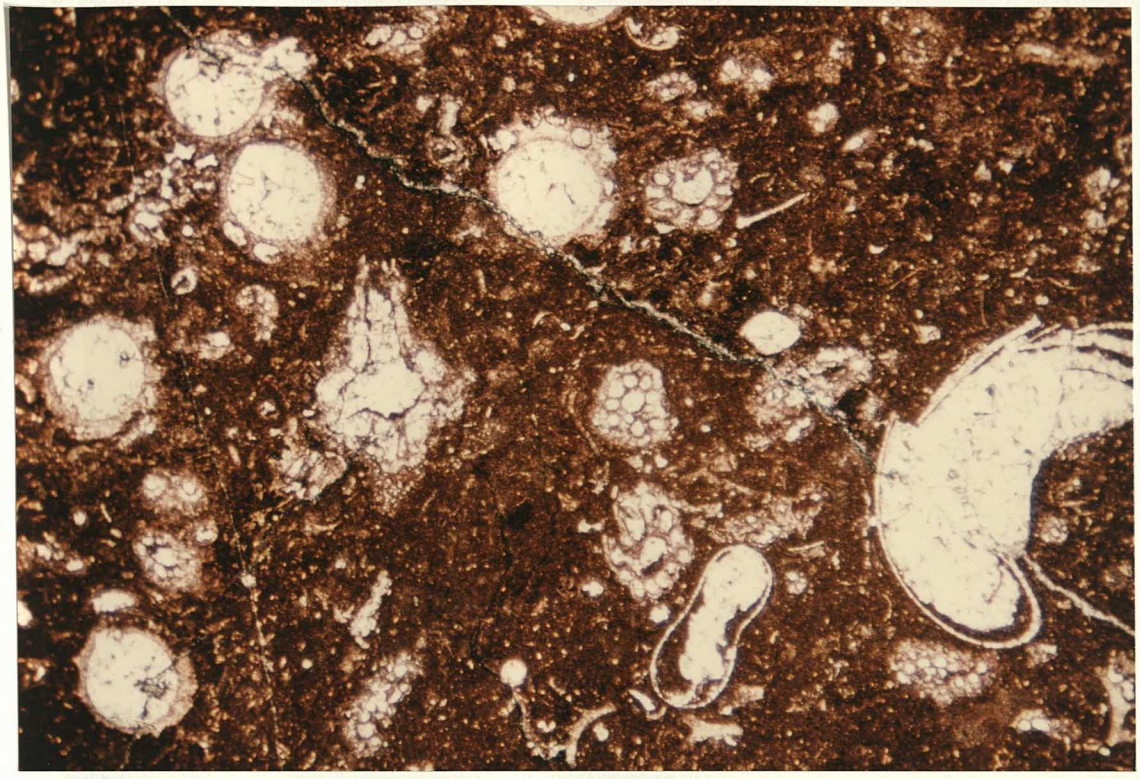

Fig 3.110. Charophyte morphology, showing structure of node sections. Modified from Sbeta (1976).

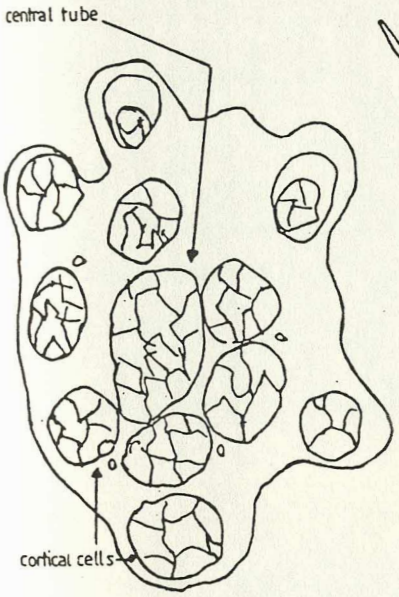

Node

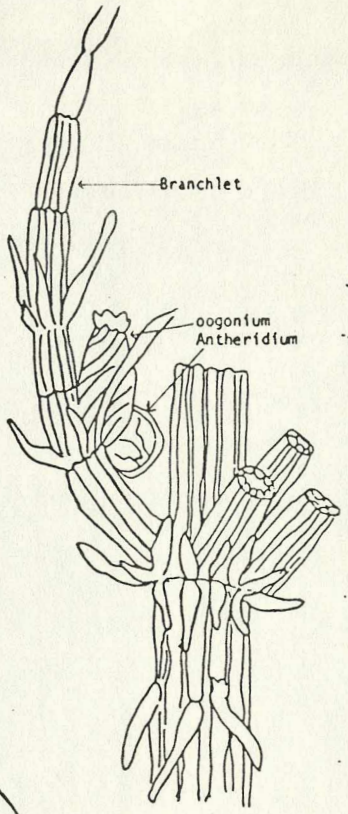

Internodes, Node, Branchlet

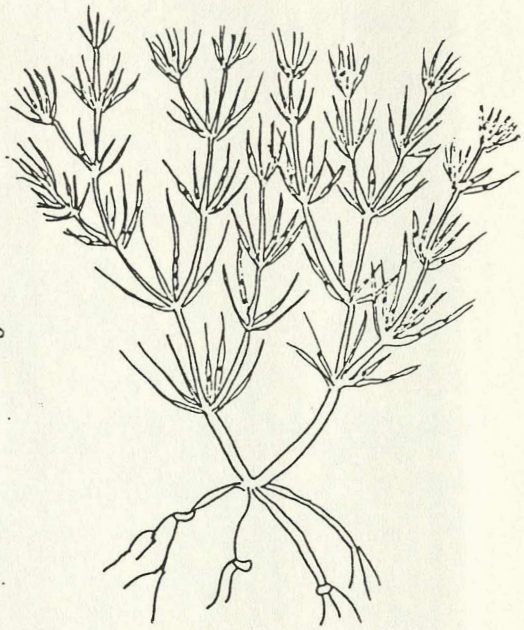

Complete plant of Chara - reduced.

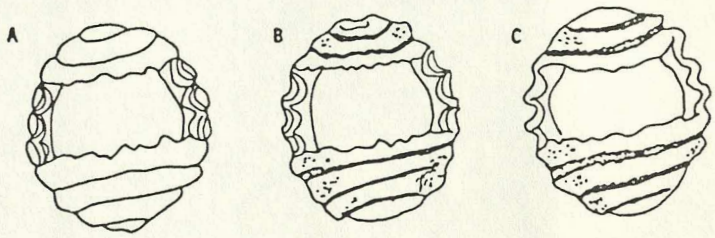

Difference in calcium carbonate deposition in enveloping cells. A - cellular ridges; B and C - cellular furrows

Charophyte morphology

Internal cast of gyrogonite (egg)

Broken gyrogonite

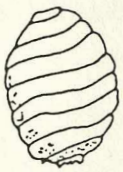

The whole surface of gyrogonite is preserved

modified after

Sbeta (1976)

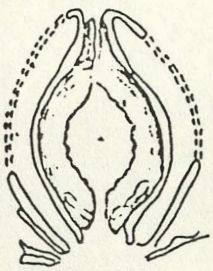

oogonium

gyrogonite

utricle

Ideal longitudinal section of oogonium enclosed by utricle.

Internal view of oogonium

Internal structure of oogonium

Fig 3.111. Biomicrite with charophyte oogonia, showing different structure according to the location and orientation of sectioning. Spiral structure evident. Stems are rare in this specimen - the oogonia are more easily transported than the larger and more delicate charophyte stems - those here may been transported into slightly deeper water. Stained section. Field of view: 9mm. Mambrillas de Lara Member. Espejon.

Fig 3.112. Biomicrite showing disarticulated charophyte stems (cortical cells removed) and oogonia. Also ostracod débris. Some evidence of compaction - flattened stems and oogonia. Late filling by ferroan cement (blue stain). Stained section. Field of view: 9mm. Mambrillas de Lara Member. Espejon.

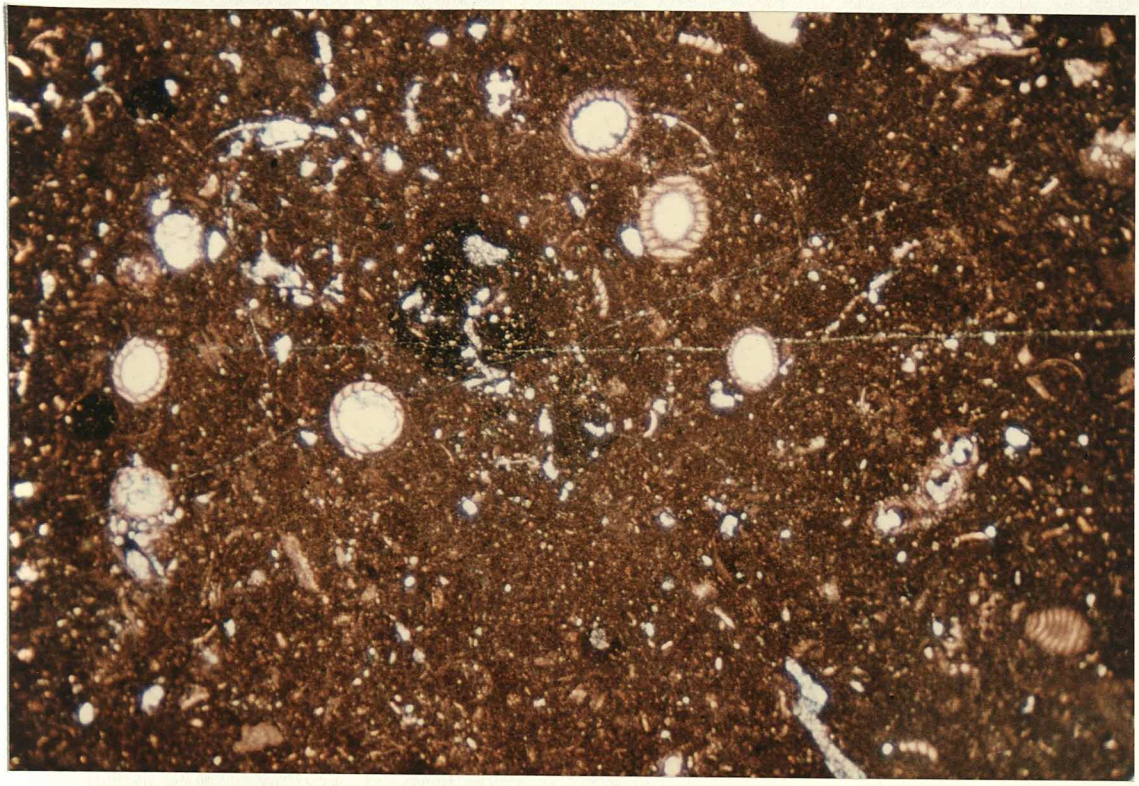

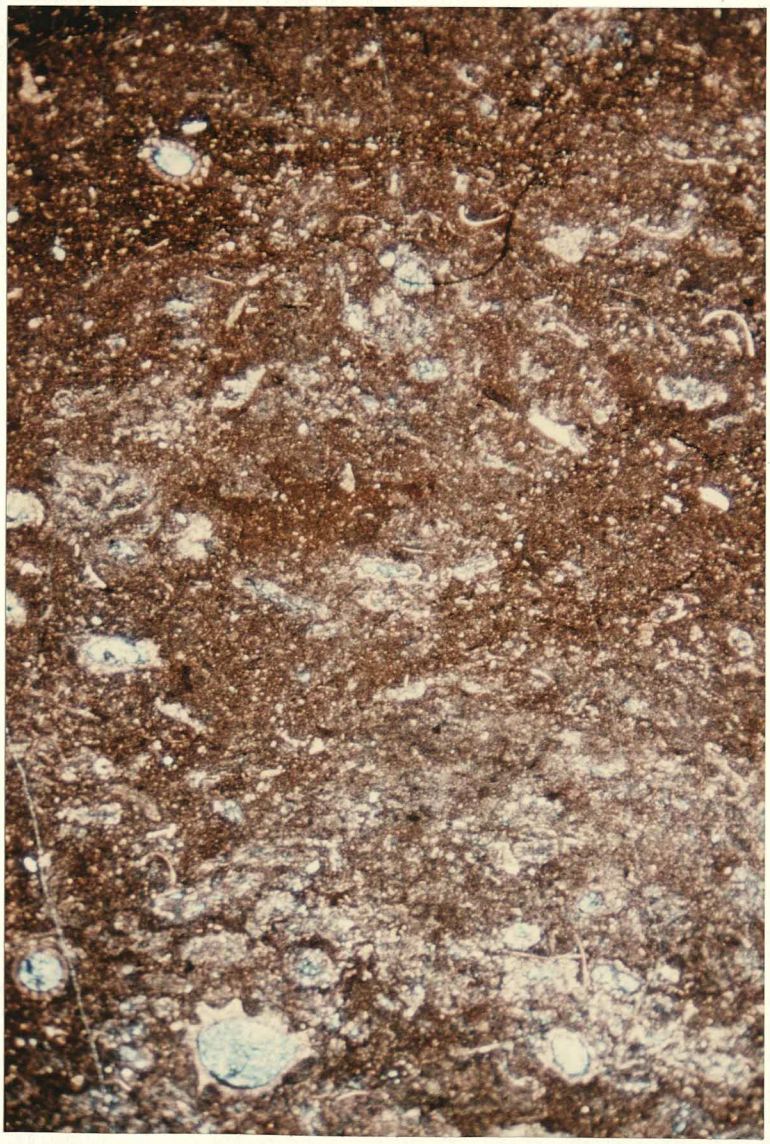

Fig 3.113. Ostracod test structure.

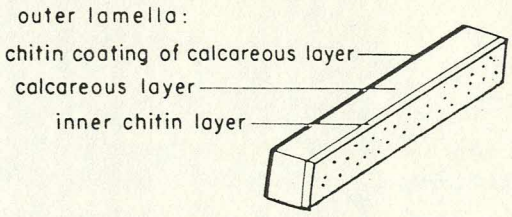

Ostracod Test Structure.

Fig 3.114. Biomicrite. Ostracod and gastropod fragments. Development of shelter porosity. Voids filled by later blocky ferroan (blue-stained) calcite spar cement. No evidence of emergence. No charophyte stems or oogonia.
Interpretation: open lacustrine, possibly deeper water.
Stained section. Field of view: 9mm. Mambrillas de Lara Member. Mambrillas de Lara.

Fig 3.115. Vertebrate débris, set in dark marly biomicrite. Sauropod bones - largest is collar rib fragment. Bones preserved in vivianite. Bones locally reworked into overlying thin marl unit.
Interpretation: Open lacustrine. Sauropods were extremely large (up to 15m) herbivores which inhabited shallow fresh-water lakes, marshes and swamps. Food supply from charophytes and other fresh-water plants.
"Dinosaur Bed", Mambrillas de Lara Member. Ladera, near Mamolar.

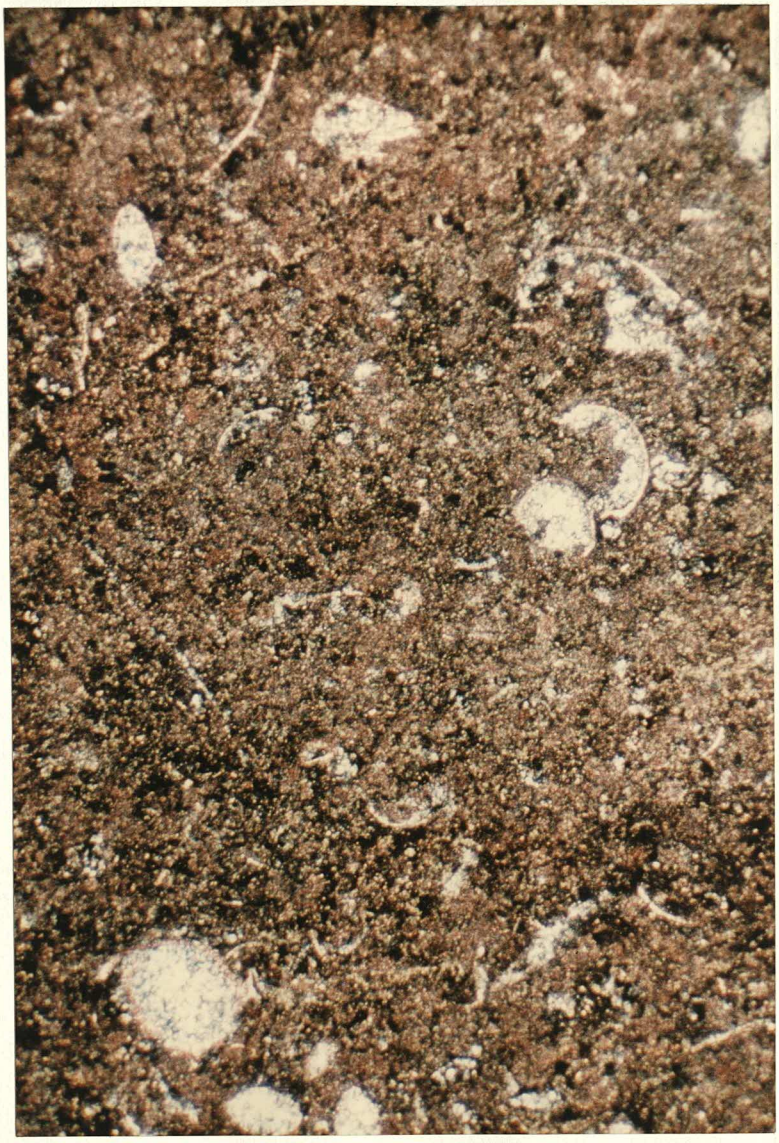

Fig 3.116. Sauropod fragments exposed on vertical bedding plane. Rock matrix rich in charophytes. Well-preserved Swiss geologist for scale (Dr A Strasser). "Dinosaur Bed", Mambrillas de Lara Member. Espejon.

Fig 3.117. Large sauropod bone fragment. Specimen is upper part of limb bone with smooth, rounded upper surface for freedom of movement in ball-and-socket joint. Other surfaces are rough - porous bone structure clearly visible. "Dinosaur Bed", Mambrillas de Lara Member. Ladera, near Mamolar.


1
cm

Fig 3.118. Close-up view of small sauropod bone fragment. Porous bone structure visible - note increased cavity size in central part of specimen. "Dinosaur Bed", Mambrillas de Lara Member. Ladera, near Mamolar.

Fig 3.119. Micrograph of sauropod bone shown in previous figure. Brown phosphate; many rounded mm-scale cavities - these represent the course of blood vessels. Partial geopetal filling of these cavities with biomicrite including ostracod fragments; later void filling spar. Unstained section. Field of view: 9mm. "Dinosaur Bed", Mambrillas de Lara Member. Ladera, near Mamolar.


1
cm

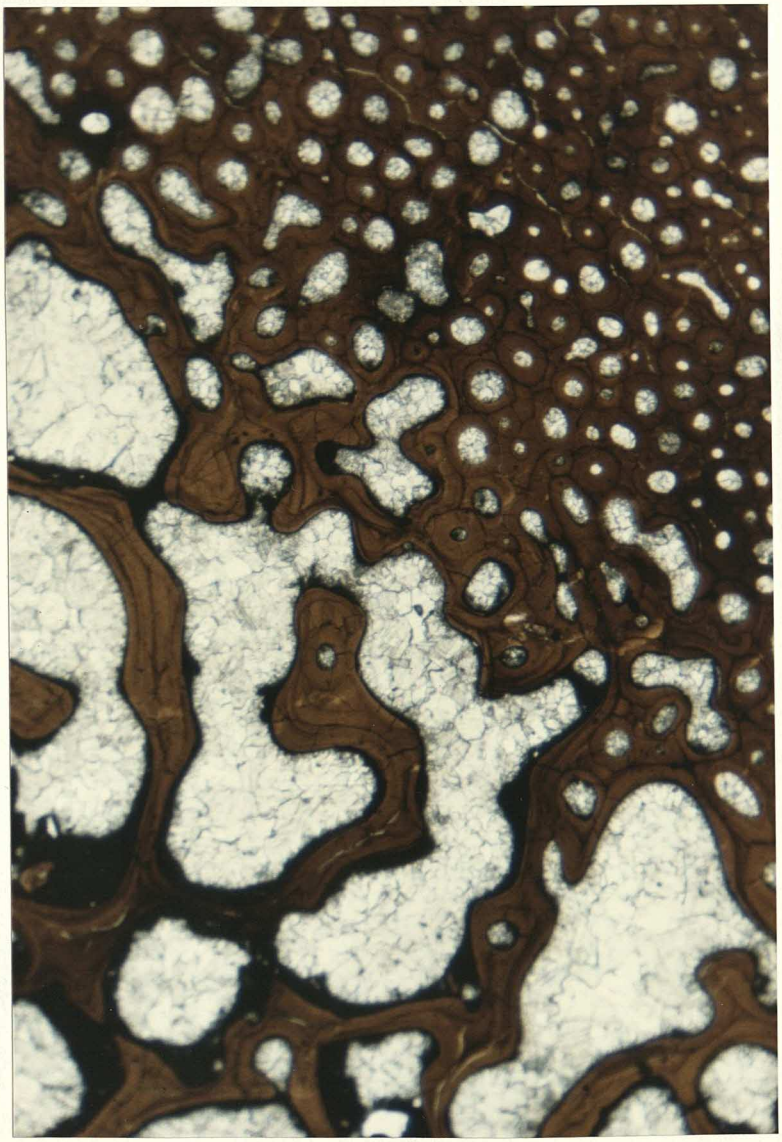

Fig 3.120. Depression on bedding plane interpreted as vertebrate (probably sauropod) footprint. Note rounded outline, and raised rim caused by displacement of soft sediment by foot. "Dinosaur Bed". Mambrillas de Lara Member. Mambrillas de Lara.

Fig 3.121. Same footprint as in fig 3.120, with human foot to give an idea of the mechanism for formation of raised rim. "Dinosaur Bed", Mambrillas de Lara Member. Mambrillas de Lara.

Fig 3.122. Depression on bedding plane interpreted as vertebrate footprint. Three protruding marks at hammer end interpreted as toe marks. "Dinosaur Bed", Mambrillas de Lara Member. Quintanilla de las Vinas.

Figs 3.123 & 3.124. Charts showing salinity tolerance of various groups of organisms.

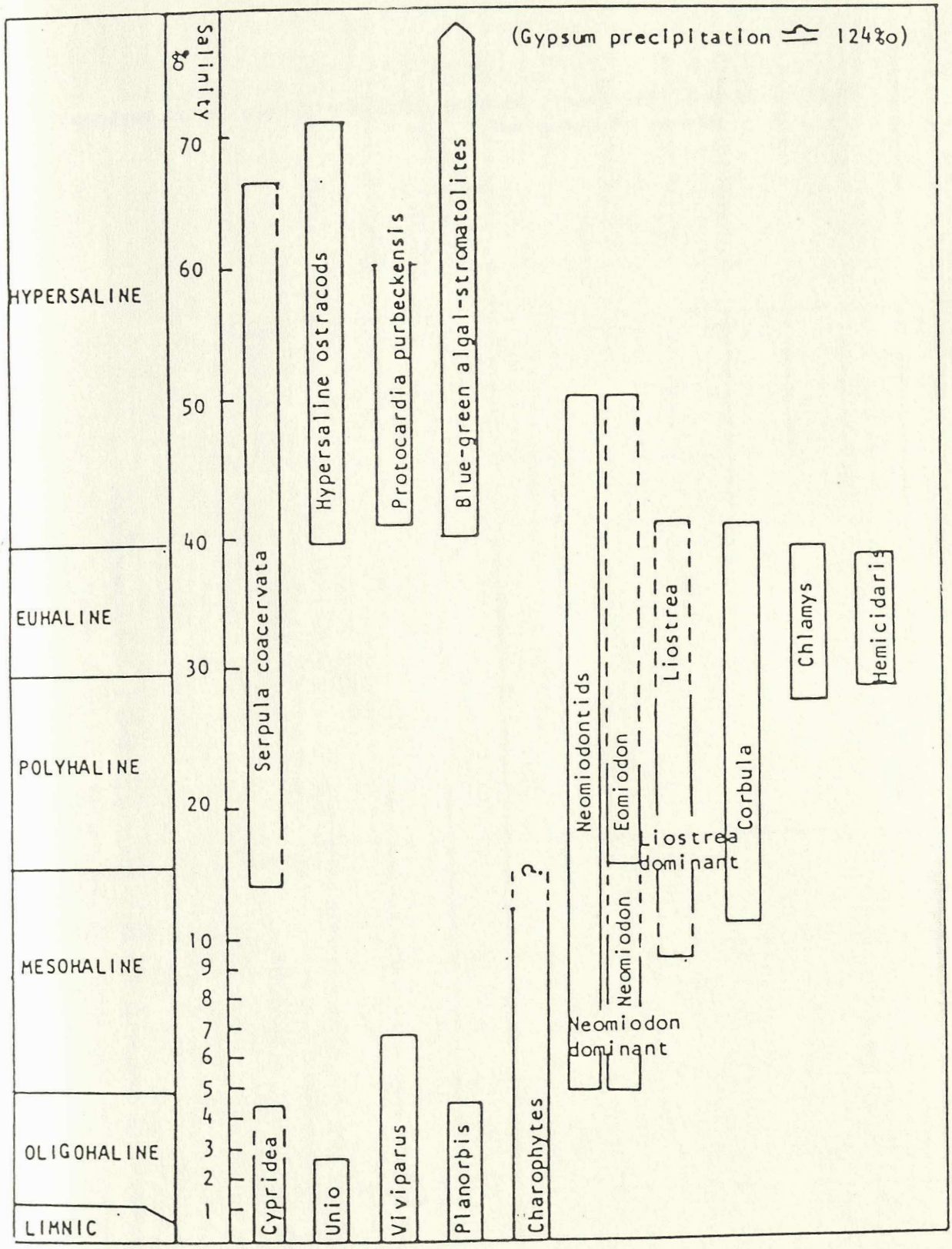

Estimates of usual salinity ranges of some Purbeck faunal and floral elements based on comparisons with certain modern and ancient assemblages and on associations with evaporites, etc. (sources include: Casey, 1955; 1971; Daley, 1972; El-Shahat, 1977; Hallam, 1976; Hudson, 1963; Huckreide, 1967; Kilenyi and Allen, 1968; Parker, 1960; West, 1975).

Figs 3.123 & 3.124. Charts showing salinity tolerance of various groups of organisms.

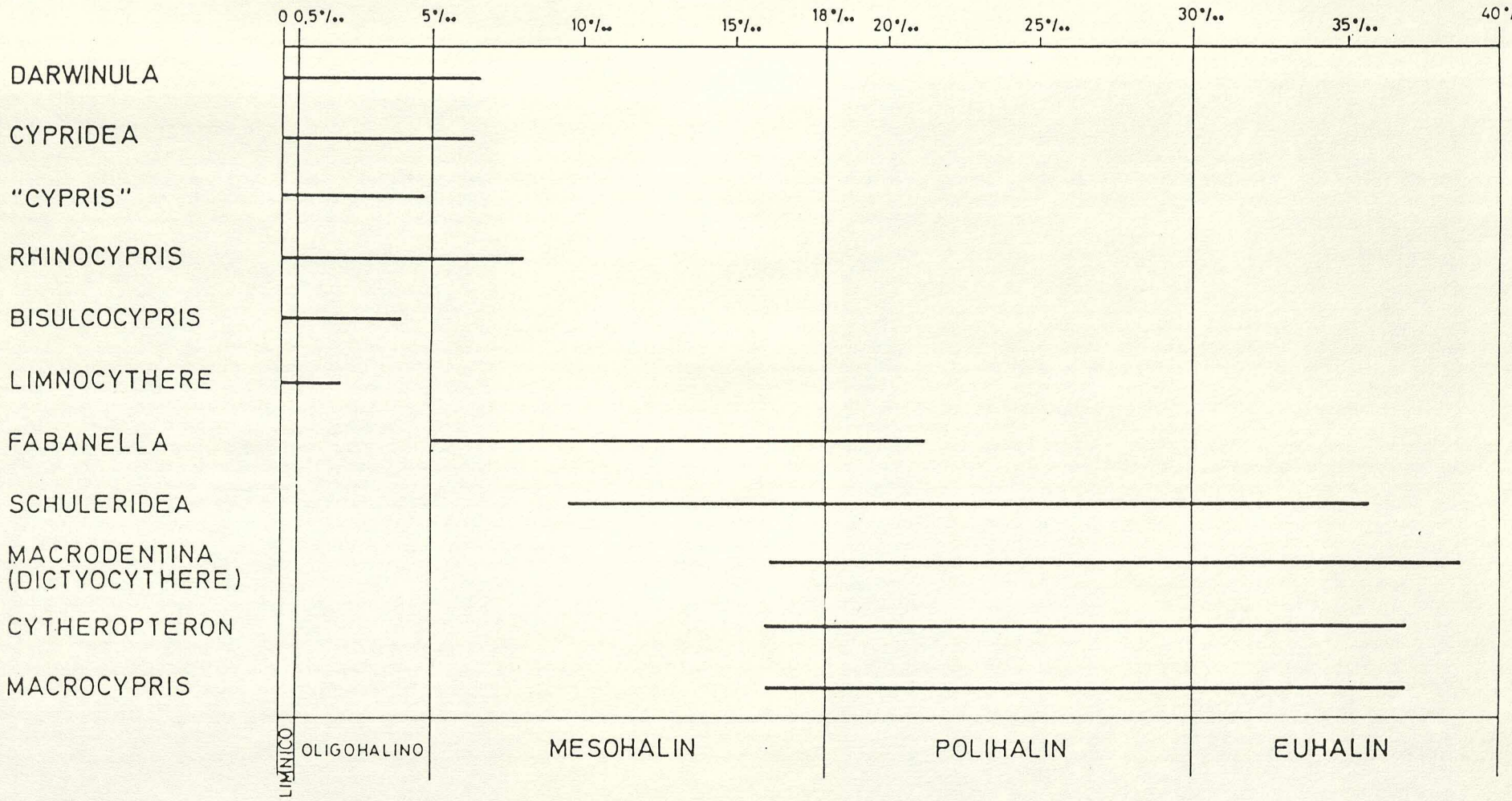

PROBABLES LIMITES DE TOLERANCIA DE SALINIDAD
DE LOS OSTRACODOS MAS FRECUENTES
EN LAS FACIES PURBECKIENSE Y WEALDENSE DEL NORTE DE ESPAÑA

Fig 3.125. Micrograph of marly biomicrite showing weak diffuse lamination. Strong compaction of charophyte fragments (oogonia and oblique stem sections). Deep red stained areas may be node fragments. Also rare quartz grains. Stained section. Field of view: 9mm. Mambrillas de Lara Member. Espejon.

Fig 3.126. Hand specimen of marly biomicrite with abundant geopetally-filled cavities. Note that the cavities are often completely filled with pure white spar, so that they may be difficult to recognise as cavities in the field. Mambrillas de Lara Member. Torrelara.

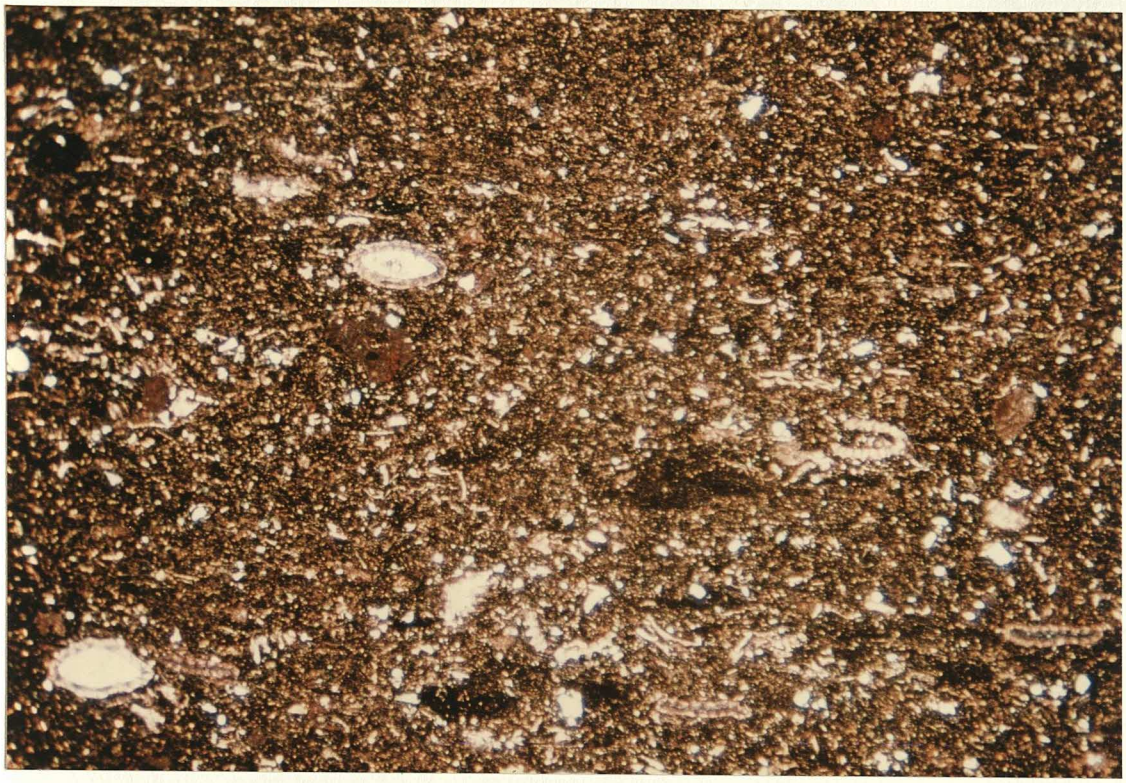

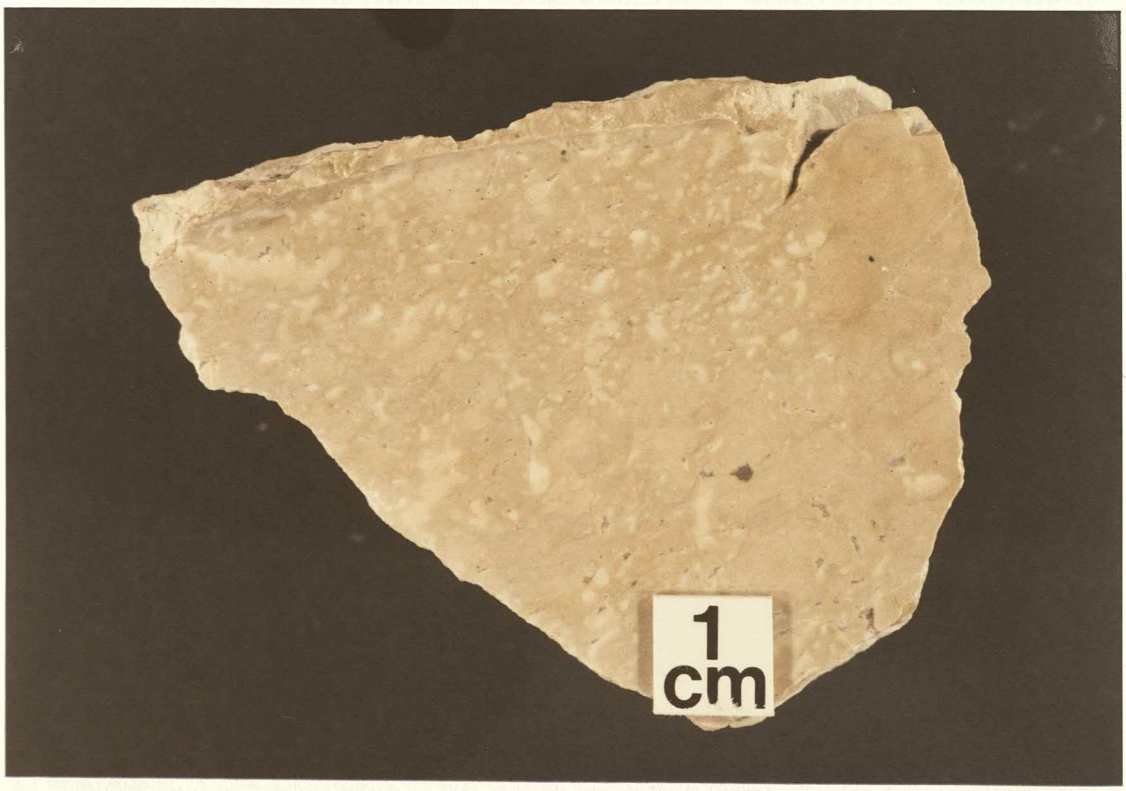
1
cm

Fig 3.127. Wackstone. Rio Cabrera Member. 800m S of Rupelo. 1-2mm rounded pale micrite intraclasts resting on irregular erosion surface in wackstone biomicrite. Note vertical variation in intraclast size and abundance.
Interpretation: reworking of pedogenically-derived and marginal lacustrine intraclasts into open-lake areas as a result of lacustrine transgression.

Fig 3.128. Close-up view of erosion surface shown in previous figure. Note: apparently two superimposed erosion surfaces with irregular bases (lower erosion surface especially); good sorting of 1-2mm rounded intraclasts at base; presence of both black (organic débris) and dark grey (open lacustrine facies) intraclasts; vertical variation in size, sorting and abundance of intraclasts.
Interpetation: several transgressive events; first one was over an irregular, possibly karstic surface.

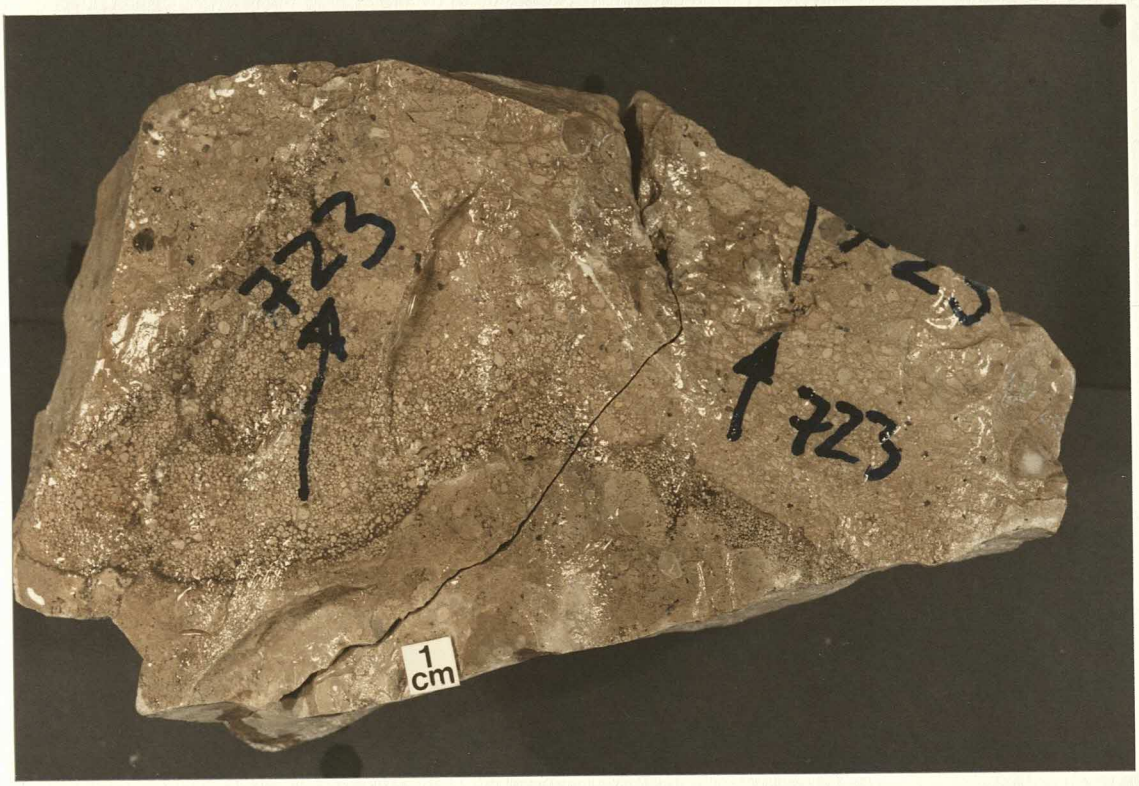
723
723
1
cm


1
cm

Fig 3.129. Formation of lacustrine wackstones and conglomerates as a result of reworking of root-brecciated marginal lacustrine carbonate. From Freytet & Plaziat (1982).

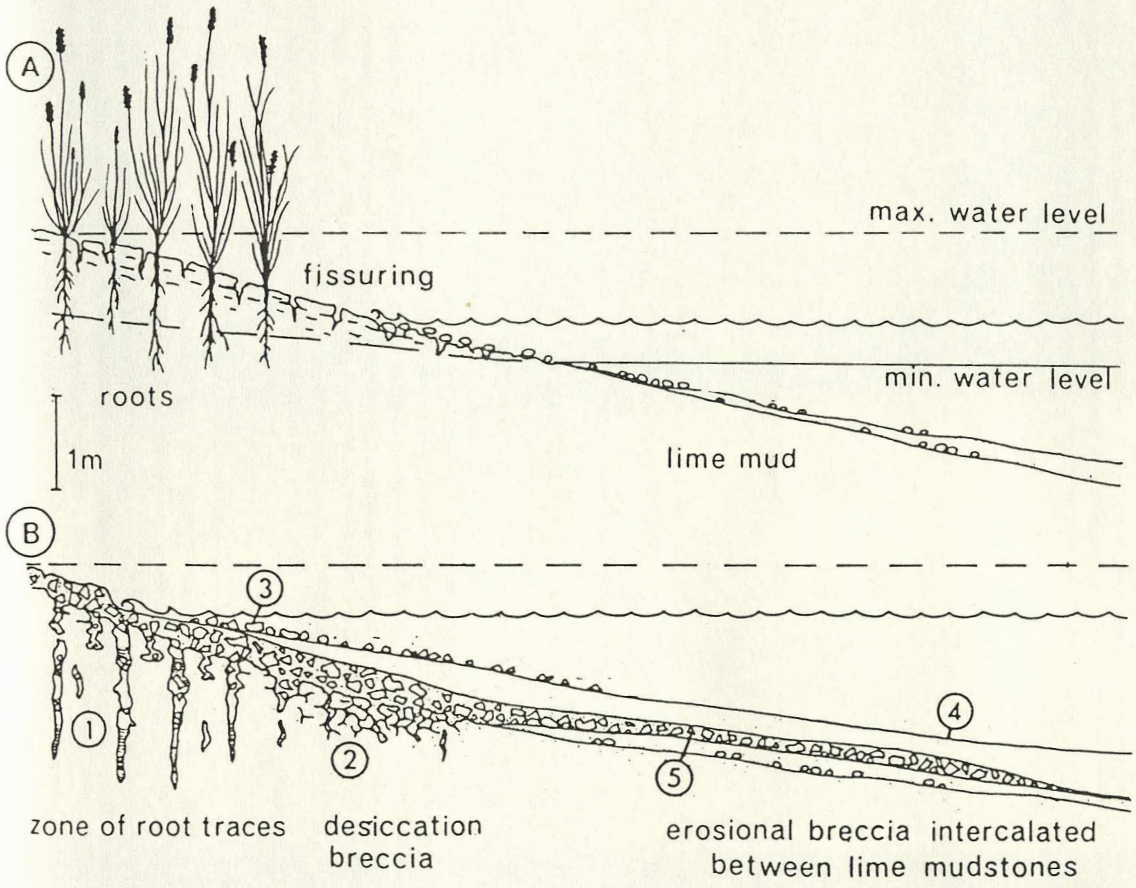

Interpretation of the origin of lacustrine and palustrine breccias based on the study of Paleocene and Eocene limestones (Corbières and Minervois).

A. Period of low water-level; exposed muds are covered with vegetation and penetrated both by roots and desiccation fissures. The formation of relatively minor quantities of gravels is due to wave action which tends to round these grains.

B. Period of high water-level: active reworking of angular desiccation clasts which tend to accumulate both in vertical cavities formed by decayed roots plus offshore lake environments.

Alternation of drying and flooding of the lake thus stimulates sediment brecciation, enlargement of the voids created by root decay, and their sedimentary infilling. Five significant facies may be distinguished: 1, limestone with root-traces filled with fine desiccation breccia and finer sediment ("pseudo-microkarst" phenomenon, see Ch. 5); 2, zone of fissured substrate filled with *in situ* breccia debris; 3, scattered elements reworked by wave action from the adjacent littoral zone; 4, lacustrine micrite; 5, interstratification of transported breccias and lacustrine micrites.

Freytet & Plaziat (1982)

Fig 3.130. Marly biomicrite with decimetre-scale polygonal desiccation cracks.

Fig 3.131. Micrograph of laminated biomicrite. Mm-scale laminae defined by fine terrigenous clastic material, perhaps introduced by river-generated subaqueous density currents. Fining upwards of laminae supports deposition by discreet events. Ostracod test, possibly reworked. Preservation of lamination could reflect either:
a) increased salinity; or
b) the onset of lake stratification (cf varves) and hence poor oxygenation and reduced bioturbation in deeper water; but probably it is the result of more rapid sediment input. Stained section. Field of view: 9mm. Mambrillas de Lara Member, 1km N of Torrelara.

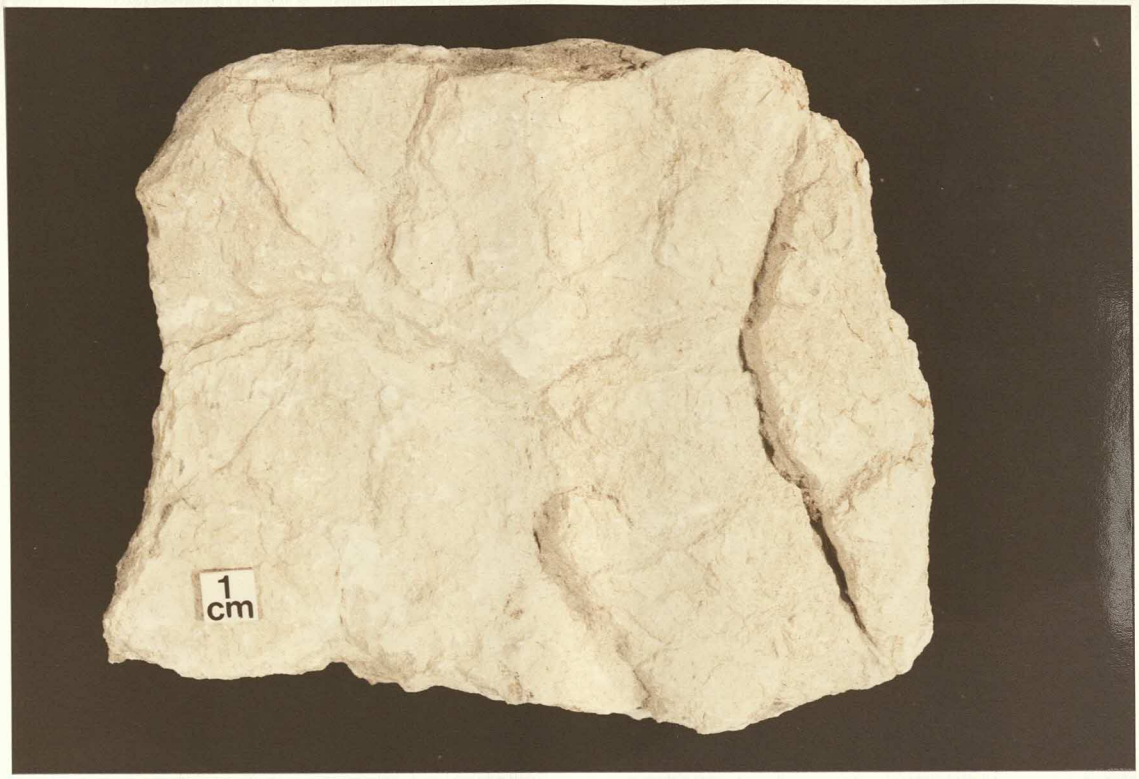
1
cm

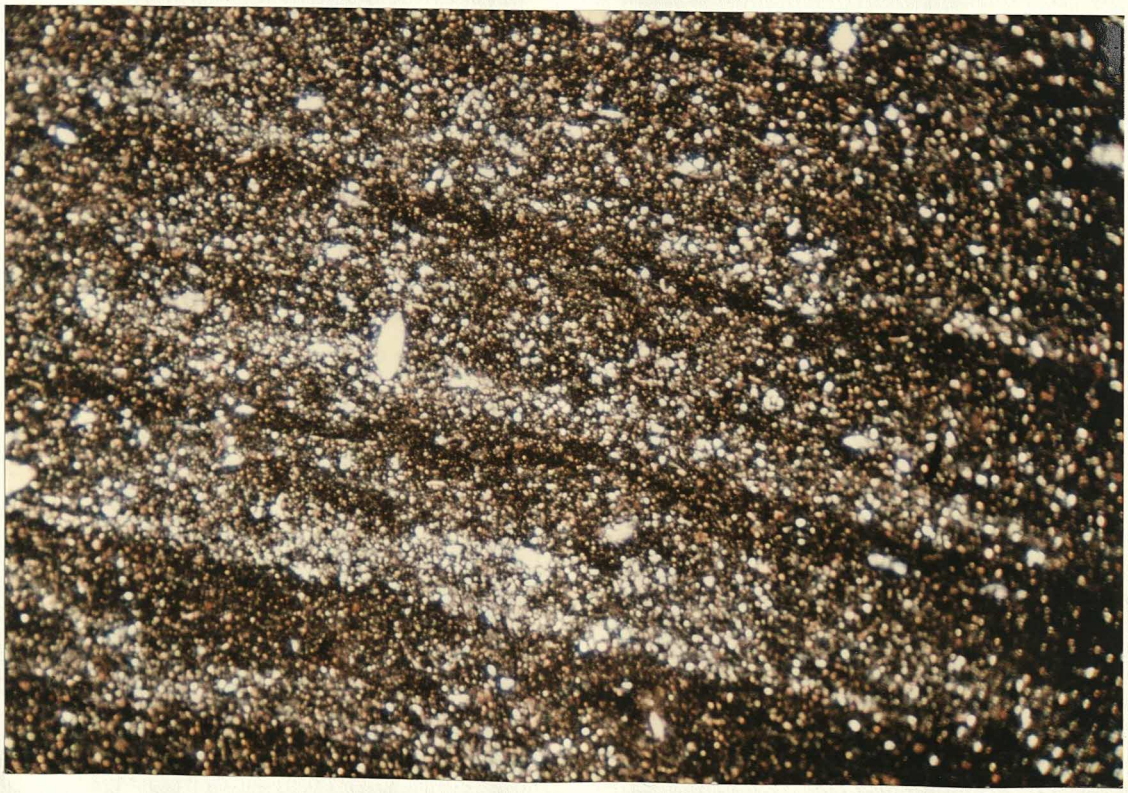

Fig 3.132. Weathered bedding surface showing characteristic "conglomeratic texture" common in Mambrillas de Lara Member. Originally thought to be a product of weathering, (fabric is only visible on weathered surface) this is now interpreted as reflecting the weathering of intraformational conglomerate with little lithological contrast between "clasts" and "matrix" - both are of fossiliferous, slightly marly biomiocrite. Clasts are irregular, 5-50mm.
Interpretation: Low-stage drainage channels.
Mambrillas de Lara Member. Mambrillas de Lara.

Fig 3.133. Erosional surface at base of unit with "conglomeratic texture". Irregular 5-50mm clasts of marly biomicrite set in marly biomicrite matrix.
Interpretation; Low-stage drainage channels.
Mambrillas de Lara Member. Mambrillas de Lara.


TAMRON

Fig 3.134. Dark marly biomicrite exhibiting strongly erosive base and many pale biomicrite and black intraclasts. Dark colour reflects greater content of organics and clays. Unit would have been originally much thicker prior to compaction - wackstone limestones above and below would not have suffered comparable compaction.
Interpretation: Low-stage drainage channel or internal (perhaps storm) reworking within lake.
Aguilar Inferior Member. Quarry 1km N of Aguilar del Campoo.

Fig 3.135. Limestone conglomerate / wackstone with abundant black pebbles (some perhaps partially corroded, eg top left) and variety of paler grey micrite intraclasts.
Interpretation: Absence of: root tubules; mottling; and desiccation cracks; suggests reworking of organic material into open lacustrine environment. Transport of black intraclasts would explain rounded and corroded margins of larger intraclasts, and would also account for the presence of numerous smaller and less well-defined dark intraclasts.
Ladera Member / Mambrillas de Lara Member? Las Pinarejas.

Fig 3.136. Similar limestone conglomerate / wackstone, many more pale micrite intraclasts. One consists of black core with corroded margins, set in pale micrite with rounded intraclast margins. Mambrillas de Lara Member? Las Pinarejas.

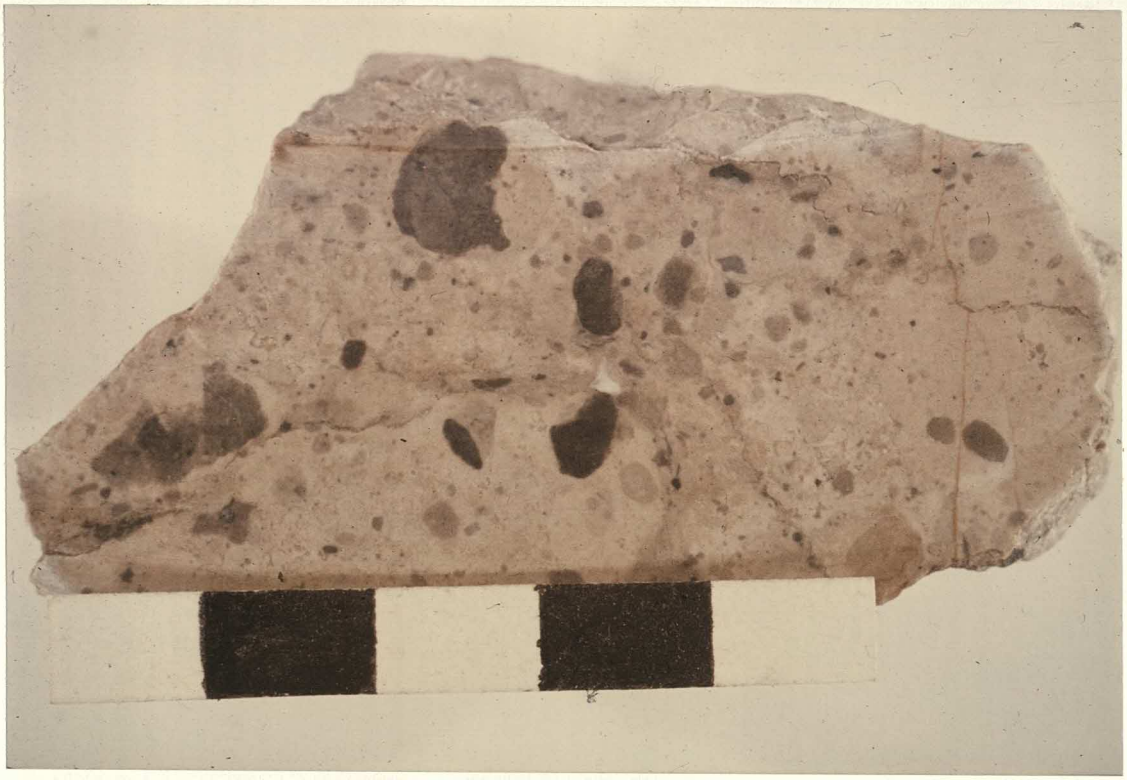

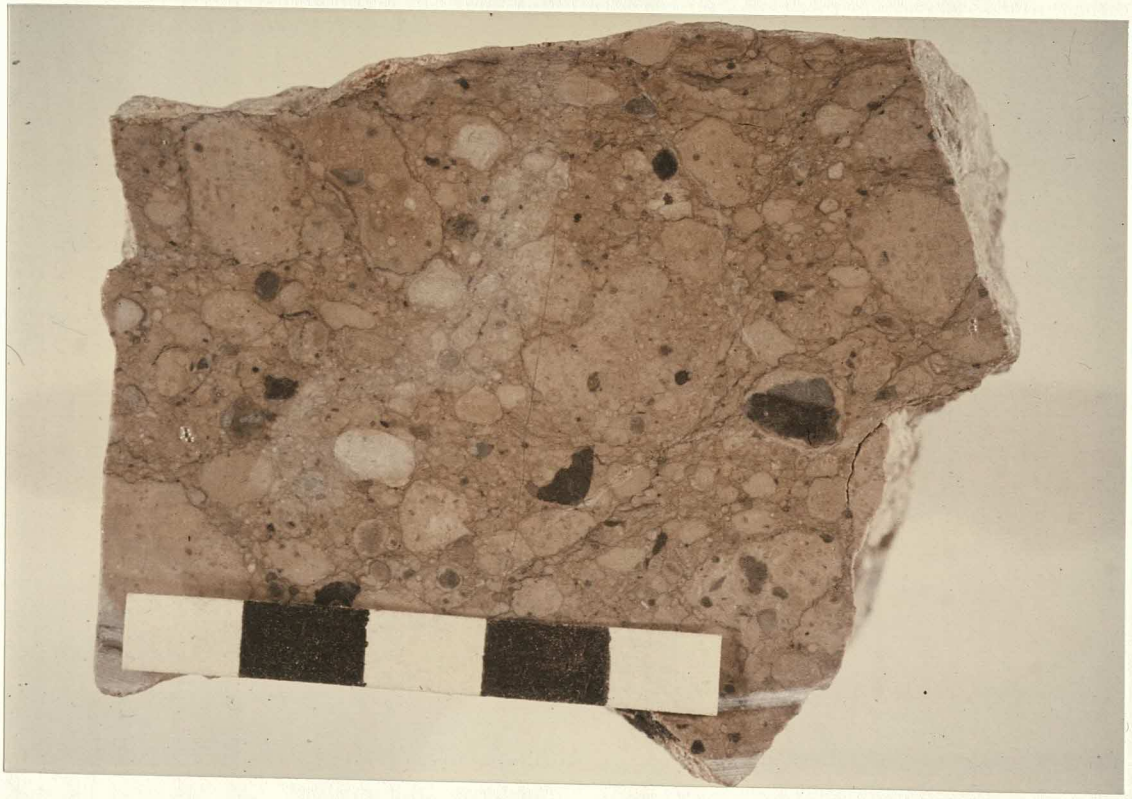

Fig 3.137. Close-up view of wackstone with rounded, and numerous smaller and more irregular black intraclasts, also many mm-scale rounded pale micrite intraclasts faintly discernible (eg lower left), all set in mid-grey biomicrite matrix. Small curved black intraclast visible right centre. Mambrillas de Lara Member. Mambrillas de Lara.

Fig 3.138. Irregular, clustered 2-40mm black pebbles in pale grey micritic limestone from the Aguilar Fm of SW Cantabria. Aguilar Inferior Member. Quarry 1km N of Aguilar del Campoo.

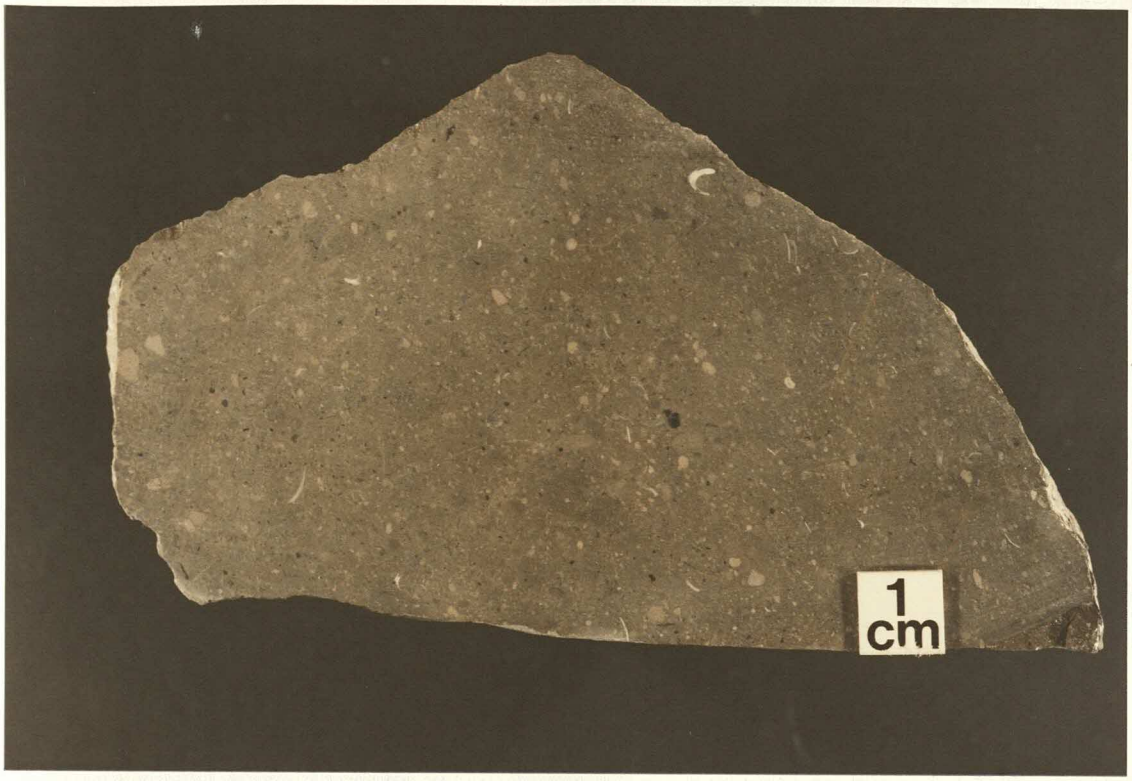
1
cm

Fig 3.139. Micrograph of black pebble. Organic-rich, dark, clotted micrite, laminar micritic coating. Unstained section. Field of view: 4mm. Ladera Member. Ladera, near Mamolar.

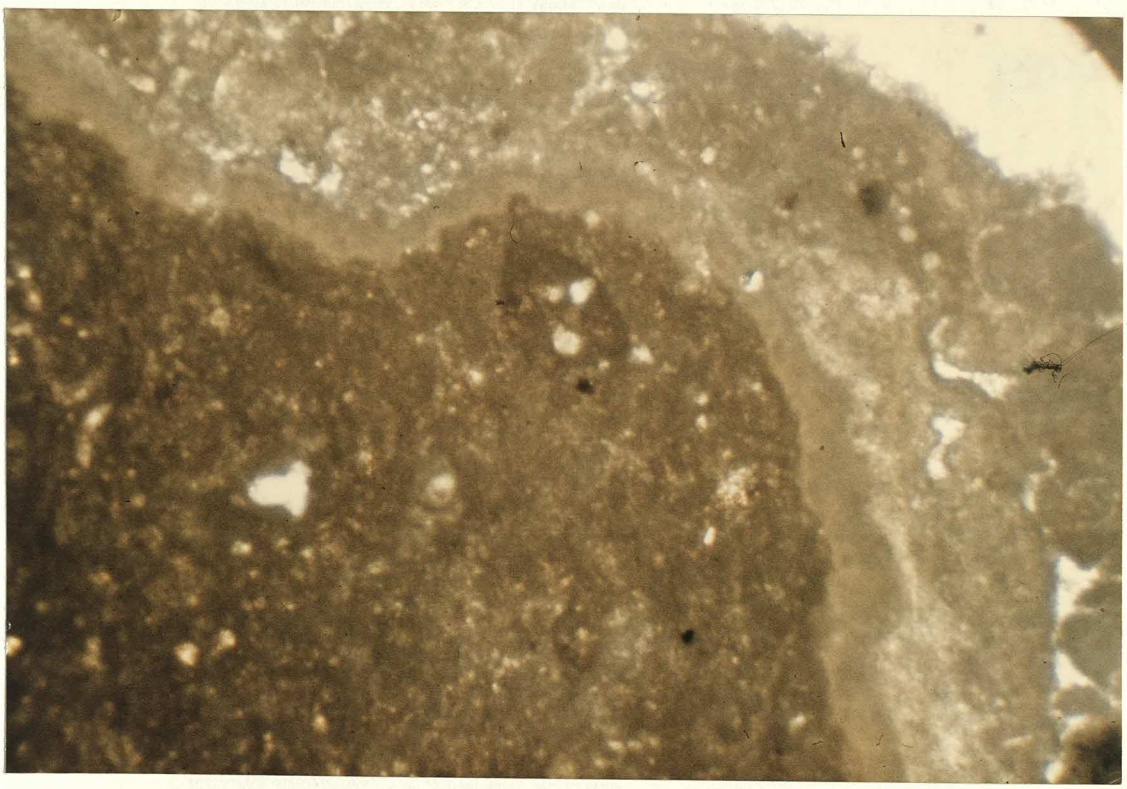

Fig 3.140. Occurrences of black pebbles: Ancient.

ANCIENT EXAMPLES OF BLACK PEBBLES.

HORIZON	LOCALITY	REFERENCE
Lr Oligocene	Basle, Switzerland	Brianza et al (1983)
Lr Oligocene	Le Puy, France	Strasser & Davaud (1983)
Oligocene	Beauce, France	Freytet (1982)
U Cretaceous - Lr Tertiary	Duero Basin, Spain	Bond (pers. comm., 1985)
	Tajo Basin, Spain	Arribas (pers. comm., 1984)
	Provence, France	Durand et al (1984)
	S France	Cayeux (1970), Freytet (1973)
U Cretaceous	Yugoslavia	Jelaska et al (1983)
	Nuevalos, Spain	Melendez, (pers. comm.,(1985)
Urgonian	Provence, France	Strasser & Davaud (pers. comm., 1984)
? Valanginian	W Cameros, Spain	This work
Purbeck	W Cameros, Spain	This work
	Swiss & French Jura	Strasser & Davaud (1983)
	S England	West (pers. comm., 1984)
		Hughes (1975)
		This work
U Jurassic	Portugal	Rey (1972)
	Pyrenees, Spain	Enay (1980)
	Aquitaine, France	Enay (1980)
	Swiss & French Jura	Enay (1980)
Bajocian	W Cameros, Spain	This work
Jurassic	Betics, Spain	This work
Triassic	Austria	Bechstadt (1979)
		Piller (1976)
Pennsylvanian	New Mexico, USA	Wilson (1967)

Data from Strasser & Davaud (1983), with additions.

Fig 3.141. Occurrences of black pebbles: Quaternary and Recent.

BLACK PEBBLES: PLIO-PLEISTOCENE, PLEISTOCENE AND RECENT OCCURRENCES.

SETTING	LOCALITY	REFERENCE
Marginal Marine	Bahamas - Bimini	Strasser & Davaud (1983)
	Bahamas - G. Bahama	Beach & Ginsburg (1980)
	Florida Keys	Strasser & Davaud (1983)
	Yucatan	Ward (1970)
	Tunisia	Strasser & Davaud (1983)
	Persian Gulf	Kendall & Skipwith (1969)
	Barrier Reef, Australia	Maiklem (1967)
Continental	SE Spain (calcretes)	Klappa (1978, 1980, 1981) Montenat (1981)

Data from Strasser & Davaud (1983), with additions.

Fig 3.142. Vertical variation in intraclast size and abundance due to reworking. Freytet & Plaziat (1982).

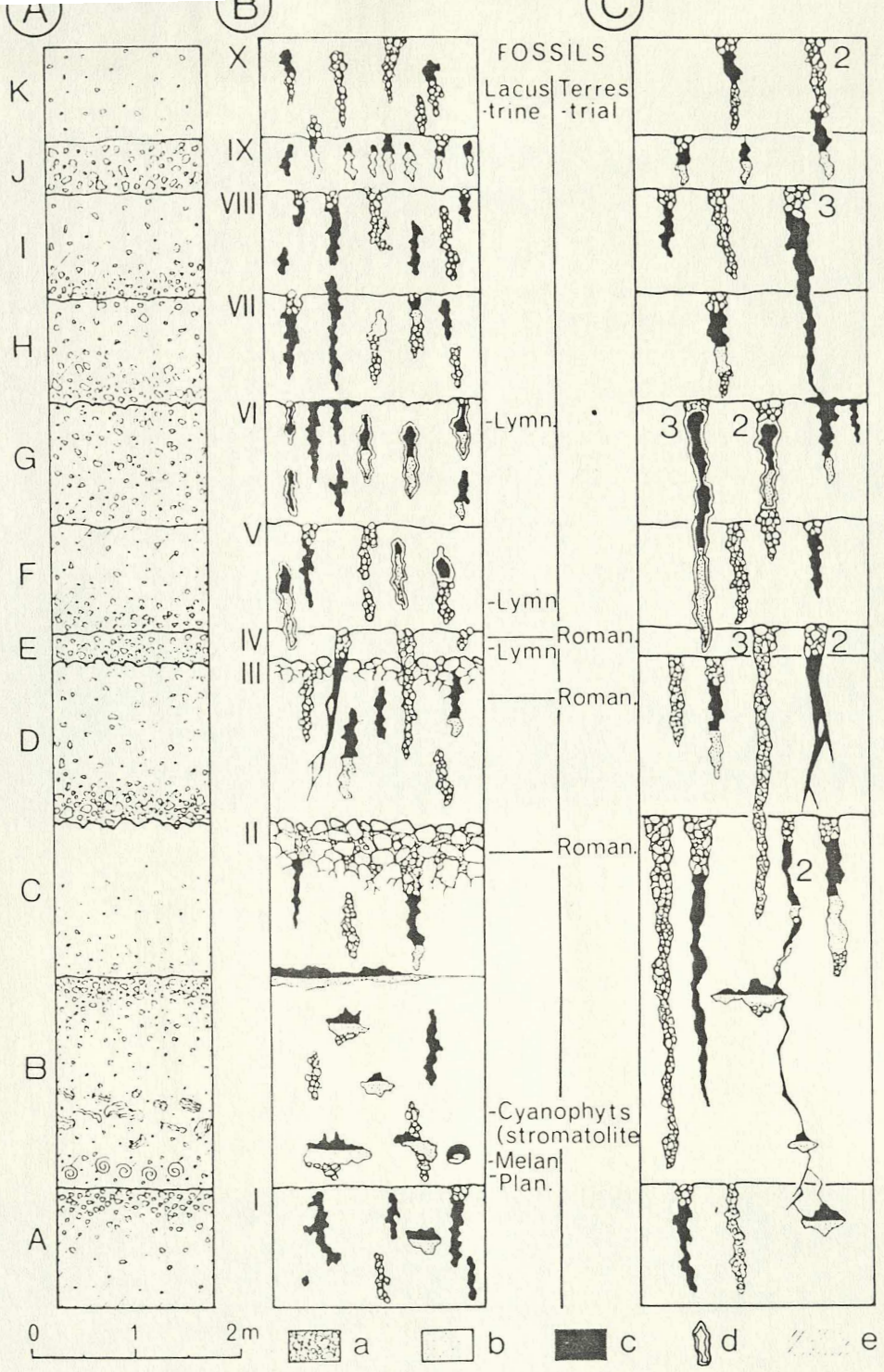

Fig. 42. Sequential analysis of part of the Ventenac Limestone showing the respective distribution of sedimentary deposits, soil, and pseudo-microkarst features. This figure shows several distinct types of sequence (sedimentary, pedological), which are superimposed and associated (Ventenac Limestone, Cuiso-Lutetian, Saint-Jean-de-Minervois).

A. Primary sedimentary sequences (A–K): within the lacustrine sedimentation with charophytes, *Lymnaea*, *Planorbis* and *Melanopsis*, one may trace a vertical change in the abundance of calcareous intraclasts (= gravels) and the intensity of dark coloration (proportional to the density of hatching). The basal sequences (A and B) exhibit an unusual abundance of intraclasts at the top of each bed, and a lighter coloration at the base that characterize progressive lacustrine filling, with increasing littoral intraclasts. Succeeding sequences exhibit inverse variations, indicative of active basal reworking due to sudden flooding of brecciated lime banks.

B and C stress pedogenetic sequences (I–X): they seem to be coordinated with the sedimentary sequences, the upper discontinuity surfaces being the same. The criteria utilized in defining the upper limit of each include desiccation surfaces (breccias) and root-traces, these latter forming subvertical canals with varied fillings (pseudo-microkarst). However, detailed observation indicates that pedological sequences tend to be thicker than sedimentary ones (C): a given root-trace can travers 1, 2 or 3 sedimentary sequences. The pedological sequences thus interfere.

It is also possible to make a sequential analysis from the internal fillings of pseudo-microkarst cavities, frequently very complexe (see Fig. 43 and Pls. 38 to 41). They demonstrate that alternative drying and wetting are the basic causes of both the sedimentary and pedological sequences. The observed fossils are lacustrine (Lymn. = *Lymnaea*; Plan. = *Planorbis*; Melan. = *Melanopsis*; incrusting cyanophytes: stromatolites) and terrestrial snails (Roman. = *Romanella*, a bulimimorph helicid). e = darker part of a sequence.

Internal fillings: a = reworked desiccation breccia; b = fine internal sediment; c = sparitic calcite, or void; d = isopachous phreatic calcite lining.

Fig 3.143. Grainstone. Abundant well-sorted, rounded 1-3mm intraclasts; some reworked black pebbles. Mambrillas de Lara Member. 2km N of Huerta del Rey.

Fig 3.144. Grainstone / reworked spar-matrix breccia, poor sorting. Abundant 1-3mm rounded intraclasts; also larger, more irregular, intraclasts 5-30mm in size. Mambrillas de Lara Member. Las Pinarejas.


1
cm

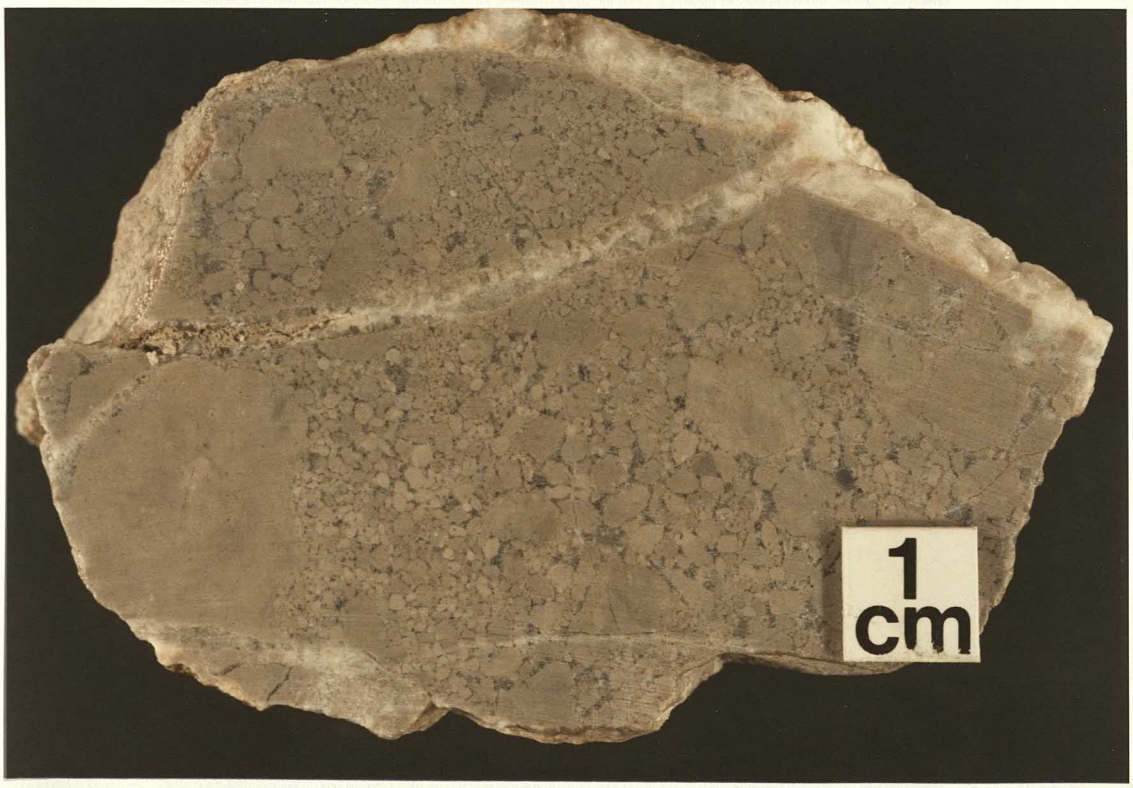
1
cm

Fig 3.145. Micrograph of grainstone showing small, rounded, and larger, more irregular, intraclasts of charophyte biomicrite. Charophytes and molluscan debris clearly visible. Cement of equant sparite crystals. No evidence of emergence. Field of view: 9mm. Mambrillas de Lara Member. Las Pinarejas.

Fig 3.146. Outcrop view showing association between facies 12 (yellow limestones) and facies 13 (cherts). Near vertical bedding. Younging to left. The repetition of these facies permits the mapping of imbricate thrust slices of the Rupelo Formation developed structurally above the San Leonardo Fault in this area. Detachment surface probably defined by yellow limestones. This outcrop occurs at a change in slope and may be associated with a thrust plane (?just to right of yellow limestones). Rio Cabrera Member. Looking SE. San Leonardo Fault Zone, 1km NE of trace of SLF. 2km SW of Mamolar, 3km NW of Pinilla de los Barruecos.

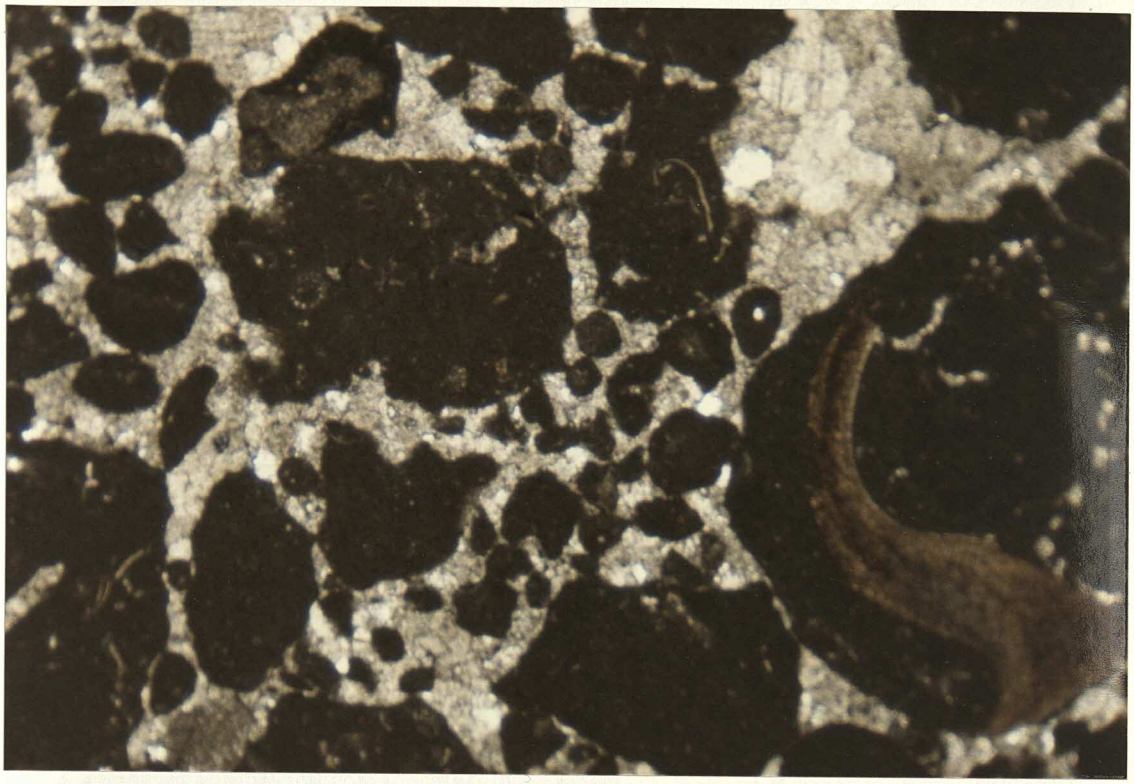

Fig 3.147. Nodules / clasts of yellow limestone at base of Ladera Member massive limestones and just above Las Vinas Member red/green marls. Also some yellow vuggy limestones and laminated cherts at this horizon (silicified root crusts?). Looking SE. Quintanilla de las Vinas.

Fig 3.148. Micrograph of yellow limestone nodule as in fig 3.147, showing microspar matrix; angular branching and abundant circumgranular cracks. Strongly peloidal fabric. Field of view: 9mm. Base of Ladera Member. Quintanilla de las Vinas.

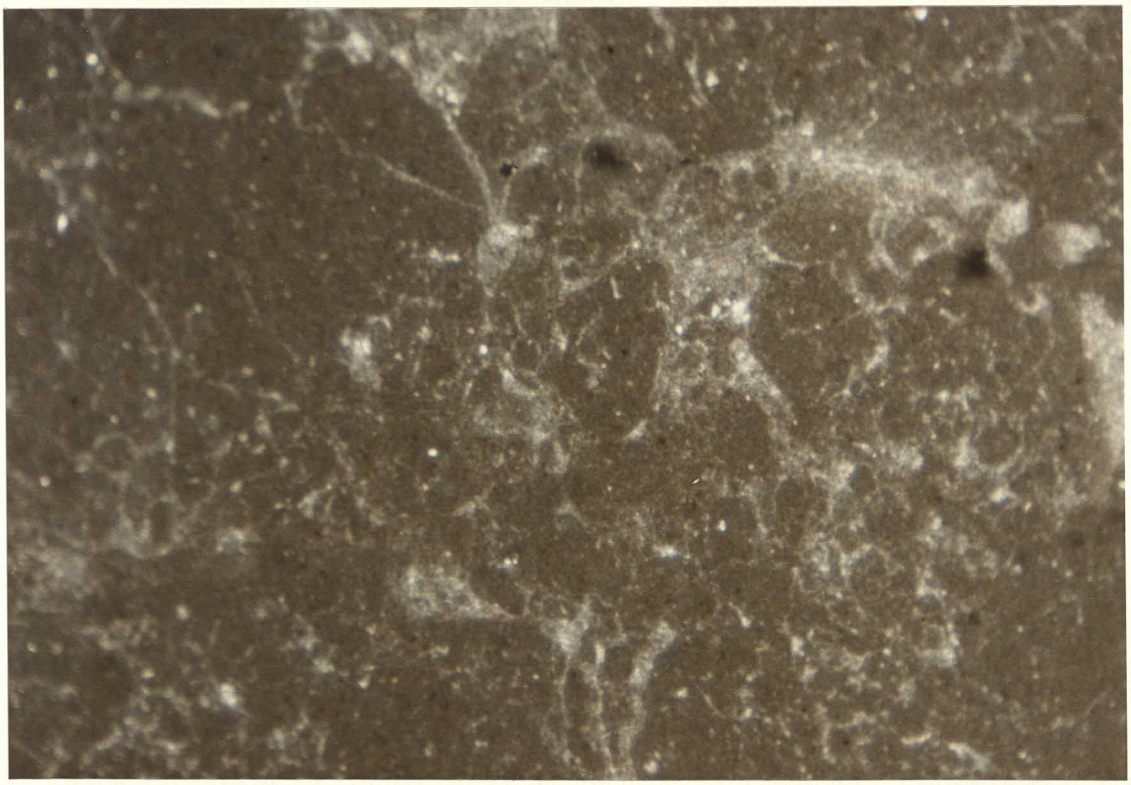

Fig 3.149/3.150. Vuggy yellow limestones. Note extremely porous, open spongy fabric. Left: appearance as in field; Right: Cut slab. Rio Cabrera Member. San Leonardo Fault Zone. 2km SE of Mamolar.


1
cm

Fig 3.151. Location of thickest chert outcrop, Rupelo football pitch. Younging towards camera. Palaeozoic of Sierra de la Demanda forming mountains far right distance. Marine Jurassic limestones forming low rise, right distance. Massive and marly white limestones of upper Ladera Member on dip slopes facing. Red mottled and rubbly limestones of lower Ladera Member behind. Yellow vuggy limestones behind bank beyond far goal-posts. Grey marls at base of outcrop, left touchline, overlain by partially silicified limestone and 1m chert bed. Charophyte-rich limestones above. Corn harvest lain out on centre line for threshing. Rio Cabrera Member. Looking N. Rupelo.

Fig 3.152. Close-up view of facies 13 chert outcrop shown in fig 3.151. Note white appearance, angular fracture. Rio Cabrera Member. Rupelo football pitch.

Fig 3.153. Outcrop of white limestone from the Aguilar Formation of SW Cantabria showing partial silicification. Brownish material at base of outcrop from weathering of vuggy yellow limestone (?/evaporite). Lomilla Member. 2km SW of Lomilla.

Fig 3.154. Bed of white chert, same locality as fig. 3.153. Lomilla Member.

Fig 3.155. Slab showing nodular fabric in white chert. ?cf chicken-wire fabric. ?Evaporite replacement. Rio Cabrera Member.

Fig 3.156. Slabs showing variable internal structure of chert - left: ?crystal growth fabric (of evaporite?); right: dense yellow-amber chert with translucent nature reminiscent of flints - ?carbonate silicification. Rio Cabrera Member.

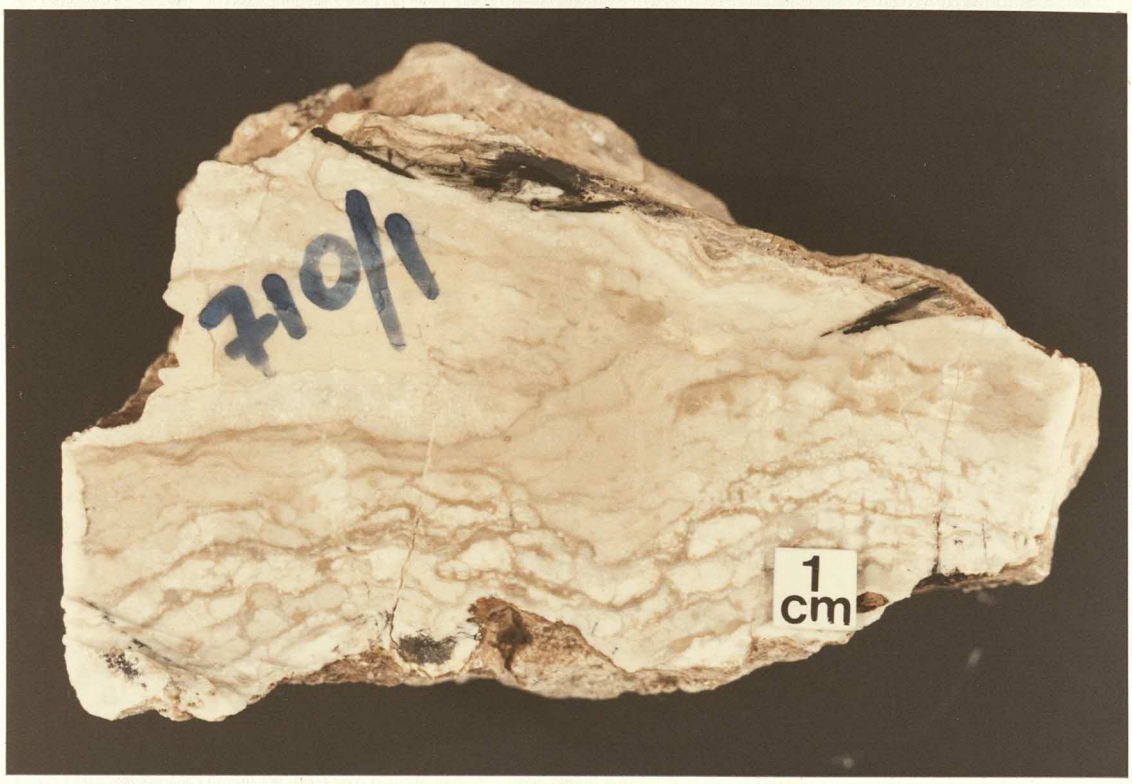
1
cm


1
cm

Fig 3.157. Chert blocks collected from soil at Rupelo near outcrop of Rio Cabrera Member. Variable habit - from massive and weakly translucent (silicification of carbonate?) to impure and apparently crystalline (evaporite replacement?).

Fig 3.158. Pseudomorph shapes in white chert. Cut chips, variable void shape, including square (left), rhomboid and irregular. Rio Cabrera Member. Tenadillas.

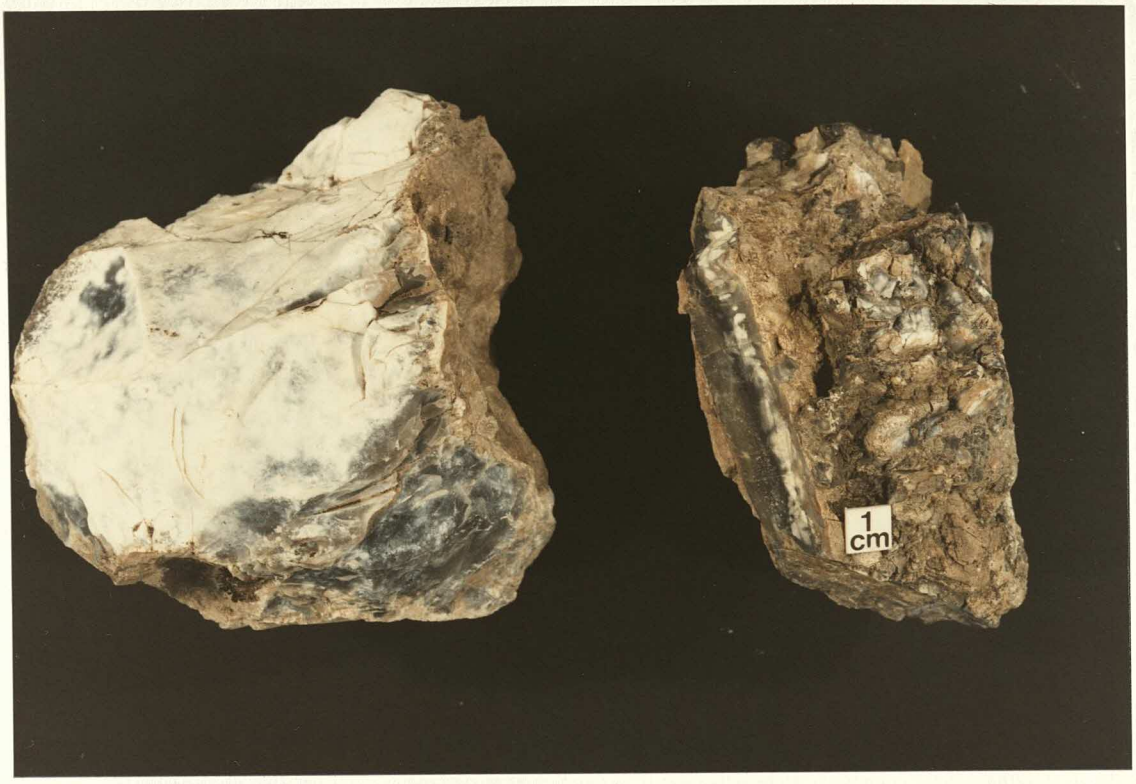
1
cm

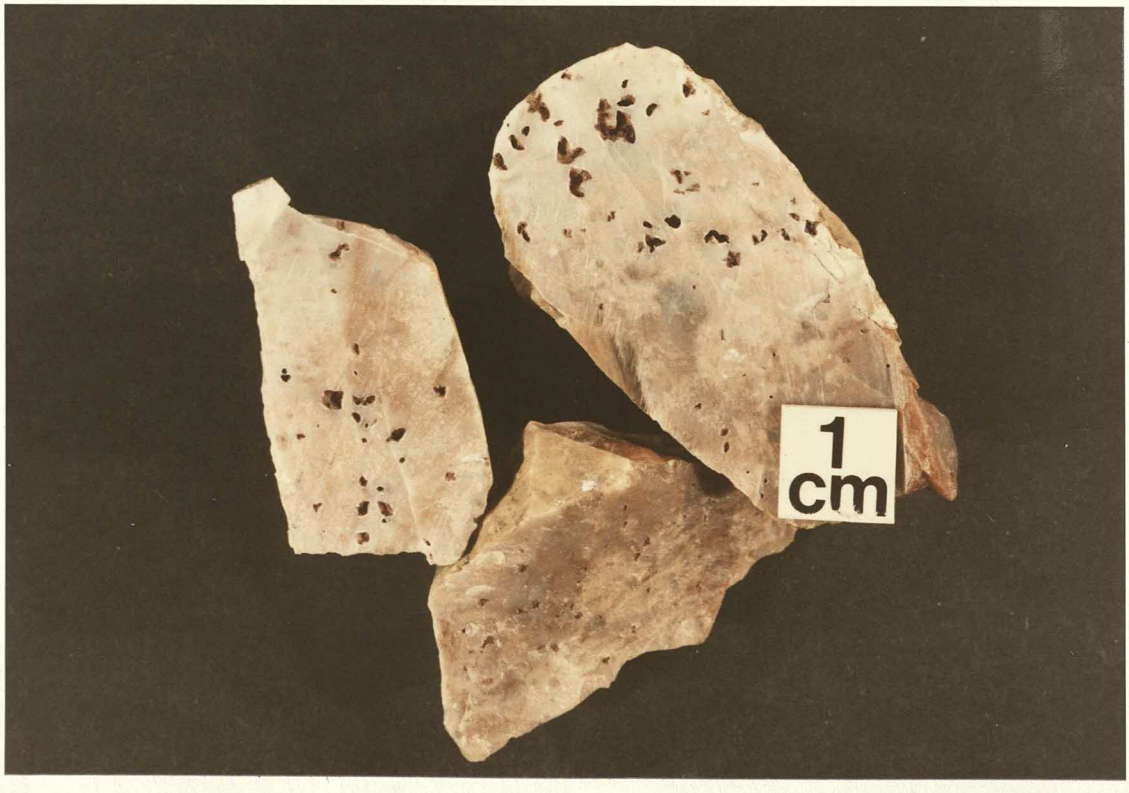
1
cm

Fig 3.159. Pseudomorph shapes in white chert. Rio Cabrera Member. Note; contrast in crystal size between pseudomorphs and matrix; inclusion of highly-birefringent clustered dolomite crystals. Field of view: 9mm. Unstained section.

Fig 3.160. Pseudomorph shapes in rather impure chert. Rio Cabrera Member. Rupelo. Left: appearance as in field; Right: Cut slab.

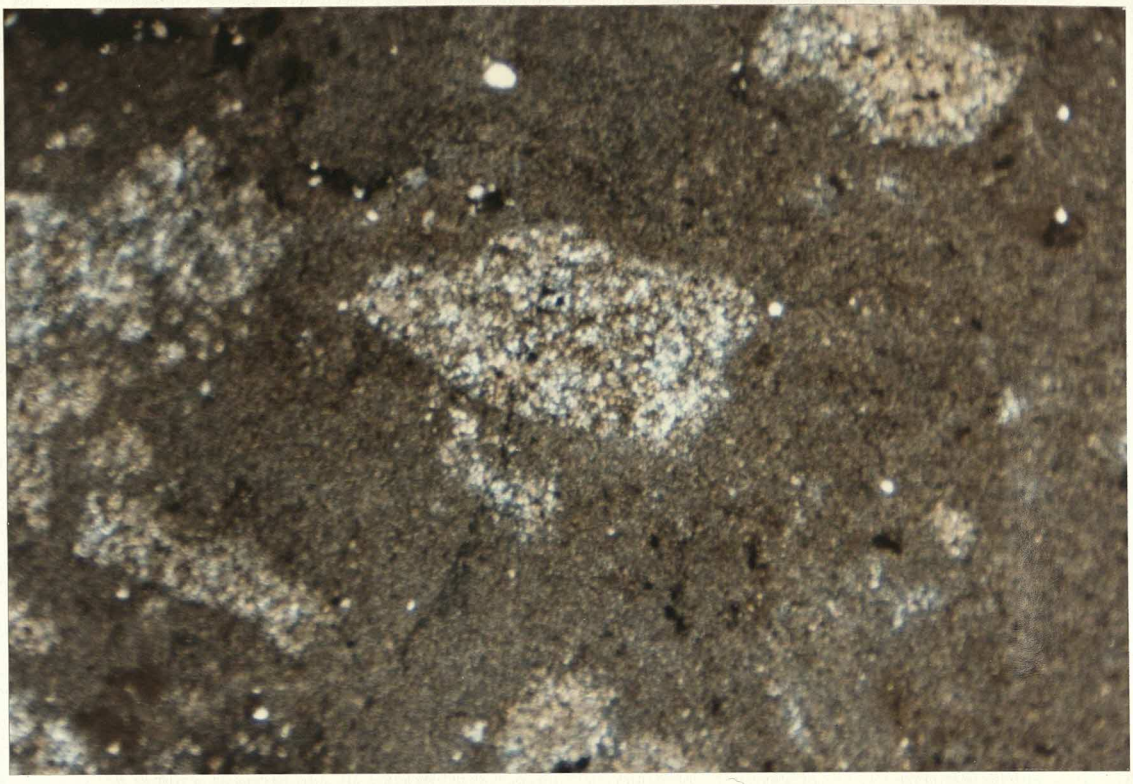


1
cm
710/7

Fig 3.161. Length-fast chalcedony inclusions and microquartz matrix of white chert. A: Plane polarised light; B: Crossed polars; C: Crossed polars, 1λ plate inserted. Field of view: 9mm. Note: retention of pale brown colour zoning visible in plane polarised light; rounded patterns suggest accretion from point nuclei on cavity wall. Rio Cabrera Member.

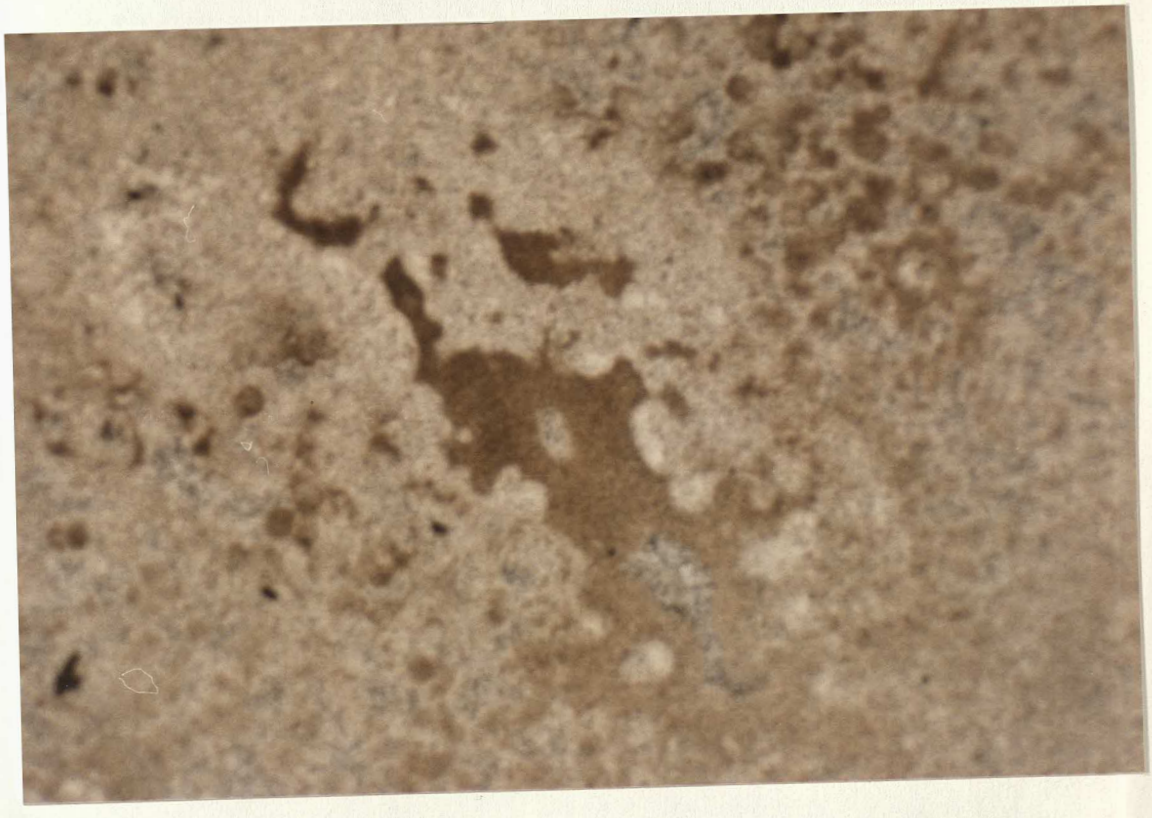

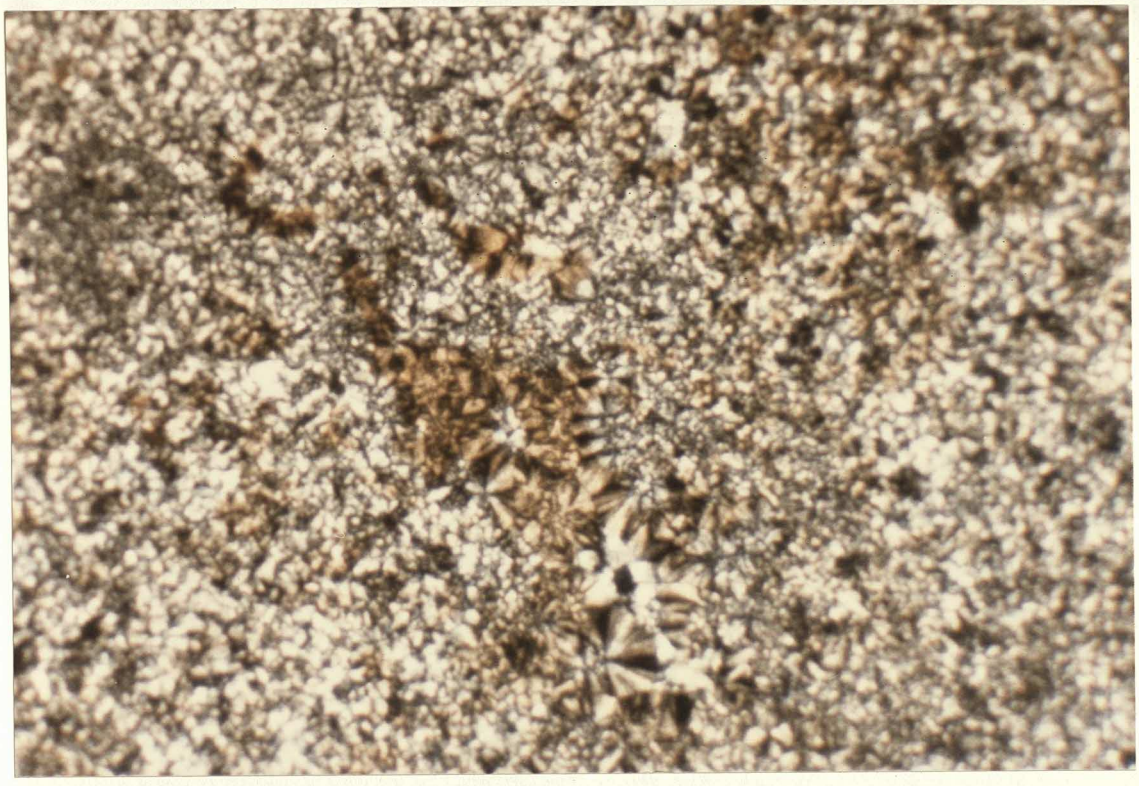

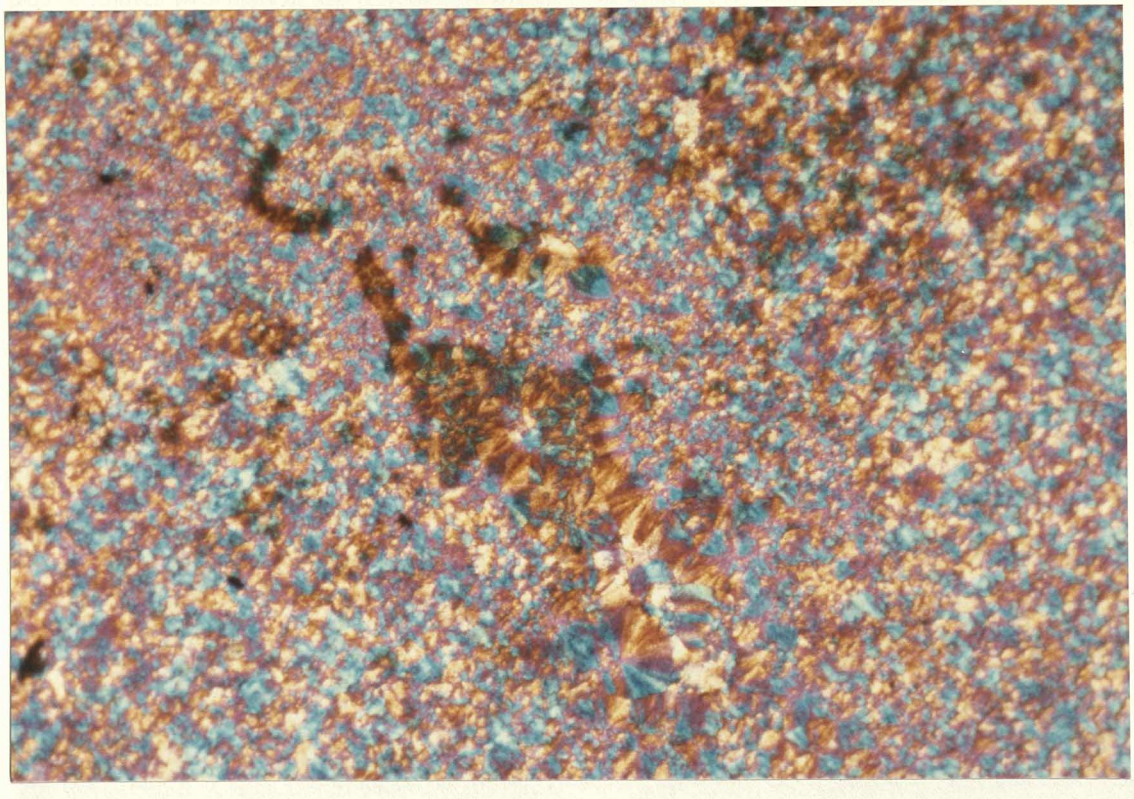

Fig 3.162. Angular void and length-fast chalcedony fill. Rio Cabrera Member. Field of view: 9mm. Top: Plane polarised light; Bottom: Crossed polars, 1 plate inserted. Note: retention of relic fabrics in matrix and of colour zoning in voids. Dirty brown patches in fine-grained chalcedony matrix are clustered dolomite crystals.

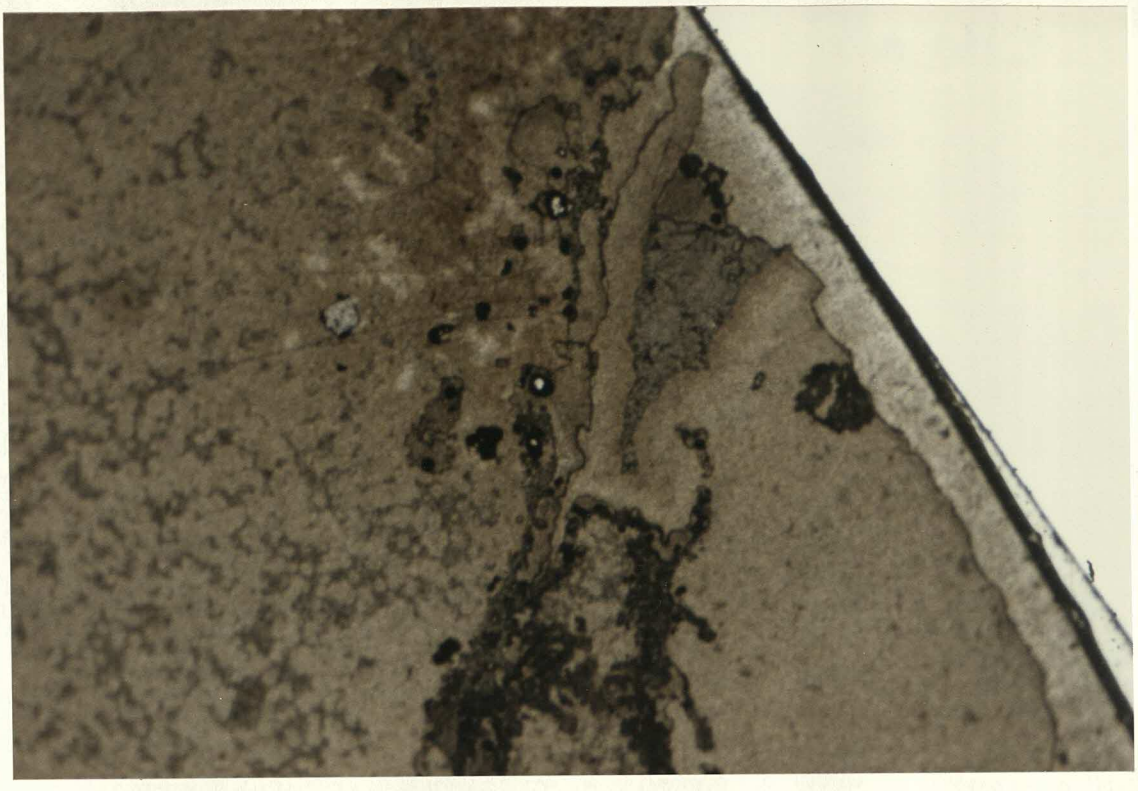

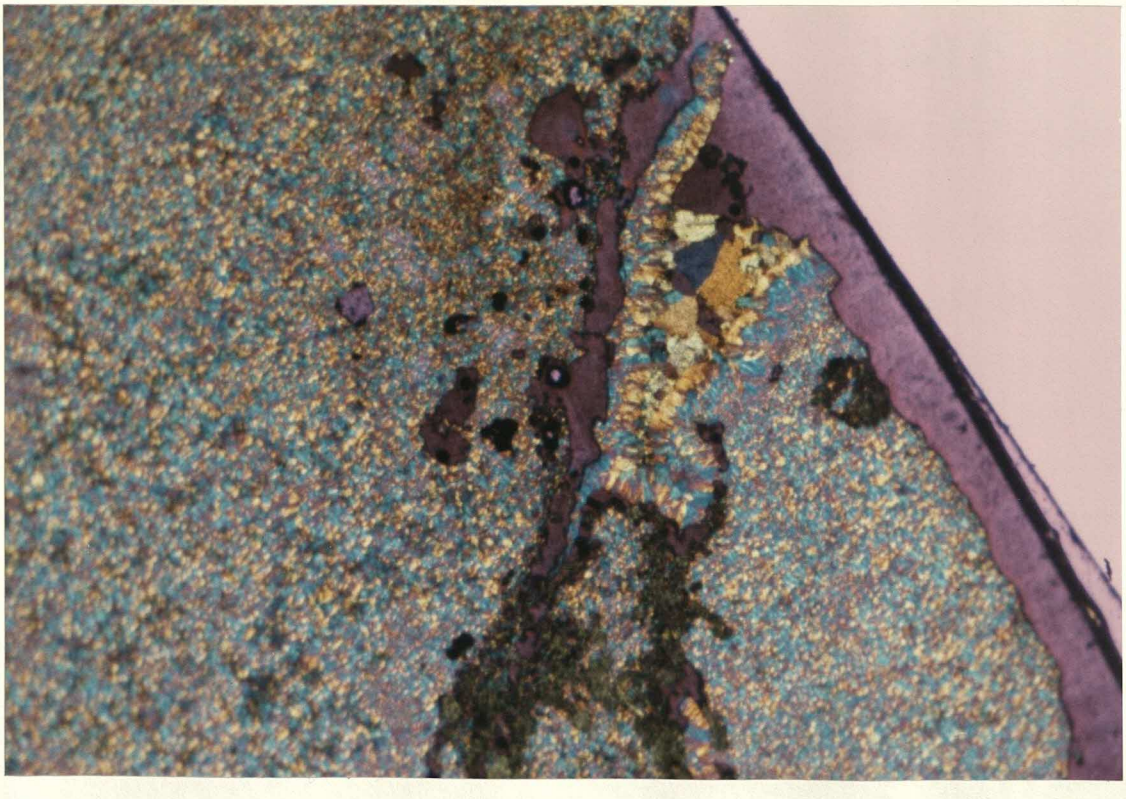

Fig 3.163. Length-slow chalcedony (quartzine) partially infilling voids in white chert. Field of view: 9mm. A: Plane polarised light, B: Crossed polars; C: Crossed polars, 1λ plate inserted. Note: retention of relict fabric; weak crystal shapes in centre of void (?pseudomorphs); rounded patterns suggesting that recrystallisation to microquartz took place by conversion from quartzine involving accretion from point nuclei along cavity margins. Rio Cabrera Member. Tenadillas. Dark brown angular shapes mark now partially- silicified and recrystallised dolomite crystals.

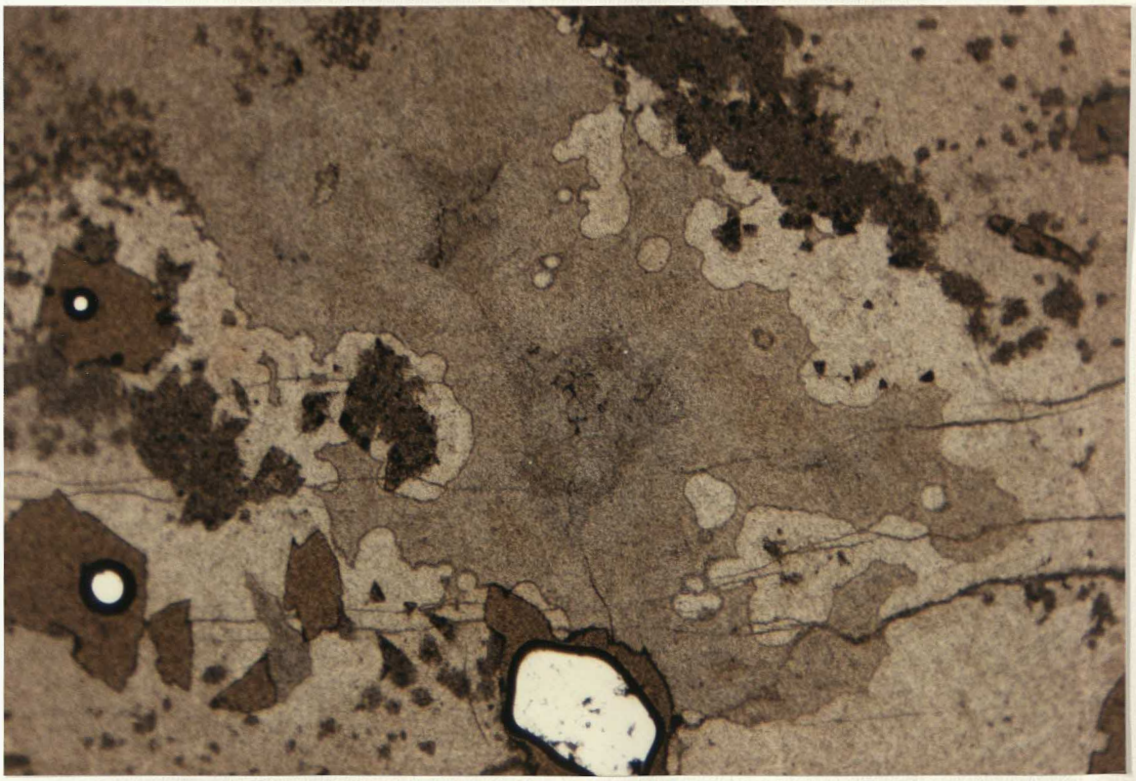

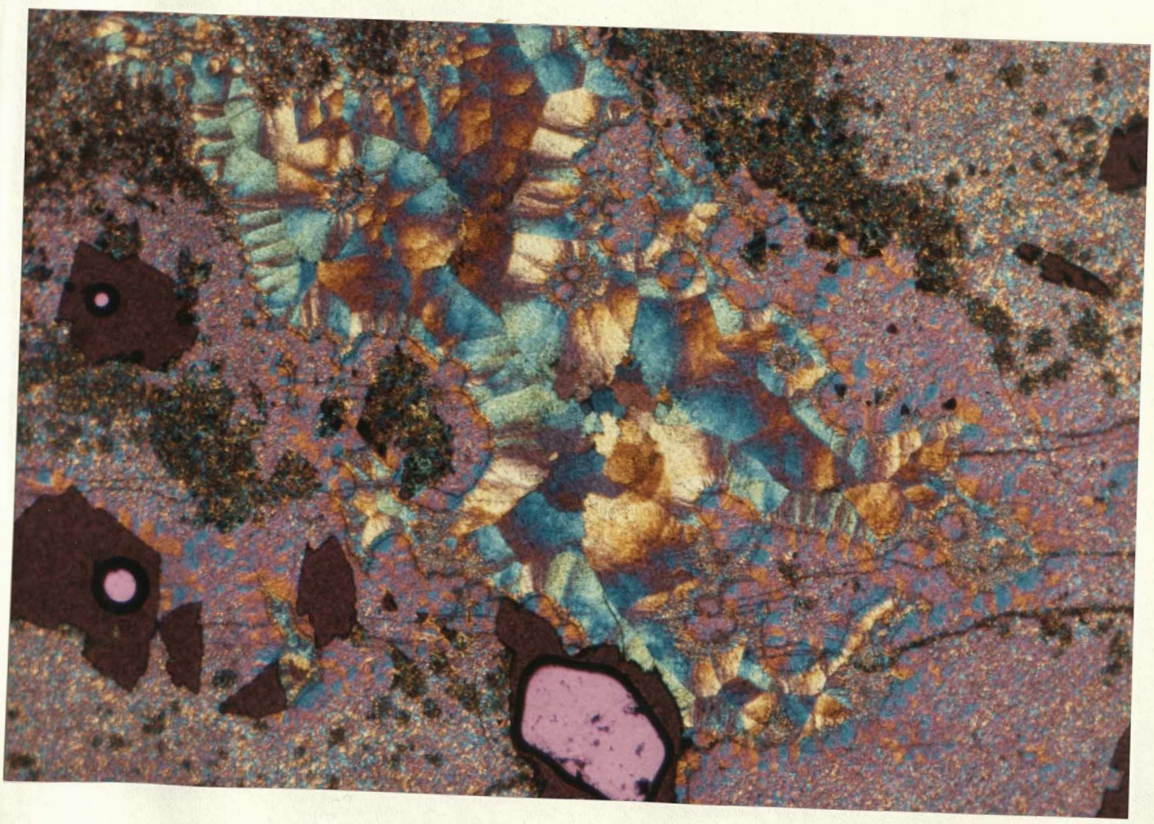

Fig 3.164. Close-up view of central part of area shown in previous figure. A, B, C: lighting conditions as above. Field of view: 4mm. Note: progressive recrystallisation of quartzine to microquartz from point nuclei and often in squarish "rosettes"; sharp linear margins to quartzine domains (compare figures in Lowenstein & Hardie, 1985); a little polygonal quartz in centre, in areas corresponding to pseudomorph shapes evident in previous figure (? evaporite fabric replacement, possibly of low-energy "foam texture").

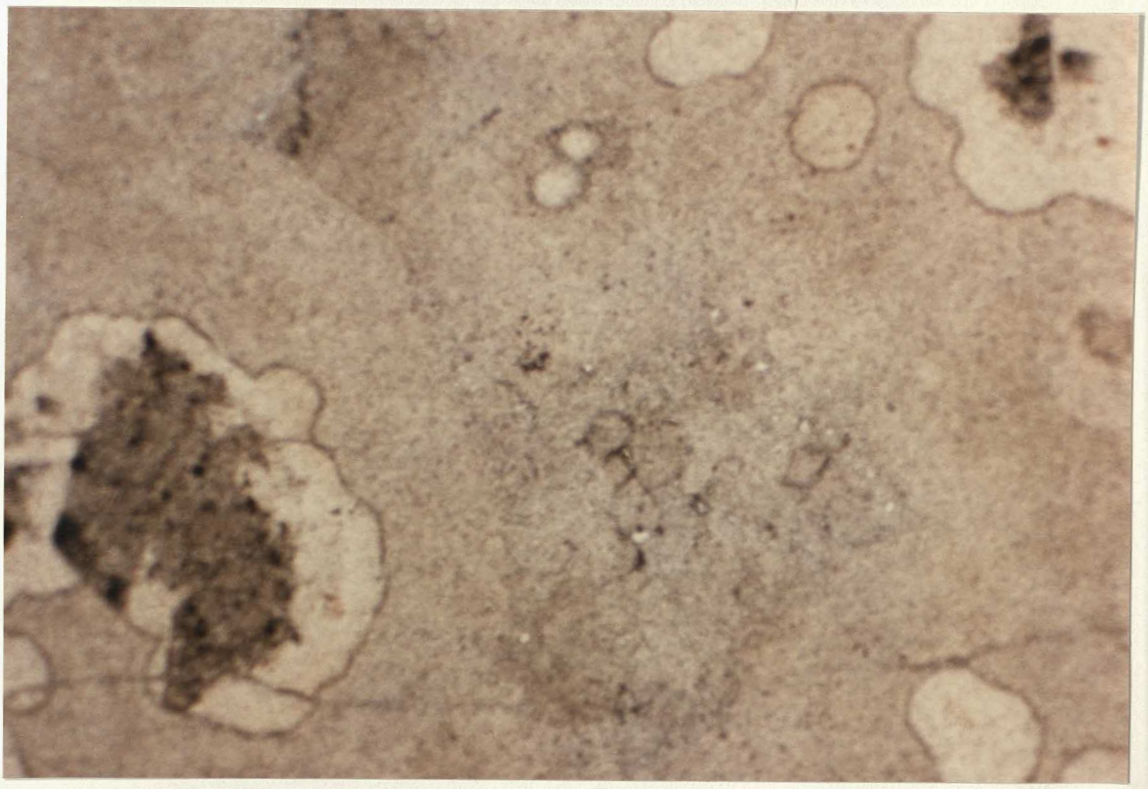

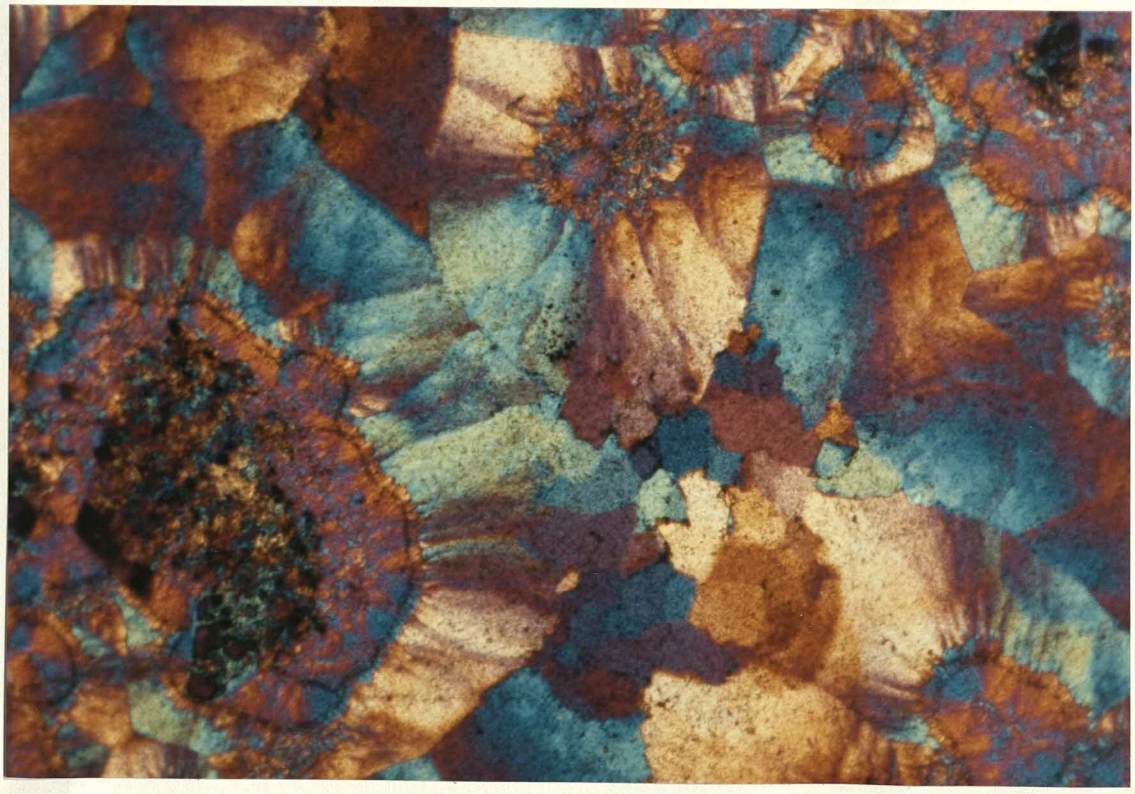

Fig 3.165. Length-fast fibrous chalcedony fill of cavity in white chert. Field of view: 4mm. A, B, C: lighting conditions as above. Rounded outline of fibrous masses indicates radial growth from point sources. Note grain size and fabric contrast with matrix. Tenadillas.

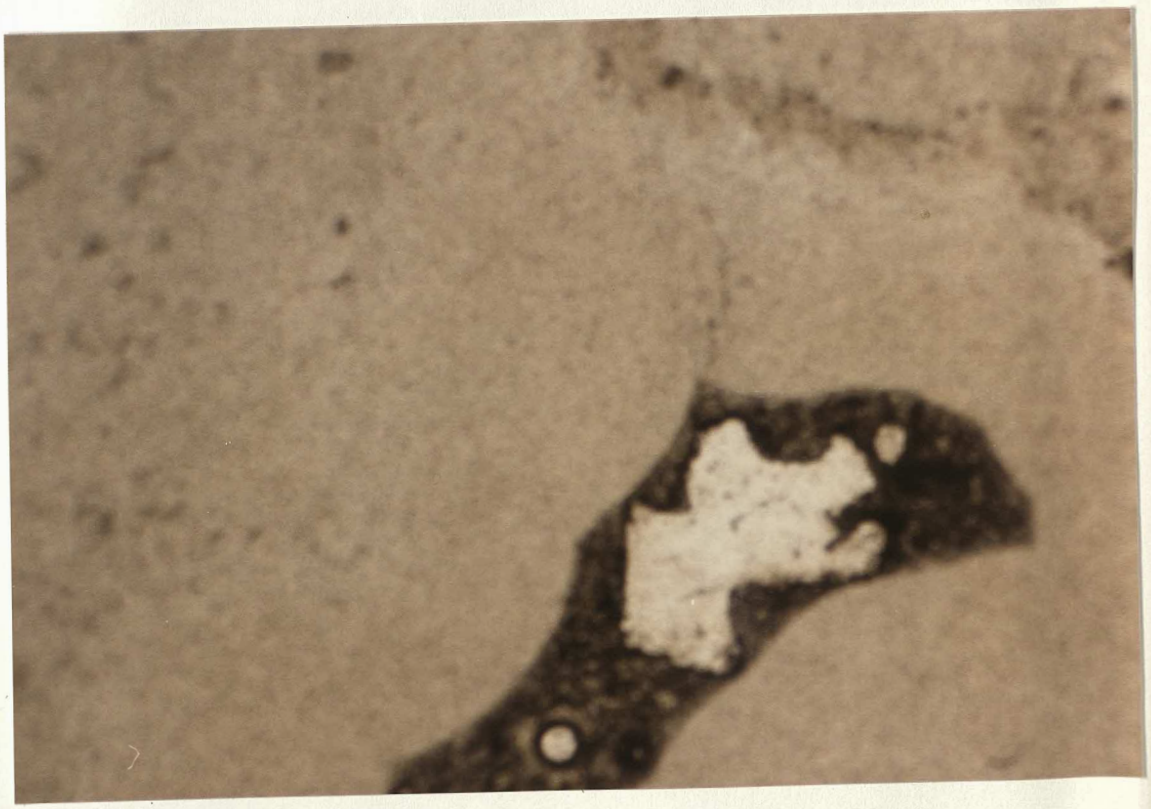

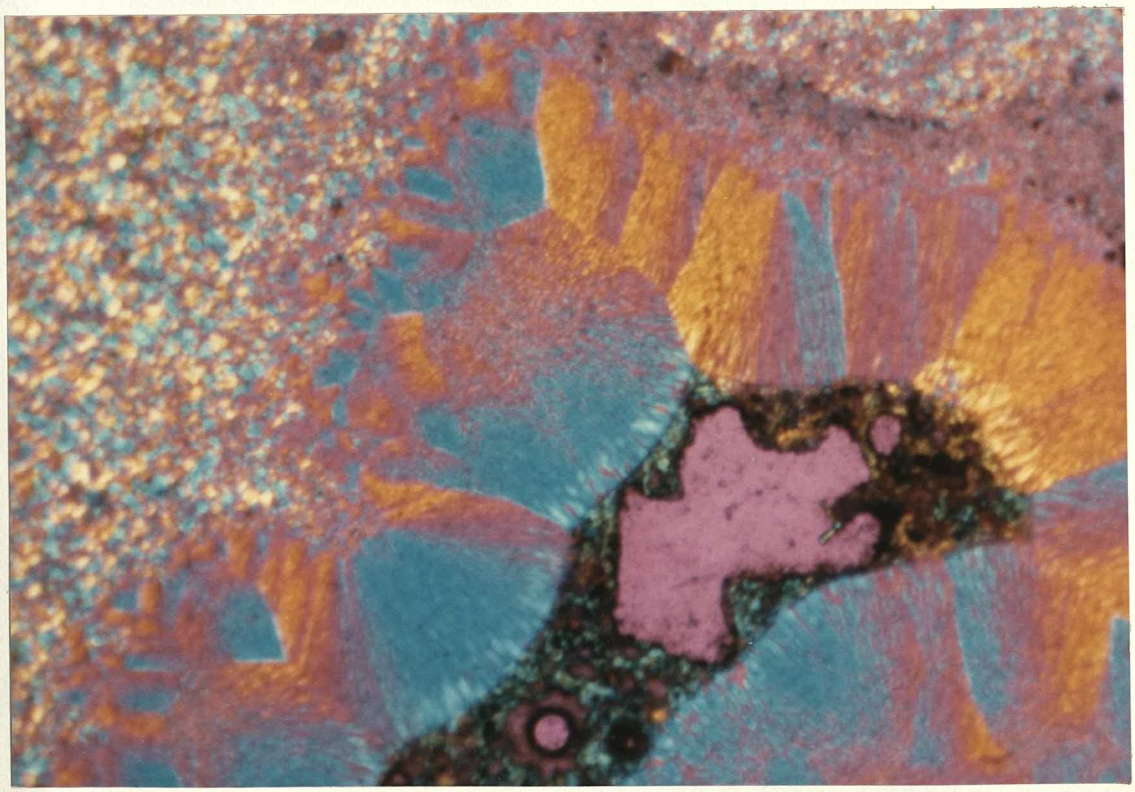

Fig 3.166. Polygonal megaquartz in white chert. Rio Cabrera Member. Field of view: 9mm.

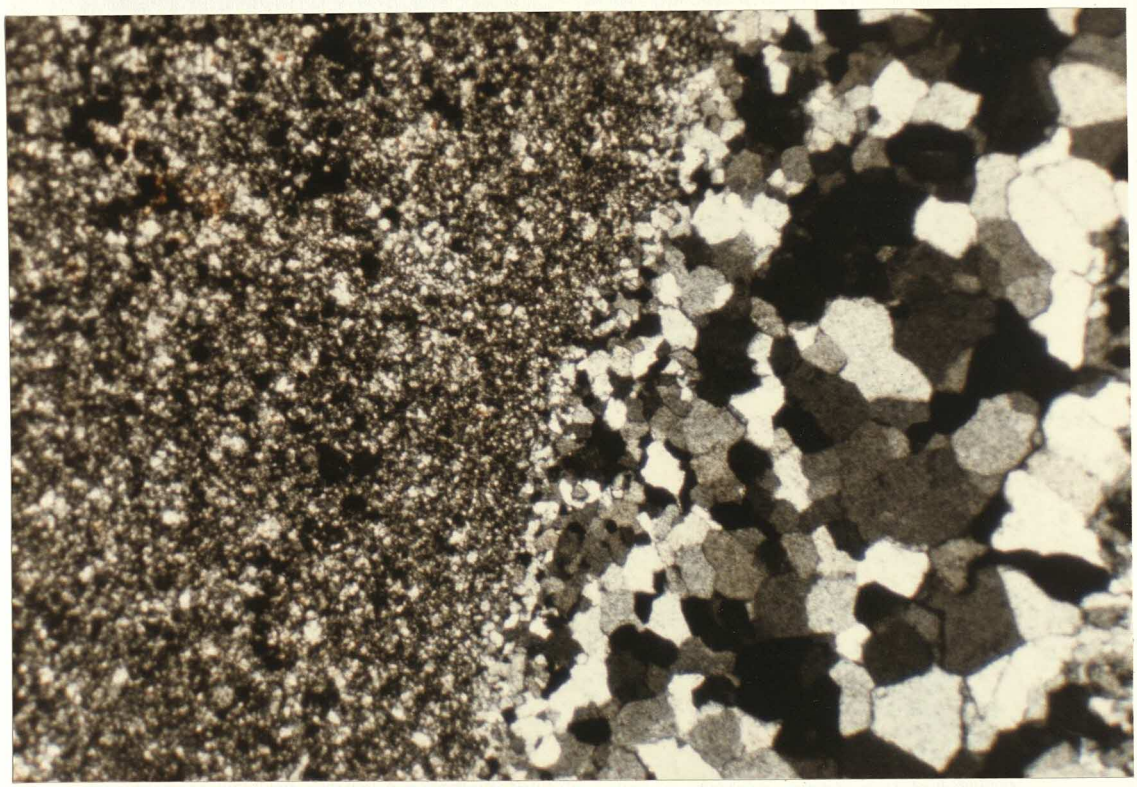

Fig 3.167. Micrograph showing silicification front. Coalescence of 50 spherulites to form chert. Rio Cabrera Member.

Fig 3.168. Relict fabric in white chert: peloids. Rhombic dolomite crystals within rounded grains. Also note presence of silicification front. Rio Cabrera Member.

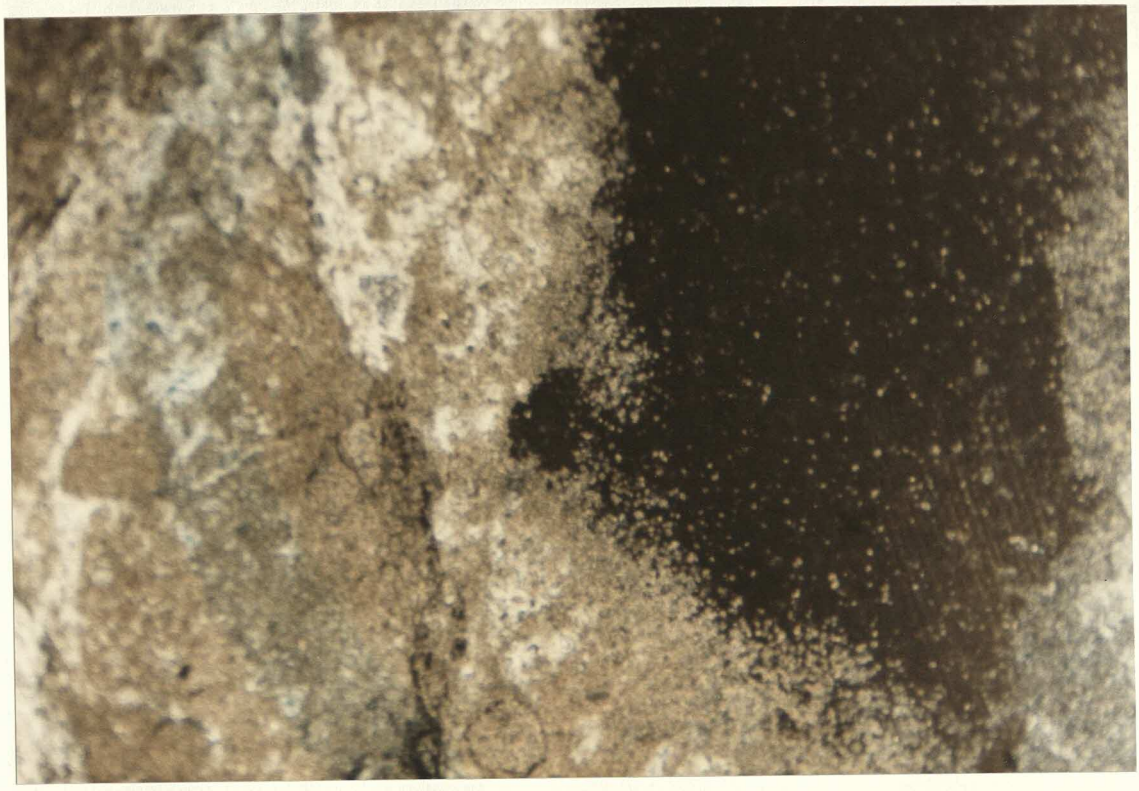

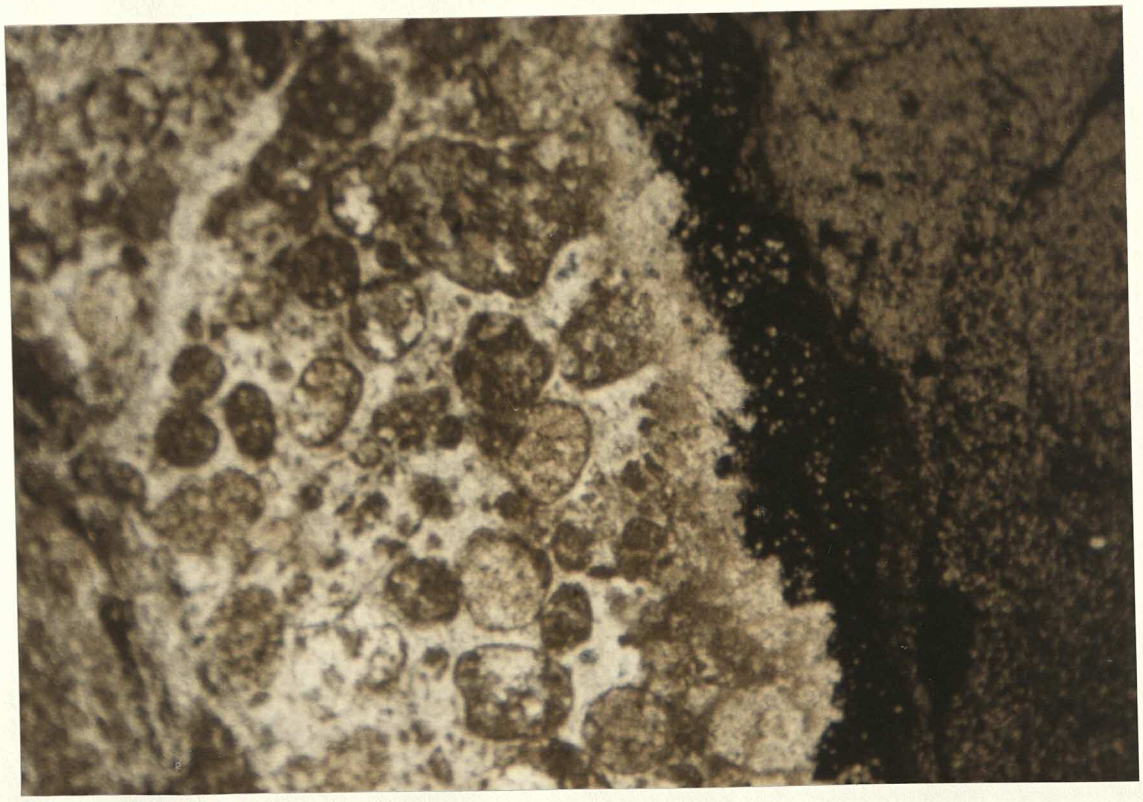

Fig 3.169. Relict fabric in white chert: root crust. Partial silicification only. Strongly peloidal fabric is visible in thin section (not figured). Base of Ladera Member. Quintanilla de las Vinas.

Fig 3.170. Relict fabric in white chert: root crust. Base of Ladera Member. Quintanilla de las Vinas.

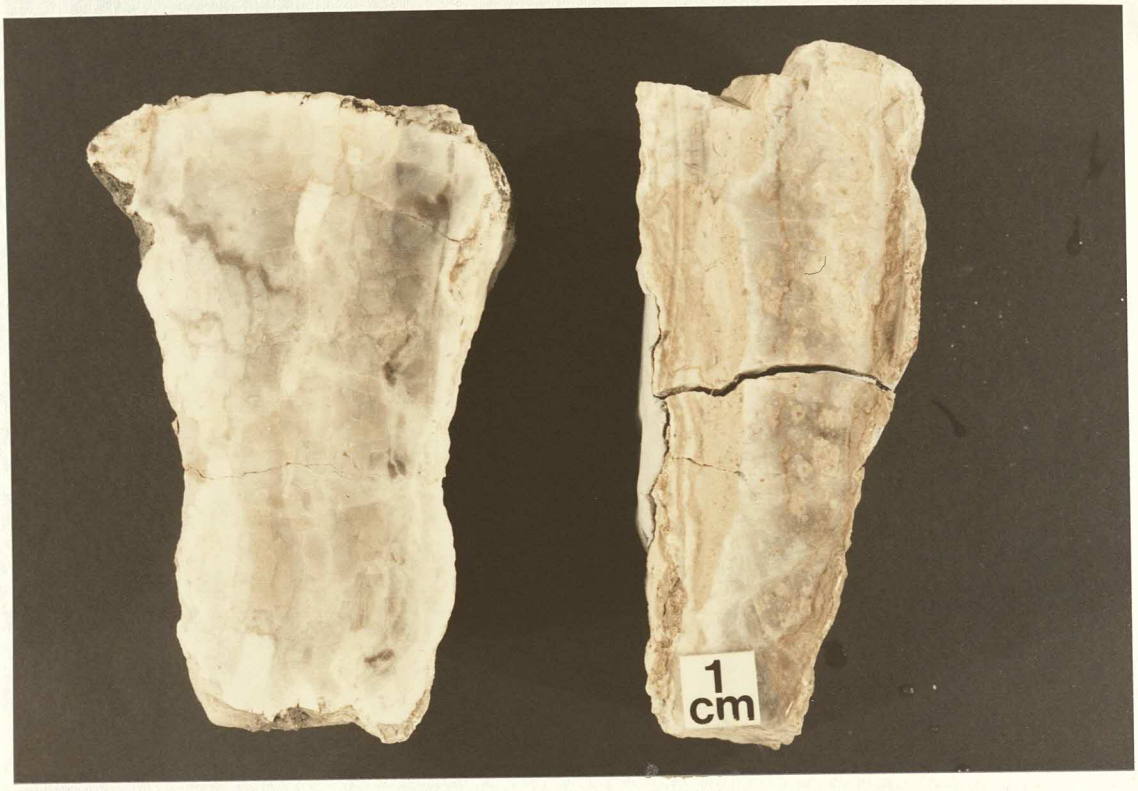
1
cm


1
cm

Fig 3.171. Relict fabric in white chert: geopetal (microkarst?) cavity. A, B, C: lighting conditions as in previous figures. Field of view: 4mm. Note: grain size variation; form of void as for microkarst cavities; fibrous length-fast chalcedony ?replacing fringing cement. Rio Cabrera Member. Tenadillas.

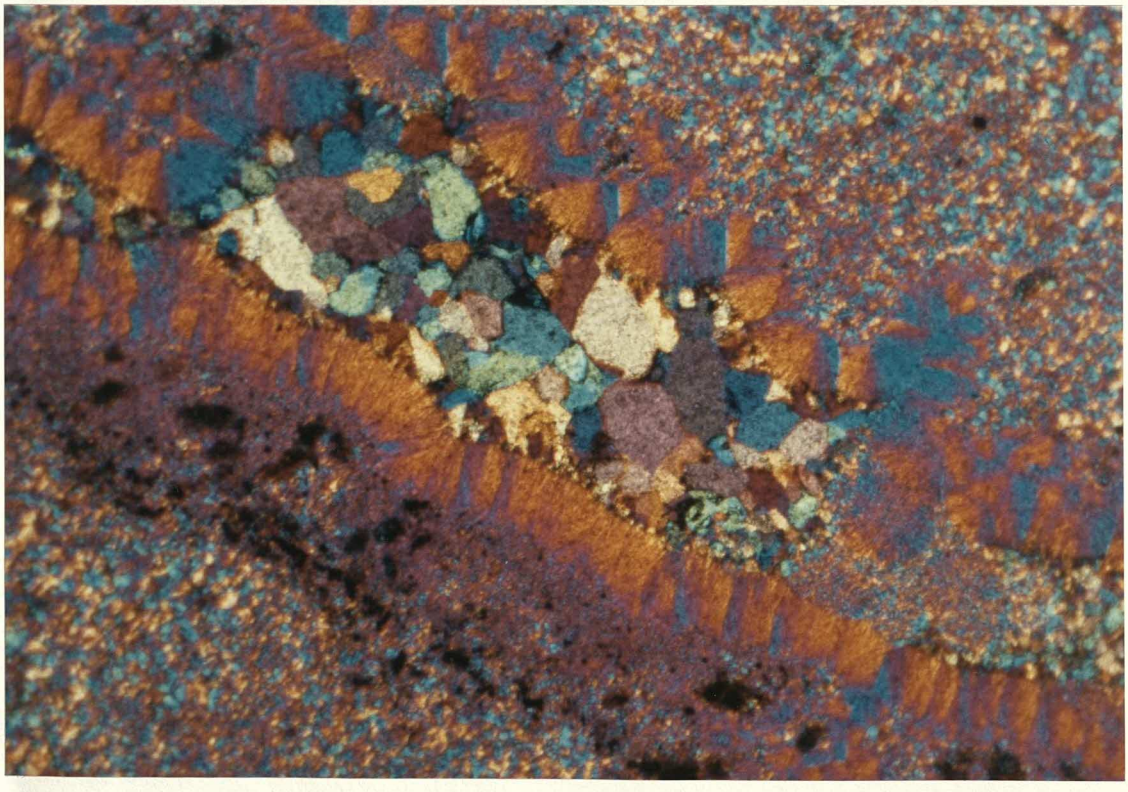

Fig 3.172. Relict fabric in white chert: charophyte stem. Central cavity and 12 cortical cells clearly visible. Rio Cabrera Member. Rupelo. Field of view: 4mm.

Fig 3.173. Fibrous satin-spar gypsum collected from road section through Rupelo Formation 2km N of Huerta del Rey. Perhaps not an original feature of the Rupelo Formation but possibly mobilised from Trias during thrusting.

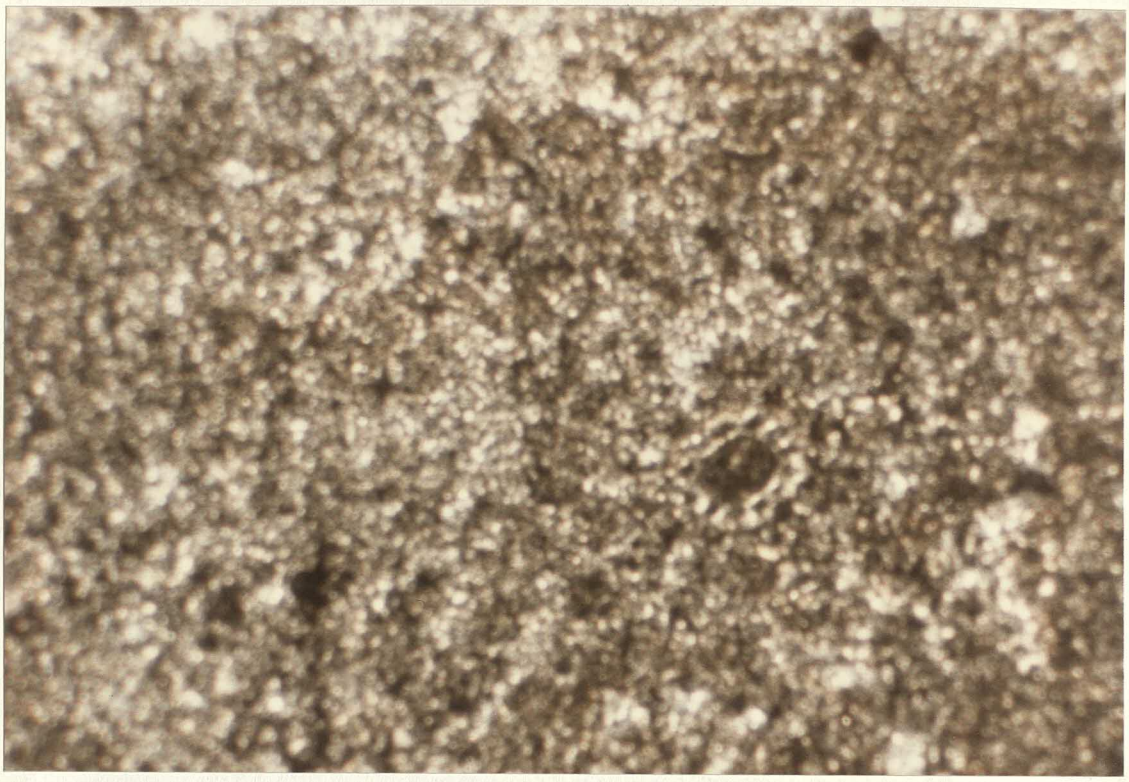


1
cm

Fig 3.174. Coarse quartzose grit overlying and truncating Ladera Member Carbonates. ?Torrelara Bed / ?Base of Hortigüela Formation equivalent. Rio Helechal, Hortezuelos.

Fig 3.175. Alternation of 5-10m charophyte dedolomite marls and 1m charophyte dedolomite limestone beds. ?Rio Cabrera Member / ?Hortigüela Formation. Rio Helechal, Hortezuelos.

Fig 3.176. Fe concretion in marls shown in fig 3.175. Rio Helechal, Hortezuelos.

Fig 3.177. Micrograph of facies 14, charophyte dedolomite. Charophyte stems in transverse, oblique and longitudinal section. Stems encrusted by rhombic sparry carbonate crystals. Matrix with abundant sparry débris. Relatively elevated organic content - note brownish matrix. TOC = 1.4%. Unstained section. Field of view: 4mm. ?Rio Cabrera Member / ?Hortigüela Formation. Rio Helechal, Hortezuelos.

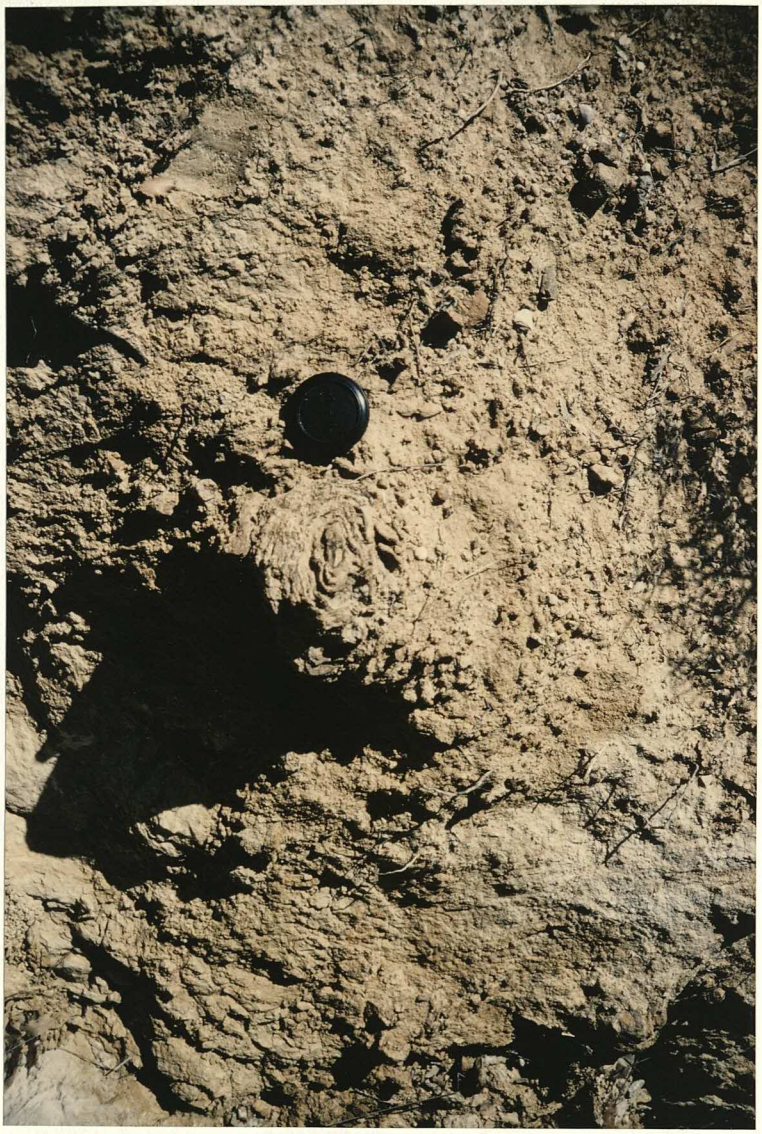

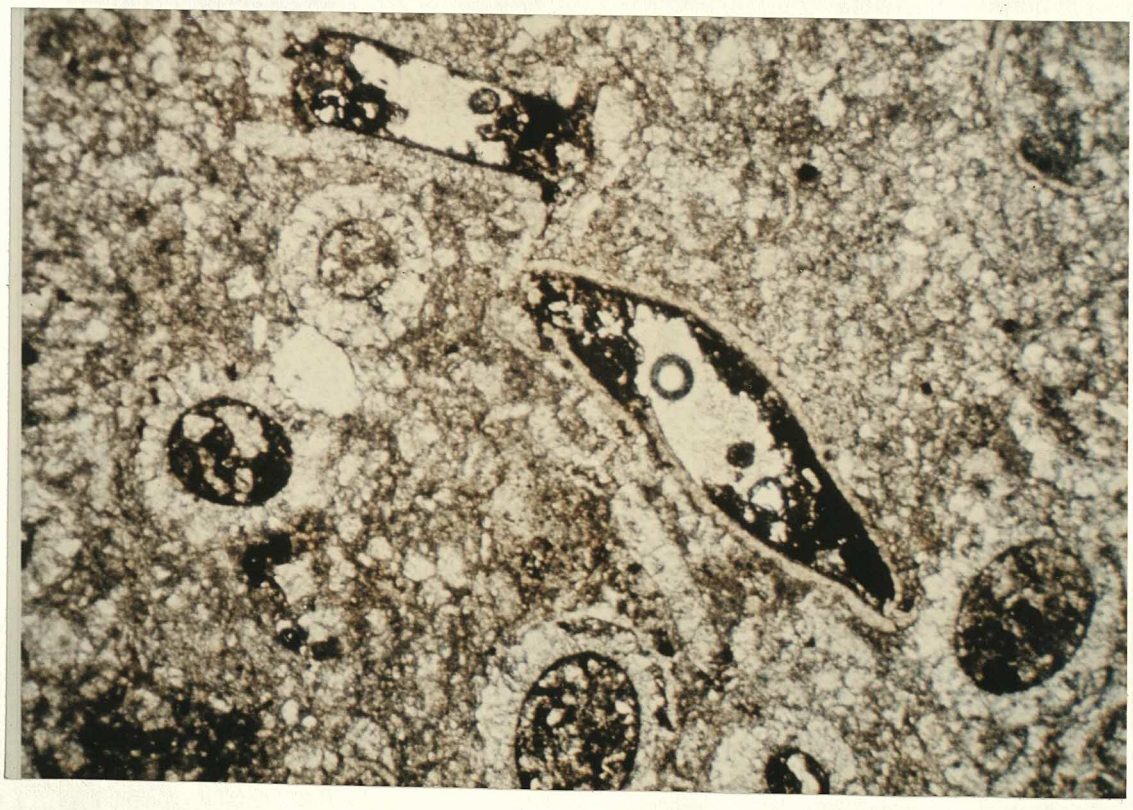

Fig 3.178. Micrographs of facies 14, charophyte dedolomite. Charophyte stems as in fig 3.177. Cortical cells of one stem still visible (right). Spar crystals (partially dedolomitised take weak stain. Strong pink stain of node fragment (left). Also pink stain, lower left, of oblique node section. Late-stage ferroan calcite cement (deep blue stain). Stained section Field of view: 12mm. ?Rio Cabrera Member / ?Hortigüela Formation. Rio Helechal, Hortezuelos.

Fig 3.179. Micrograph of facies 14, charophyte dedolomite. Charophyte stems, longitudinal, transverse and oblique sections. Stained section. Field of view: 4mm. Locality / horizon as figs 3.178 & 3.179.

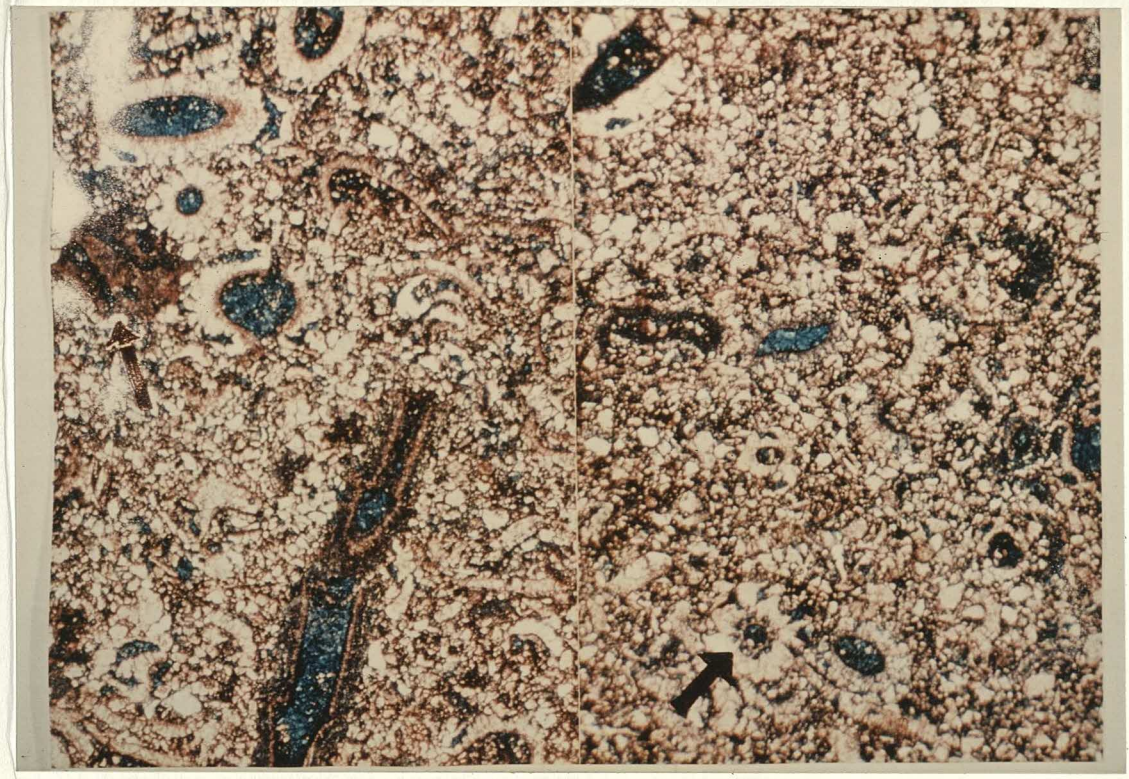

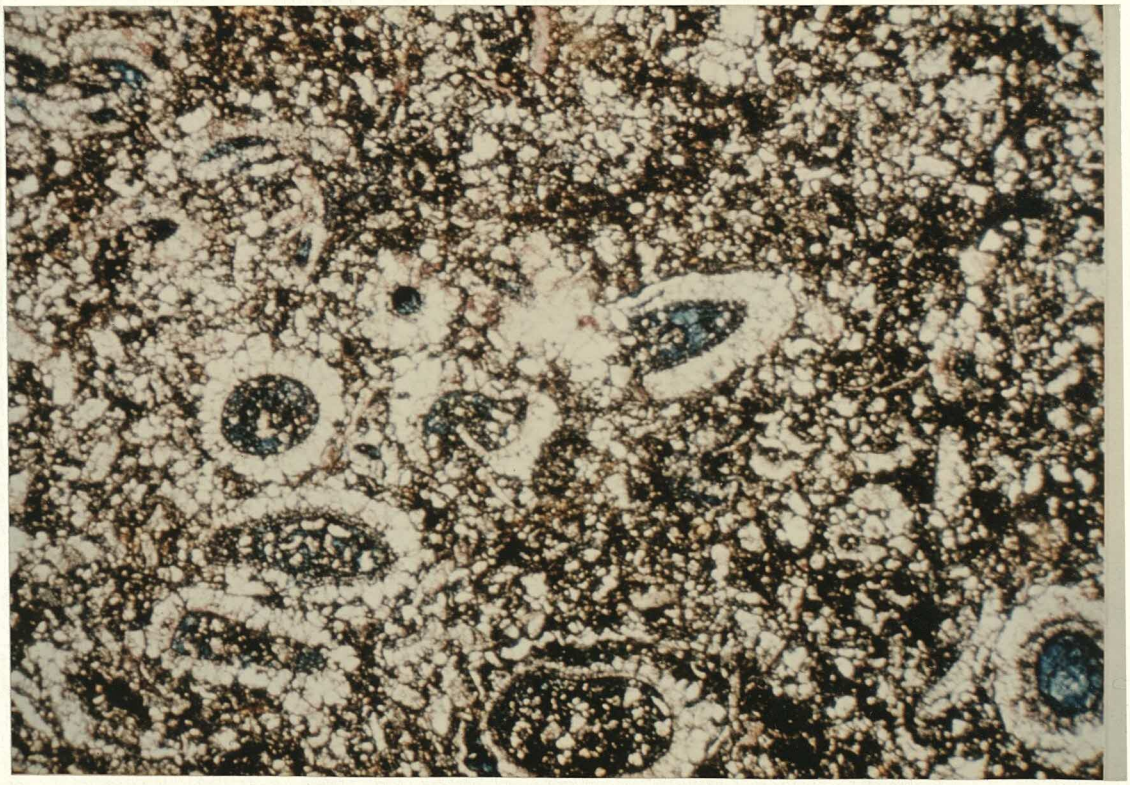

Fig 3.180. Micrographs of micritic limestone (biomicrite facies) with geopetal cavities. A: Plane polarised light; B Cathodoluminescence showing micrite (dull luminescence, variable intensity of luminescence picking out constituent intraclasts), vadose silt (non-luminescent). Later void-filling blocky spar cement is strongly luminescent (honey yellow areas). Biomicrite also contains some detrital clastic material - quartz grains (dull luminescence) and feldspar (blue luminescence). Field of view: 4mm. Mambrillas de Lara Member. Torrelara.

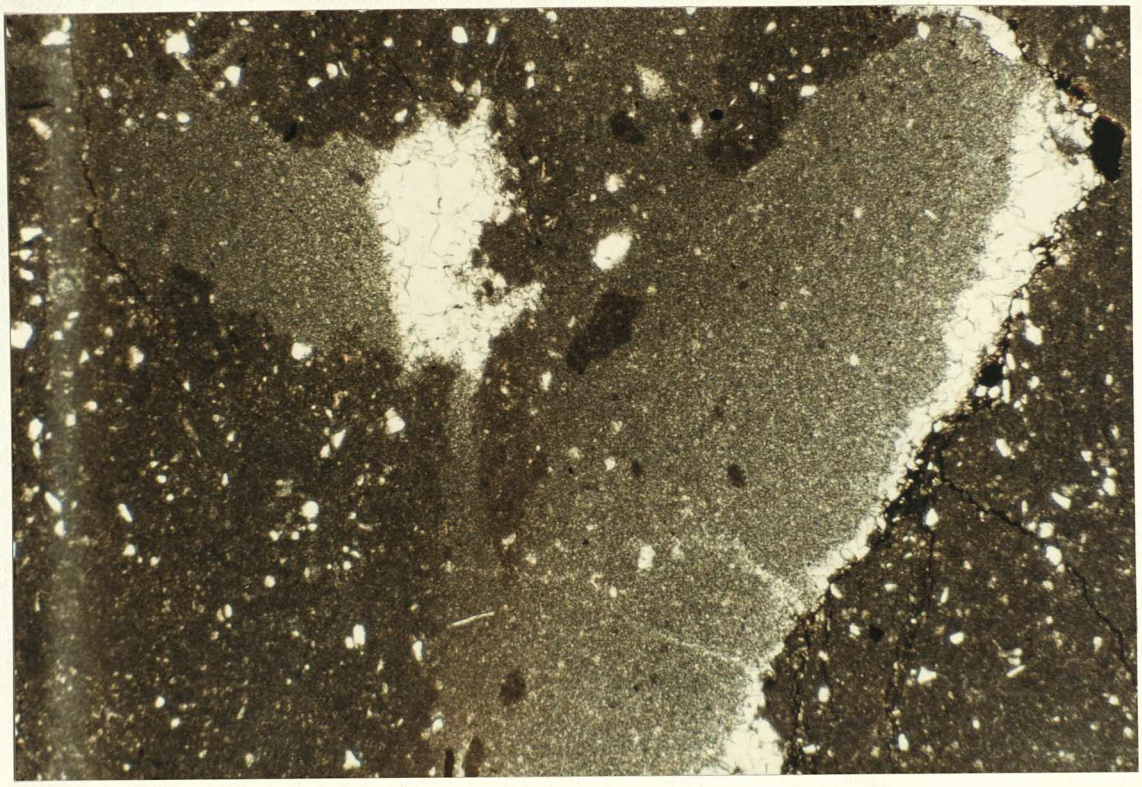

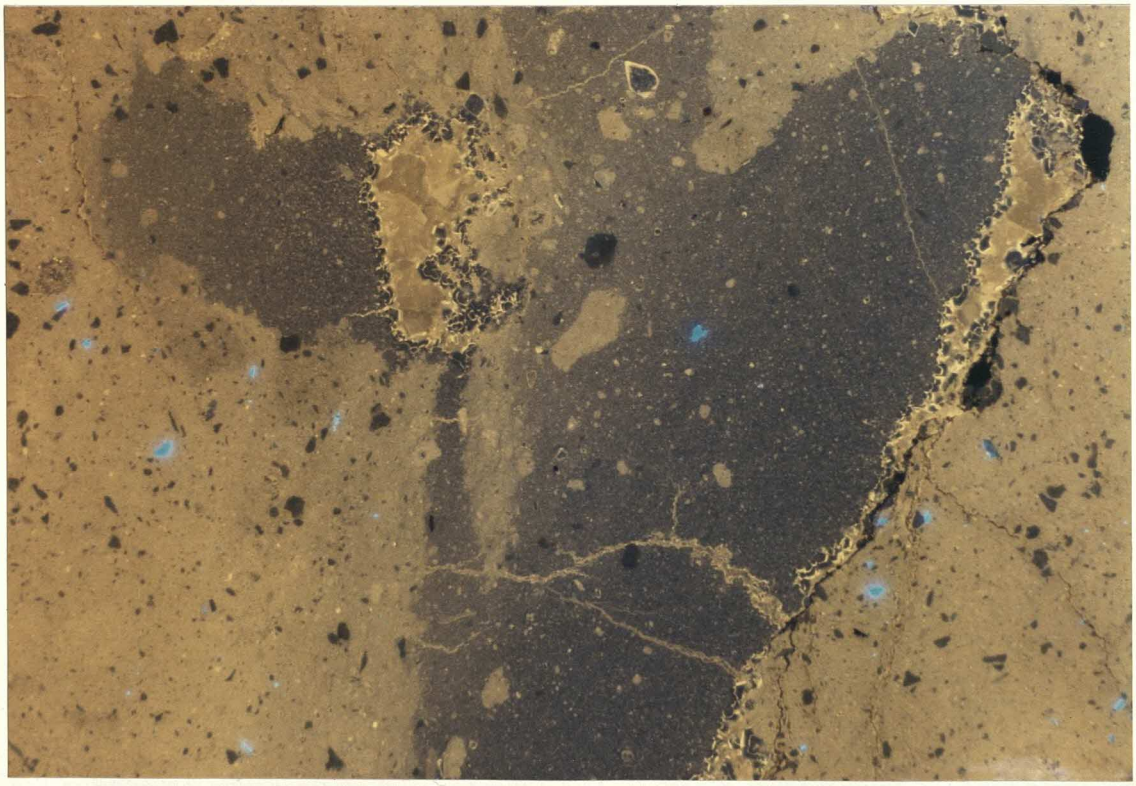

Fig 3.181. Micrographs of micritic limestone with geopetal cavities.
A: Plane polarised light, unstained section, note presence of detrital clastic grains, ostracod tests;
B: Cathodoluminescence showing micrite (dull luminescence), vadose silt (non-luminescent, except in upper cavity with perched luminescent crystal silt fill), later luminescent blocky cavity-filling spar cement, feldspar grains (blue luminescence). Field of view: 4mm. Mambrillas de Lara Member. Torrelara. Note that cathodoluminescence in this and the previous figure shows inclusion of some detrital material in vadose silt - probably washed into cavity or internally derived from cavity wall collapse.

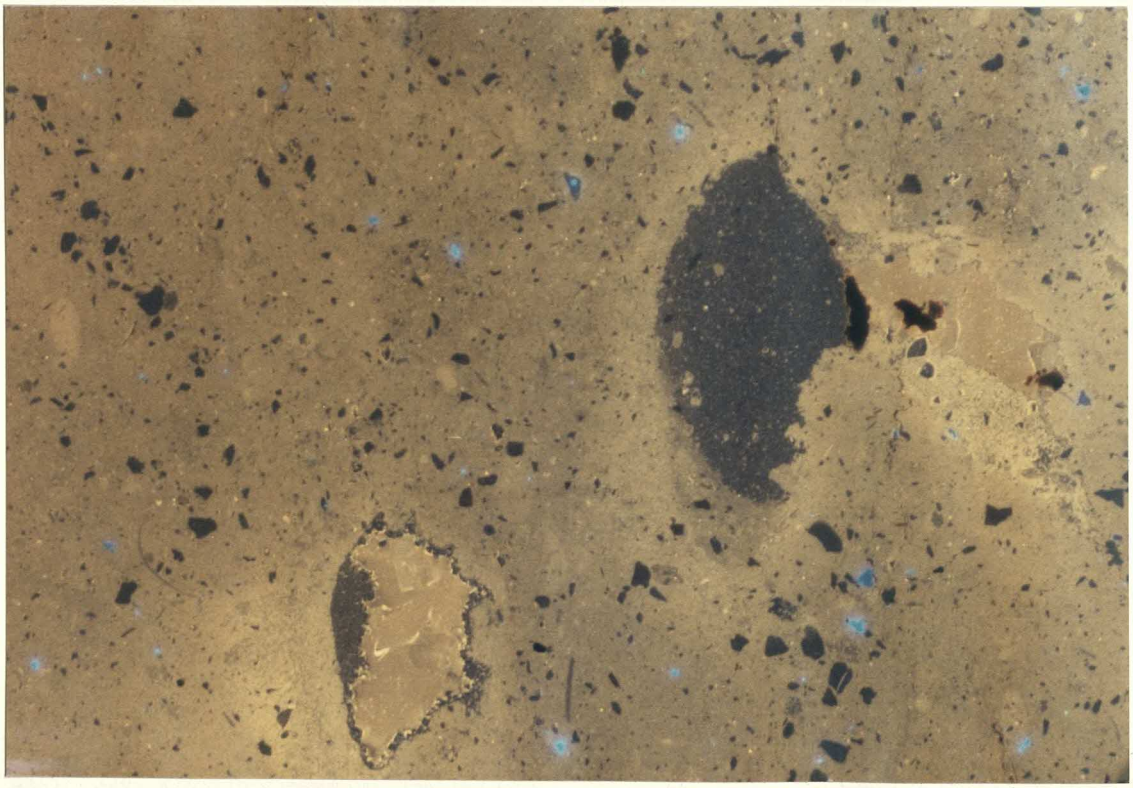

Fig 3.182. Micrographs of facies 11 grainstone.
A: Plane polarised light;
B: Cathodoluminescence. Biomicrite shows dull luminescence. Cement consists mostly of weakly zoned, non-luminescent spar; remaining void space is filled by later generation of brightly luminescent, zoned spar. Field of view: 4mm.
Mambrillas de Lara Member. Las Pinarejas.

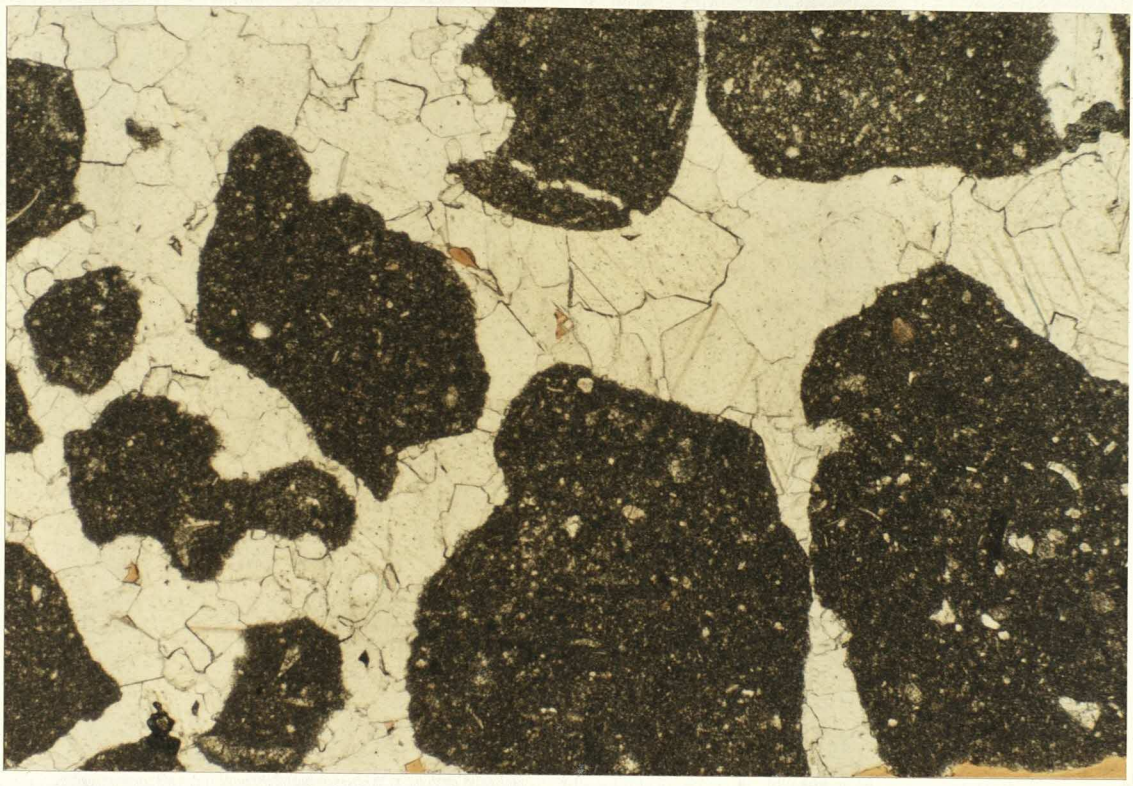

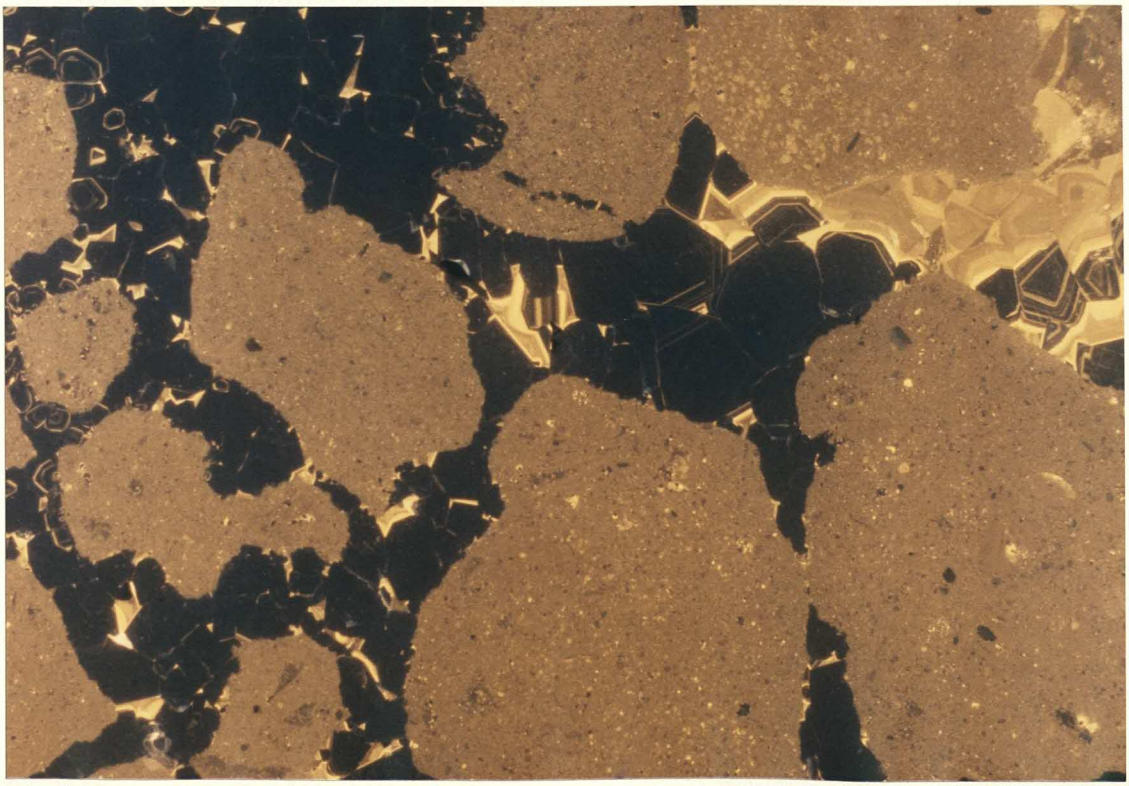

Fig 3.183. Micrograph of facies 2 micrite showing pendent cement. Vadose "drips" developed beneath glaebules / peloids, but post-dating an early isopachous fringing cement. Stained section. Ladera Member. Mambrillas de Lara.

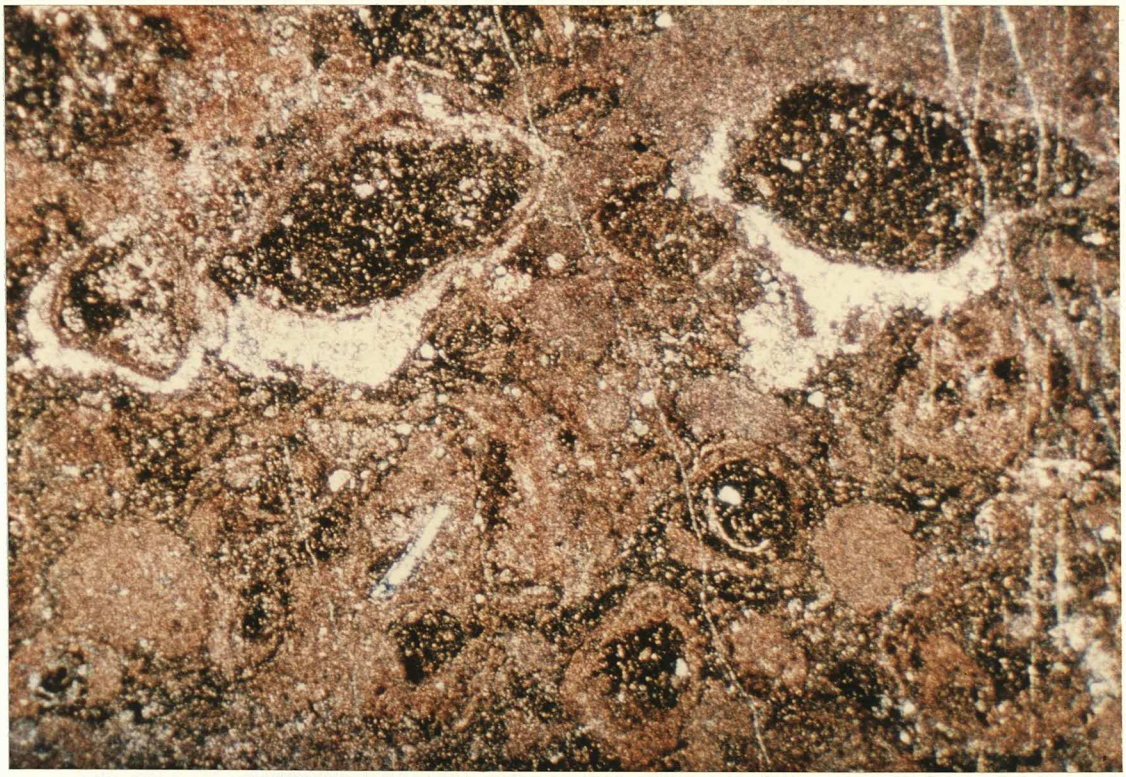

Fig 3.184. Micrographs of micritic limestone with larger cavities. A: Plane polarised light, unstained section;
B: Cathodoluminescence. Study of both micrographs allows recognition of:

1) biomicrite (weakly luminescent)
2) isopachous fringing cement (non-luminescent)
3) multiphase geopetal cavity fill of vadose crystal silt (also non-luminescent)
4) spar.

Spar appears in PPL to consist of one generation only, but CL permits distinction between earlier palisade crystals (weakly zoned but generally non-luminescent) and later blocky fresh-water phreatic cement, showing bright, zoned luminescence. Field of view: 4mm. Top of Mambrillas de Lara Member. Senora de Brezales.

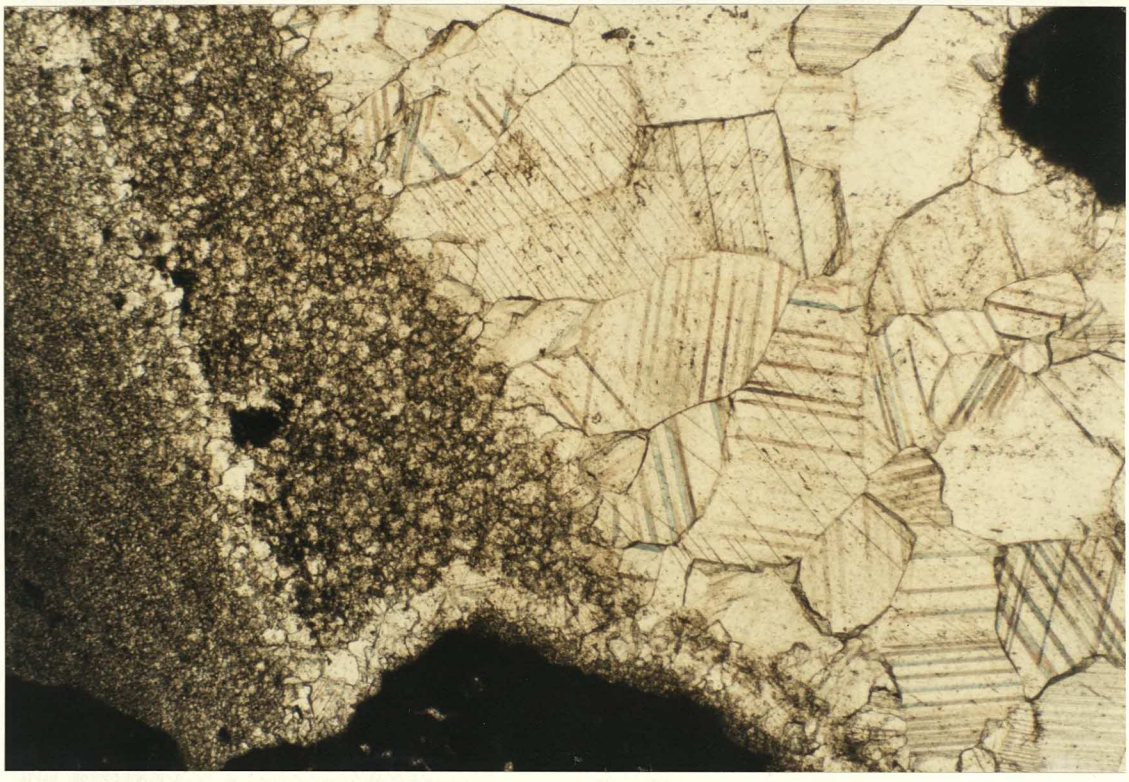

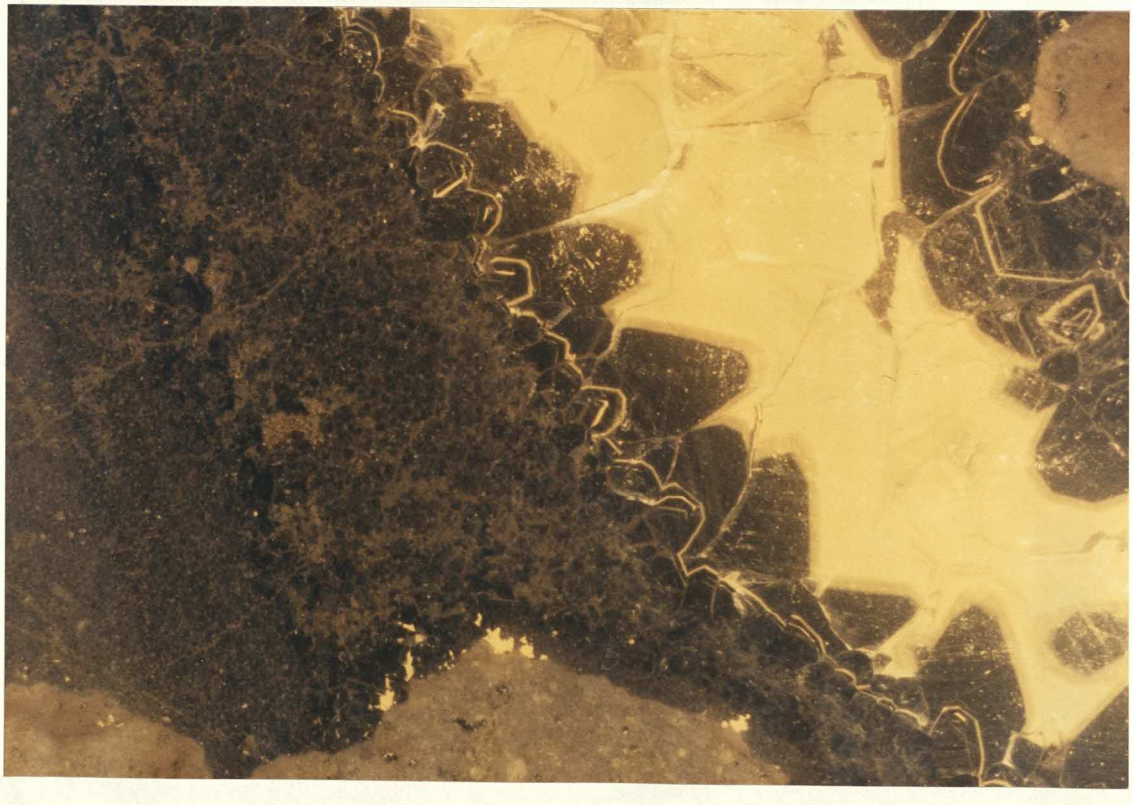

Figs 3.185 & 3.186. Micrographs of same specimen as in fig 3.54. Micritic limestone with larger cavities, some vadose silt, initial palisade crystals of zoned, non-luminescent spar, late-stage blocky fresh-water phreatic cement, showing bright, zoned luminescence, sometimes grown in optical continuity. Note great variation in crystal size. Field of view: 4mm. Top of Mambrillas de Lara Member. Senora de Brezales.

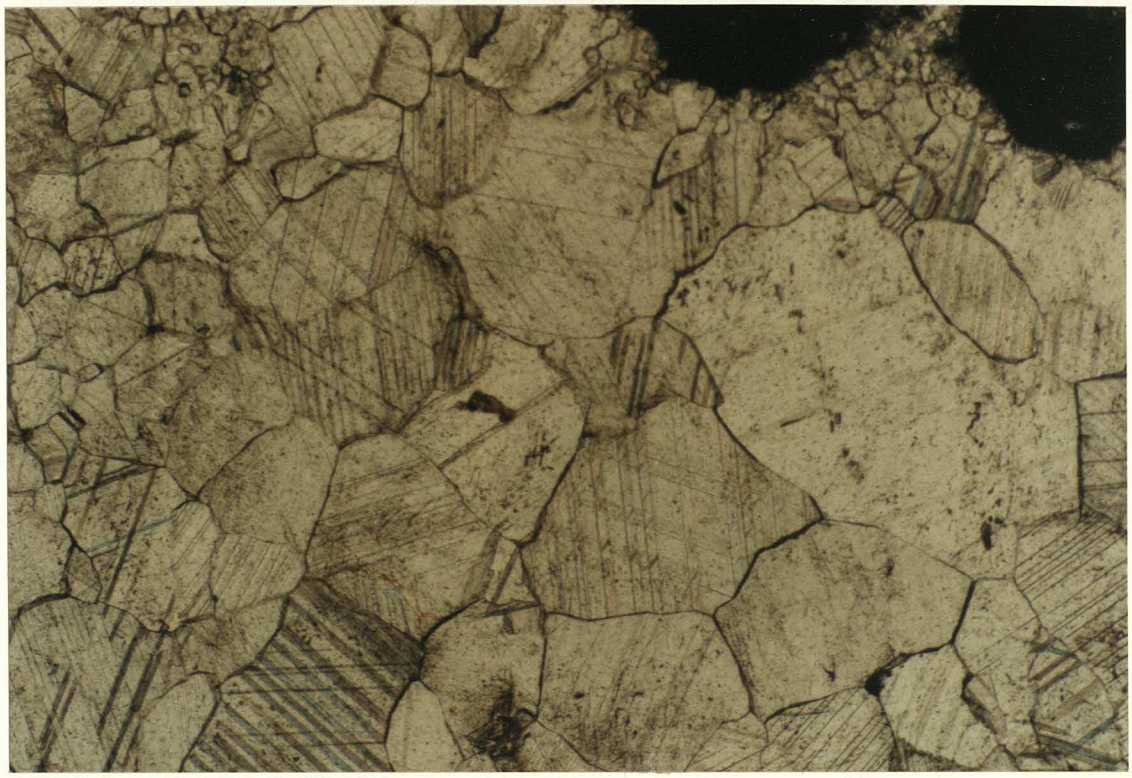

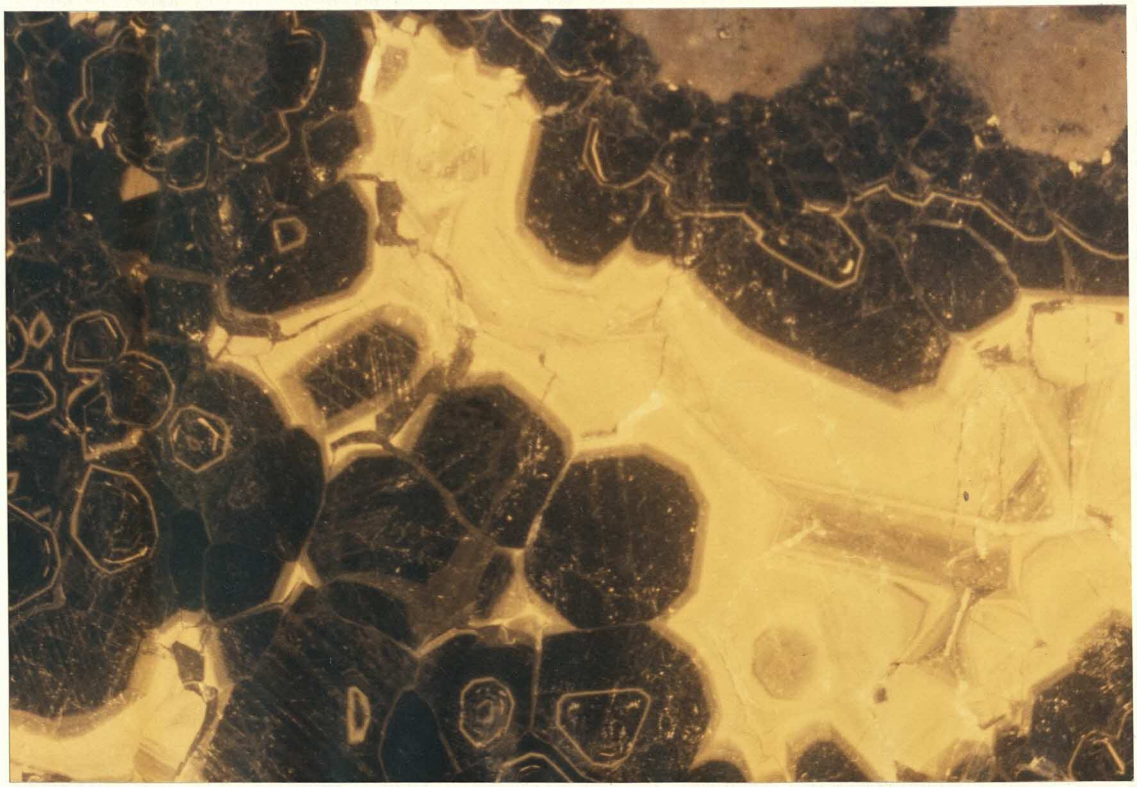

Figs 3.185 & 3.186. Micrographs of same specimen as in fig 3.54. Micritic limestone with larger cavities, some vadose silt, initial palisade crystals of zoned, non-luminescent spar, late-stage blocky fresh-water phreatic cement, showing bright, zoned luminescence, sometimes grown in optical continuity. Note great variation in crystal size. Field of view: 4mm. Top of Mambrillas de Lara Member. Senora de Brezales.

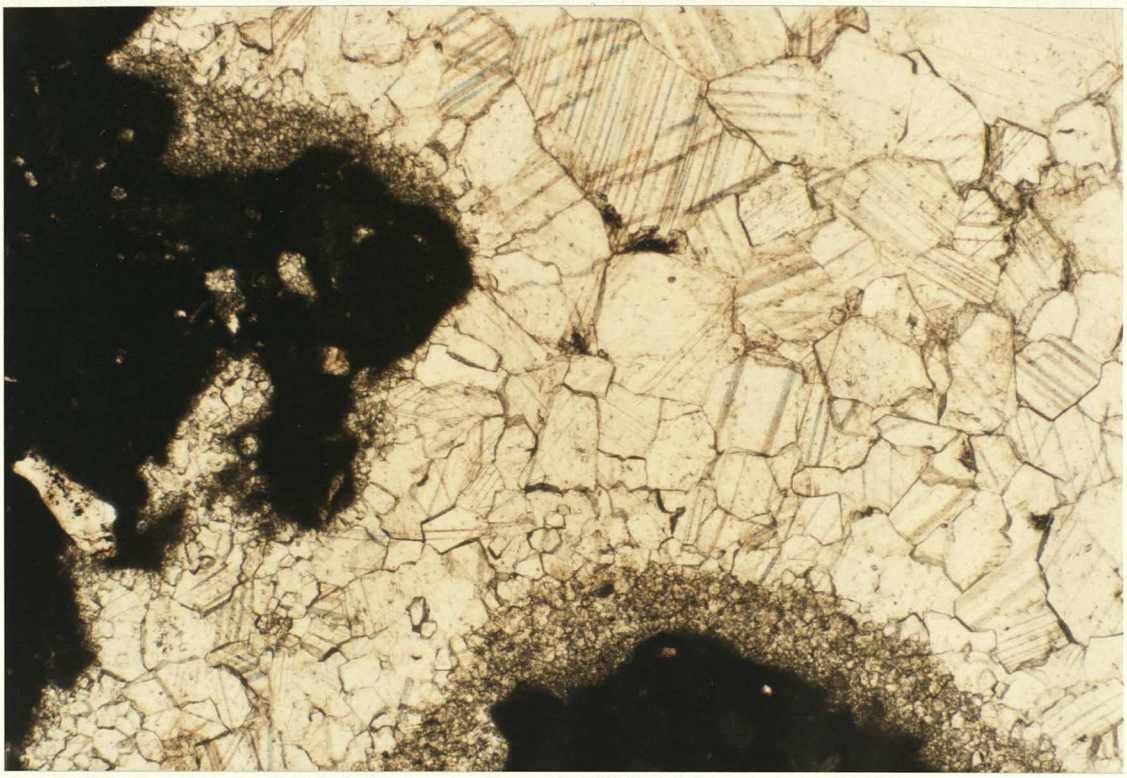

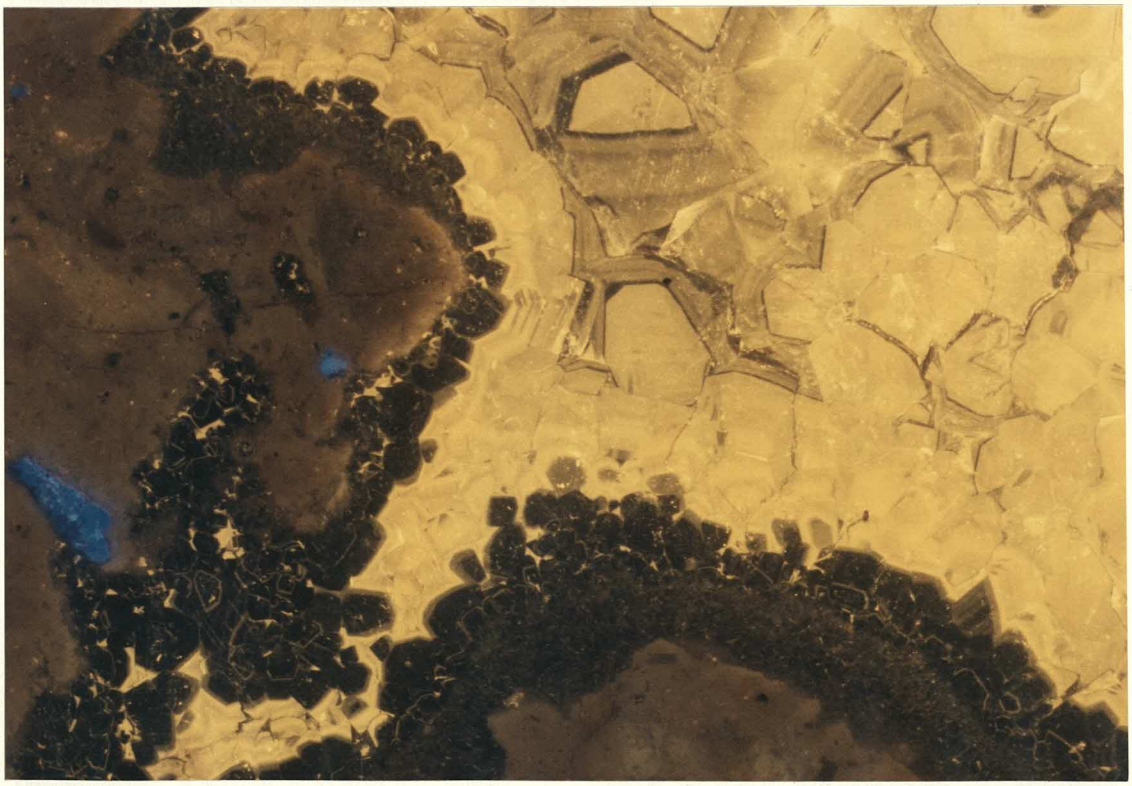

Figs 3.187 & 3.188. Cements from large cavity shown in fig 3.58.
A: Crossed polars, unstained (and unpolished) sections;
B: Cathodoluminescence. Note: Zoned non-luminescent cement crystals have palisade morphology beautifully displayed in cathodoluminescence, similar to speleothem columnar calcites described by Kendall & Broughton (1978); multiphase zoning clearly evident, some crystals in sheath-like arays; later generation of zoned luminescent cement, sometimes grown in optical continuity. Intensity of luminescence reflects concentrations of trace elements, particularly transition metals such as Mn (favours luminescence) and Fe (quenches luminescence). Field of view: 4mm. Ladera Member. Mambrillas de Lara.

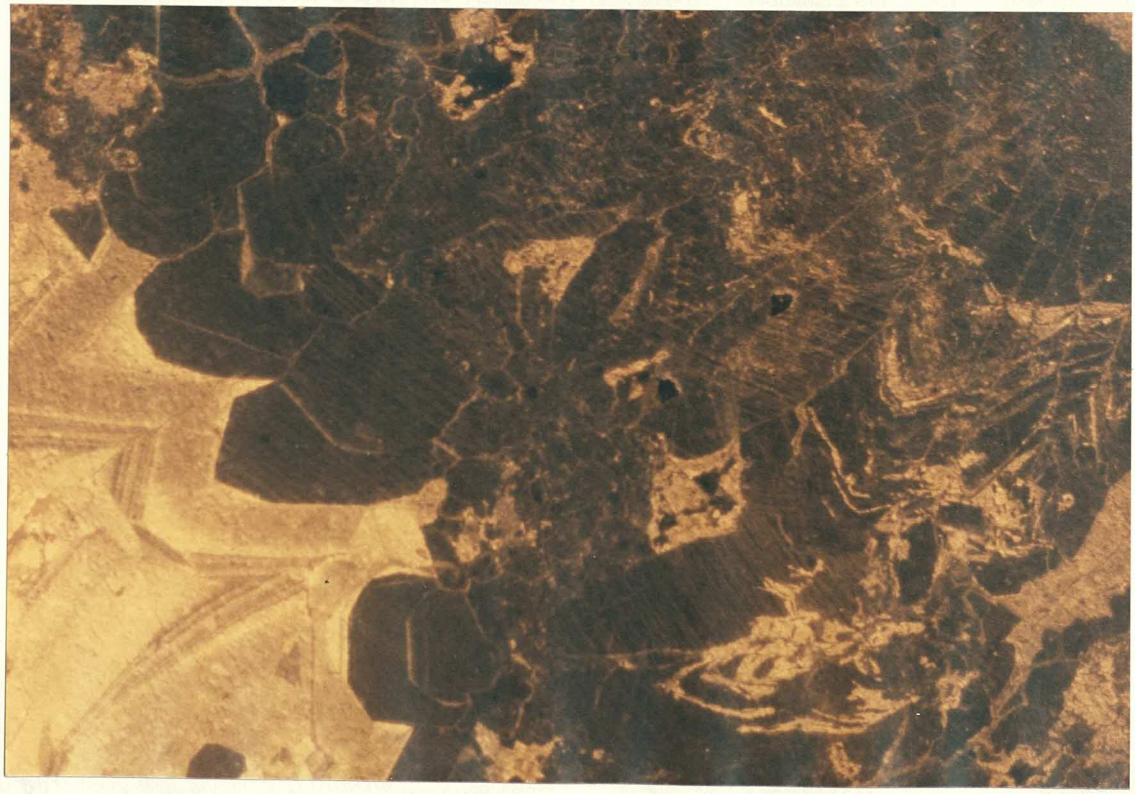

Figs 3.187 & 3.188. Cements from large cavity shown in fig 3.58.
A: Crossed polars, unstained (and unpolished) sections;
B: Cathodoluminescence. Note: Zoned non-luinescent cement crystals have palisade morphology beautifully displayed in cathodoluminescence, similar to speleothem columnar calcites described by Kendall & Broughton (1978); multiphase zoning clearly evident, some crystals in sheath-like arays; later generation of zoned luminescent cement, sometimes grown in optical continuity. Intensity of luminescence reflects concentrations of trace elements, particularly transition metals such as Mn (favours luminescence) and Fe (quenches luminescence). Field of view: 4mm. Ladera Member. Mambrillas de Lara.

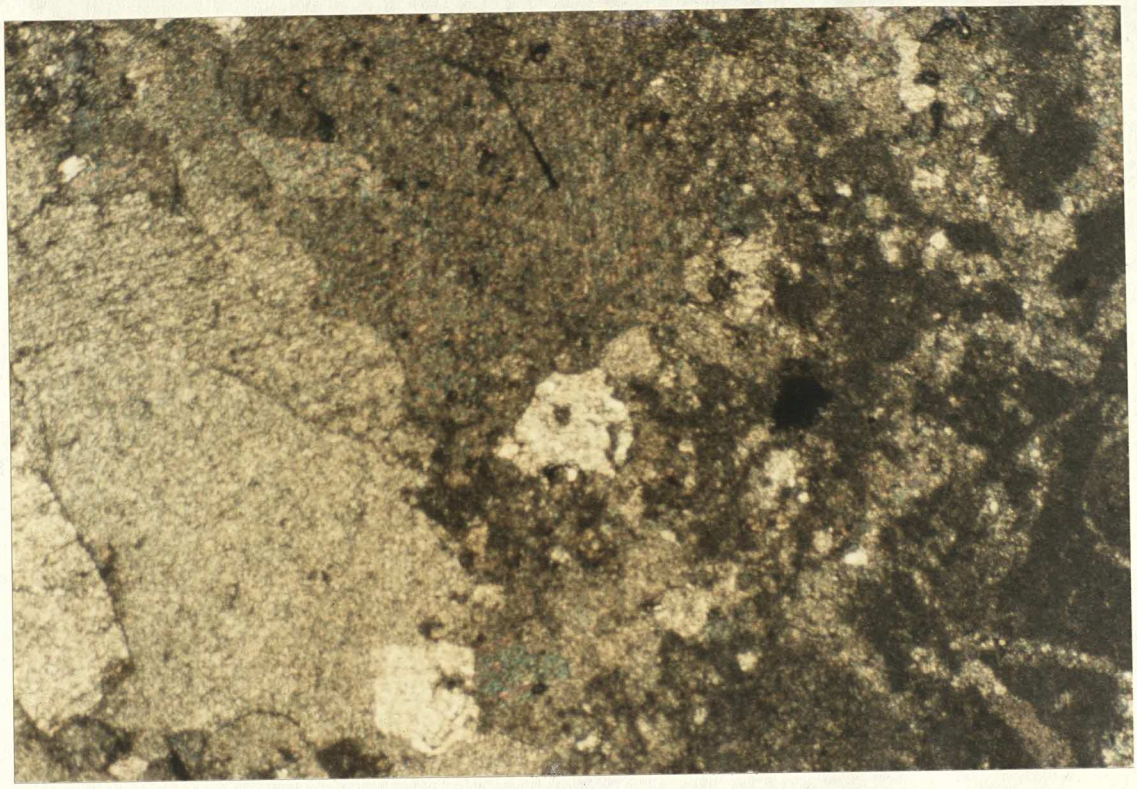

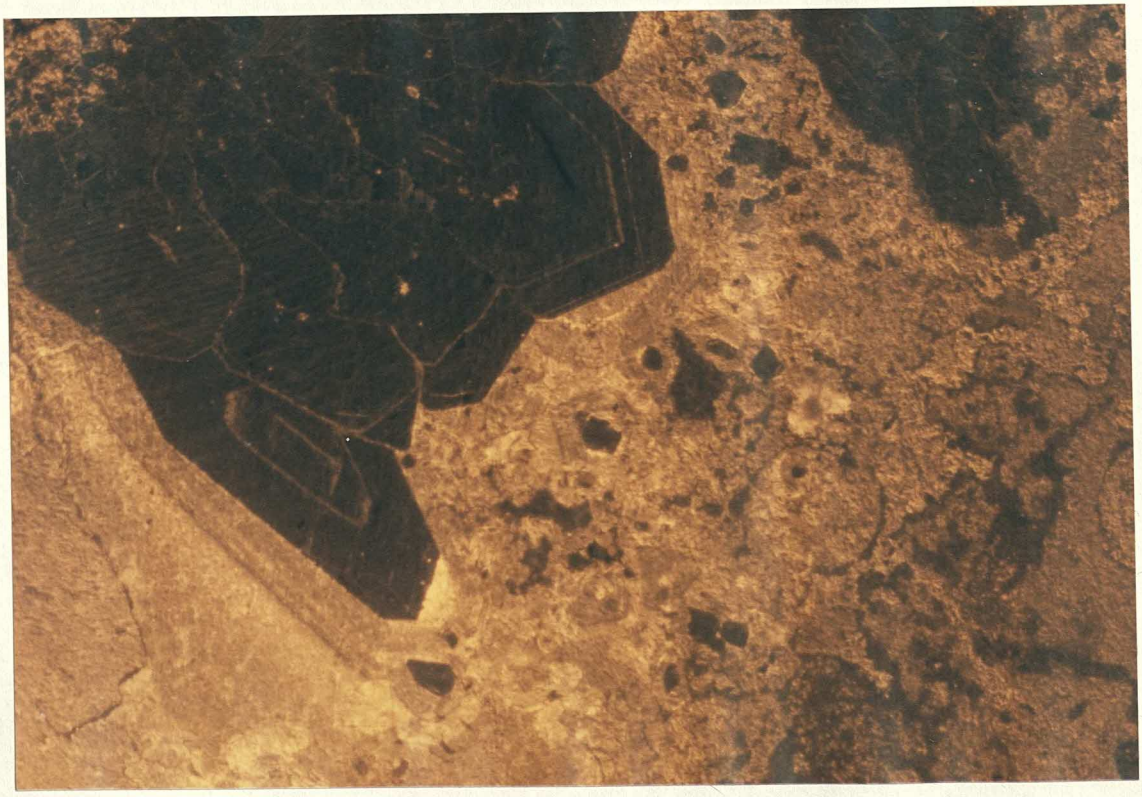

Fig 3.189. Most frequent facies associations in the Tierra de Lara Group, W Cameros Basin.

TIERRA DE LARA GROUP: FACIES ASSOCIATIONS.

FACIES ASSOCIATION	INTERPRETATION
SENORA DE BREZALES FORMATION	
1) conglomerates-sands-rubbly mottled carbonates	small-scale alluvial fans: channels, sandsheets and interdistributary pedogenesis
2) red marls-"laminites"-sands	alluvial fan toe encroaching on temporary lake with water plants
3) red marls-white limestone lenses	periodically inundated floodplain, ponded carbonates
RUPELO FORMATION	
Ladera Member	
4) peloidal limestones-rubbly horizons-"terra rossa"-red marls	marginal lacustrine: frequently exposed, tectonics rapid terrigenous progradation
5) green marls-root crusts-white carbonates with microkarst	marginal lacustrine: less frequent exposure, subaqueous fine clastic input marls
Mambrillas de Lara Member	
6) lst conglom-arenites-clastic laminated biomicrite	clastic input at lake margin river-generated density currents in lake
7) grainstones-biomicrites	open lacustrine, alternating high and low energy
8) biomicrites-marls-chara-oastracs-gastrops-bones + prints	open lacustrine, shallow, unstratified fresh water perennial lake
9) dk grey biomicrs-grey/black biomicrs + diffuse lamination	open lacustrine, partly anoxic, sulphide rich bottom at hypolimnion
10) biomicites-grey marls-intraformational conglomerates	more central open lacustrine, low-stage lake-flat drainage channels periodic reworking on emergence
Rio Cabrera Member	
11) cherts-yellow lsts-yellow vuggy lsts	desiccating lake flat, evaporitic pumping of subsurface brines
12) wacksts-wh.biomicrites + desiccation cracks-green/red marls	periodically desiccating marginal lacustrine carbonate flat

PLATT N (1986)

Fig 3.190. Integrated facies model for the Senora de Brezales Formation, W Cameros Basin.

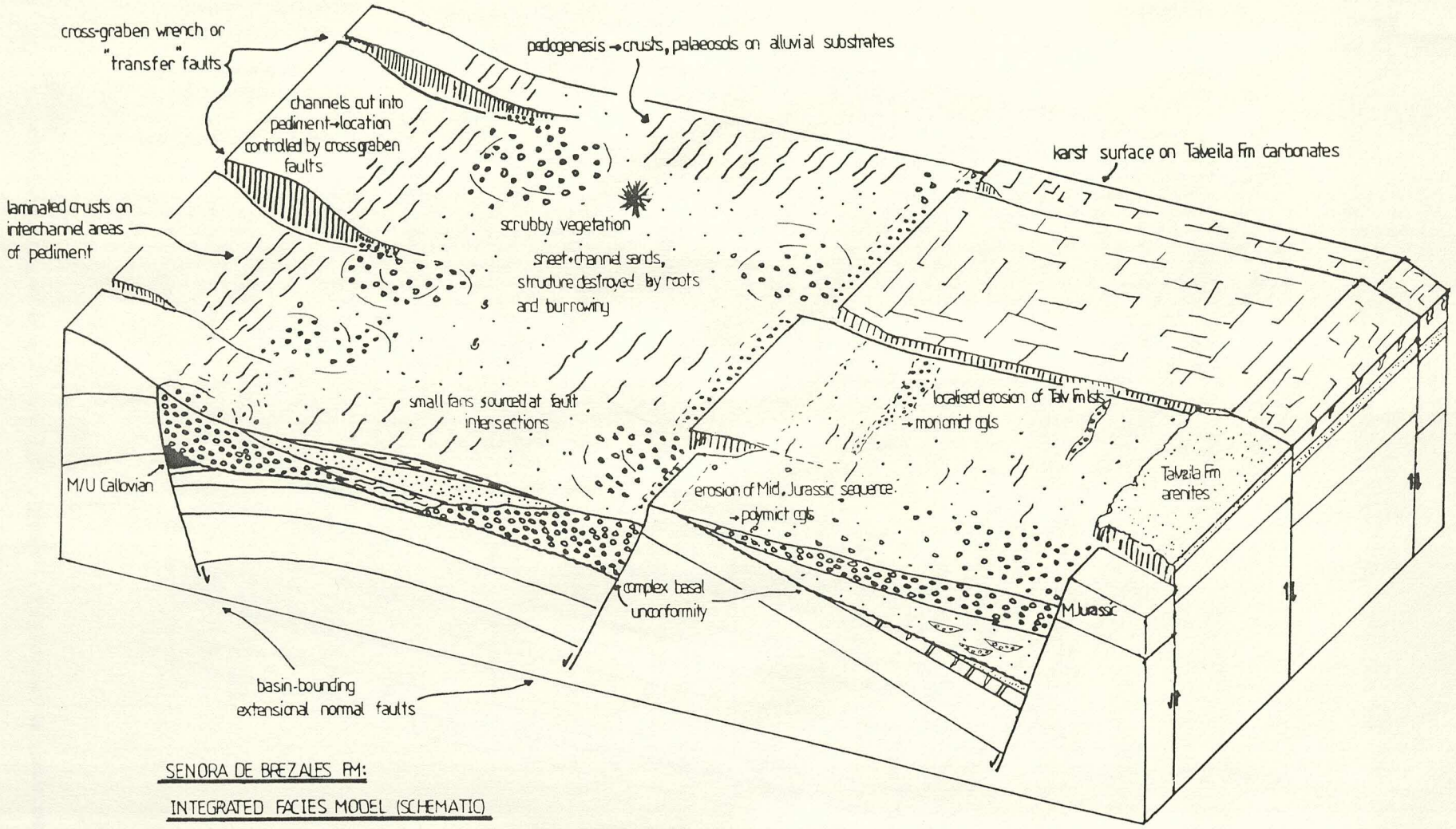

SENORA DE BREZALES FM:

INTEGRATED FACIES MODEL (SCHEMATIC)

Fig 3.191. Integrated facies model for the Rupelo Formation, W Cameros Basin.

RUPELO FORMATION:
INTEGRATED FACIES MODEL

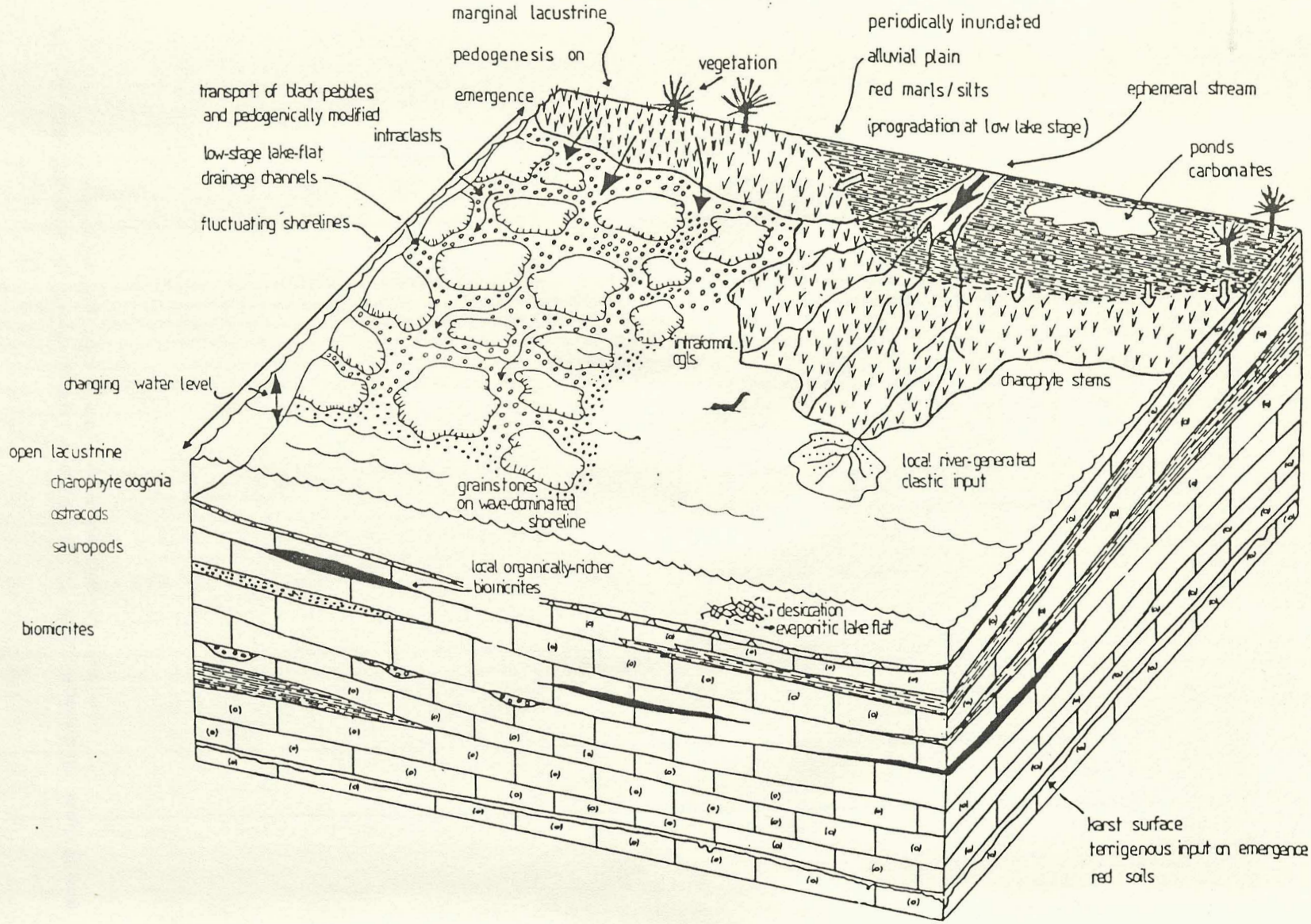

Fig 3.192. Tierra de Lara Group: Evolution of environmental conditions indicated by the observed sequence of facies.

TIERRA DE LARA GROUP: EVOLUTION OF ENVIRONMENTS.

FORMATION	MEMBER	CLIMATE	CLASTIC SUPPLY	CARBONATE PRODUCTION	
	RIO CABRERA	semi-arid → intermittently arid	low to zero	important	- shallow fresh-water - frequent emergence and desiccation - occasionally elevated pH, salinity
	MAMBRILLAS DE LARA	moderately humid	low to zero	important	- shallow fresh-water - more continuous - rare emergence only
RUPELO					
	LADERA	semi-arid	low	important emergence	- shallow fresh-water - frequent emergence → clastic input & pedogenesis
	LAS VINAS	semi-arid	higher	intermittent	- in ponds
SENORA DE BREZALES		semi-arid	high fault control	intermitte	nt pedogenic - mottled carbonates - crusts

PLATT N (1986)

Fig 3.193. Photograph showing typical and consistent facies evolution of the Rupelo Formation. Strata overturned, younging to left. Marls of Las Vinas Member overlain by "laminites" (alternations of marl and bedded root crusts), both out of view, right. Next (in view, right) are massive and mottled limestones of Ladera Member. Prominent rubbly/red horizon just to right of bush. Fossiliferous biomicrites of Mambrillas de Lara Member show typical thickness of 1-2m and form thin beds at left end of last tree trunk. Fauna/flora of Mambrillas de Lara Member: charophytes, ostracods, gastropods, vertebrate bones. Two thicker limestone beds, left, show upward increase in pedogenic modification - ?top of Mambrillas de Lara Member / ??Rio Cabrera Member. Extreme left - marls, 1m intercalated limestones above - probably Hortigüela Formation. Sequence truncated below basal Utrillas conglomerates here at more deformed SW basin margin. Looking NW. Espejon.

Fig 3.194. Photograph showing evidence of repeated desiccation cycles. Thinly-bedded alternations of white biomicrites with polygonal desiccation cracks and green marls. Massive white limestone above shows more intense pedogenesis (nodular fabric, brecciation, weak mottling etc.). Top of Rio Cabrera Member. 1km S of Rupelo. Looking E.

Fig 3.195. Facies sequences: characteristic style of pedogenic modification of various lithofacies within the Tierra de Lara Group.

FACIES SEQUENCES REFLECTING PEDOGENESIS.

"HOST" SEDIMENT LITHOLOGY	CHARACTERISTIC MANIFESTATIONS OF PROGRESSIVE PEDOGENESIS
CLASTICS	→ mottling → cracking → nodular carbonates
MARLS	a) → mottling → nodular carbonates
	b) → root crusts
CARBONATES	a) → cracking → glaebules → mottling → brecciation → clastic input
	b) → microkarst cavities → microkarst brecciation → mottling

PLATT N (1986).